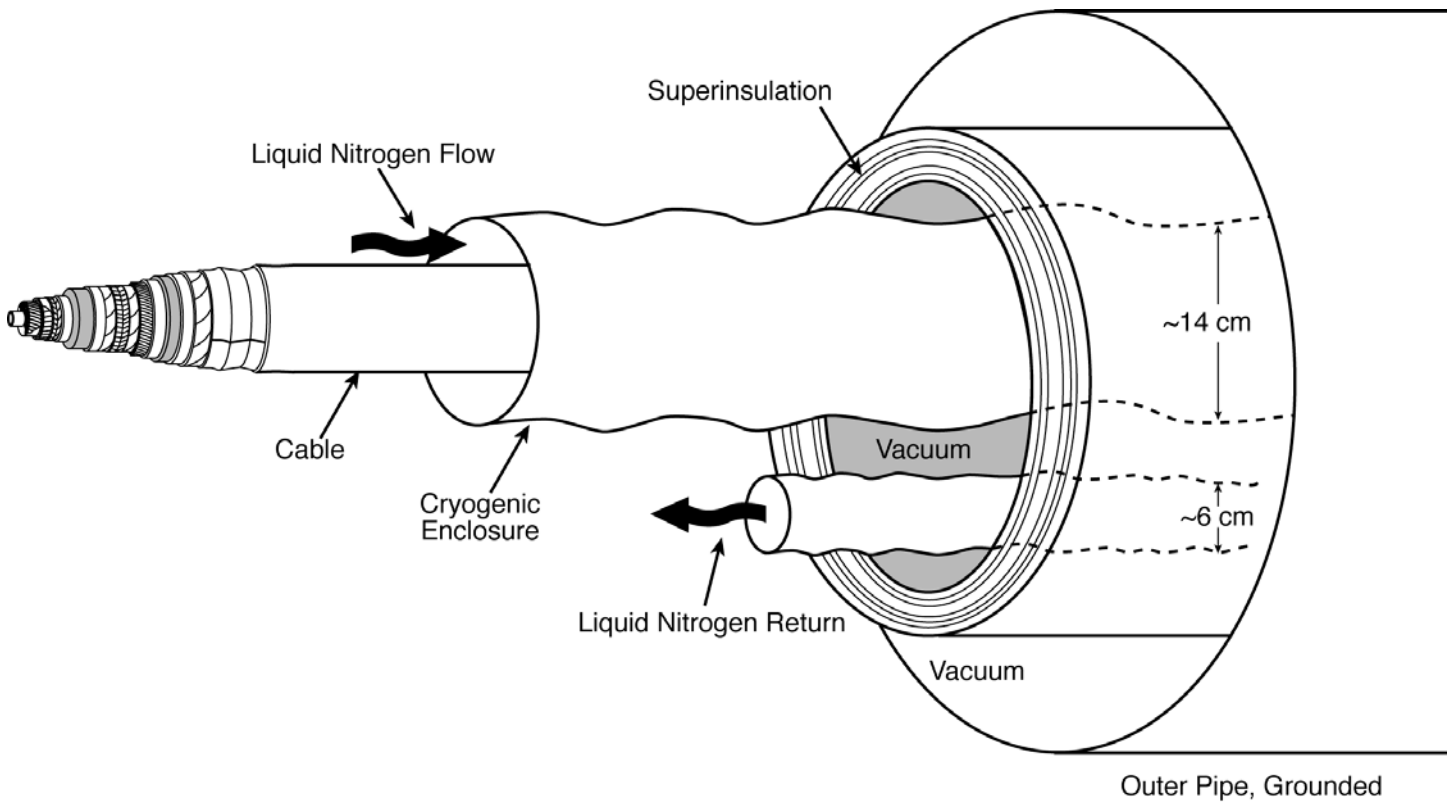


Program on Technology Innovation: a Superconducting DC Cable



Program on Technology Innovation: a Superconducting DC Cable

1020458

Final Report, December 2009

EPRI Project Manager
S. Eckroad

DISCLAIMER OF WARRANTIES AND LIMITATION OF LIABILITIES

THIS DOCUMENT WAS PREPARED BY THE ORGANIZATION(S) NAMED BELOW AS AN ACCOUNT OF WORK SPONSORED OR COSPONSORED BY THE ELECTRIC POWER RESEARCH INSTITUTE, INC. (EPRI). NEITHER EPRI, ANY MEMBER OF EPRI, ANY COSPONSOR, THE ORGANIZATION(S) BELOW, NOR ANY PERSON ACTING ON BEHALF OF ANY OF THEM:

(A) MAKES ANY WARRANTY OR REPRESENTATION WHATSOEVER, EXPRESS OR IMPLIED, (I) WITH RESPECT TO THE USE OF ANY INFORMATION, APPARATUS, METHOD, PROCESS, OR SIMILAR ITEM DISCLOSED IN THIS DOCUMENT, INCLUDING MERCHANTABILITY AND FITNESS FOR A PARTICULAR PURPOSE, OR (II) THAT SUCH USE DOES NOT INFRINGE ON OR INTERFERE WITH PRIVATELY OWNED RIGHTS, INCLUDING ANY PARTY'S INTELLECTUAL PROPERTY, OR (III) THAT THIS DOCUMENT IS SUITABLE TO ANY PARTICULAR USER'S CIRCUMSTANCE; OR

(B) ASSUMES RESPONSIBILITY FOR ANY DAMAGES OR OTHER LIABILITY WHATSOEVER (INCLUDING ANY CONSEQUENTIAL DAMAGES, EVEN IF EPRI OR ANY EPRI REPRESENTATIVE HAS BEEN ADVISED OF THE POSSIBILITY OF SUCH DAMAGES) RESULTING FROM YOUR SELECTION OR USE OF THIS DOCUMENT OR ANY INFORMATION, APPARATUS, METHOD, PROCESS, OR SIMILAR ITEM DISCLOSED IN THIS DOCUMENT.

ORGANIZATION(S) THAT PREPARED THIS DOCUMENT

Advanced Energy Analysis

Cable Consulting International Limited

Electric Power Research Institute

Exponent Failure Analysis Associates

W2AGZ

NOTE

For further information about EPRI, call the EPRI Customer Assistance Center at 800.313.3774 or e-mail askepri@epri.com.

Electric Power Research Institute, EPRI, and TOGETHER...SHAPING THE FUTURE OF ELECTRICITY are registered service marks of the Electric Power Research Institute, Inc.

Copyright © 2009 Electric Power Research Institute, Inc. All rights reserved.

CITATIONS

This report was prepared by

Advanced Energy Analysis
1020 Rose Avenue
Piedmont, CA 94611

Principal Investigator
W. Hassenzahl

Cable Consulting International Limited
PO Box 1
Sevenoaks, Kent
TN14 7EN, UK

Principal Investigator
B. Gregory

Electric Power Research Institute (EPRI)
1300 West W. T. Harris Blvd.
Charlotte, NC 28262

Principal Investigator
S. Eckroad

This report describes research sponsored by EPRI.

The report is a corporate document that should be cited in the literature in the following manner:

Program on Technology Innovation: a Superconducting DC Cable. EPRI, Palo Alto, CA:
2009. 1020458.

Exponent Failure Analysis Associates
149 Commonwealth Drive
Menlo Park, CA 94025

Principal Investigators
S. Nilsson
A. Daneshpooy

W2AGZ
1147 Mockingbird Hill Lane
San Jose, CA 95120

Principal Investigator
P. Grant

PRODUCT DESCRIPTION

Shortly after the beginning of the twentieth century, dc power transmission was replaced by ac in order to achieve efficient transmission of electric power over long distances with available conductors and at safe distribution voltages. However, dc power was not completely abandoned, and the advent of solid-state power electronic ac-to-dc conversion equipment has reinvigorated its application. High-voltage dc power is more desirable for long-range transmission than ac in many ways: dc uses two wires rather than three, uses a simpler conductor, eliminates capacitive elements to cancel inherent inductive behavior, and can use the earth as one of the current-carrying elements. When justified by a lower cost per kilometer, dc transmission is now used for long-distance, high-power transmission lines as well as for interconnecting asynchronous ac systems.

Results and Findings

This report describes the design of an interregional, superconducting dc cable system that is intended to achieve 10 GW power capacity with a nominal current and voltage of 100 kA and 100 kV. When installed, it will enhance the safety, reliability, and efficiency of the existing ac power grid and enable a level of bulk power transfer that is not conceivable with today's conventional technology. Superconducting dc cable systems are inherently suitable for long-distance, high-power, bulk energy transfer without the disadvantages of either high-voltage dc or extrahigh-voltage ac systems. The superconducting dc cable is projected to have greater reliability and security, substantially lower losses, a smaller right-of-way footprint, fewer siting restrictions, and the ability to be terminated at distribution voltages in or near load centers. An underground superconducting dc cable system could transport many gigawatts of power from remote energy farms (wind, hydropower, coal, or nuclear facilities) to urban load centers with minimal impact on the environment. The superconducting dc cable will serve multiple, distributed generators and loads, using voltage source converter-based technology for the power on and off ramps.

Challenges and Objectives

The objectives of this program are to research, develop, and demonstrate a superconducting dc cable system at a level suitable for use on an electric power grid. From the outset, a system capable of being built with today's technology was envisioned. In developing the design of the superconducting dc cable, the research team relied heavily on existing, commercially available cable, cryogenic, and superconductivity technologies. A challenge in the present design has been to determine whether and where new approaches might be better than existing capabilities, especially in light of the goal of producing a conceptual design that could realistically become the basis for the final engineering design of a commercial prototype system within a five- to ten-year timeframe. Despite these challenges, the authors present an engineering-based design that can be expected to function effectively as a new component of the power grid. The major

technical challenge for the future of this technology will be to test some of the novel concepts using a model cable that has the full transverse dimension proposed, if not the full power-carrying capability at first.

Application, Value, and Use

This report provides insight into the groundbreaking research sponsored by the Electric Power Research Institute (EPRI) on superconducting dc cable systems. It will provide utilities and others with a basic understanding of the design concepts and the potential benefits of such a system and a well-thought-out starting point for further engineering design and optimization activities by both institutional research bodies and industrial organizations.

EPRI Perspective

In 2001, Dr. Chauncey Starr, founder and president emeritus of EPRI, introduced the concept of the SuperGrid, a superconducting dc cable cooled by liquid hydrogen to link underground nuclear power plants that would produce both the electricity and the hydrogen that flowed on the dc cable. The nitrogen-cooled superconducting dc cable project described in this report is a first step toward—but is considerably less ambitious in scope than—the SuperGrid. It must be considered on its own merits, and it is viewed as having a nearer-term payoff that is independent of the longer-term SuperGrid vision while still being supportive of it. In the present program, the superconducting dc cable has been taken to a level of engineering design at which the team is confident of the practicality of the concept and its readiness for commercial development.

In his welcome address to the first EPRI workshop on superconducting dc cables in October 2005, Dr. Starr described the values that determine “big systems” as the ability to provide energy under difficult conditions, to avoid the enormous social costs of off-design events, and to move huge amounts of power over long distances. He went on to say that the timeframe for the development, application, and acceptance of the superconducting dc cable system would likely be 20–30 years, as it has been for other major innovations in the power industry. It took 50 years for the power industry to move from wood to coal; it took 10 years to develop advanced turbines and another 10 years for them to be accepted. We do not expect that this project will be an exception. However, EPRI has historically been a leader in innovative transmission cable design work, including the initial development of superconducting ac cables, and considerable progress has now been made in developing the conceptual design of a superconducting dc cable.

Approach

In 2005, EPRI held a workshop on the technology of superconducting dc transmission cables in order to bring together a small group of experts in technologies relevant to the development of such a cable. The goals were to enumerate potential issues and technical challenges, to bring all the participants to a fundamental level of familiarity with the various technologies, and to discuss a timetable for development. Following that initial workshop, a team of researchers began a three-year trek toward the development of a feasible superconducting dc cable design.

Keywords

Cryogenic systems

DC transmission systems

Green power transmission

Superconductors

Superconducting dc cable

Voltage source converters

CONTENTS

- 1 INTRODUCTION AND SUMMARY 1-1**
 - 1.1 Historical Background 1-1
 - 1.2 The Superconducting DC Cable Program 1-4
 - 1.3 Report Outline 1-7

- 2 AC GRID INTERFACE AND CABLE SYSTEM DRIVERS 2-1**
 - 2.1 Vision: Reinventing the North American Transmission System 2-1
 - 2.2 Existing DC Links and Lines 2-3
 - 2.3 Interaction of DC Cables and Lines with Ground 2-5
 - 2.4 Converter Technology 2-5
 - 2.5 The Superconducting DC Cable with Multiple Local Connections to the Grid 2-7
 - 2.6 Issues and Future Work on the Superconducting DC Cable 2-9

- 3 SUPERCONDUCTORS: PAST, PRESENT, AND FUTURE 3-1**
 - 3.1 General Properties of Superconductors 3-1
 - 3.1.1 Early Developments 3-1
 - 3.1.2 The Bardeen-Cooper-Schrieffer Theory of Superconductivity 3-2
 - 3.1.3 Type II Superconductors: Technically Useful Materials 3-3
 - 3.2 The High-Temperature Superconductors 3-7
 - 3.2.1 The Search for Higher-Temperature Superconductors 3-7
 - 3.2.2 Status of High-Temperature Conductors 3-9
 - 3.2.2.1 Gen 1 Technology and Process 3-10
 - 3.2.2.2 Gen 2 Technology 3-11
 - 3.3 High-Temperature Superconductor Performance Targets for Cable Design 3-11
 - 3.4 Cable Losses Due to Time-Dependent Current Flow 3-21

| | |
|--|------------|
| 4 CABLE DESIGN AND FABRICATION | 4-1 |
| 4.1 Introduction | 4-1 |
| 4.2 Background..... | 4-1 |
| 4.2.1 Conventional Cables | 4-2 |
| 4.2.2 Superconducting AC Cables | 4-8 |
| 4.3 Superconducting DC Cable Design | 4-11 |
| 4.3.1 Approach..... | 4-11 |
| 4.3.2 Conductor Mandrel..... | 4-13 |
| 4.3.3 Inner and Outer Quench Conductors | 4-14 |
| 4.3.4 Inner and Outer Superconductor Layers..... | 4-14 |
| 4.3.5 Conductor Shields..... | 4-15 |
| 4.3.6 Insulation..... | 4-16 |
| 4.3.7 Outer Shield and Insulator | 4-16 |
| 4.3.8 Sheath and Skid Layer..... | 4-17 |
| 4.4 Superconducting DC Cable Dimensions..... | 4-17 |
| 4.5 Superconducting DC Cable Fabrication..... | 4-19 |
| | |
| 5 VACUUM SYSTEM | 5-1 |
| 5.1 Introduction | 5-1 |
| 5.1.1 Overview | 5-1 |
| 5.1.2 Heat Input..... | 5-4 |
| 5.1.2.1 Heat Conduction by Residual Gas..... | 5-4 |
| 5.1.2.2 Thermal Radiation..... | 5-5 |
| 5.1.2.3 Combined Radiation and Gaseous Convection | 5-6 |
| 5.1.3 Some Units Used in Vacuum Systems..... | 5-7 |
| 5.2 Getters | 5-7 |
| 5.3 Vacuum Pumps | 5-10 |
| 5.3.1 Purpose..... | 5-10 |
| 5.3.2 Types | 5-11 |
| 5.3.3 Pumping Speeds and Pressure Drop | 5-12 |
| 5.4 Superconducting DC Cable Vacuum Issues..... | 5-14 |
| 5.4.1 Conductance and Pressure Drop in a Vacuum System..... | 5-14 |
| 5.4.2 Residual Gas, Outgassing, and Leaks..... | 5-15 |
| 5.4.2.1 Water Vapor and the Need for Purging with a Dry Inert Gas..... | 5-15 |

| | | |
|----------|--|------------|
| 5.4.2.2 | Leaks | 5-16 |
| 5.4.2.3 | Impact of Cryogenic Surface on Gas Adsorption and Freezing | 5-17 |
| 5.4.3 | Superconducting DC Cable Vacuum Pump Capacity and Spacing | 5-17 |
| 5.5 | Conclusions and Observations | 5-18 |
| 5.5.1 | Comparison of These Results to the Previous Study | 5-18 |
| 5.5.2 | Issues for the Next Stage of Vacuum System Design | 5-18 |
| 6 | CRYOGENICS | 6-1 |
| 6.1 | Introduction and Summary | 6-1 |
| 6.1.1 | Introduction | 6-1 |
| 6.1.2 | Summary | 6-2 |
| 6.1.2.1 | Refrigerator Station Separation | 6-3 |
| 6.1.2.2 | Initial Temperature of the Cryogen | 6-3 |
| 6.1.2.3 | Temperature Rise Along the Cable Between Refrigerator Stations | 6-3 |
| 6.1.2.4 | Maximum Pressure Drop Between Refrigerator Stations | 6-3 |
| 6.2 | Heat Flow into the Cold Mass | 6-5 |
| 6.2.1 | Radiation and Conduction Through the Vacuum | 6-5 |
| 6.2.2 | Heat Conduction Along Mechanical Supports | 6-6 |
| 6.2.3 | Losses Associated with the Flow of the Cryogen | 6-8 |
| 6.2.4 | Heat Generated Within the Cable Conductors | 6-10 |
| 6.2.5 | Heat Input at the Vacuum and Refrigerator Stations | 6-11 |
| 6.2.6 | Heat Flow Through the Power Leads | 6-12 |
| 6.2.7 | Summary of Heat Inputs | 6-14 |
| 6.3 | Cryogen Flow | 6-14 |
| 6.3.1 | Practical Cable Flow and Tube Dimensions | 6-17 |
| 6.3.2 | Effect of Altitude Changes | 6-19 |
| 6.3.3 | Temperatures During Normal Operation | 6-20 |
| 6.3.4 | Counterflow Heat Exchange | 6-21 |
| 6.4 | Refrigerator Separation Issues | 6-24 |
| 6.4.1 | Case 1, Urban or Suburban Environment | 6-25 |
| 6.4.2 | Case 2, Rural Environment | 6-26 |
| 6.4.3 | Case 3, Mountainous Environment | 6-26 |

| | | |
|----------|---|------------|
| 7 | END STATIONS AND CONVERTERS | 7-1 |
| 7.1 | Converter Topology | 7-1 |
| 7.2 | Superconducting Cable System Assumptions | 7-2 |
| 7.3 | Converter Station Design..... | 7-5 |
| 7.4 | Grounding of the Superconducting Cables | 7-10 |
| 7.5 | Energization of the DC System..... | 7-13 |
| 7.6 | Further Research and Development Needs | 7-14 |
| | | |
| 8 | FABRICATION AND INSTALLATION | 8-1 |
| 8.1 | Factory-Fabricated Components | 8-2 |
| 8.1.1 | Vacuum Pipe..... | 8-2 |
| 8.1.2 | Cleaning Vacuum Pipe and Installing Internal Reflective Coating | 8-4 |
| 8.1.3 | Cryogenic Enclosure and Return Pipe | 8-4 |
| 8.1.4 | Cryogenic Supports..... | 8-5 |
| 8.1.5 | Multilayer Insulation | 8-5 |
| 8.1.6 | Getters | 8-6 |
| 8.1.7 | Factory Welds | 8-7 |
| 8.1.8 | Instrumentation | 8-8 |
| 8.1.9 | Installation of Collar and Protective End Caps..... | 8-8 |
| 8.2 | Field Fabrication and Final Assembly | 8-8 |
| 8.2.1 | Site Preparation | 8-8 |
| 8.2.2 | Transportation | 8-10 |
| 8.2.3 | Positioning in Trench..... | 8-10 |
| 8.2.4 | Welding of Cryogenic Pipes and Connecting Instrumentation | 8-12 |
| 8.2.5 | Welding Collars to Connect the Vacuum Pipe | 8-13 |
| 8.3 | Vault and Manhole Installation..... | 8-13 |
| 8.3.1 | Cable Pulling..... | 8-15 |
| 8.3.2 | Cable Splicing | 8-18 |
| 8.3.3 | Vacuum Pump Installation and Pumpdown | 8-22 |
| 8.3.4 | Vacuum and Cryogenic Component Sectioning | 8-23 |
| 8.3.5 | Cryogenic Station Installation..... | 8-23 |

| | |
|--|-------------|
| 9 FUTURE WORK | 9-1 |
| 9.1 System Test..... | 9-1 |
| 9.2 Cryogenics and Vacuum..... | 9-2 |
| 9.3 Insulation and Dielectrics | 9-2 |
| 9.4 Cable Design and Fabrication..... | 9-5 |
| 9.5 Converters | 9-5 |
| 9.6 Grid Interface | 9-6 |
| 9.7 Optimization and Tradeoffs..... | 9-7 |
| 9.8 Costs..... | 9-8 |
| 9.9 Superconductors..... | 9-8 |
| 9.10 General | 9-9 |
| | |
| 10 REFERENCES | 10-1 |
| | |
| A ABBREVIATIONS AND ACRONYMS | A-1 |
| | |
| B SYSTEM STUDY OF LONG-DISTANCE LOW-VOLTAGE TRANSMISSION USING HIGH-TEMPERATURE SUPERCONDUCTING CABLE | B-1 |
| | |
| C ECONOMIC CONSIDERATIONS | C-1 |

LIST OF FIGURES

| | |
|---|------|
| Figure 1-1 Cable cross section | 1-6 |
| Figure 2-1 Single-phase, two-level voltage source converter | 2-7 |
| Figure 2-2 A simplified, six-node drawing of the superconducting dc cable as connected to various parts of the ac grid | 2-8 |
| Figure 3-1 A replication of the original observation of zero resistance in mercury in 1911 | 3-2 |
| Figure 3-2 A simplified view of the interaction between a phonon and a lattice in the Bardeen-Cooper-Schrieffer theory | 3-3 |
| Figure 3-3 Phase diagram of a typical type II superconductor..... | 3-4 |
| Figure 3-4 Illustration of the vortex dynamics of a type II superconductor..... | 3-5 |
| Figure 3-5 The irreversibility line..... | 3-6 |
| Figure 3-6 Origin of ac hysteretic losses in a type II superconductor | 3-7 |
| Figure 3-7 Observed increase in T_c since 1911 | 3-8 |
| Figure 3-8 The two categories of high-temperature superconductor tapes currently available | 3-10 |
| Figure 3-9 The two principal methods of manufacturing Gen 2 high-temperature superconductor tape | 3-12 |
| Figure 3-10 Dependence of the critical current, J_c , of Gen 2 YBCO on the magnetic field (data from SRL-ISTEC, Japan) | 3-14 |
| Figure 3-11 Effect of various pinning impurities on the anisotropy of J_c with respect to the direction of applied magnetic field (data from Los Alamos National Laboratory) | 3-15 |
| Figure 3-12 Comparison of I_c per unit tape width of representative samples | 3-16 |
| Figure 3-13 Variation of I_c per unit width as a function of the direction of a 1-T externally applied field with respect to the tape plane (a-b)..... | 3-17 |
| Figure 3-14 Specification sheet for American Superconductor copper-stabilized Gen 2 tape | 3-18 |
| Figure 3-15 E-J characteristic, typical of both Gen 1 and Gen 2 | 3-19 |
| Figure 3-16. Representative Fourier decomposition of rectified current from a general purpose n -phase passive rectifier | 3-22 |
| Figure 4-1 Cable transport drum, fully loaded with cable..... | 4-2 |
| Figure 4-2 Loaded cable transport drums being transported from manufacturing facility to installation site..... | 4-3 |
| Figure 4-3 A 400-kV ac cable with extruded, solid insulation (left) and oil-impregnated paper insulation (right) | 4-4 |
| Figure 4-4 A tape-lapping machine in a humidity-controlled enclosure | 4-5 |

| | |
|---|------|
| Figure 4-5 One of the tape-lapping heads | 4-5 |
| Figure 4-6 Layout of a horizontal extrusion machine for cable insulation | 4-6 |
| Figure 4-7 An extruded cable core emerging from the extrusion and cross-linking machine..... | 4-7 |
| Figure 4-8 Triple extrusion equipment in a vertical line. The conductor appears as a vertical, white line to the left of the foremost extrusion press..... | 4-7 |
| Figure 4-9 A warm dielectric, single-phase superconducting ac cable | 4-8 |
| Figure 4-10 A superconducting triplex with nitrogen-impregnated, cold insulation between phases | 4-9 |
| Figure 4-11 Three cold-dielectric, superconducting, single-phase ac cables in a single pipe | 4-10 |
| Figure 4-12 Superconducting dc cable design..... | 4-13 |
| Figure 4-13 Conductor stranding machine..... | 4-19 |
| Figure 5-1 Simplified design for cryogenic and vacuum calculations | 5-2 |
| Figure 5-2 Design of the cable developed for the EPRI report <i>System Study of Long-Distance Low-Voltage Transmission Using High-Temperature Superconducting Cable</i> | 5-3 |
| Figure 6-1 Cable in pipe envelope showing various components..... | 6-4 |
| Figure 6-2 Temperature increase along the superconducting dc cable (base case) | 6-8 |
| Figure 6-3 Pressure drop along the superconducting dc cable for the flow of liquid nitrogen | 6-9 |
| Figure 6-4 Pressure drop along the superconducting dc cable for the flow of supercritical nitrogen | 6-9 |
| Figure 6-5 Temperature along a warm-to-cold power lead for different operating currents..... | 6-13 |
| Figure 6-6 Saturation pressure of liquid nitrogen over the operating range..... | 6-15 |
| Figure 6-7 Saturation density variation of liquid nitrogen over the operating range..... | 6-15 |
| Figure 6-8 Pressure-specific volume diagram for liquid nitrogen..... | 6-16 |
| Figure 6-9 Pressure drop along the cryogenic enclosure as a function of tube diameter..... | 6-18 |
| Figure 6-10 Pressure drop along the return tube as a function of tube diameter..... | 6-19 |
| Figure 6-11 Pressure changes in a 10-km length of cable with an altitude change of 150 m | 6-20 |
| Figure 6-12 Nominal temperature rise along the superconducting dc cable..... | 6-21 |
| Figure 6-13 Hypothetical example of counterflow heat exchange in a constrained flow loop | 6-22 |
| Figure 6-14 Temperatures along the superconducting dc cable for medium heat transfer..... | 6-23 |
| Figure 6-15 Temperatures along the superconducting dc cable for good heat transfer | 6-24 |
| Figure 7-1 Switching arrangement to transfer converter A from a failed to a healthy cable; similar switches would be required on converter B..... | 7-3 |
| Figure 7-2 Single-phase, two-level voltage source converter | 7-5 |
| Figure 7-3 Output voltage from a single-phase, two-level pulse-width modulation converter | 7-6 |

| | |
|--|------|
| Figure 7-4 Three-phase, two-level voltage source converter..... | 7-7 |
| Figure 7-5 Switched phase-to-phase output voltage and fundamental ac component for the three-phase, two-level voltage source converter..... | 7-8 |
| Figure 7-6 Ripple current through the capacitor at no load..... | 7-9 |
| Figure 7-7 Highly simplified superconducting cable design | 7-12 |
| Figure 7-8 Cable in pipe envelope showing various components..... | 7-13 |
| Figure 8-1 Simplified design of factory-assembled pipe for superconducting dc cable | 8-2 |
| Figure 8-2 Example of gas pipeline being delivered to site in preparation for welding | 8-9 |
| Figure 8-3 Artist's concept for truck transport of pipe sections for the superconducting dc cable..... | 8-10 |
| Figure 8-4 Side view of two pipe sections for the superconducting dc cable that are nearly in place | 8-11 |
| Figure 8-5 Diagonal view of two pipe sections for the superconducting dc cable that are nearly in place | 8-11 |
| Figure 8-6 After the vacuum pipe of the left section is in place, the two cryogenic pipes are welded together by an automatic welder. | 8-12 |
| Figure 8-7 The final step in installing a section of cable is welding the collar to both pipe sections. | 8-13 |
| Figure 8-8 Artist's concept of the vault with the two vacuum pipes installed | 8-14 |
| Figure 8-9 Vacuum vault with vacuum pump installed and an extended section of pipe..... | 8-15 |
| Figure 8-10 Extensions of the cryogenic enclosure to accommodate cable pulling and joint fabrication | 8-15 |
| Figure 8-11 Cable pull for a superconducting cable | 8-16 |
| Figure 8-12 The superconducting dc cable core in place and ready to be pulled into the cryogenic enclosure | 8-17 |
| Figure 8-13 Cable cores extending into a vault in preparation for splicing | 8-17 |
| Figure 8-14 The electrical splice for the superconducting dc cable | 8-18 |
| Figure 8-15 The cable core..... | 8-19 |
| Figure 8-16 A completed splice | 8-21 |
| Figure 8-17 Vault for vacuum and cable splice after full installation | 8-22 |
| Figure 8-18 Vault for refrigeration and vacuum | 8-24 |
| Figure 8-19 Cryogenic refrigerator and the associated vault for cryogenics and vacuum. | 8-24 |
| Figure 8-20 Pumping station for a natural gas pipeline | 8-25 |

LIST OF TABLES

| | |
|--|------|
| Table 4-1 Dimensions of the various layers of the superconducting dc cable..... | 4-18 |
| Table 6-1 Design parameters of the superconducting dc cable..... | 6-4 |
| Table 6-2 Weights of materials in the cold mass of the superconducting dc cable..... | 6-7 |
| Table 6-3 Summary of heat inputs..... | 6-14 |

1

INTRODUCTION AND SUMMARY

Economic, environmental, and political forces will change the nature of energy distribution and use in the next decades. As a result, future electricity generation and consumption is quite uncertain. Increased use of large generating facilities such as remote nuclear power plants or huge wind farms forms one possibility, and small distributed energy sources such as renewable and hydrogen sources form another. Should large, 5–10 GW power generation facilities become the norm in a couple of decades, methods of transmitting power of this level over long distances will be required. In addition, there is a growing recognition of the necessity for improved efficiency, stability, and reliability of a power grid that can provide continent-wide sharing of electric power. One way to accomplish these goals is to use dc cables based on high-temperature superconductors. The technology to build such dc cables exists today. However, existing superconducting materials and other system components that are technically capable of meeting such a mission would not today deliver a competitive alternative to existing technologies. Fortunately, both recent progress and ongoing research in these areas promise to improve performance and reduce cost so that competitive parity with conventional transmission is expected in a few years' time.

The Electric Power Research Institute (EPRI) conducts research and development related to the generation, delivery, and use of electricity for the benefit of the public. In pursuit of this mission, EPRI explores scenarios that would impact future electricity production, transmission, and use. Thus, in the fall of 2005, EPRI took a long-range view and convened a workshop on the present and future technology of superconducting dc transmission cables. The project described in this report—the development of a long-distance superconducting dc cable—was conceived during that workshop, which began with an address by Chauncey Starr. Dr. Starr gave some of his insights to workshop participants on future needs and challenges for the electric power industry. He reflected that this could be a major change in the electric power industry and that significant changes have typically required 40–50 years to become standard operations. His early contribution to the project has guided the team to the design of what amounts to a new component for future electric power systems.

1.1 Historical Background

Shortly after the beginning of the twentieth century, the use of dc for electric power transmission was largely replaced by ac. The reason for the change was that achieving efficient transmission of electric power over long distances with conductors made of normal metals requires the use of low currents and thus high voltages, whereas safety issues for residential and commercial use demand a low voltage. This difference is easily achieved by ac transformers, so ac power systems proliferated. There are, however, individual choices involved in the selection of voltage and frequency for ac power systems. Thus, two electric power systems that are physically

adjacent might use different frequencies. In addition, for reasons of security and stability, it might be desirable for two adjacent systems that use the same frequency to be isolated and yet have the capability of exchanging power [1]. Thus, although ac power became the norm, dc power was not completely abandoned, because a dc element provides an effective and efficient interface between two independent ac systems. For example, the Eel River back-to-back dc converter station connects Hydro-Québec's power generation capacity with other transmission systems in North America. The back-to-back converter uses silicon-controlled rectifiers (SCRs) that exchange power between the two systems through a common dc bus. Eel River was commissioned in 1972 and was the first of its kind in the world. Such converters are common today.

Notwithstanding the rationale for an ac power grid, the use of high voltage dc for long-range transmission is, in many ways, more desirable than ac. For example, two wires are used for dc rather than three for ac, the conductor for dc can be simpler than one for an ac system, the dc line does not need capacitive elements to cancel the inherent inductive behavior of ac lines, and the earth can act as one of the current-carrying elements. As a result, dc has been used for several long-distance high-power transmission lines—both overhead and underground (or undersea). In each case, the selection of dc has been based on an economic comparison with ac for the same power corridor. The typical case in which dc has been chosen is for distances that exceed the *breakeven length*, which is the distance at which the lower cost per kilometer of the dc line more than compensates for the additional cost of the ac–dc converters at each end of the line. Bahrman and Johnson recently published an understandable description of the present status of high-voltage dc technology [2].

The ever-increasing use of electric power and the continuing improvement in superconducting materials (zero-resistance materials) suggest that a very high power superconducting dc cable might be an effective component of an electric power system. Thus, the concept developed here is based on the use of superconductivity in a dc power cable. This effort was preceded by several other explorations of superconducting dc systems. Perhaps the earliest relevant work in the area was an assessment of massive power transfer in a superconducting dc cable by two physicists, Garwin and Mattisoo [3]. In 1967, they evaluated the possibility of transferring 100 GW in a single dc power cable. Their plan was to use the recently discovered superconducting compound Nb₃Sn and to operate at about 4 K. Of all the elements, only helium remains a liquid at that temperature, and helium coolant is incorporated in that design. The depth of their work was limited, and engineering details of the cable were not addressed.

A few years later, Bartlit, Edeskuty, and Hammel, three engineers from the Los Alamos Scientific Laboratory (LASL), advanced a more practical power transfer system [4]. Their scheme recognized the limitations and advantages of the flow of cryogenics and combined multiple fuels as liquefied coolants with a superconducting dc cable. In particular, they incorporated the use of liquid hydrogen. At the time, liquid hydrogen was primarily used as a fuel for spacecraft operating beyond the earth's atmosphere, and there was also an effort to use it as the fuel for large commercial jetliners. Then as now, one of the major limitations of the use of hydrogen as a fuel was the need to develop an infrastructure for its delivery.

A short time later, the LASL team proposed the development of a superconducting dc cable. Over the next decade, a group of scientists at LASL worked on scientific and engineering details of such a system [5]. The results showed that a superconducting dc cable could be built and made

to operate within a large ac power grid. One conclusion at the end of the program was that further developments in superconducting materials would be necessary in order to achieve a practical device. In addition, a financial analysis indicated that a superconducting dc cable operating with liquid helium would be an expensive solution. By far the biggest issue with operation at liquid helium temperatures is the combination of capital and operating costs associated with maintaining the operating temperature. Heat flow into a cryogenic system occurs by a variety of mechanisms and cannot be completely avoided, even with the best of designs. Any heat that enters a cryogenic environment must be removed with a special refrigeration system. Approximately 500 W of electric power is required to run a refrigerator for each watt that enters the 4 K temperature environment. At the time of the LASL dc cable work, ac–dc converter systems were based on SCR technology. These converters required special control systems or an exceptionally strong ac power grid or both to convert the dc to ac at the receiving end of a cable. In addition, individual SCRs were limited to currents of a few hundred amperes. Both of these constraints have disappeared in the almost three decades since their pioneering work.

The discovery of high-temperature superconductors by Bednorz and Müller in 1986 opened a new perspective for superconducting power applications [6]. The main stimulus was the reduced energy cost associated with operating a refrigerator at a higher temperature. Instead of a factor of 500 for the refrigerator's power requirement, the factor is only 15 or so at 77 K and less than 20 at the design temperature of 66 K that was chosen for the present program. This amounts to an improvement by a factor of 25 in a critical part of the system.

In parallel with the development of superconductors, ac–dc power converters evolved with the development of higher-current and higher-power silicon-based devices. The SCR has been supplemented by other silicon devices that can be controlled directly to open and close, thereby providing precise control of the current. In addition, some control schemes now allow ac–dc converters to operate in a rapid switching mode, which allows the converter to pattern the outgoing power to match the variations in the current and voltage of the receiving power grid. The result is that harmonic distortion of the power is reduced and the filters required are considerably smaller.

The next relevant efforts in the process leading to this project were the SuperCity and SuperGrid concepts introduced by Grant and Starr, respectively, in 2001 [7–9]. These concepts combined liquid hydrogen flow and a superconducting dc cable. It was never developed to an engineering design, but the SuperCity concept was put forward as a complementary development for large scale and integrated power systems. The SuperGrid is the parent of the present program to develop a long-distance, high-power superconducting dc cable system.

1.2 The Superconducting DC Cable Program

The superconducting dc cable is separate from and considerably less ambitious in scope than the SuperGrid. It can be considered on its own merits, without the further development to a hydrogen-cooled system as envisioned in the SuperGrid. It is viewed as having a nearer-term payoff and, in this program, has been taken to a level of engineering design at which the team is confident of the practicality of the concept and its readiness for commercial development. In the initial 2005 EPRI workshop and a follow-on meeting, the discussions covered a variety of topics, but the focus was determining the optimum power capacity and optimum length of a superconducting dc cable. There were two rather different opinions as to these variables. One was that an intraregional cable operating at up to 2 GW and 300–500 km in length could find commercial application. This cable has power capacity much like the 765-kV power lines in use today. The second concept was an interregional cable that would carry 10 GW over a distance of 1000 km or more.

Transmission systems with 2–10 GW power capacity will integrate large electric power grids and will be optimally effective only if they have multiple power connections over long distances. That means that there must be several power sources and several loads. This functionality will be a generally new development for dc cables and lines. In particular, multiterminal operation has significant implications for the control algorithms that govern the converters on the cable and for the interface with the surrounding power grid—particularly when the transmission line (cable) is superconducting. The cable can be thought of as a store of energy that can be extracted at will, but that is somewhat simplistic because a voltage gradient is needed to achieve and control power flow along the cable from one location to another. Although the possible application of these high-power superconducting dc cables can occur in many places, the most likely current location for such a system is in North America, where large distances separate highly electrified regions, as well as some potential future generation resources, and some interconnection already exists.

From the beginning of the program, reliability and availability were paramount in the thought process of the development team. There are many aspects of this approach and they are discussed in some detail in the various sections. However, a critical decision was to design for full redundancy in the cable system. To achieve this goal, each circuit would have two cables in parallel, each of which would have the full 10-GW power capability. During normal operation, each would carry approximately half of the power. If there were a limitation of one cable, the other cable would act as a reserve to carry the total load. The major impact of this choice falls not on the cable design but rather on total cost, which is yet to be explored, and on the end station ac–dc converters and how they can be switched from feeding two cables to feeding one. Although the development effort has been based on the assumption that loss of a line carrying many gigawatts has the possibility of causing cascading failure of the ac system, the results of a subsequent study commissioned under this program have suggested otherwise, at least in some sections of the continent (see Section 2.5, *The Superconducting DC Cable with Multiple Local Connections to the Grid*, for details).

Both interregional and intraregional systems became part of the program, but emphasis was placed on the higher-power, interregional cable, which, as expected, has proven to be the more challenging. It is this interregional cable that is described in this report. The nominal current and

voltage selected to achieve 10 GW is 100 kA and 100 kV, although other combinations are possible. Perhaps the biggest challenge seen in the development to date is designing the fabrication process to produce conductor bundles that can carry 100 kA. The insulation level of 100 kA is easily achieved with currently available insulation schemes. In fact, the voltage level is so low that insulation thickness is determined by structural capabilities and ruggedness rather than by voltage standoff capabilities. A higher voltage could be readily achieved and would help meet the challenges posed by the high current. However, the advantages of keeping the voltage as low as possible (such as ac connection to urban sub-transmission-voltage systems without the need for voltage transformation; improved reliability of splicing joints, smaller-diameter cable, resulting in more cable on shipping reels; and fewer splicing chambers, leading to lower costs and higher reliability) are not to be ignored. By setting the bar high, researchers hope that the result will be continued motivation for the industrial research and development needed to produce very high current conductor bundles. High-power transmission at relatively low voltage is a hallmark of superconducting power transmission systems, both ac and dc, and is a key component of their economic viability.

It is clear from the cable cross section shown in Figure 1-1 that a great deal of the superconducting dc cable design is based on the extensive development of underground cables over the last century. That base is supplemented by applying recent developments on prototype superconducting ac cables, some of which are presently installed and operating daily.

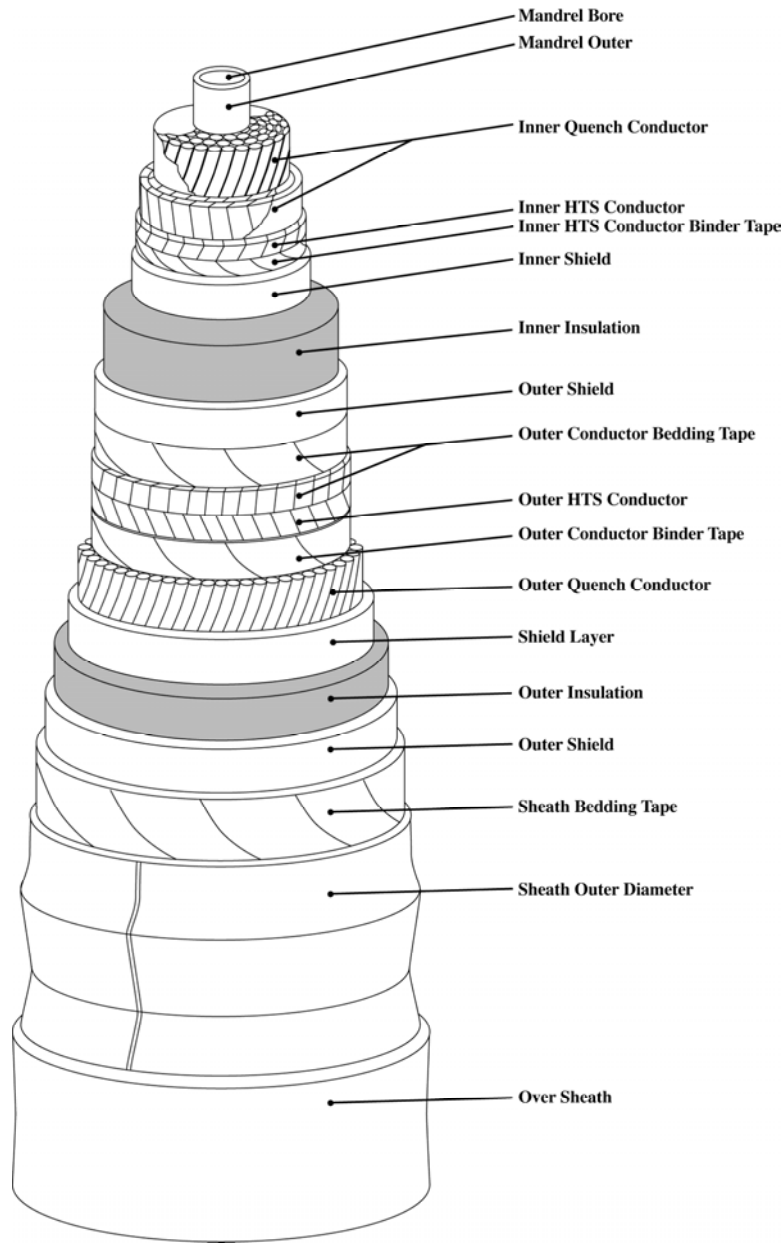


Figure 1-1
Cable cross section

1.3 Report Outline

This report consists of the following sections that describe the various aspects of the superconducting dc cable:

- Section 2 addresses what is perhaps the most critical aspect of the cable, the way in which it will interact with an existing ac power grid. There is no intention in this project of having the cable act as a point-to-point power transfer system. Rather, it is designed to function with bidirectional power flow and to incorporate multiple power nodes for feeding power into the cable or extracting it for local use.
- Section 3 describes the status and capabilities of superconducting materials, including commercially available materials that could be used in the proposed cable. Several materials might be considered for a superconducting dc cable, and research is still under way for future, large-scale systems. At this time, most of the effort toward a practical superconducting wire for the superconducting dc cable is in the area of improving the fabricated material so that it can carry sufficient current in the presence of the approximately 1-tesla magnetic field that will occur within the cable. In addition, the lowering of cost through mass production methods continues, with recent progress exceeding government and industry goals.
- Section 4 describes the design of the cable core. The cross section of the superconducting cable looks much like that of a conventional cable, and the fabrication process is similar. However, there are more individual conductors and additional layers to accommodate the peculiarities of all superconducting materials, and the cable design must allow for cooling to cryogenic temperatures in operation.
- Section 5 describes the vacuum insulation process, the practical issues of maintaining a vacuum along a 1000-km section of cable, and the reliability aspects of segmented, permanent vacuum sections. To achieve a low heat flow from ambient conditions to the cryogenic environment of the superconducting dc cable, it is necessary to have some form of thermal insulation. Vacuum with multiple layers of aluminized Mylar film forms the best-known thermal insulation. It is about five times as effective as any other known insulation and is about 50 times as good as the typical fiberglass used in a house.
- Section 6 describes the design choices made for the cryogenic system. The operation of large cryogenic systems is well developed by the industrial gas community. As a result, the design of the cryogenics for the superconducting dc cable is rather straightforward.
- Section 7 describes the functionality and topology of the end stations and converters along the length of the cable. It includes a description of the harmonics that will be produced by the stations and will exist for some length along the cable itself.
- Section 8 describes one possible scenario for system fabrication and installation. The approach uses many of the procedures that have been well developed in the installation of high-pressure gas pipelines—a commercially mature enterprise. This section also describes special considerations for the use of vacuum for thermal insulation.
- Section 9 describes the future work needed in order to develop the superconducting dc cable to a practical technology for use on an electric power grid.

- Section 10 contains a list of references.
- Appendix A defines the acronyms and abbreviations used in this report.
- Appendix B contains a previously unpublished report that was developed for EPRI in 1996, *System Study of Long-Distance Low-Voltage Transmission Using High-Temperature Superconducting Cable*. It describes a point-to-point, 5-GW, superconducting dc cable that was designed to operate between a source of energy—such as a farm of nuclear power plants or a large oil or coal field—and a population center, at a distance of 1600 km.
- Appendix C is an update of the cost analysis provided in Appendix B. It is a conceptual engineering-level cost estimate, based in part on the understanding developed in the current program and incorporating appropriate contingencies to account for final design development. Although it is not the major focus of the present program, this cost estimate is believed to be the best publicly available cost estimate today for a large-scale superconducting dc cable system.

2

AC GRID INTERFACE AND CABLE SYSTEM DRIVERS

2.1 Vision: Reinventing the North American Transmission System

Two major challenges faced by the power grid in North America today are the needs for enhanced transmission system capacity and improved control. It will be seen that the superconducting dc cable has the ability to provide both. Increasing the overall power capacity of the grid will require the addition of transmission lines using one or more of four technologies: overhead, high-voltage ac lines; overhead, high-voltage dc lines; underground, high-voltage dc cables; and underground, superconducting dc cables. (Underground ac cables are not suitable for long-distance, high-voltage power transmission, due to high reactive power consumption.) Improving control of the grid will involve a suite of different technologies and approaches, including the use of wide area phasor measurements, flexible ac transmission systems (FACTS), and ac–dc–ac transmission links, one form of which are the back-to-back dc converter links used to interconnect the five major North American ac grids, which are not synchronous with one another.

A common approach used by utilities today to achieve increased power levels over existing or planned transmission corridors, and one with which they are both comfortable and familiar, is to increase the ac transmission voltage. This is simply a variation on a well-developed theme. Multiple interconnections are easily accommodated, but control of power flow paths can be an issue, particularly in deregulated power markets, which leads to the potential for serious voltage problems and even system collapse. For long lines, the need for reactive power compensation is a significant cost and operations burden. Although high-voltage ac transmission is, and will continue to be, the norm for increasing power flow in the near term, it has undesirable characteristics that are increasingly coming under public scrutiny. These characteristics include the substantial right of way required for the power corridor, the notable and sometimes objectionable visibility of high transmission line towers, and the need for physically large substations to accommodate the high-voltage components. It is also difficult, if not impossible, to terminate these lines in the dense urban load centers whose power needs they feed.

As an alternative, high-voltage dc lines are effective for transmitting massive amounts of power over long distances, and they are generally more efficient than ac lines. Furthermore, they are ideal for providing control within an ac system, due to the inherent controllability of the ac–dc converters that interface the lines to the ac grid. A number of long-distance, high-power, overhead dc lines are used in several locations around the world. The equipment to convert from ac to dc and then back to ac constitutes a significant cost adder. Even so, for long distances, a high-voltage dc line is generally less expensive than an equivalent ac line. However, unlike ac lines, dc lines typically carry power only along a specific, single power corridor, without interconnections along the way (that is, they provide only point-to-point service). They share

with high-voltage ac the public concerns about right-of-way, substation size, and urban termination issues, although to a reduced extent due to their reduced number of conductors (two instead of three). High-voltage dc transmission is increasingly being used around the world, particularly for bringing massive quantities of remotely generated energy to dense population centers.

When high-voltage dc overhead lines are compared to conventional ac lines, a major factor in deciding which of the two technologies to use in a specific installation is the *breakeven distance*—the length at which dc becomes less expensive than ac, which occurs when the lower cost per unit length of the dc line more than compensates for the cost of the ac–dc converters at each end of the line. Other factors notwithstanding, the dc line would be chosen for corridors longer than this distance, and the ac line would be chosen for shorter applications. In general, this is a rational first approach to selecting the optimum technology.

High-voltage dc underground cables using conventional conductors (such as copper) with voltage source converters (VSCs), instead of the current source converters (CSCs) used by overhead dc lines, are a relative newcomer for land-based applications. (High-voltage dc submarine cables using CSCs are a well-developed and mature technology.) Like overhead dc lines, underground dc cables also provide inherent control to the interconnected ac system via their ac–dc converters (in fact, even greater control flexibility than overhead lines because of the different converter technology used). Land cables promise to mitigate visibility and siting issues of overhead lines and to deliver power reliably at multiple off-ramps. However, voltage ratings for land cables (as distinct from submarine cables) have not reached the levels of their overhead line counterparts. Thus, power transfer over conventional dc cables equivalent to that available from overhead lines would require multiple circuits, increasing costs for a technology that is already generally more expensive to install than an overhead line. Underground cables offer greater reliability, having greater protection from natural and man-made catastrophic events, but usually require a lengthier repair period that reduces their availability in comparison to overhead lines, which are relatively quickly repaired.

Superconducting dc cables are the focus of the work described in this report. The promise of this technology is that it will provide many of the advantages of conventional high-voltage lines without some of the disadvantages. In this respect, a superconducting dc cable has the following:

- The massive power transmission capability of conventional high-voltage ac and dc lines
- The efficiency and cost advantages of high-voltage dc lines (although it has even lower losses)
- The multiple-interconnection capability of high-voltage ac lines and underground dc cables with VSCs
- The unobtrusiveness and higher reliability of underground dc cables
- The system control features of dc transmission lines and links

Key to understanding the advantage of a superconducting dc cable is the realization that the cable itself (excluding the converters) has essentially no electrical losses. This means that the energy lost in transmitting power is completely independent of the amount of power transferred. This is quite unlike the situation for all other means of high power transmission, for which losses

increase with power transmitted. For overhead lines, the resistive component of these losses is roughly proportional to the square of the current and corona losses are proportional to voltage. In addition, for ac lines, the reactance of the line causes the current and voltage to be out of phase. This is referred to as *reactive power consumption*. It causes ac currents (and hence, losses) to increase because the reactive power consumption is added to the real power transmission. The exact losses in a superconducting dc cable will depend on the engineering approach and specific design details. However, above some suitable, high power level (>2 GW), the percentage losses in a superconducting dc cable will be substantially less than those of any other means of transmission. Thus, the higher the power that is transferred, the more desirable this technology becomes.

For ac applications, superconducting cables are practical only for distances of a few tens of kilometers. The need for numerous shunt reactors spaced at close intervals along ac cables for reactive power compensation, as well as the cryogenic power requirements, preclude the use of superconducting ac cables for high-power, long-distance applications.

Eventually, it will be necessary to establish a figure of merit for comparing a superconducting dc cable with conventional transmission lines. That figure of merit might be similar to the breakeven distance that is used to compare ac and dc lines, but it is likely to be considerably more complicated. Finding a good metric will require considerably more information than is available today about the transmission system that will be in place 20 or so years from now as well as some unknown amount of research on the technology itself. For example, it is not clear how the trade-off will be affected by voltage, current, and power levels. On the cost side, the ac-dc converters will play a relatively minor role because their cost will be roughly proportional to the peak power and will depend little on the selection of current and voltage. The cost of the cable itself will be influenced by many factors. For this conceptual design, we assume that, at some time in the future, there will be a need for a highly interconnected electric power system in North America and that a major component of the interconnection will be a gridwork of superconducting dc cables.

2.2 Existing DC Links and Lines

The use of dc transmission, including both transmission lines and back-to-back dc links, is enjoying an unprecedented growth worldwide. Extrahigh-voltage overhead dc lines, longer and higher-power dc submarine cables, and back-to-back converter installations that interconnect asynchronous ac systems are being proposed and built at an increasing rate. This growth is being fueled partially by demand for power—particularly renewable power—from remote regions as well as by the growing interdependence of electricity markets in which dc interconnections provide the most reliable means of exchanging power across political, geographical, and electrical boundaries. The increasing dependence on dc transmission bodes well for the eventual deployment of superconducting dc lines.

There are dozens of back-to-back dc links around the world, many of which are in North America. The term *back-to-back* refers to the fact that two converters are associated with each dc link—one changes ac to dc, and the other changes it back to ac. The dc section isolates the two

systems on either side of the link. These systems can be at the same frequency but not synchronized, or they can operate at different frequencies with the receiving systems controlling the relative magnitudes of real and reactive power.

The North American links include installations such as Eel River, which partially isolates Hydro-Québec's power grid from other areas to the south and west and provides asynchronous power flow from the hydropower available in Québec mainly to the United States. A few dc links interconnect the three major electric grids in the 48 contiguous United States: the Eastern Interconnect, for states east of the Rocky Mountains; the WECC (Western Electricity Coordinating Council), for states west of the Rocky Mountains; and ERCOT (the Electric Reliability Council of Texas) for substantially the state of Texas. These are mostly modest installations of a few hundred megawatts (with a total capacity of only about 1 GW).

Worldwide, there are a number of high-power dc transmission projects in operation and a growing number proposed or under construction. Among these are the Pacific Intertie and the Intermountain Power Project in the United States, the Itaipu system in Brazil, and the Three Gorges project in China.

Power flow along the Pacific Intertie is generally from north to south. Hydroelectric power from the Pacific Northwest of the United States and parts of British Columbia is converted to dc at the northern terminus of the Intertie and transmitted to Southern California. The Pacific dc Intertie originally used mercury arc diodes at the northern terminus. These were converted to conventional thyristor valve technology in several stages. The first step was a modest addition of 50 MW in 1977. This additional power was specifically for control purposes. It allowed the Pacific Intertie to damp oscillations that had been observed on the existing ac interconnection between the Pacific Northwest and Southern California. Under certain conditions of high power demand in the south, these oscillations limited power flow on the ac lines to about half their capacity [10, 11]. Success of this installation and improvements in SCR technology eventually led to the complete replacement of the mercury arc valves. Today, the Pacific Intertie operates at 500 kV and has a power rating of 3100 MW.

The Itaipu dam is on the Parana River between Brazil and Paraguay. Power from the dam is shared by Brazil and Paraguay. At present, Paraguay does not use its entire share of the power, so that excess power is sold to Brazil. However, the generators at the dam produce power at the frequency used by the owning country. Paraguay's generators operate at 50 Hz, whereas Brazil's operate at 60 Hz. For power from Paraguay's generators to be used by Brazil, the frequency must be converted from 50 Hz to 60 Hz. This requires two converters with a dc link between them. Because there is no incremental cost for the converters, and because the per-kilometer cost of high-voltage dc lines is less than that of high-voltage ac lines, in this unique case in which back-to-back converters must be used in any event, the breakeven distance is zero kilometers. Thus, a high-voltage dc line is clearly the most economical solution, and it was chosen as the means of transmitting this part of the power from Itaipu to the load centers of Rio de Janeiro and Sao Paulo. The power rating of the dc line is 3100 MW at 600 kV and 2.5 kA.

The Three Gorges dam on the Yangtze River in China will be the largest dam in the world, and even though the entire power generation capability has not been reached, it already produces more electric power than any other hydroelectric installation. Construction of the dam began in

1994, and all of the originally planned civil and power generation capability was completed in 2008. This is an impressive feat for a dam whose primary justification was flood control. Power from the dam will be delivered to load centers by both high-voltage ac lines and high-voltage dc lines.

Power from the dam is sent in three directions: 12,000 MW is carried on several 500-kV ac transmission lines to Central China; 7200 MW is carried on three 500-kV dc transmission lines to the East China Grid; and 3000 MW is supplied through one 500-kV dc transmission line to Guangdong.

2.3 Interaction of DC Cables and Lines with Ground

High-voltage dc transmission can be either bipolar or monopolar, referring to the disposition and connection of the transmission line conductors. In a bipolar configuration, the two conductors (poles) operate at equal and opposite polarities with respect to ground, and the current circulates around the bipolar circuit. In this configuration, there is no need for a return current path. In a monopolar configuration, only a single conductor operates at a potential that is significantly different from ground. This single conductor is used for the transmission of power. Either a second metallic conductor (ground conductor) provides a current return path, or the earth itself (through an anode–cathode earth contact system) can be used for the return. In the case of undersea cables, the sea can provide the ground return through a similar anode–cathode contact system. Monopolar systems are more cost effective than bipolar systems at power transmission levels up to approximately 600–800 MW [12].

With respect to the return current path, one significant difference between the superconducting dc cable and a high-voltage dc transmission line is the operating current. The superconducting cable is expected to carry up to 100 kA, whereas the conventional high-voltage dc line carries at most a few kiloamps. The result is that an earth current return option is not possible with the superconducting dc cable. For example, the effective resistance of an earth–sea ground is about 0.3Ω , which causes a voltage drop of a few kilovolts if it is used to carry the entire current in a transmission cable or line with conventional conductors. This is similar to the voltage drop in the wires themselves. However, in the case of the superconducting dc cable operating at 100 kA, the voltage drop if the current went through the ground would be tens of kilovolts. The power absorbed (the losses) would be a significant fraction of the total power capacity of the cable. In addition, such a high ground current could be a potential hazard. As a result, every effort must be made to fully isolate the cable system from ground except at one single node.

2.4 Converter Technology

Converters come in a variety of configurations and can use several different types of components, depending on the application. Today, the switching elements in most high-power converters are thyristors or silicon-controlled rectifiers (SCRs). They are installed at each end of most dc links and are about 99.35% efficient at maximum power. However, their efficiency at any moment depends on the power level—the lower the power, the lower the efficiency. Converters of this type typically require a strong ac system at the connection to the ac grid, where the reversing voltage in the grid forces them to turn off (commutate) the current in each

SCR near the zero voltage crossing of each cycle. Gate turnoff devices (GTOs) and insulated-gate bipolar transistors (IGBTs), on the other hand, do not need the ac grid to turn off; rather, the current is turned off by a separate signal to one layer of the semiconductor in the device. Thus, GTOs and IGBTs are more likely to be elements in converters that feed power into a weak ac system (that is, VSCs; see the next paragraph). There is, however, a drawback to these devices. The voltage drop across a GTO when it is carrying current is much greater than that of an SCR. As a result, converters based on GTOs are only about 98.4% efficient. In addition to the ability to feed into a weak system, converters based on IGBTs can operate at much higher frequencies than the fundamental. As a result, the harmonic currents on the dc side of the circuit can be controlled to a high degree. Reducing the amplitude of the harmonic current will permit the use of smaller filters and reduce the amount of heat generated in the superconducting dc cables.

There are two principal converter topologies: VSCs and CSCs. (They are described in Section 7, End Stations and Converters). Both types convert ac to dc and dc to ac. However, they are quite different in terms of operation, controllability, and overall functionality. Existing point-to-point dc transmission (overhead lines and submarine cables) use CSCs almost exclusively. VSCs are used for a variety of applications, such as variable-speed motor controllers, and are critical components of FACTS devices. The VSC-based dc cable for land and sub-sea applications, incorporating cross-linked polyethylene (XLPE) insulation, was introduced in 1997 [12]. This resulted in the implementation of several underground cable projects using VSCs, the most notable of which is the ± 150 kV, 220 MW Murraylink Project (Australia), which was installed in 2002. The route length is 112 miles (180 km), which is to date a world record for long-length underground cable installations. VSCs have not been desirable for use with overhead lines because of their susceptibility to failure due to line-to-ground faults, to which overhead lines are frequently exposed (for example, due to lightning or tree branch contact). However, VSC systems may become available for overhead lines when suitable means of protection are developed. Although less efficient than a CSC, a VSC offers greater controllability in its interface to the ac grid (such as its ability to control reactive power and voltage in the ac system) as well as the possibility for multiple on and off ramps (see Section 7, End Stations and Converters).

A single-phase, two-level VSC is shown in Figure 2-1. The dc voltage is constant and independent of the dc current because the superconducting cable has no voltage drop. Pulse width modulation techniques can be used to control the real and reactive power delivered to the ac system. In such a converter, the ac voltage is synthesized by varying the current amplitude and the phase angle of the ac current. This is often referred to as *four-quadrant control*; it enables full control over the phase current flowing into (or out of) the ac system.

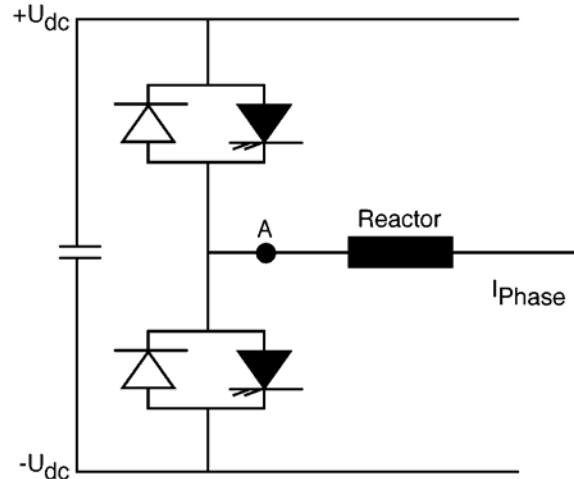


Figure 2-1
Single-phase, two-level voltage source converter

2.5 The Superconducting DC Cable with Multiple Local Connections to the Grid

A critical component of a large grid is the ability to feed power into and extract power from the system at many locations. One characteristic that is crucial for this functionality is the ability to change the direction of the power flow at many different nodes. The VSC provides this capability in a manner that is compatible with both conventional XLPE cables and superconducting cables—it can reverse the power flow by reversing the direction of the current. (Rapid voltage reversal in a dc cable can lead to insulation failure with certain types of insulation.) Consider, for example, a 200-MW VSC connected to a superconducting dc cable operating at 100 kV with a local current of 40 kA. If the local grid requires power from the cable, a current of up to 2 kA dc can be extracted from the cable and converted to the appropriate three-phase ac current. The VSC can be controlled so that the current in each ac phase will be in phase with the voltage of the local grid. The current beyond the converter on the superconducting dc cable will be reduced to 38 kA. Equivalently, the converter can extract less current from the dc cable and deliver ac current that is not exactly in phase with the local grid voltage. Thus, the VSC can provide both real and reactive power as required. If, at some other time, the local grid requires less power than is generated nearby, power can be delivered by the local grid to the dc cable. If 200 MW were to be delivered to the cable, which is again carrying 40 kA, the current in the superconducting cable beyond the converter station will increase to 42 kA.

Possibly the most effective configuration for connecting the superconducting dc cable to the grid is to use a combination of CSCs and VSCs. Where the cable is connected to a source of power such as a single large generator or a wind farm, a CSC will function perfectly well and would be the converter of choice because it is more efficient. Complete power control is not needed at a site whose sole purpose is power injection. The CSC can provide power flow in both directions, but it requires an additional reversing switch. This is an effective solution when the power flow reverses infrequently, which is the case for the injection of power on the Pacific Intertie. Power typically flows from the Pacific Northwest to Southern California, but it can be reversed in the

evening when there is more than adequate power available from sources in California, Arizona, and Nevada. This reversal helps maintain the water reserves in the Columbia Basin and in southern British Columbia.

A system using VSCs requires keeping the voltage across the cable fixed and reversing the current in order to reverse the power flow. The maximum allowable rate of current change depends on the inductance of the cable, the losses in the superconductor associated with the changing current, and other limits determined by the conductor and the overall cable design.

The simplest and possibly the most effective solution would be to use CSCs at the generation nodes on the line and VSCs at nodes at which power is extracted from the cable and injected into an ac system, particularly where power flow reverses frequently. This removes the problem of ac voltage support at the receiving ac system because VSCs can control the ac voltage and power flow. In addition, the VSC allows for *black start* (the ability to provide power to restart the area of a blackout), which is an important advantage of a dc cable with multiple sources and loads.

A multinode system of the superconducting dc cable is shown in Figure 2-2. This figure shows six nodes, each of which has the ability to inject or extract power. The power capacities of the individual nodes are not indicated in the figure and are not necessary to understand the principle of operation. Consider for the moment a simple case in which power is injected into the cable at node 1 and some power is extracted at each of the other five nodes. In this case, a single, large high-power converter is needed near the site of generation, and several lower-power, and thus physically smaller, converters are needed at each node. One advantage of using multiple small converters is that they can be located nearer the load centers than could a large converter associated with a point-to-point power delivery system. In addition, both real and reactive power can be injected into the local ac system at the most advantageous location. This ability decreases the need for additional means of VAR (volt-amperes-reactive) compensation within the power system.

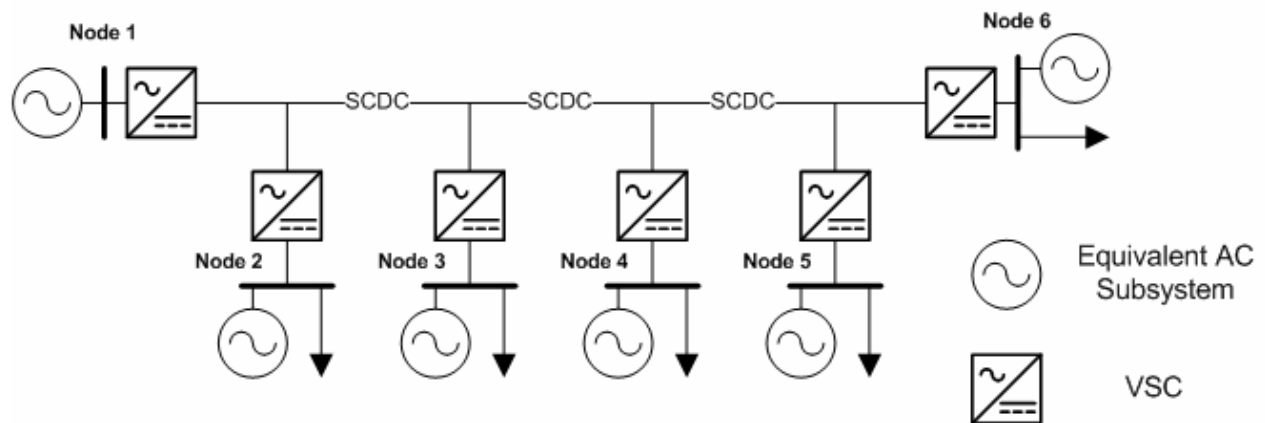


Figure 2-2
A simplified, six-node drawing of the superconducting dc cable as connected to various parts of the ac grid

The control system for the cable system shown in Figure 2-2 is similar in many ways to that for any grid that includes a major transmission line. Dispatch and scheduling must have some forward-looking plans for the total power needs at all nodes at any given time. This knowledge is converted into control signals to the generators connected to the cable, node 1 in this example. There must also be feedback mechanisms similar to those in conventional systems. In addition, the control system must provide power flow control signals to each node. This is somewhat more sophisticated than the controls needed for transformers and circuit breakers at the nodes of a conventional system. Part of the additional complication in control is the ability of VSCs to control both real and reactive power. However, conventional control technology will remain as an overriding element. For example, the need for spinning reserve (emergency power to offset the loss of a generating unit or major transmission link) will be equally important as it is in conventional systems. However, the sharing of spinning reserve will require reevaluation because the power ability of the dc cable will integrate wide geographic areas and will allow spinning reserve in one area to contribute instantaneously to system stability and help to limit voltage sag at all locations along the cable.

A potential downside of having many taps could be a decrease in overall reliability and availability. The converter at each small tap is likely to have the same reliability as does the large converter near the generation source, and so failure in any converter could impact system operation. One solution is to design a robust converter that has high availability and failure modes that do not impact operation of the cable itself or any other converter along the cable. In this regard, one possibility is to have a fail-safe configuration in which a failed converter automatically separates itself from the dc cable.

It is generally held that loss of a line carrying many gigawatts has the possibility of causing cascading failure of the ac system. This aspect has been investigated in a separate study, the results of which were published as the EPRI report *Study on the Integration of High-Temperature Superconducting Cables Within the Eastern and Western North American Power Grids* (1020330) [13]. The study showed that the power grid in the eastern part of the United States can accommodate the loss of a 10-GW superconducting dc cable and that the western United States grid can accommodate an 8.5-GW loss. This was not a sensitivity study, so these are not limits; it is not clear how much more power the dc cable systems could carry before some problem occurred.

2.6 Issues and Future Work on the Superconducting DC Cable

Loads will vary with time, and thus the power requirement will cycle. The superconducting dc cable must be able to follow such load variations. For a long-distance cable, the current direction could change over some cable sections as a result of short-term, daily, and even seasonal power flow changes. This is not considered to be an issue in the design of the cable, but an assessment of the effects of current direction changes must be an early task for the next stage of the program.

The operational case of a fault to earth (for example, an overhead line insulator flashover on the ac system) can cause a transient drop in voltage and double the ac current for up to 20 ms before the converter regains control. The design described in this report can accommodate twice the design current for a period of 0.5 seconds. Decreasing the time of a fault and the magnitude of the current would reduce the required size of the quench conductor.

In the case of a superconducting dc cable, a fault to earth on the high-voltage side would be a disastrous event with potentially disruptive violence. For example, an explosion and vaporization of components could severely damage the cable and take it out of operation for a long time. The design must accommodate the eventuality of dc-side faults and isolate the cable before it is damaged.

Traditional multi-terminal dc systems using CSCs have major control issues that limit them to three or four terminals. The basic problem occurs at each converter during transient events in which there is a significant, current-dependent dc voltage between terminals. If the superconducting dc cable has multiple power insertion nodes, each of which uses CSCs, this same control issue might become important. Because traditional CSC systems are complicated and need a carefully customized overall control scheme, this might well apply to a large and extended superconducting cable system, even though the expectation is that the dc voltage will be constant, or nearly so, on the superconducting dc cable.

Superconducting cables change several key system characteristics and will have a major impact on control options. There is no longer a current-dependent dc voltage drop. Voltage regulation sets a single voltage level for all the terminals, which can be keyed from one or a few crucial converters, probably those associated with major power feeds. However, transient changes in dc voltage will propagate rapidly throughout the dc system. It is expected that these transients could be used for control in a fashion similar to that of a change in frequency on ac systems.

The control systems for a multi-terminal VSC-based superconducting dc cable system must be fully assessed for all possible system conditions, events, and ac and dc faults. Although VSCs will no doubt have superior performance compared to grid-commutated CSCs, more detailed modeling and simulations must be conducted with multiple converters at the actual current and power levels proposed for the superconducting dc cable system. Superior VSC controls plus active and passive filtering can mitigate the challenging transients associated with the low ac resistances of superconducting dc cables. A start in this direction has been initiated with a study of the effects of transients on the cable and converter system, the results of which were published in the EPRI report *Transient Response of a Superconducting DC, Long Length Cable System Using Voltage Source Converters* (1020339) [14].

The practical issues of integrating a high-power superconducting dc link into the existing, lower-power ac transmission and distribution systems and the operation and control of the link are key to the viability, usefulness, and acceptance of the concept. It is likely to be necessary as part of the project to develop a plan to show how the ac network will radiate from the remote dc and ac terminals. Critical questions to ask about a high-power superconducting link are “What are the economic and operational trade-offs between carrying very high power on one cable versus deploying distributed resources and multiple, lower-power transmission lines?” and “Even if there were significant benefits, what are the system impacts of the loss of the single, large line?”

3

SUPERCONDUCTORS: PAST, PRESENT, AND FUTURE

Some of the information in this section is adapted with permission from “Superconductivity and Electric Power: Promises, Promises...Past, Present, and Future” [15].

3.1 General Properties of Superconductors

3.1.1 *Early Developments*

At the close of the nineteenth century, great advances in physics were under way. Maxwell had unified all the phenomenology of electricity gathered together by Faraday, Ampere, Henry, Oersted, Kirchoff, Ohm, Hertz, and Heaviside into four beautifully exquisite equations. Although it was unrecognized at the time, those equations contained the essential principles of Einstein’s coming formulation of the Special Theory of Relativity. In 1899, J. J. Thompson proved experimentally that the fundamental unit of electric charge was the electron and that its motion was the basis of electric current both in vacuum and in a metal. By 1905, Rutherford had guessed that the electron was also the basis of the structure of the atom and was responsible for all chemical reactions and bonding.

This period also witnessed major progress in practical thermodynamics, especially the liquefaction of most common and not-so-common gases. In 1908, Heike Kamerlingh-Onnes of the University of Leiden succeeded in liquefying helium at the incredibly low temperature of 4.2 Centigrade degree increments above absolute zero (4.2 K). His laboratory began extending measurements on the resistance of metals down to this new lower limit. It was by then well known that metals were peculiar in that their resistance decreased with lower temperature. At the time, most physicists expected that, according to the Rutherford picture, if a sufficiently low temperature could be reached, the electrons moving throughout the metal would “freeze out,” and thus the metal would become an insulator. A significant problem was that at very low temperatures residual impurities in the metal impeded the motion of the electrons and made interpretation difficult. Gilles Horst, a researcher in the Leiden laboratory, got the idea of measuring mercury inasmuch as it is a high vapor pressure liquid at room temperature and could be made extremely pure by multiple distillations before being cooled into a solid and brought to lower temperatures for electrical measurement. Much to his amazement, he found its resistance to totally disappear, rather fortuitously, at the boiling point of liquid helium (see Figure 3-1) [16].

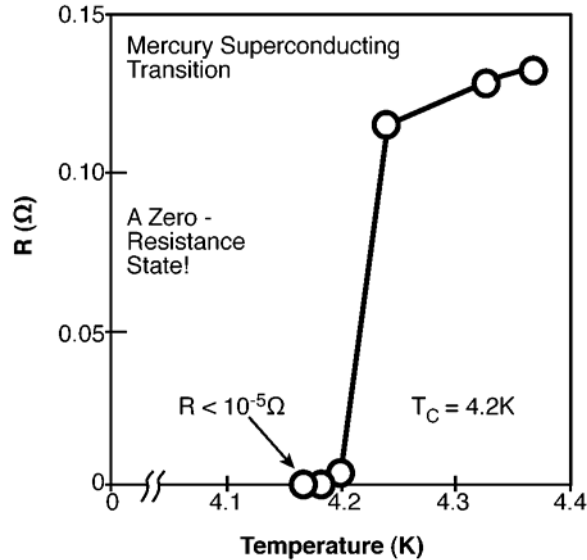


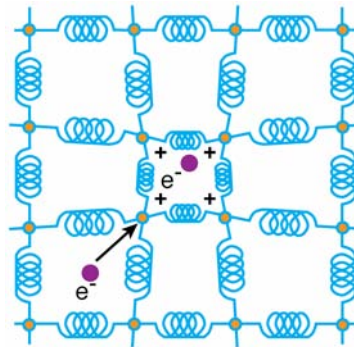
Figure 3-1
A replication of the original observation of zero resistance in mercury in 1911 [16]

A microscopic description of this remarkable phenomenon was attempted by the best minds of early twentieth-century physics without success. Clues arrived slowly. In the early 1930s, it was found that not only was an applied magnetic field excluded from penetrating a superconductor by virtue of its perfect conductivity but also a field that had been applied above its transition temperature was expelled as it cooled below this temperature. This was a key finding, as it established that a superconductor was something more than just a perfect conductor. Moreover, at about the same time, a jump in specific heat was observed to occur at the transition temperature. As with transitions in materials such as water at the freezing point, this suggested that a phase condensation of some sort was part of superconductivity. These experimental observations led to the empirical reformulation of the boundary conditions on Maxwell's equations for the case of fields applied to a superconductor, and most importantly, a macroscopic thermodynamic and phenomenological theory of the suspected superconductivity condensate. This latter development took place in the midst of World War II in the Soviet Union; it is now known as the Ginzburg-Landau theory. Today, it remains the most useful engineering tool for practical applications of superconductivity. A separate observation of early superconductors was that their ability to carry a superconducting current could be completely and abruptly destroyed by a modest magnetic field. As more materials were found to be superconducting, those with this characteristic were designated *type I superconductors*.

3.1.2 The Bardeen-Cooper-Schrieffer Theory of Superconductivity

In 1950, it was found that the onset temperature of superconductivity in mercury depended on isotopic weight. This discovery and subsequent measurements on other metals strongly suggested that atomic inertial mass, and therefore lattice vibrations, were a key ingredient of superconductivity. In addition, there were hints within the Ginzburg-Landau picture that the current-carrying elements had twice the charge of a single electron. In a brilliant, elegant, and amazingly simple exercise in quantum mechanics, Leon Cooper showed in 1956 that an arbitrarily weak, attractive interaction between electrons in a metal inevitably led to their pairing

(physicists refer to them as *Cooper pairs*) and suggested that their interaction with lattice vibrations, or *phonons*, could give rise to such an attraction. A crude picture of this model, along with the dependence of the transition temperature of material properties, is shown in Figure 3-2. The figure illustrates the phonon-mediated pairing of two electrons, shown as a lattice contraction resulting from one electron producing a locally positive region to draw in an additional negative charge. T_c is the onset temperature (or *transition temperature*) for this superconducting state. The parameters are θ_D , the characteristic temperature of a lattice vibration, and λ , the coupling strength of the electrons to the lattice. Their values for niobium are 275 K and 0.28, respectively.



$$T_c = 1.14 \theta_D \exp(-1/\lambda)$$

$$\theta_D = 275\text{K}$$

$$\lambda = 0.28$$

$$\therefore T_c = 9.5\text{ K (Niobium)}$$

Figure 3-2

A simplified view of the interaction between a phonon and a lattice in the Bardeen-Cooper-Schrieffer theory [17]

A year later, Cooper, along with John Bardeen and Robert Schrieffer, formalized this picture into the macroscopic quantum theory known as the *Bardeen-Cooper-Schrieffer* or *BCS* theory, which successfully united all previous empirical theories into a single explanation of superconductivity. In its broadest interpretation, the BCS model encompasses all known examples of fermion (such as electrons or holes) pairing mediated by a boson field (such as phonons). The terms *fermion* and *boson* honor Enrico Fermi and Satyendra Bose, who carried out seminal work on the different statistical forms of physical interactions. The pairing process has wide application, ranging from superfluid helium-3 to neutron stars. Theories of superconductivity are qualitative, not quantitative, in nature, providing essentially guides to the eye in their understanding. Today, this situation is beginning to change, and it is now possible to compute some properties of simple, high-symmetry, low atomic number metals such as aluminum and magnesium diboride as accurately as they can be measured.

3.1.3 Type II Superconductors: Technically Useful Materials

Most applications of superconductivity depend on the ability of the material to carry current in the presence of a significant magnetic field. Fortunately, superconductors come in two varieties, type I and type II, depending on their behavior in a magnetic field. The discovery of type II superconductors in the decades following World War II opened the door to the possibility of

significant and wide-ranging power applications. The difference in magnetic properties—and inferentially, current-carrying capacity—as a function of temperature between the two varieties is shown schematically in Figure 3-3. The phase diagram is characterized by two critical magnetic fields—a lower, H_{C1} , and an upper, H_{C2} . Below H_{C1} and at sufficiently low temperatures and fields, both types will completely shield an externally applied magnetic field. Moreover, both will completely expel an internal field of strength below H_{C1} that is applied above the critical temperature, T_c . In a purely type I superconductor (which most elemental materials are) this is all that happens— H_{C1} is a single critical field, H_c , which also primarily defines J_c , the maximum current density that such a superconductor can sustain. Typically, H_c is a few hundred oersteds, J_c is a few tens of amperes per square centimeter, and T_c is in the single-digit kelvin range, none of which is very practical for power uses.

A qualitatively similar diagram holds for critical current as the vertical axis. Figure 3-3 uses the modern notation, B , rather than the traditional H , as the applied field. For superconductors, this distinction is largely irrelevant; throughout this report, we use the notation H within the superconductor. *Normal state* refers to the usual high-temperature state of a metal, and *Meissner state* refers to the non-field-penetrating state, named for its discoverer. *Vortex state* is described in the next paragraph. The region in green is designated as a type II phase, and the region in yellow is a type I phase.

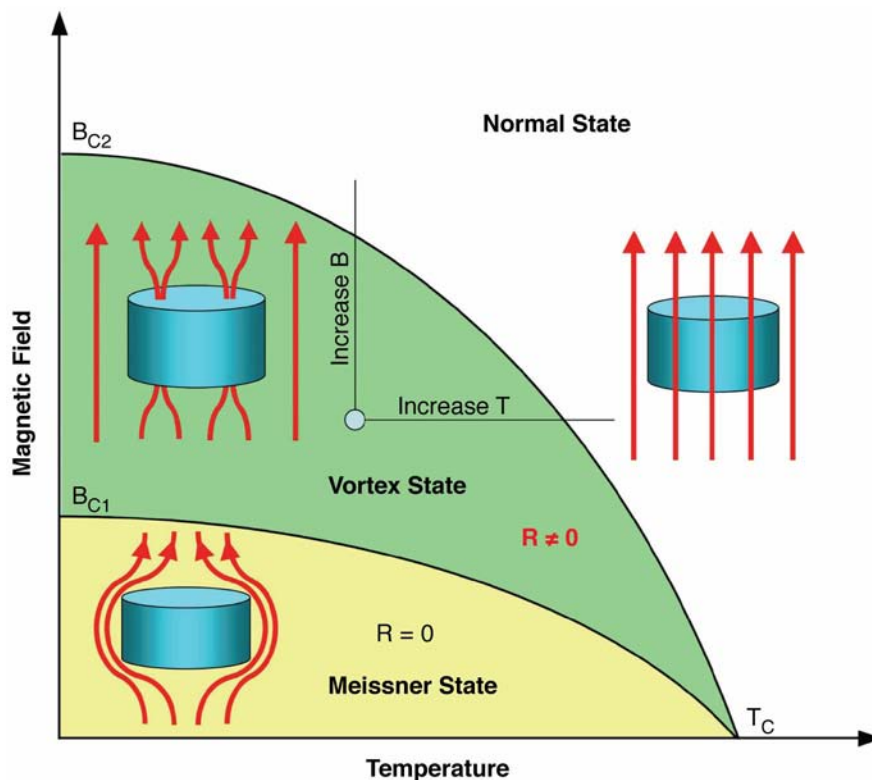


Figure 3-3
Phase diagram of a typical type II superconductor

Nearly all superconductors with $T_c > 10$ K are type II. In these materials, magnetic fields greater than H_c (H_{c1} in Figure 3-3) are neither completely expelled from nor completely pervade the volume of the superconductor. Instead, magnetic flux penetrates through many small tubes with a radius that is approximately the paired electron coherence length, ξ (roughly, the distance between the paired electrons or holes). The material in these tubes is in the normal state (see Figure 3-4[a]). If there are multiple nonsuperconducting columns, they are separated by a distance—the penetration depth, λ —that an applied magnetic field can reach before it is completely screened by Lenz's law. In fact, the ratio $\kappa \equiv \lambda/\xi$ essentially determines whether a material is type I (κ roughly less than unity) or type II ($\kappa > 1/\sqrt{2}$). Each tube, or *vortex*, contains one quantum of magnetic flux, Φ_0 , the collection of which forms a periodic lattice, the *Abrikosov vortex lattice*. As the applied field increases, so do the number of vortices until a field of order $H_{c2} \approx \Phi_0/\xi^2$ is reached at which the superconductor volume can contain no more and thus enters the normal state. For obvious reasons, the region between the lower and upper critical fields in a type II superconductor is called the *mixed state*. The value of H_{c2} at low temperatures can be as large as several hundred tesla (in a vacuum, 1 tesla is 10,000 oersteds; for reference, the earth's magnetic field is a few oersteds).

The determining factors of critical current density in the mixed state are complex and, by and large, extrinsic in nature. The vortices formed by the self-field of a flowing current are perpendicular to that current and thus experience a sideways Lorentz force that is perpendicular to the current and the vortex field and proportional to the magnitude of their vector product. This force produces vortex motion, which results in frictional energy loss and therefore electrical resistance. Thus, a type II superconductor in the mixed state fundamentally cannot transport electrical current losslessly. However, as the vortices move, some become trapped or pinned at various material impurities or defects. Figure 3-4 illustrates the vortex dynamics of a type II superconductor (a) in the mixed state, when the vortices dissipatively move under an applied Lorentz force, (b) when the motion of the entire vortex lattice is pinned by point defects, and (c) when the vortex is pinned by columnar defects. Both point defect pinning and columnar defect pinning can be operative in high-temperature superconducting (HTS) compounds.

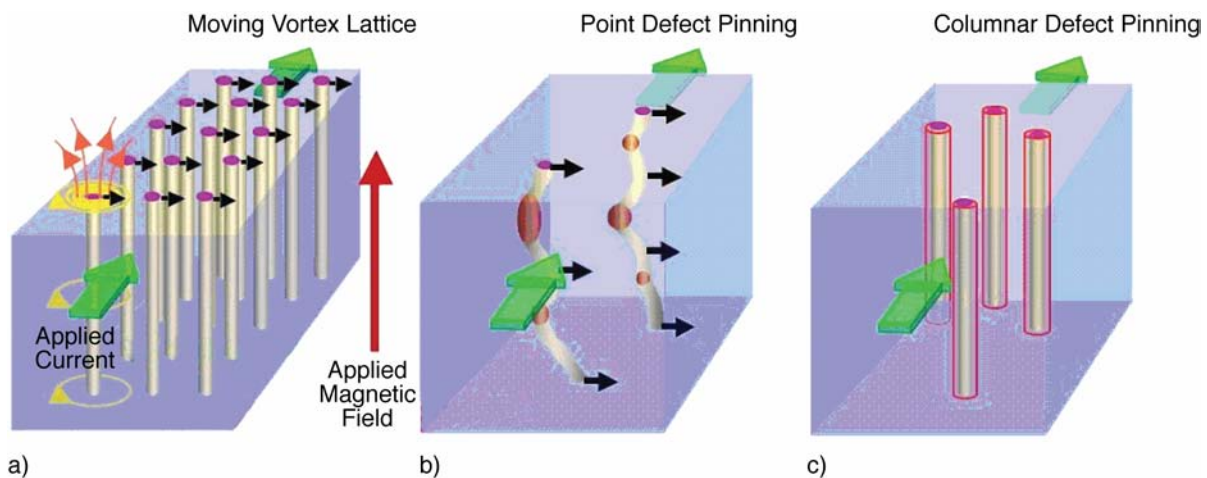


Figure 3-4
Illustration of the vortex dynamics of a type II superconductor

Due to the repulsive force between vortices, pinning a small fraction freezes the motion of the entire lattice and ensures a lossless state. This is true only for constant current and magnetic field and only below the irreversibility line (see Figure 3-5). The field at the irreversibility line is a function of temperature.

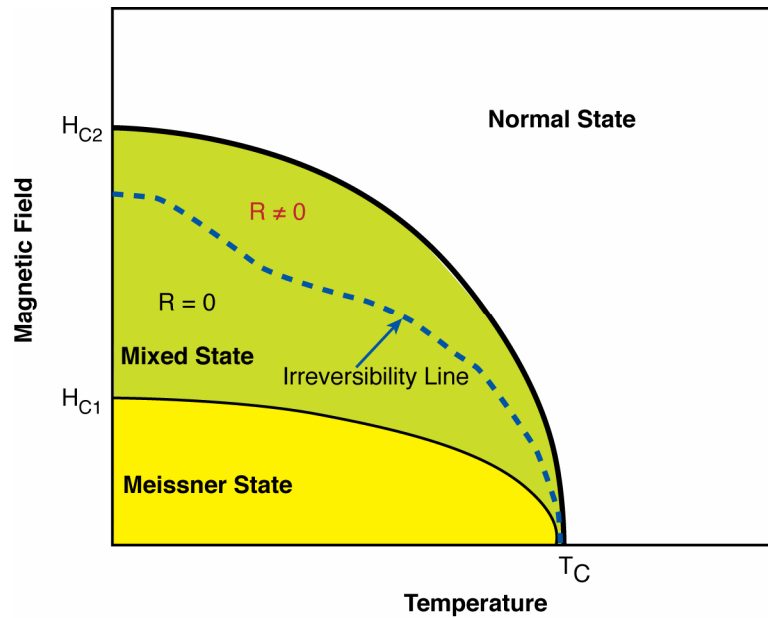


Figure 3-5
The irreversibility line

© 1997 IEEE; reprinted with permission [15]

The result of pinning the vortex lattice with defects is to restore a portion of the mixed state of a type II superconductor to perfect conductivity for fields less than the dipole or Lorentz force required to collectively de-pin it. The demarcation between these regions is the *irreversibility line*, defining a temperature-dependent usability field, H_{IRR} . Whenever one encounters field or critical current data versus temperature on a given compound or wire, what is plotted is H_{IRR} , not the upper critical field, H_{C2} .

Below H_{IRR} , upon current polarity reversal, some vortices remain pinned as the current passes through zero. Much like domain wall hysteresis in ferromagnets, the vortex lattice reappears each cycle in a geometrically different equilibrium. The thermal losses associated with vortex motion are proportional to the area within the loop. These vortices result in a trapped flux remaining in the superconductor, quite analogous to the remanent field of a ferromagnet. Thus, under alternating current conditions, a type II superconductor experiences hysteresis, which dissipates energy (see Figure 3-6), again similar to the same effect in a soft ferromagnet. Due to both vortex motion and hysteresis, transport of ac power in a type II superconductor in the mixed state is never lossless.

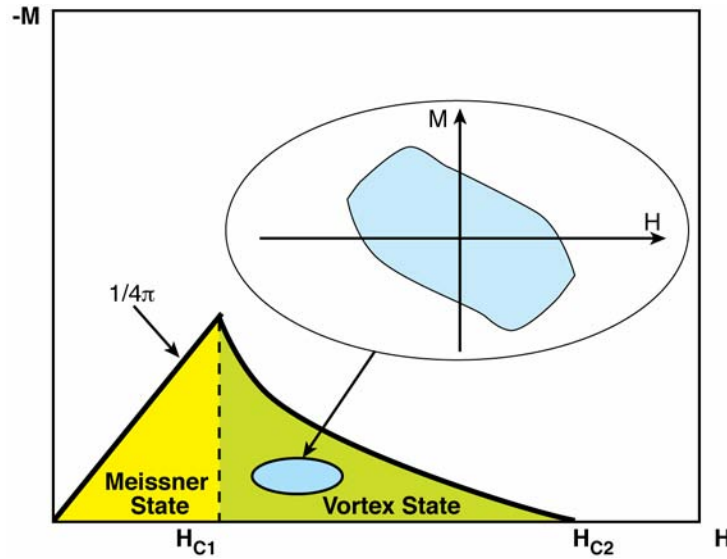


Figure 3-6
Origin of ac hysteretic losses in a type II superconductor [17]

These basic physical attributes of type II superconductors dominate all superconducting magnet designs and all superconducting power applications. One final remark—how to produce extrinsic vortex pinning sites in a type II superconductor is at the heart of superconductor materials science, yet to this day it remains pretty much a black art, ranging from standard metallurgical “heat ’em and beat ’em” processing to, in the case of HTS compounds, bombardment with energetic fundamental particles.

The discovery of HTS, arguably the epitome of type II superconductors, only magnified the importance of understanding vortex dynamics. In fact, due to the low-dimensional nature of both their physical and electronic structure and the higher operating temperature, losses due to flux motion are relatively higher than for low-temperature superconductor (LTS) materials. Although this report focuses specifically on dc cables, there will inevitably be ripple and thermal losses associated with all HTS materials.

3.2 The High-Temperature Superconductors

3.2.1 The Search for Higher-Temperature Superconductors

Progress in finding superconducting materials with ever-higher transition temperatures (T_c) proceeded, as with the theory, haltingly, after the initial 1911 discovery. By the early 1980s, the highest temperature achieved was approximately 23 K, slightly above the atmospheric boiling temperature of hydrogen, in vanadium silicide. On the other hand, it had become clear that the overwhelming majority of metals, both elemental and alloys, became superconducting at some temperature. The exceptions were few—ferromagnetic metals and extremely good metals such as the alkali series and noble metals. These exceptions were well explained within the BCS framework. Even many exotic superconductors—organics, polymers and actinides—had been discovered, albeit all at quite low temperatures. Nevertheless, the golden rule for finding new

superconductors has always been, “If you find a new metal, it’s good idea to cool it down. Someday you might be pleasantly surprised.” This is exactly the path taken by Bednorz and Mueller in 1986 in their investigation of the low-temperature properties of conducting transition metal oxides. In January of that year, they discovered superconductivity at the then unheard of temperature of 30 K in one of the planar copper oxide perovskites, a family of compounds now numbering over 100, with transition temperatures up to 165 K. The perovskites include materials such as mica and have many of the physical characteristics of ceramics. In particular, they are quite inhomogeneous and usually brittle.

The chronology of discovery of materials with increasing T_c is summarized in Figure 3-7. The layered copper oxide superconductors are highly anisotropic compared to the low-temperature materials. The crystallographic convention for these materials is to refer to the basal plane of the red pyramids as the *a-b plane* and the apical direction as the *c-axis*. The particular structure shown to the right in Figure 3-7 has the chemical formula $\text{YBa}_2\text{Cu}_3\text{O}_{7-y}$. Note the uncertainty, *y*, in oxygen concentration, a feature of all superconducting copper oxides, one at the heart of why they indeed are superconducting. In fact, if $y = 0$, even then seven oxygens leave Cu with an effective charge of +2.3, with the excess +0.3 available for electrical transport.

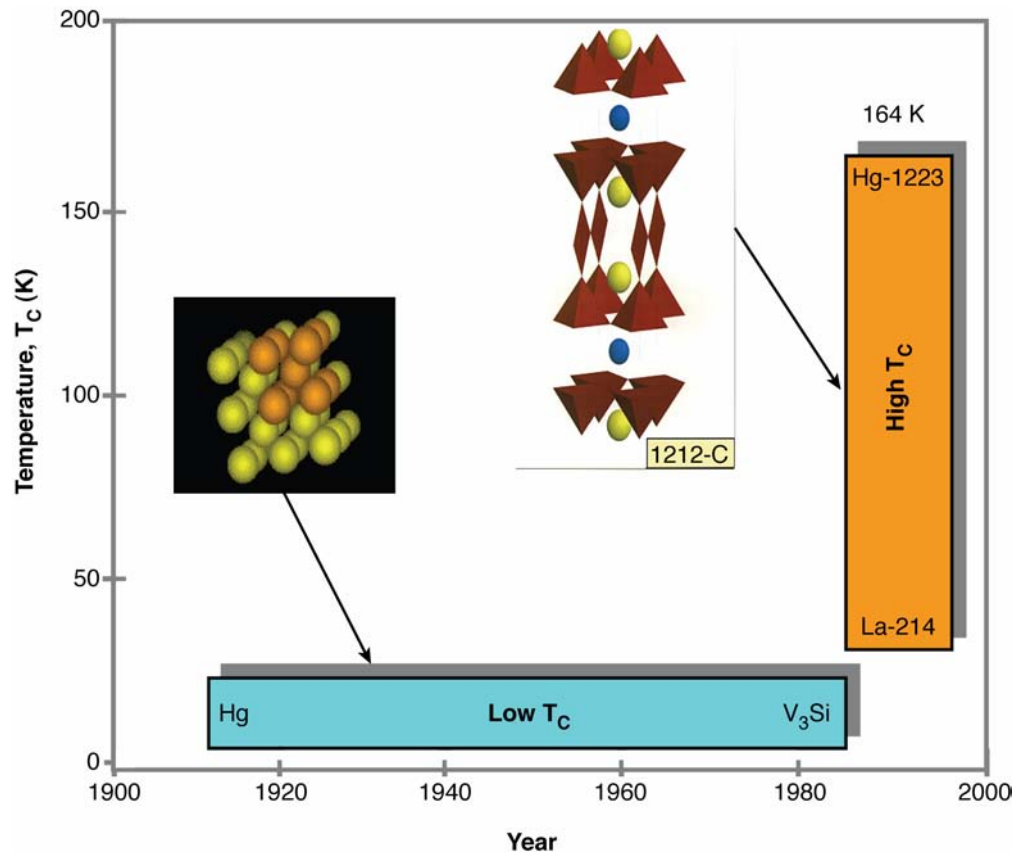


Figure 3-7
Observed increase in T_c since 1911 [17]

These new discoveries prompted renewed interest in power applications of superconductivity because many of these HTS compounds were operative above 77 K, the normal boiling temperature of nitrogen, a much cheaper and easier to handle cryogen than helium or hydrogen, and they could, in principle, be fabricated into long-length wires and tapes. Actually, dreams of applying superconductivity to electric power emerged shortly after its discovery in Kamerlingh-Onnes' institute. However, limitations of the early, elemental materials under conditions of even moderate amounts of current and magnetic fields quickly dispelled such hopes. From the 1960s through the early 1980s, there were extremely high-performance superconducting materials such as NbTi and Nb₃Sn. These materials, particularly NbTi, enabled applications such as magnets for magnetic resonance imaging and particle accelerators. Considerable effort went into developing them for power applications, but the operating cost of keeping them cooled with liquid helium at 4 K was found to be a showstopper.

3.2.2 Status of High-Temperature Conductors

Essentially every application of superconductivity to electric power technology, especially with regard to transmission and distribution cables, depends on the successful development of suitable wire or tape in long lengths. Progress toward this end using the new HTS materials has moved much more rapidly in the 20 years since their discovery than what at first appeared to be likely given the universally poor ductility (one might say nonductility) of ceramic materials. An added factor, easily seen from Figure 3-7, is the high degree of crystalline, and therefore electronic, anisotropy of the HTS compounds. The two decades since their discovery have seen more than two dozen successful prototype and demonstration projects worldwide involving the new discoveries—ac cables, motors, generators, current limiters, power leads, small superconducting magnetic energy storage units, transformers, reactive power controllers, flywheels, and more. The technology and manufacture of HTS wires (more aptly described as *tapes*) are summarized in Figure 3-8, under the categories of Generation 1 (Gen 1) and Generation 2 (Gen 2), roughly descriptive of their order of development and maturation stage. In Gen 1, the HTS material is packed and swaged inside a silver ribbon, whereas in Gen 2, the HTS material is evaporated, or coated, onto a substrate with crystallographic orientation compatible to the superconductor.

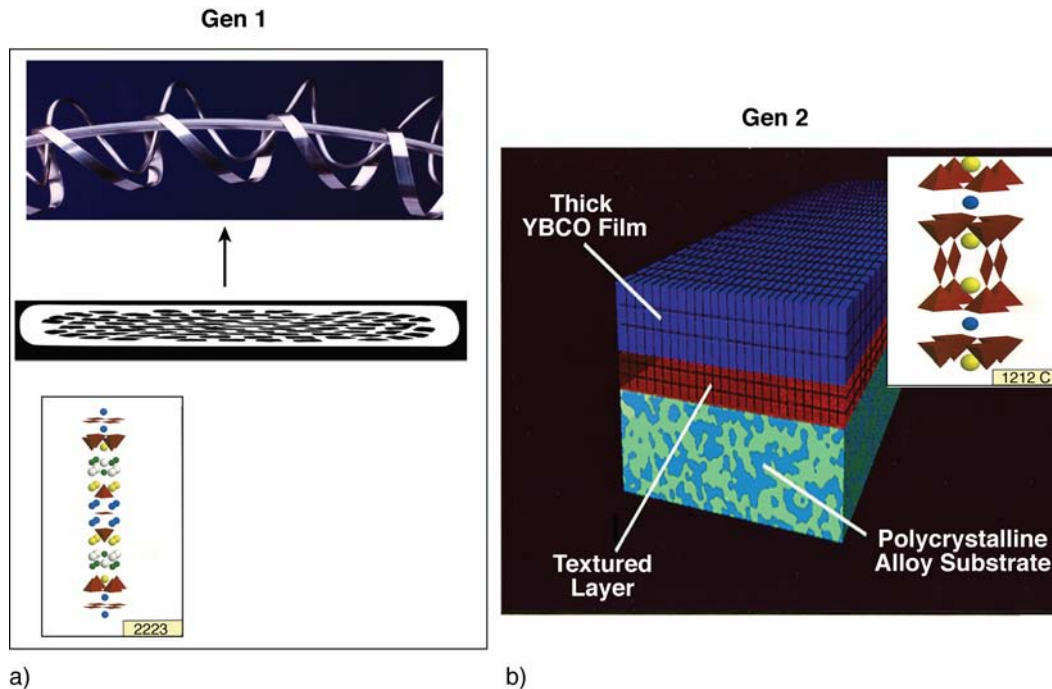


Figure 3-8
The two categories of high-temperature superconductor tapes currently available

© 1997 IEEE; reprinted with permission [15]

3.2.2.1 Gen 1 Technology and Process

The Gen 1 technology is based on HTS materials with the generic elemental content BiSrCaCuO (BSCCO) and the stacking structure shown in Figure 3-8(a). Electrical conduction (and superconduction) is primarily along the basal planes of the red CuO pyramids and planes, separated by green BiO interlayers. Thus, it is paramount that coplanarity of the entire unit cell be preserved as much as possible throughout the entire length of the final tape. The particular stoichiometry chosen is usually Bi:Sr:Ca:Cu::2:2:2:3, or *Bi-2223*, because its transition temperature is 110 K, comfortably above that of liquid nitrogen at 77 K.

Metal oxide precursors of the respective elements (carbonates of Sr and Ca are used because of the general instability of oxides of alkaline earth metals in air) are mixed and reacted (calcined) at temperatures ranging between 800°C and 850°C, usually undergoing several cycles of regrinding and reheating, to produce a cation-stoichiometric powder of the target compound. The powder resulting from either approach is then tightly packed into a cylindrical silver billet. The filled billet next undergoes repeated draw and swaging operations, using equipment almost identical to that used for common wire production, until an overall diameter of approximately 1 mm or less is obtained. Several tens to over a hundred of these wires are then inserted into another silver billet, which undergoes the same draw and swaging operations. The resulting ~1-mm-diameter multifilament wire is then rolled into a tape of the order 4–6 mm wide by <0.3 mm thick. A final step is to wind a given length of tape on a mandrill (spool). The entire assembly is then annealed at high temperature for several days under oxygen atmosphere. (See the tape cross-section in Figure 3-8[a].) The process was named the *silver-containing oxide-*

powder-in-tube (Ag OPIT) method. The main supplier at present is Sumitomo Electric Industries, with American Superconductor Corporation selling from inventory. The OPIT process is now at the state where tapes of kilometer length containing several hundred BiO-based copper oxide filaments can be routinely made. All in all, suppliers have manufactured about 100,000 kilometers of Gen 1 tape as of 2008.

The micaceous nature of the intermetallic oxide layer is one of the keys to the success of the OPIT approach because the draw-swage-roll process shears it, much like spreading out a deck of playing cards, which produces an unexpectedly high degree of crystallographic alignment of the copper oxide planes from a randomly oriented powder. The increased correlation of crystalline planes along the tape results in significantly improved critical current. In addition, a quasi-melt processing phenomenon, which is still not completely understood, aids in the texturization process. Most of the critical current flows within several microns of the Ag-HTS interface. Gen 1 tape has been used successfully in all demonstration and prototype projects mentioned previously, but its properties in high magnetic field are not as robust as one would desire. This lack is addressed by the next generation.

3.2.2.2 Gen 2 Technology

Soon after its discovery, it was found that single-crystal, epitaxial films of $\text{YBa}_2\text{Cu}_3\text{O}_{7-y}$ (YBCO) could be processed to yield critical currents greater than 10^8 A/cm^2 . However, these same efforts also made clear that long-range propagation of these enormous currents in wires and tapes would be severely inhibited by wide-angle grain boundary contacts between the CuO planes of neighboring crystallites. (See the crystal structure of YBCO in Figure 3-8[b]). Unlike BSCCO, YBCO lacks the interplanar micaceous intermetallic oxide spacer, and thus it is extremely brittle and not amenable to conventional metallurgical processing, as is BSCCO. Nonetheless, workers in Japan, and later in the United States, were able to deposit oriented films of YBCO on suitably prepared, buffered tapes. The topology of this Gen 2 technology is sketched in Figure 3-8. It now yields tape of reasonably long lengths (~400 m as of 2008) whose performance at 77 K—especially in magnetic fields as high as 1 T—greatly exceed Gen 1 capabilities. (It is expected that “self fields” in high-current superconducting dc cables will reach or exceed 1 T.) Although Gen 1 tape may well be employed in early superconducting dc cable prototypes and demonstrations, it seems clear today that Gen 2 will dominate the commercial deployment. The remainder of this section addresses only Gen 2 technology.

3.3 High-Temperature Superconductor Performance Targets for Cable Design

There are two quite different approaches to the fabrication of Gen 2 tape (see Figure 3-9). The rolling-assisted biaxially textured substrates (RABiTS) technique uses metallurgical texturing, or orientation, of transition metals, in this case a nickel alloy, by repeated heating and rolling, to align the underlying atomic cubic crystalline grains in a more or less uniform three-dimensional array, a giant single crystal, if you will. This technology actually has roots in the late nineteenth century, when grain-oriented iron was found to greatly reduce ferromagnetic hysteresis losses in transformer cores. The resulting crystalline orientation of the nickel alloy is then imprinted, or transmitted, through several intervening buffer layers to

permit the formation of a quasi-epitaxial, high-performance YBCO film. The purpose of the buffer layers in the RABiTS process is primarily to provide an element diffusion barrier for, and chemical isolation of, the YBCO film.

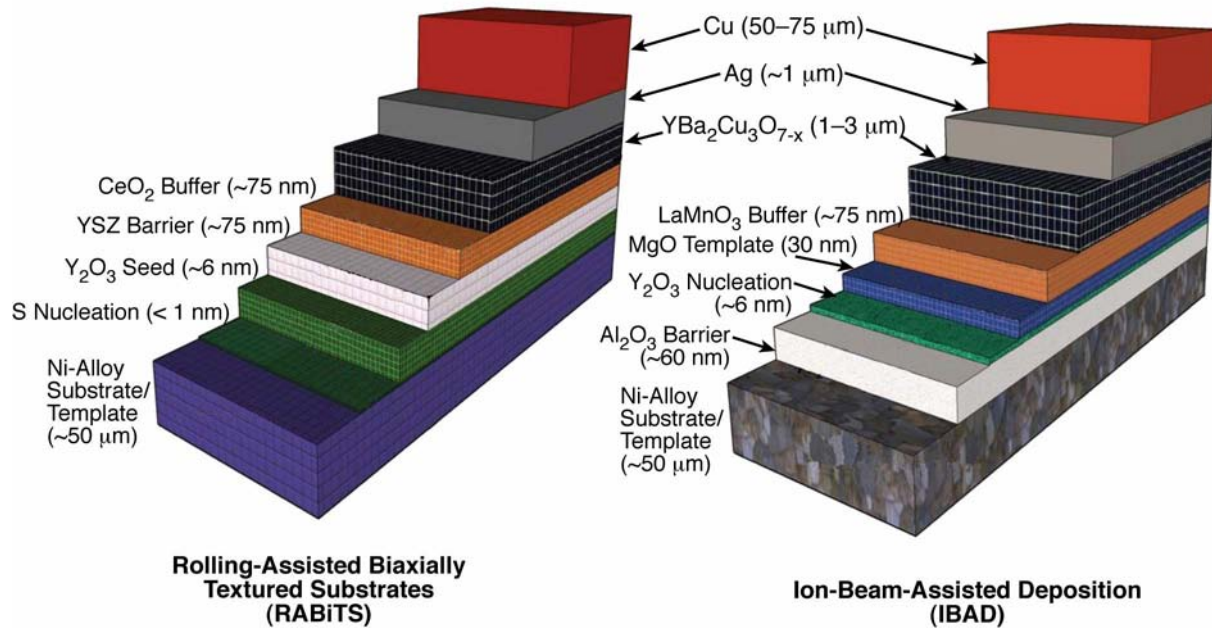


Figure 3-9
The two principal methods of manufacturing Gen 2 high-temperature superconductor tape

The alternative to RABiTS is to atomically pattern one of the diffusion barriers, rather than the base metal tape itself. The tape stack that results from this process, ion-beam-assisted deposition (IBAD), is shown in Figure 3-9. Here the MgO buffer layer provides the crystalline template for the superconductor, and is textured by a sandblasting beam of directed inert gas ions during its growth. The stacking in Figure 3-9 is not to scale, and the overall tape thickness is dominated by the base metal substrate and the Cu stabilization layer, with a final value of approximately 130 μm.

Although both methods might superficially appear to yield the same result, they differ significantly in detail. For example, the preferred method to grow the YBCO film on the RABiTS stack is by thermal decomposition of a fluoroacetate solution of the cation precursors. (The result of this process is sometimes termed a *coated conductor*.) In the IBAD approach, the YBCO layer is grown by a metal-oxide, chemical-vapor deposition process similar to that used in the semiconductor industry, although in principle, the same YBCO growth approach is interchangeable. RABiTS was pioneered by Oak Ridge National Laboratory and transferred to American Superconductor Corporation for commercialization, whereas IBAD is from Los Alamos National Laboratory and is the manufacturing method of choice for Gen 2 tape produced by SuperPower, Inc.

The application to cable manufacturing is more or less invariant to the details of each process. On the other hand, the dimensions shown of each component for both processes is representative and can be used for engineering analysis. They are not to scale in Figure 3-9; in both processes, the thickness of the superconductor comprises an almost insignificant portion of the overall stack. The importance of this is that a presumptive threefold to fourfold increase in YBCO thickness, and therefore current capacity, would not change the overall tape dimensions in a major way. However, a central issue in Gen 2 development has been that the critical current density within the YBCO layer is thickness dependent—that is, the current density decreases with increasing thickness, so that the net critical current does not scale with layer thickness.

Figure 3-10 is representative of the state-of-the-art (circa 2008) critical current density performance of Gen 2 YBCO tape as a function of temperature and of both the direction and magnitude of the applied magnetic field. The current-carrying capability of YBCO is considerably limited by the presence of perpendicular magnetic fields. Figure 3-10 illustrates the dependence of the critical current, J_c , on the magnetic field, for the field applied (a) perpendicular and (b) parallel to the crystallographic c -axis. (This notation is often reversed by various institutions.) J_c is much more robust near 77 K for the perpendicular direction than for the parallel. The critical current density normalization factor used in Figure 3-10 is square meters (m^2) and not square centimeters (cm^2) as is usually seen.

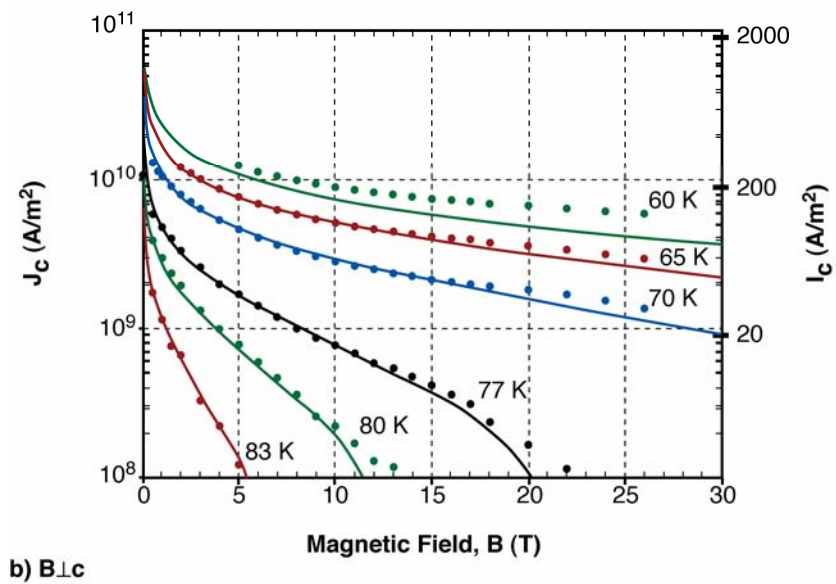
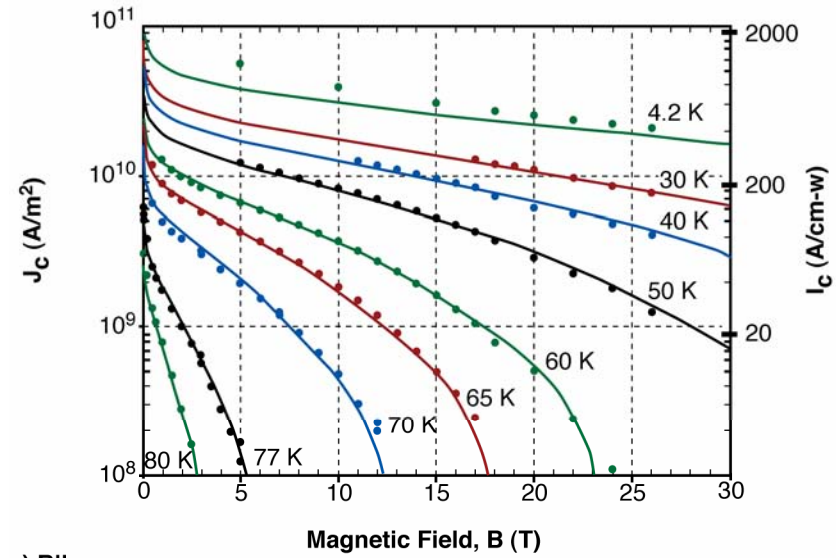


Figure 3-10
 Dependence of the critical current, J_c , of Gen 2 YBCO on the magnetic field (data from SRL-ISTEC, Japan)

In addition to specifying critical current areal density relative to the thickness of the YBCO layer, it is now common to report critical current per unit width of tape. Gen 2 tape is generally slit to specification from multicentimeter-wide sheets obtained from the basic manufacturing line. This normalization provides a method of performance comparison across various end applications. Also, the engineering-critical current density, J_E —the critical current normalized to the actual overall end-use tape dimension—is vital to design efforts. For example, tape widths of 4 mm seem now to have been accepted as nominal for cable application. Thus, for tapes of the thickness shown in Figure 3-9, J_E at self field and 77 K is roughly 15,000 A/cm² or 80 A per 4-mm wide tape. (At the time of publication, both U.S. manufacturers of Gen 2 tapes were offering long-length tapes with current-carrying capability of greater than 100 A; see the following paragraphs. At the operating temperature for the superconducting dc cable described in this report, this translates to approximately 200 A.)

Note the extreme performance degradation for fields perpendicular to the plane of the tape. For example, at 77 K in a 1-T perpendicular field ($B \parallel c$), the critical current is perhaps only 20% that for a field parallel to the tape surface ($B \perp c$), the usual self field direction for axially flowing current in a cylindrically symmetric conductor. Because of the high currents (≥ 20 kA) that we expect a superconducting dc cable to carry, perpendicular fields that might arise in the cable from departures from perfect coaxial symmetry (axial offsets, bends, dents, and so on) can lead to serious performance issues. However, it is possible that recent advances in engineering flux pinning anisotropies in Gen 2 tapes might ameliorate, or in fact completely eliminate, this issue.

Figure 3-11 shows the latest efforts in reducing directional effects of external magnetic fields on Gen 2 tape performance. The introduction of a particular type of defect—barium zirconate (BZO) nanotubes—can completely reverse the usually observed and typical field anisotropy displayed in Figure 3-10.

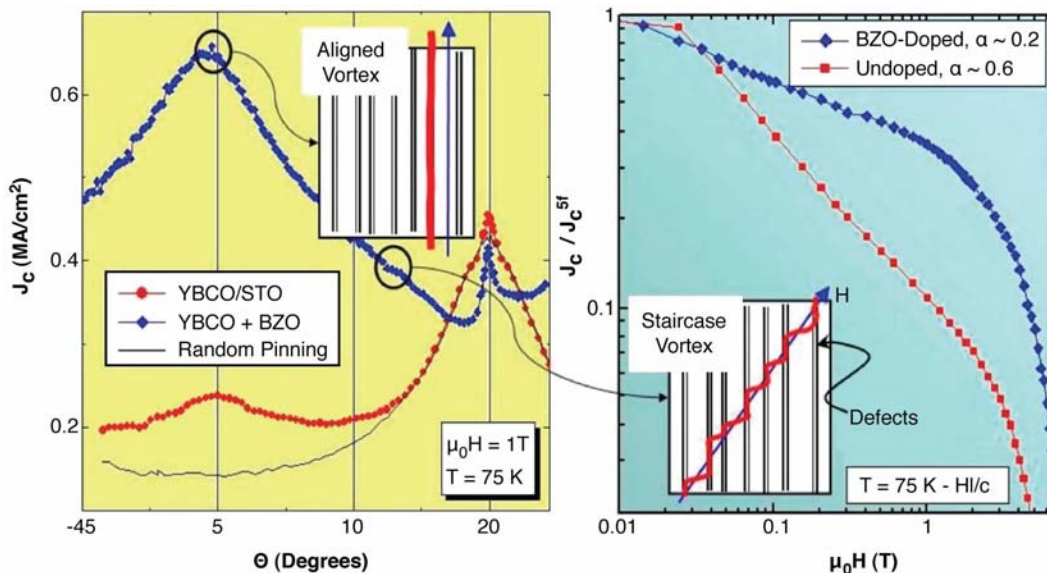


Figure 3-11
Effect of various pinning impurities on the anisotropy of J_c with respect to the direction of applied magnetic field (data from Los Alamos National Laboratory)

The eventual implication of this finding is revealed by measurements on Gen 2 tapes produced recently at Brookhaven National Laboratory. Figure 3-12 compares the “best of show” results as of the end of 2006 from the three U.S. national laboratories involved in Gen 2 tape development. The data are at 77 K for field applied in the “bad” direction (perpendicular to the surface). The field dependence is dramatically reduced in the Brookhaven National Laboratory samples. (These data have been independently verified at Los Alamos National Laboratory and Oak Ridge National Laboratory).

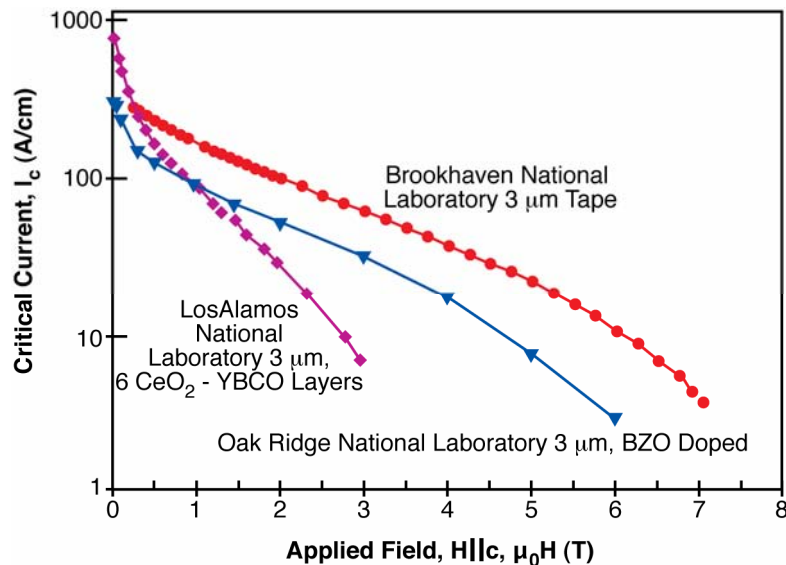


Figure 3-12
Comparison of I_c per unit tape width of representative samples

Figure 3-13 shows the magnetic field directional dependence of an externally applied 1-T magnetic field for the Brookhaven National Laboratory tape. The response is almost independent of angle. Note the almost complete lack of anisotropic response and performance degradation relative to the data in Figure 3-10. Moreover, the Brookhaven National Laboratory team states that they have developed a metal-oxide decomposition method, similar to that used by American Superconductor, that overcomes the thickness dependence of the microscopic critical current density. We might be able to assume that isotropically pinned 1000 A/cm at 77 K and 1 T will be available in the future. Such a development would have important consequences for superconducting dc cables.

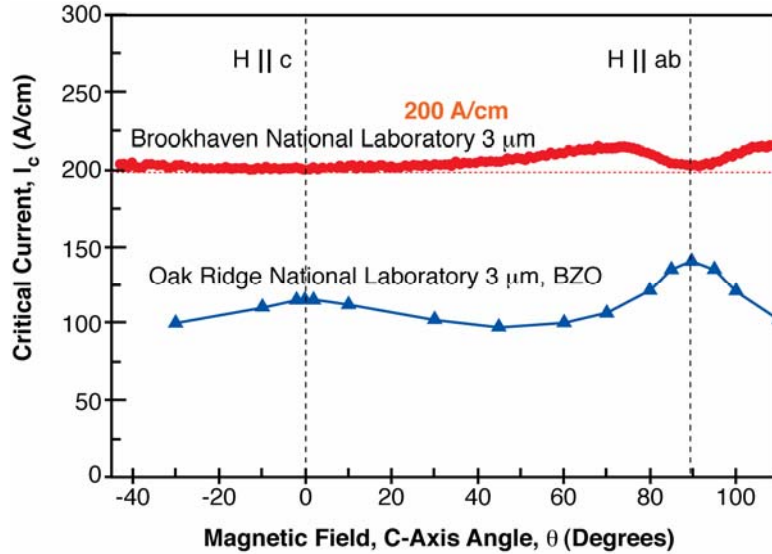


Figure 3-13
Variation of I_c per unit width as a function of the direction of a 1-T externally applied field with respect to the tape plane (a-b).

Presently, two U.S. manufacturers—SuperPower, Inc. (Schenectady, NY) and American Superconductor Corporation (Devens, MA)—offer Gen 2 tapes commercially in lengths up to 1 km and with ampacity exceeding 100 A (77 K, self field). Prices for the tapes have declined dramatically in the last few years. Although they are manufactured by different methods, both manufacturers' tapes have similar performance characteristics, and the tape ampacity is expected to continue to increase as manufacturing yields are improved.

Figure 3-14 shows a typical specification sheet for presently available Gen 2 tape from American Superconductor Corporation that is suitable for preliminary cable design. Splice resistance at 77 K is stated separately as 100 n Ω for tape-to-tape overlaps of 100 mm. No standards are yet in place to determine what specifications should be reported by manufacturers to allow for design, and therefore cost, optimization. For example, the universal E-J characteristic of superconductor wire of any variety, high or low transition temperature, is given by the power law represented in Figure 3-15.


Type 344C HTS Wire Fact Sheet

344 Superconductors

Type 344C: Copper stabilized YBCO second generation HTS wire

- HTS wire laminated on both sides with hardened copper for stabilization and strength
- Solder fillets at edges provide hermeticity, corrosion protection, and enhanced electrical stability
- Robust product with excellent mechanical strength and bend tolerance
- Optimized for use in power dense coils and magnets

344 superconductors are American Superconductor's new YBCO second generation HTS wires.



Mechanical Properties::

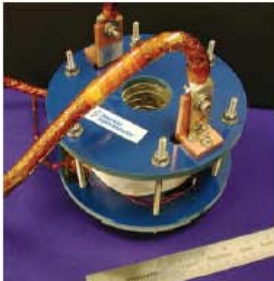
| | |
|-------------------------------------|----------------------|
| Average thickness: | 0.18 - 0.22 mm |
| Minimum width: | 4.27 mm |
| Maximum width: | 4.55 mm |
| Minimum double bend diameter (RT): | 25 mm ⁱ |
| Maximum rated tensile stress (RT): | 200 MPa ⁱ |
| Maximum rated wire tension (RT): | 12 kg |
| Maximum rated tensile strain (77K): | 0.3% ⁱ |

Electrical Properties:


| Minimum amperage (Ic) ⁱⁱ | Average engineering current density (Je) ⁱⁱⁱ |
|-------------------------------------|---|
| 70 A | 7,900 A/cm ² |
| 80 A | 9,100 A/cm ² |
| 90 A | 10,200 A/cm ² |
| ≥100 A | Contact factory |

Spliced wire available in long lengths
 Insulation options: Contact factory
 Certificate of Conformance provided.
 Certificate of Analysis optionally available. Contact factory.
 Leaders and tailers optionally available. Contact factory.

ⁱ With 95% Ic retention
ⁱⁱ 77K, self-field, 1 μV/cm
ⁱⁱⁱ Je is a calculated value based on average thickness and width



1.2 T HTS coil using Type 344C superconductors.



American Superconductor Corporation
 64 Jackson Road
 Devens, MA 01434 USA
 htswire@amsc.com
 tel +1 978 842 3519
 fax +1 978 842 3364
 www.amsc.com

©2009 American Superconductor. All rights reserved. American Superconductor and design, AMSC, POWERED BY AMSC, Revolutionizing the Way the World Uses Electricity are trademarks of American Superconductor Corporation. Printed in USA.

WFS_344C_0300_A4

Figure 3-14
Specification sheet for American Superconductor copper-stabilized Gen 2 tape
 Courtesy of American Superconductor

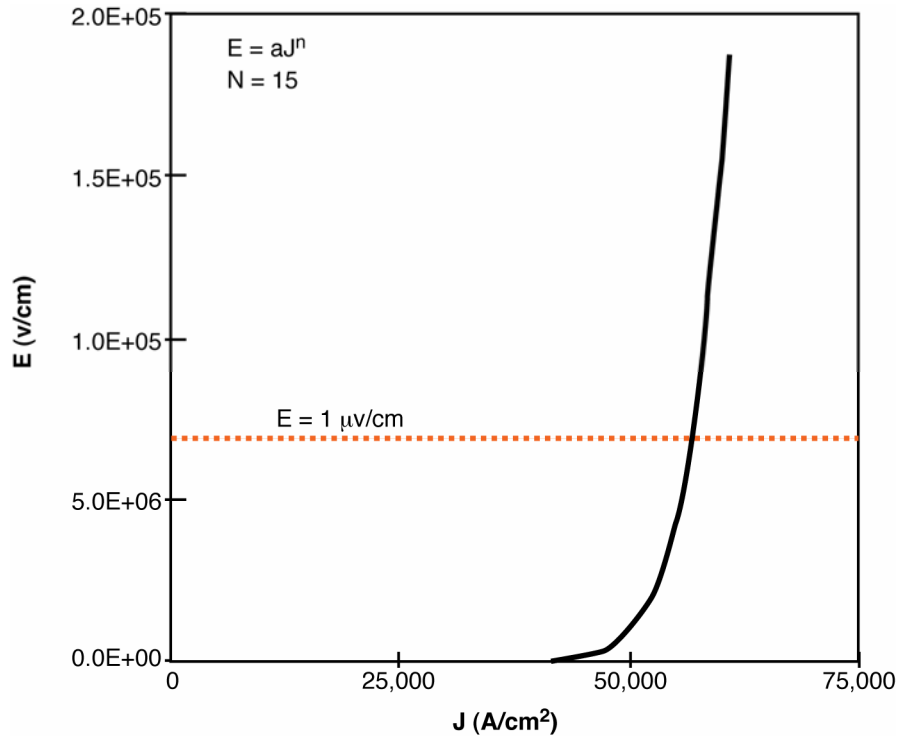


Figure 3-15
E-J characteristic, typical of both Gen 1 and Gen 2 [17]

The overall quality factor for superconducting wire is the value of n , which can range all the way from 5 for early BSCCO tape to 50 for premium Nb₃Sn and Nb-Ti magnet wire that operates at 4 K. In addition, the threshold voltage drop for establishing zero resistance is rather arbitrary and is not dictated by physics considerations. (The criterion for determining critical current is not zero resistance.)

LTS wire is typically described by its performance (critical current) at an electric field of 0.1 $\mu\text{V/cm}$, whereas for HTS tape, it is the performance at 1.0 $\mu\text{V/cm}$. Originally, the LTS wires also used the weaker criterion, but it was found to provide ambiguous results in terms of device performance. In fact, this power law is a function of many engineering-independent variables whose values must be known for proper design exercises. In general, the field E , or the measured voltage drop per unit length, is given by Equation 3-1.

$$V = f(I, T, B, \theta, \omega, A, l) \quad \text{Eq. 3-1}$$

Where:

V is the voltage drop per unit length.

I is the current.

T is the temperature.

B is the magnetic field.

θ is the crystallographic orientation.

ω is the frequency.

A is the cross-sectional area.

l is the wire length.

The voltage is a nonlinear function of all the parameters. The cost/performance of any given wire, measured as $\$/kA \times m$, would then be given by Equation 3-2.

$$C/P = \$/I \times l = \$/l \times g(V, T, B, \theta, \omega, A, l) \quad \text{Eq. 3-2}$$

Where:

C/P is in $\$/kA \times m$.

$g(V, T, B, \theta, \omega, A, l)$ is the inversion of Equation 3-1 with respect to current, I .

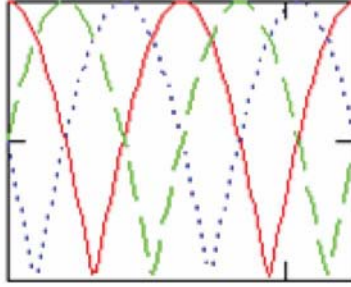
In addition, engineering safety and performance margin must be taken into consideration. For example, almost no applications would perform properly at $1.0 \mu V/cm$, so a derating factor must be applied, perhaps 30%, thus raising cost by a factor of three for HTS materials. The condition is quite different for materials in which the n value is high. For them, the difference between performance at $1.0 \mu V/cm$ and $0.1 \mu V/cm$ is only a few percent. At present, manufacturers are reluctant to state a specific price bracket, preferring to bid each order independently. As reported anecdotally, C/P values at $1.0 \mu V/cm$ range from 150–300 $\$/kA \times m$ (77K, self field). This represents approximately a fourfold decrease in price in three years. Commercial breakthrough is generally assumed to require a C/P figure around 30 $\$/kA \times m$ [18].

However, current capital cost estimates for a dc superconducting cable developed as part of this project (see Appendix C, Cost Considerations) indicate that in order to compete head to head with long-distance, high-power, conventional overhead transmission (ignoring the benefits of a superconducting line associated with smaller right of way, lower losses, environmental impact, and so on), wire costs would probably have to decline to around 15–20 $\$/kA \times m$. At current trends in price, that goal could be reached in five to six years. But, owing to the dependence of price on volume of manufacture, at some point there would have to be substantial production to reach these price levels, and therein lies the well-known “chicken and egg problem” in which substantial orders do not occur until price is reduced, and price is not reduced until substantial orders are received.

3.4 Cable Losses Due to Time-Dependent Current Flow

No type II superconductor is a perfect conductor under time-varying current flow; only at strictly constant current does such a condition apply. Such is also ideally the case for type I superconductors or type II in the Meissner state. Although the energy gap of the ground state of all superconductors is of order several terahertz, by the same laws of physics that govern dispersion of radiation in the visible range, a measurable amount of energy at 50–60 Hz will be absorbed across this gap, and the net current will eventually vanish. Interestingly, one of the first proposals to use superconductivity for power cables was to propose operating Nb wire in the Meissner state at high voltage and low current simply to recover the cost of reduction in generation resulting from the consequent energy savings [19]. This is seldom the case for practical dc transmission of electric power. There is the loading and deloading of the line and a multitude of other transients and interruptions from faults and “ripple” introduced into the line by inversion-conversion connections into the surrounding ac grid and generation system. These time-dependent fluctuations induce losses in a nominally direct current transmission system in several ways—eddy current and skin effect dissipation, hysteretic losses in the ferromagnetic packaging, dielectric losses, and even radiation. However, the overriding source will derive from vortex lattice hysteretic motion (see Section 3.1.3, Type II Superconductors: Technically Useful Materials), but these are likely to be quite controllable—and small.

Figure 3-16 depicts the general Fourier decomposition of an n -pulse rectification of ac input to a conversion station servicing a prototypical dc line or cable. For example, if the outside line frequency is 60 Hz, a six-phase (12-pulse) rectification station, results in a fundamental ripple at 360 Hz. If the effective dc current is taken as 20 kA, with a ripple efficiency of 1.5% (typical of today’s overhead high-voltage dc systems), the total heat dissipation to be relieved by the cable cryogenic system, from the fundamental up to the tenth harmonic, is approximately 0.013 W/m, an extremely low load on the cryogenic system compared to ac cables. In addition, these estimates do not include application of cable impedance characteristics.



$$f_p(t) = \frac{a_0^p}{2} + \sum_{n=1}^{\infty} a_n^p \cos(2\pi n v_p t), \text{ where } v_p = p v;$$

$$a_0^p = 2 \frac{\sin(\pi/p)}{\pi/p} \text{ and } a_n^p = \left\{ \frac{\sin(\pi(1/p+n))}{\pi(1/p+n)} + \frac{\sin(\pi(1/p-n))}{\pi(1/p-n)} \right\}$$

Where:

v = fundamental of one phase of a multiphase source undergoing full-wave rectification (for example, 50 or 60Hz).

p = "pulse number," or number of half-waved-generated greater-than-zero waveshapes thus generated. (For example, the figure illustrates the case for a 3-phase input in which each phase is advanced 120°.)

"dc" or average value = $a_0/2$. Any ac voltage or current must be peak and not rms.

"Ripple Factor," R_n = $(2a_n/a_0)$ in percent.

Figure 3-16. Representative Fourier decomposition of rectified current from a general purpose n -phase passive rectifier

4

CABLE DESIGN AND FABRICATION

4.1 Introduction

The purpose of the design of all components of the superconducting dc cable is to have a system that can be built and that will be functional in an engineering sense. That is not to say that it is possible to finalize all the details of a conceptual design at this time. A great deal of work remains before a final system can be fabricated and installed. Along the way, several options must be explored. Of major importance is the type of insulation that will be used. It is possible to finesse this decision and still come up with a placeholder in the design that is the correct size to accommodate several different insulation types. A second choice is the dimensions and current-carrying capacity of the superconducting tapes that will carry the dc current. It is clearly too early to attempt a detailed design for a 100-kA conductor with existing 200-A tapes. Nevertheless, the goal of this effort has been to design a reliable, high-power, long-length, underground, superconducting dc cable line with a maximum power rating of 10 GW and a length of 1500 km or more.

Hundreds of kilometers of conventional power cables have been installed at various places around the world, and the technology is commercially mature, with some 75 km of new cable cumulative circuit length installed each year. The knowledge base developed in reaching the present status of development in conventional cables is generally applicable to the present superconducting dc cable. In fact, those developments have already contributed to the development of superconducting ac cables. Several prototype superconducting ac cables are now installed in various locations around the world, and experience in operating and maintaining them is increasing as this analysis proceeds.

4.2 Background

This section touches on the wealth of information on conventional cables and existing superconducting ac cables that is available in the literature and in several EPRI publications. The EPRI report *EPRI Underground Transmission Systems Reference Book* (1014840), which is commonly known as “the Green Book,” is an extensive resource for information on underground cables [20]. Additional, valuable references include the EPRI report *Design Concepts for a Superconducting Cable* (TR-103631) as well as industry publications [21–25]. The developments in the areas of both conventional and superconducting ac cables form a base for the development of the superconducting dc cable described in this report.

4.2.1 Conventional Cables

Before exploring the design of the superconducting dc cable, we will describe the approach that is generally used in the fabrication of a conventional cable, including the constraints on its fabrication. The overriding boundary condition for a conventional cable is related to the maximum length that can be economically transported from the factory and then installed and jointed together at the installation site. Joints are complex and are fabricated on site under less-controlled conditions than are present in the cable factory. In practice, joints are the weakest link in the reliability of the cable system. In addition, they are expensive, and their long assembly times can significantly increase the overall project time. The most economical solution is obtained by an iterative costing analysis, with the objective of supplying the maximum possible cable length to reduce the number of joints. The actual determination of length on a drum is an iterative process between customer and vendor, involving a number of customer-specified design and performance requirements together with manufacturer capabilities, which are usually worked out in the bidding process for a new cable system.

Land cables are usually transported on a large drum or spool (see Figures 4-1 and 4-2). Drum size is limited by the physical dimensions of the roads and bridge clearances and the maximum weight allowable on the particular route. The drum shown in Figures 4-1 and 4-2 has a total capacity of about 60 tons; it is one of the larger drums used for transporting underground cables. Such a spool would carry 1–4 km of conventional cable; the exact length would depend on the specified current rating and system voltage of the cable. The cable cross section and components must be selected to allow winding of the cable onto and off of the drum.



Figure 4-1
Cable transport drum, fully loaded with cable



Figure 4-2
Loaded cable transport drums being transported from manufacturing facility to installation site

The strain that occurs in each cable component on the drum is proportional to the cable core diameter and inversely proportional to the diameter of the drum's hub. Thus, the larger the hub and the smaller the diameter of the cable, the lower the strain that is produced when the cable is wound onto the drum for transport. However, the thickness of the insulation depends on the design voltage. Thus, the higher the cable's design voltage, the greater the overall cable diameter and, thus, the greater the strain when the cable is wound onto a drum. To limit the strain in a high-voltage cable to an acceptable level, the diameter of the hub is increased, with the downside that the cable length is reduced. Conventional ac cable circuits are made of three identical, single-phase cables, each of which is wound onto a separate drum and transported to the installation site, where the three phases are connected to the grid.

Several insulation schemes are possible for a conventional cable. They can be divided into two general classes: 1) extruded, solid insulation, also known as *dry insulation*; and 2) impregnated, paper tape insulation or laminated paper polypropylene (LPP) insulation, also known as *wet insulation*. Both types of insulation have worked effectively in the field. For new ac applications, dry insulation is mostly superseding wet insulation at all transmission voltages. The advantages are elimination of fluid leaks and ease of monitoring and maintenance. For new dc applications, there is also a preference for dry insulation; however, applications to date have been limited by the lower insulation strength to system voltages of 150–250 kV. The development of improved dry insulation is being actively pursued, and prototype 500-kV dc cables have been tested. Figure 4-3 illustrates the difference between the two insulation types for a 400-kV ac application. The thickness required to insulate at a specific voltage is similar for the two types.

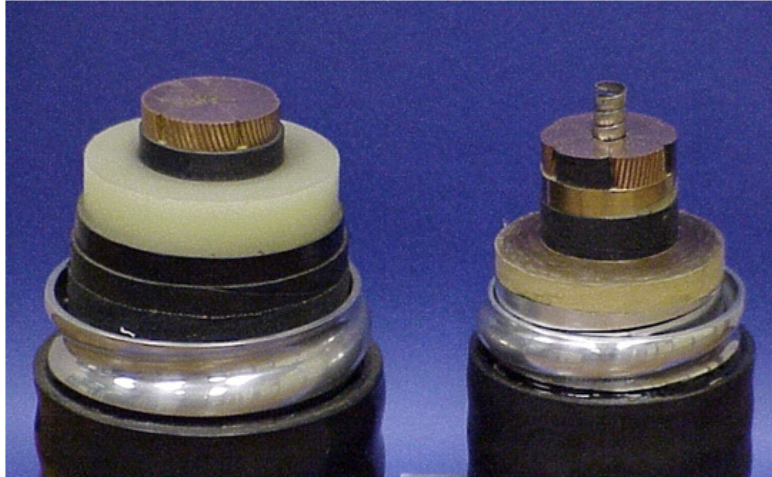


Figure 4-3
A 400-kV ac cable with extruded, solid insulation (left) and oil-impregnated paper insulation (right)

The impregnated, wet type insulation on the right in Figure 4-3 has a central tube that is filled with hydrocarbon oil. The oil penetrates the paper and contributes to the electrical strength of each tape. The oil also fills in the gaps along the sides of each tape. The size of this gap ultimately dictates the maximum electrical design strength and, hence, the thickness of the insulation. The cable system is designed to permit the oil to flow out of the cable through special joints into reservoirs. An outward oil flow occurs when the temperature of the cable increases as it is electrically loaded, and conversely, an inward flow occurs when the cable cools down. In some special instances, the oil is made to flow along the cable, thereby supplying cooling by way of forced convection.

Figures 4-4 and 4-5 show a paper-lapping machine, in which up to 200 layers of tape are applied to the cable as it is pulled along the machine. This same tape-lapping technique has been used to insulate most of the superconducting ac cable designs to date. The insulation has been impregnated with either liquid nitrogen or liquid helium, rather than oil, which cannot flow at low temperature.



Figure 4-4
A tape-lapping machine in a humidity-controlled enclosure

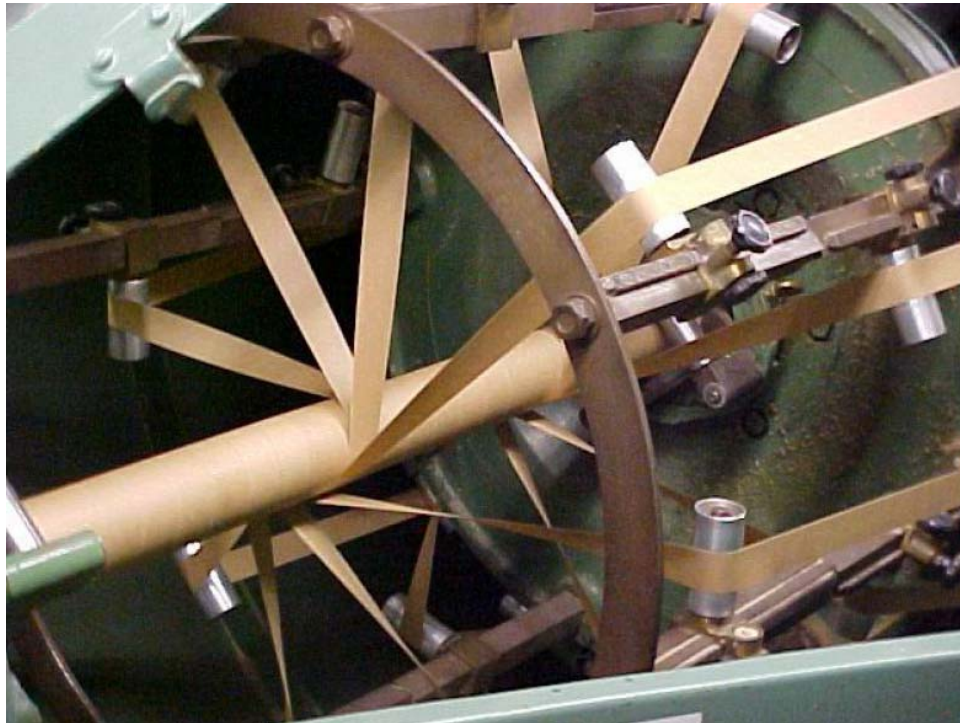


Figure 4-5
One of the tape-lapping heads

The cable on the right in Figure 4-3 has a solid insulation that is formed by a pressurized extrusion of a plastic material. Typically, there are three extrusion heads that together apply the material in multiple layers. The inner layer is a semiconducting, carbon-impregnated layer, usually an elastomer that provides both mechanical and electrical uniformity between the conductor and the insulation. The second layer is the insulator, which is white in the figure. A variety of insulating materials are used today, and the specific choice depends on a variety of factors, including the maximum temperature at which the cable will operate. Some highly cross-linked plastics, such as XLPE, can maintain their shape and strength under extreme thermal conditions. Finally, an outer semiconducting layer, usually of the same material as the inner layer, is applied. The general layout of a horizontal extrusion machine is shown in Figure 4-6.

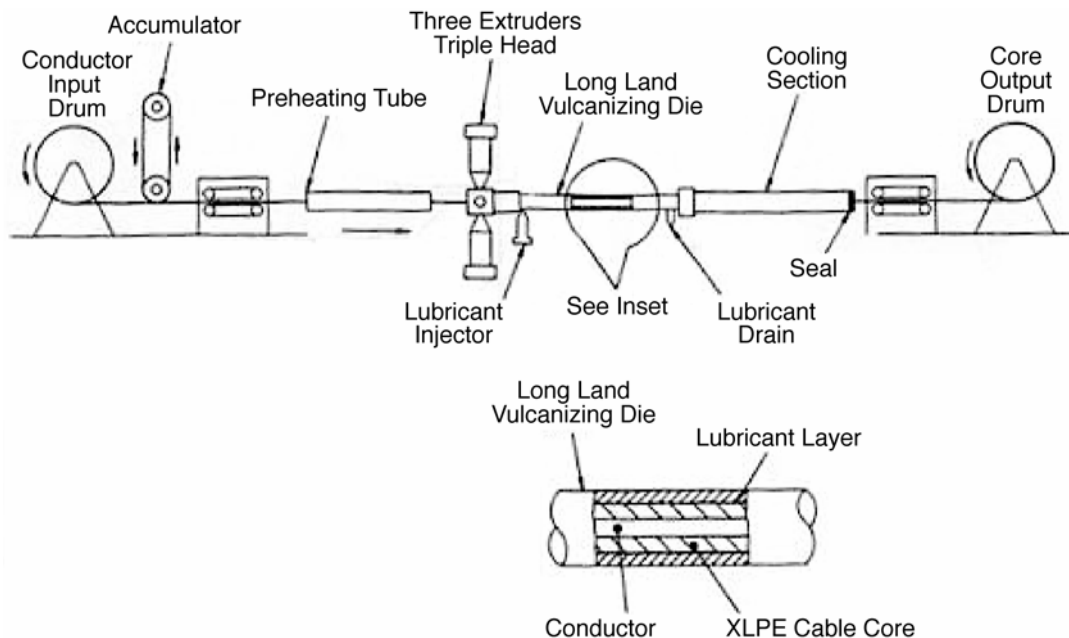


Figure 4-6
Layout of a horizontal extrusion machine for cable insulation

Figure 4-7 shows a cable as it exits the extrusion equipment. Often, the insulation is extruded onto the cable in a vertical orientation (see Figure 4-8) so that it can be heated to cross-linking temperature and then cooled while it is contained in the free space within a gas-filled tube. The vertical orientation keeps the conductor central, and the insulation shape cylindrical, during the process.

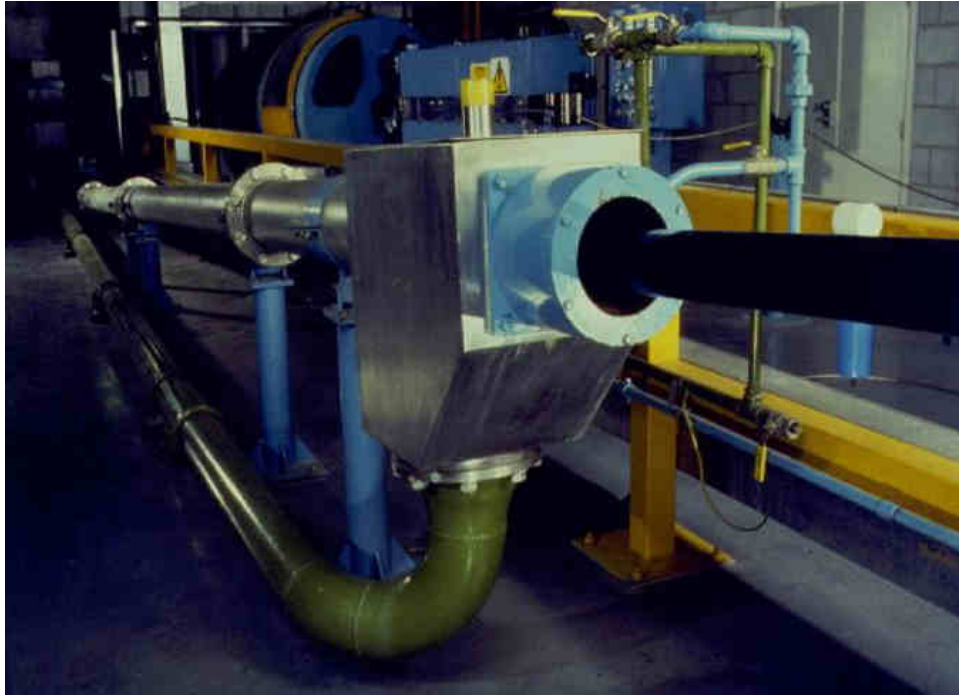


Figure 4-7
An extruded cable core emerging from the extrusion and cross-linking machine

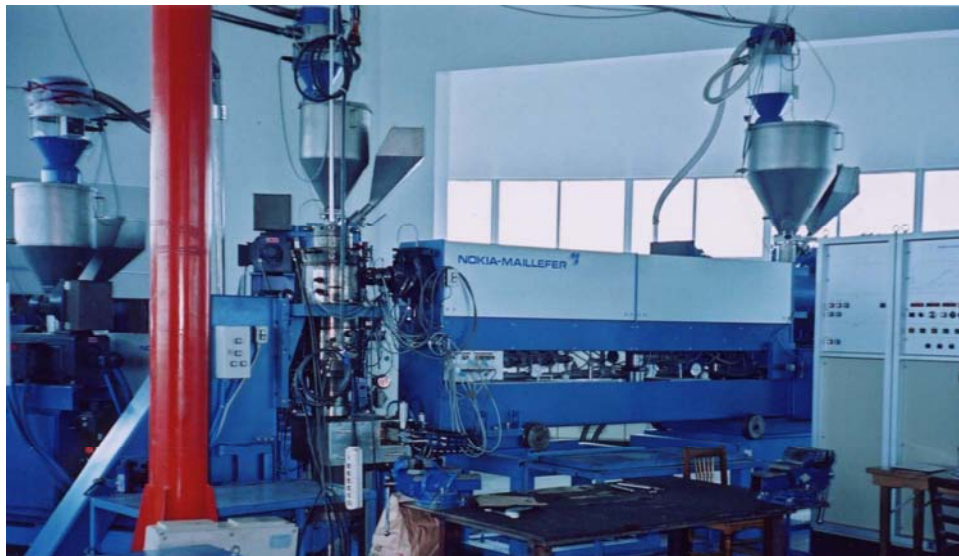


Figure 4-8
Triple extrusion equipment in a vertical line. The conductor appears as a vertical, white line to the left of the foremost extrusion press.

4.2.2 Superconducting AC Cables

Several HTS ac cables have been installed in niche situations, where they can be studied before issues associated with their commercial development are addressed. That is not to imply that these systems do not provide a service where they are installed. The designs of almost all superconducting ac cables installed to date are based on the design of the conventional, impregnated, wet cable. However, several differences relate to the unique characteristics of the superconductors. First, they must operate at a low temperature in a cryogenic environment. Second, most of the superconducting materials available today can operate only when the magnetic field is relatively low. Third, the materials have no resistance when the current and field are constant, but they do have a resistive component under ac conditions. Finally, the superconductor tries to shield itself from magnetic fields by producing an opposing electromotive force, which is not damped as it is in most resistive systems.

The combination of these effects has led to several different approaches to the design of superconducting ac cables. Most use cold dielectrics, which use liquid nitrogen in much the same way as the oil is used in an impregnated cable, but some are much like the conventional cable that has an extruded, warm dielectric surrounding the superconducting material and the cryostat. The first superconducting ac cable was of this warm dielectric design (see Figure 4-9).



Figure 4-9
A warm dielectric, single-phase superconducting ac cable

The cable was developed by Pirelli Cavi e Sistemi SpA (Milan, Italy) based on an EPRI-patented design and initial research that was conducted by both EPRI and the U.S. Department of Energy [26, 27]. The Pirelli cable was installed at Detroit Edison, but it was not operated due to problems with the cryostat [28]. Two different designs for superconducting ac cables seem the most likely to be effective elements of the future power grid. Both use a cold dielectric that is permeated with liquid nitrogen. However, they are quite different from the warm dielectric design and from each other.

One popular superconducting ac cable design is a *triplex*—that is, the three phases are wound concentrically on a single inner core. Figure 4-10 shows a cable of this type made by Southwire and installed at an American Electric Power substation. The advantage of the triplex cable design is that it uses half as much superconductor as the three single-phase cables.



Figure 4-10
A superconducting triplex with nitrogen-impregnated, cold insulation between phases

The second design consists of three separate, single-phase cables, which are typically installed either in a single pipe or in three separate pipes. This design has been used by Sumitomo, American Superconductor, and Nexans in several installations. The single-phase ac cables typically have two layers of superconductor, separated by the high-voltage insulation (see Figure 4-11). The outer layer of superconductor has a return current that contains the magnetic field, thereby shielding everything outside each phase from the magnetic field.

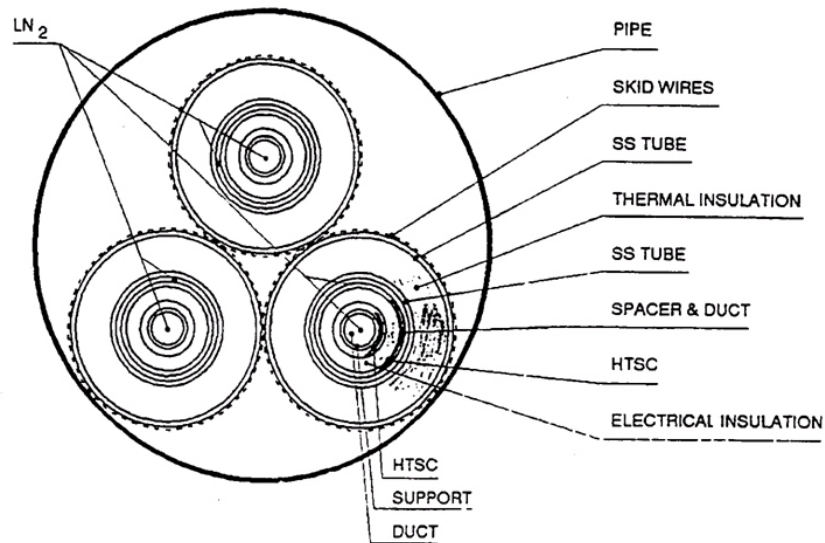


Figure 4-11
Three cold-dielectric, superconducting, single-phase ac cables in a single pipe

Existing designs of both cold and warm dielectric cables have used a hollow-center conductor to carry the liquid nitrogen coolant. The liquid nitrogen cooling systems have typically been designed to operate at high pressure limits of 20-bar inlet (go) pressure and 10-bar outlet (return) pressure. Thus, the central conductor duct is required to be a leak-tight pressure vessel. This requirement has a significant effect on the design of the cable joints. This pipe must be joined end to end as the first step of assembling an electrical straight joint, before the overlying layers of conductor and insulation can be reapplied. This is a significant disadvantage; the requirements for the liquid nitrogen to flow out of the duct, which is at high voltage, through the joint insulation to the heat exchangers at ground voltage, while segregating the liquid nitrogen pressure from that on the opposite side of the joint, makes the joint design quite complex. Furthermore, any pressure leak from the central duct within the cable would prospectively disturb and damage the insulation, and it would be inaccessible for maintenance and repair.

4.3 Superconducting DC Cable Design

4.3.1 Approach

This study for a long-length superconducting dc cable system has identified several design approaches to overcome some of the limitations of existing superconducting ac cables, including the following:

- Simplifying the cable design and manufacture by removing the functions of the liquid nitrogen cooling system and the vacuum-containing cryogenic system from the specification. The cable core construction then becomes similar to that of a conventional cable, and so it benefits from the use of proven manufacturing, installation, and jointing methods. The benefits are increased economies of scale, increased cable and joint reliability, and the provision of independent access for operation and maintenance to the liquid nitrogen system and the cryogenic vacuum system on the installed line.
- Developing a dry type of cold dielectric insulation that permits a standard high-voltage acceptance test to be performed to verify the integrity of the cable insulation on each shipping reel length before it is dispatched from the factory.
- Minimizing cable costs by reducing the cable outer diameter, thereby accomplishing the following:
 - Reducing the material content
 - Increasing the cable length to be delivered to the site on the factory dispatch reel
 - Reducing the number of hand-assembled joints (splices) needed during site installation

One target for the superconducting dc cable is to achieve a minimum of 1 km length together with a high power (5 GW and greater) capability, which will be a significant step in making it competitive with conventional transmission voltage cables, which are typically applied in lengths of 0.5–0.8 km and carry less than 4 GW at most. For special applications, conventional cables have been supplied in lengths of up to 1.5 km on special long-hub reels. The achievement of these lengths will also require the development of low-friction cable coverings and techniques to reduce pulling tensions and forces experienced by the ducts within the cryogenic enclosure. The ultimate, low-temperature service operation will affect the use of typical oils, greases, and water-soluble gel lubricants for cable pulling.

In manufacture of a cable, every millimeter of the insulation over the length on the reel (0.5–1.5 km) must be perfect. Thus, factory shipping tests are always performed on each piece of cable. These tests include an overvoltage withstand test. Superconducting cables that use wet designs of liquid nitrogen-impregnated paper or LPP insulation cannot easily be tested without cooling the shipping reel to 77 K, which is probably impractical for the mass production that is expected for the superconducting dc cable system. Thus, it would not be possible to confirm the integrity of the insulation and the absence of possible damage until all the lengths had been delivered to the site, jointed together, and impregnated with liquid nitrogen.

Similarly, to reduce risk, it is highly desirable—and is included in the specifications for conventional cables—that the resistance of the conductor be measured. This is not possible with any design of a superconducting cable without cooling the conductor. Therefore, a significant risk exists that some superconducting tapes might have suffered unrecorded damage during manufacture that will not become apparent until they fail in service.

The 10-GW superconducting dc cable design selected for this project is shown in Figure 4-12. The dimensions of each component of the cable are given in Section 4.4, Superconducting DC Cable Dimensions. These dimensions are based on calculations carried out in a spreadsheet that is, in essence, a design algorithm for the superconducting dc cable. Data within the program include characteristics of most of the materials that could be used in such a cable. Operation of the program is such that changing the voltage, the current, or the maximum operating temperature will result in a new cross section. The design that is described is for a 10-GW, 100-kV, 100-kA cable that operates at temperatures less than 69 K.

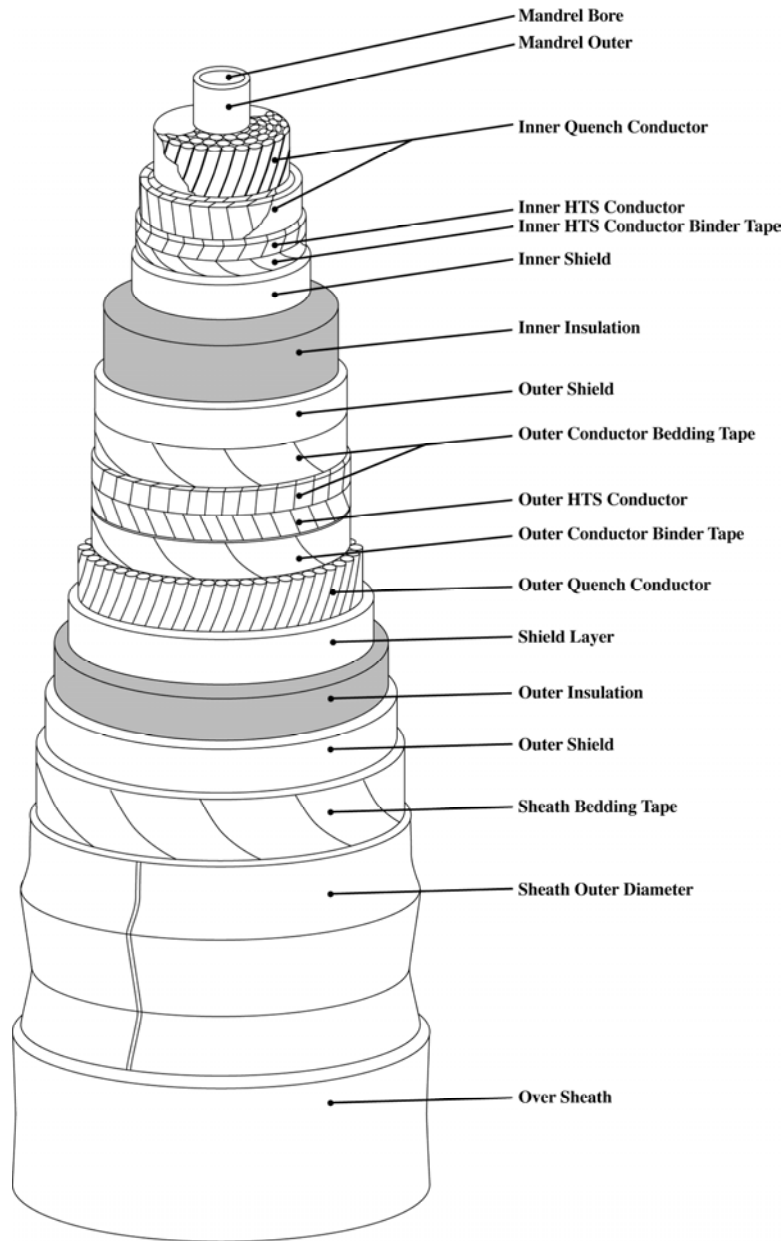


Figure 4-12
Superconducting dc cable design

4.3.2 Conductor Mandrel

The *mandrel* (also called a *former*) is a support tube for the conductor components. Unlike a conventional copper wire conductor, a superconducting wire (a flat tape) has a limiting, minimum bending radius based on a maximum permissible bending strain. The strain is reduced by stranding (laying or winding) the tapes in a helical pattern onto a sufficiently large diameter of a mandrel. The outer diameter of the mandrel must be large enough that the combination of stresses from bending around the diameter and the helical lay of the tapes is less than the strain limit of the material.

The mandrel can be tubular, or it can be helical, formed from a tape material. It can be made of a metal or some type of reinforced plastic or elastomeric material. The mandrel could also be a solid rod, which would have an advantage of increased tensile strength and stability, whereas a hollow mandrel is more flexible and lower in cost.

4.3.3 Inner and Outer Quench Conductors

The quench conductors are made of copper wires that form one or more concentric layers. The inner quench conductor is on top of and in good electrical contact with the mandrel. The individual copper wires can be of either round or flat cross section, and they will be applied in alternate right-hand and left-hand lays for mechanical flexibility and stability during cable bending. The role of the conductor is to carry the current momentarily should the overlaying superconductor be driven out of its superconducting state (such as during a fault). Having low-resistance copper, rather than the superconductor, carry the current limits the temperature rise. Specifically, it controls the maximum temperature reached between the time that a fault occurs and the time that the ac–dc converters clear the event. For this design, the short-circuit current was taken to be twice the nominal current and the maximum time duration to be 20 cycles. The maximum permitted temperature rise was taken to be 1 K, so that the superconductivity could be reestablished immediately after the fault was cleared.

As a further explanation, the cross-sectional area of a quench conductor is calculated to minimize the production of heat during the fault condition and to provide the thermal capacity to absorb that energy without exceeding the desired temperature. A copper conductor at 69 K is more effective than at ambient temperatures because its resistance is less by a factor of ten. The reduced resistance allows a relatively small cross section of copper to provide this functionality.

The inner quench conductor is positioned inside the first layer of superconductor, because there is no magnetic field. Similarly, the outer quench conductor is placed outside the second superconductor layer to be in a region that is free of magnetic fields. These zero-magnetic-field zones isolate the copper from most stray fields and from the harmonic currents that are produced by the ac–dc converters at the end stations. In addition, the position allows good contact between the copper and the superconductor. In both cases, radial pressure within the cable lowers contact resistance. The result is that current transfers easily between conductor and superconductor during current ramps as the power is changed. Because the function of the two quench conductor layers is similar, they have the same cross section.

4.3.4 Inner and Outer Superconductor Layers

The HTS wires are actually flat tapes. These tapes can include a YBCO or Bi-2223 superconductor or some other superconducting material that will be developed in the future. In either case, the nominal dimension of each tape used here is 4.3 mm wide \times 0.24 mm thick, which was established early in the program. Because the important parameter is the critical current density of the superconducting material, the exact dimension has little impact on the overall cable dimensions. The tape size and operating current, however, will affect the number of tapes that are wound into the cable to form the inner and outer HTS conductors and some details of the HTS conductor stranding process (the winding of the HTS tapes to form the conductor).

The current-carrying capacity of each tape is determined by its critical current at the operating magnetic field and temperature and a suitable margin. The total number of tapes is calculated from this current and the 100-kA total current in the cable. Each layer is laid in a helical pattern, as described previously for the copper conductors. The lay alternates between left-hand and right-hand helicity in adjacent layers. If all the layers had the same helicity, an axial magnetic field would be produced due to the unbalanced, circumferentially rotating component of current. This field would be similar to that of a solenoid, producing a magnetic field inside the diameter of the windings. Fields of this form might have the effect of reducing the current-carrying capacity of the conductors.

The magnetic field has a maximum value at the outer surface of the inner HTS conductor, proportional to I/r , where r is the outer radius of the conductor. As a result, the maximum field can be substantially reduced by using as large a mandrel as possible. The reduced magnetic field would also increase the current-carrying capacity of each tape. An optimal diameter exists at which the cost reduction resulting from the decrease in the number of HTS tapes is balanced by the increased cost of the volume and diameter increase of the overall cable (and the associated reduction in transportation length).

Having applied the HTS tapes to form the inner HTS conductor, a *semi-conducting* (low conductivity) high-strength fabric binder and bedding tape is laid over it. This accomplishes several purposes, including holding the tapes in position during cable manufacture and providing a cylindrical surface onto which the conductor shield is extruded. A similar bedding tape is applied over the extruded insulation shield to form the bedding for the HTS tapes in the outer HTS conductor.

The outer HTS conductor and outer quench conductor nominally operate at ground potential. At the same time, the inner HTS conductor and inner quench conductor operate at the maximum system voltage. The voltage can be positive or negative with respect to ground. However, after a polarity is chosen, all cables that are directly interconnected must have the same polarity. Because the overall philosophy adopted for the superconducting dc cable system was to achieve redundancy by having two cables in each circuit, it is possible to have the inner conductor of one cable positive with respect to ground and the other negative with respect to ground.

4.3.5 Conductor Shields

The conductor shields provide controlled interfaces between the HTS conductors and the insulation. The intent here is to use the same insulating geometry as the conventional, single-phase ac cable. In the proposed use of an extruded insulation, the shield, typically an annular layer of a graphite-filled elastomer, is extruded hot onto the binder tape over the inner conductor. It is immediately followed in the same fabrication line by an extruded layer of hot insulation, so that the surfaces of the two materials coalesce to form a mechanically bonded, smooth, cylindrical layer that is free of electrically weak impurities, such as air voids, screen asperities, and particulate contamination. Similarly, a second layer of elastomer is extruded onto the outside of the insulation layer as the core conductor continues along the fabrication line (see Figure 4-8).

The thicknesses of these layers are determined by the mechanical properties of the material itself and the structure of the adjacent layers of conductor. If appropriate materials can be made to function in a cryogenic environment, existing techniques and equipment can be used to fabricate this part of a superconducting dc cable.

4.3.6 Insulation

The inner surface of the insulation, the second layer in the extrusion process, experiences the highest electrostatic stress in the cable. The variation of this stress and the voltage gradient radially across the insulation are results of the geometry of the cable. The highest magnetic field in the cable is just at the outside of the inner HTS conductor layer, and the maximum voltage gradient would be at the same radial location if it were not for the binding tape and the elastomeric layer. The gradient at this location is taken to be the insulation design stress. The magnitude of the design stress is calculated to ensure that the insulation will operate satisfactorily for the specified design life of the cable at its normal operating voltage and under sporadic, transient over-voltages. The design life of conventional cables is typically specified to be 40 years.

The effect of a constant voltage on an insulator for a long period is a polarization of the material. Various materials become polarized at different rates, and the polarization becomes saturated at a level that depends on the material and, most likely, the temperature. Polarization does not occur in an ac cable, because the polarity of the voltage alternates at the fundamental frequency. Polarization and space charge enhancement are expected to be negligible at cryogenic temperatures due to the extremely low charge carrier mobility. However, this prediction must be verified by measurement (electrical breakdown strength at elevated dc voltages and under short-term, transient impulse voltage). In addition, if polarization does occur, the reduced carrier mobility at low temperatures will cause the polarization to persist for long periods. This could be a potential hazard for maintenance and repairs.

The selection and validation of a suitable, extruded insulation material is identified as a key development in the superconducting dc cable project. The mechanical strength of the insulation and its ability to withstand its internally generated thermal contraction forces (longitudinal and radial) must also be quantified.

4.3.7 Outer Shield and Insulator

During normal operation, the outer HTS conductor layer and the outer quench conductor will be at ground potential. However, under certain upset conditions, the outer HTS conductor can reach an elevated voltage that can be as high as half the voltage of the inner HTS conductor (see Section 7.4, Grounding of the Superconducting Cables). As a result, this component of the superconducting dc cable must be well insulated from the outer sheath, which always remains at ground, to avoid arcing. A layer of insulation is introduced between the outer quench conductor and the outer shield. The thickness of this layer is about half that of the main insulator. Just as in other transition areas, shields and bedding are needed to limit locally enhanced electrostatic stress caused by material irregularities.

4.3.8 Sheath and Skid Layer

An outer sheath of stainless steel contains the entire cable core structure. The outer diameter and thickness of this layer have a major effect on the ability of the cable to be wound onto the transport drum and to go through various bends while being pulled into place on site. The sheath is corrugated (see Figure 4-12), which will require the sheath bedding tape (or other material) to vary in diameter along the length of each cable section. A layer of protective material is typically applied to the outside of the sheath on conventional cables. This layer might not be necessary for the stainless material used for the superconducting dc cable. Alternatively, a thin, welded, stainless steel sheath of cylindrical shape bonded to, and mechanically reinforced by, an outer protective layer of the composite type now being used on conventional extruded cables should be investigated, as this would reduce the diameter of the cable.

4.4 Superconducting DC Cable Dimensions

A spreadsheet program was developed to determine the dimensions of the cable based on input parameters that include overall cable system requirements, such as power level, operating voltage, and operating current; and material characteristics, such as voltage breakdown strength, material density, resistivity, and the operating current of the superconductor tape. The design that is addressed here is a 10-GW, 100-kV, 100-kA cable that operates at temperatures less than 69 K. The program calculates the dimensions of each layer of material shown in Figure 4-12. In addition, several small layers (which are not described in the previous section and are not shown in Figure 4-12) are included for completeness in the program. These dimensions are summarized in Table 4-1. By far, the largest components of the cable are the quench conductors. This is a direct result of choosing a limited temperature rise of 1 K during an upset condition. Future analyses might well suggest that allowing a larger temperature rise would be an acceptable tradeoff with the size of the cable.

Table 4-1
Dimensions of the various layers of the superconducting dc cable

| Layer | Description (see Figure 4-12) | Thickness (mm) | Outer Diameter (mm) |
|-------|---|----------------|---------------------|
| 1 | Mandrel bore | | 30.00 |
| 2 | Mandrel outer | 1.5 | 33.00 |
| 3 | Inner quench conductor | 20.32 | 73.63 |
| 4 | Binder (not shown in Figure 4-12) | 0.15 | 73.93 |
| 5 | Inner HTS conductor | 1.98 | 77.89 |
| 6 | Inner HTS conductor binder tape | 0.20 | 78.29 |
| 7 | Inner shield (or screen) | 1.00 | 80.29 |
| 8 | Inner insulation | 3.68 | 87.64 |
| 9 | Outer shield (or screen) | 1.00 | 89.64 |
| 10 | Outer conductor bedding tape | 2.00 | 93.64 |
| 11 | Outer HTS conductor | 1.54 | 96.72 |
| 12 | Outer conductor binder tape (reinforcing and bedding) | 0.15 | 97.02 |
| 13 | Outer quench conductor | 10.11 | 117.25 |
| 14 | Reinforcing binder (not shown in Figure 4-12) | 0.15 | 117.55 |
| 15 | Shield layer (screen) | 1.00 | 119.55 |
| 16 | Outer insulation | 1.84 | 123.22 |
| 17 | Outer shield (screen) | 1.00 | 125.22 |
| 18 | Sheath bedding tape | 0.50 | 126.22 |
| 19 | Sheath (metal) | 3.70 | 133.62 |
| 20 | Over sheath (outer jacket) | 2.00 | 137.62 |

The spreadsheet program permits an optimum transmission voltage to be selected for the specified power transmission level, while achieving the maximum transportable length cable and the minimum number of HTS tapes and minimum material content.

Table 4-1 does not show the number of superconducting wires needed and the number of superconducting layers. The program calculates both of these quantities and then adjusts the structure to have an even number of layers, with the lay of the superconducting turns adjusted to the diameter of the layer. For this cable, there are approximately 500 superconducting tapes in

each of the inner and outer HTS conductors. This number is considerably greater than the capability of existing cabling machines. Either stranding machines with more feed bobbins must be developed or the current-carrying capacity of each superconducting tape must be increased.

4.5 Superconducting DC Cable Fabrication

The anticipated fabrication procedure for the superconducting dc cable is much the same as that for conventional ac cables. However, the extra layers on this cable require several extra steps. Here we assume that all insulation is of the solid-core, dry-extruded type. A similar description could be given if impregnated tape were to be used, and the number of steps would remain the same. In all the steps, cleanliness of the facilities is critical. The slightest metal chip can lead to failure of the cable. Imperfections in the insulation can lead to electric field enhancements that, over time, will cause breakdowns or affect the sensitivity of the cable to over-voltages and voltage changes. Although there are many steps in the fabrication, the process can be separated into 11 stages, as follows:

- Stage 1. The starting point in the fabrication process is the inner mandrel, which is supplied in a cleaned condition on a spool. The mandrel is passed through a stranding machine, where the inner quench conductor, which consists of copper wires, is applied. This conductor stranding machine will look much like the one shown in Figure 4-13. The conductor wires will preferably be applied in one pass. The cable now consists of the mandrel and the inner quench conductor, and it is wound onto a take-up spool. This spool can be stored or moved directly into position to carry out stage 2. If the spool of conductor is stored in this condition, great care must be taken to avoid contamination—in particular, the surface contact among the copper wires and between the copper wires and the superconducting layer that will be applied must be kept in a dry and oxygen-free environment.



Figure 4-13
Conductor stranding machine

- Stage 2. The spool of cable from stage 1 will be placed in position for the cable to enter a strander that applies the inner HTS conductors. Just as for the quench conductor, the superconductor must be applied in several steps. In this case, because the layers alternate in helicity, each layer must be applied from a separate feed head. Because the superconductor tapes are more sensitive to mechanical strain than the copper quench conductor is, it will probably be necessary to apply all the layers during a single pass through a fabrication line, essentially a sequential set of stranding heads. After the final layer is in place, the conductor binding tape and a disposable, protective tape will be applied before the cable is wound onto a take-up spool. To reduce strain on the conductors, these take-up spools can be considerably larger in diameter than the eventual transport drum.
- Stage 3. The spool with the cable on it will be moved to a separate location, where the insulation and shield layers will be applied. This process will be identical to the one described in Section 4.2.1, Conventional Cables. Although the details are different for wet insulation, the purpose of this stage will remain unchanged. The insulated cable will be respooled and transported back to the winding facility.
- Stage 4. The outer HTS conductor will be applied over the insulation. The details will be similar to those for the inner HTS conductor. However, the diameter of the outer HTS conductor is greater than that of the inner HTS conductor, so it will have fewer layers. Because of the sensitivity of the HTS material to strain, the ideal situation would be to go directly to the next stage without respooling. However, this might not be an option. If not, the material must be maintained in a clean, oxygen-free environment before moving to stage 5.
- Stage 5. The outer quench conductor (copper wires) will be applied in the same fashion as for the inner conductor layers in stage 1, and then the cable will be put onto a spool.
- Stage 6. The spool of cable, with the outer conductors in place, will be moved to the location where the outer insulation and shield layers will be applied. The insulated cable will be respooled and transported back to the winding facility.
- Stage 7. The outer sheath bedding tape will be applied, and the cable will be respooled.
- Stage 8. The cable will be taken to a location where the outer sheath will be fabricated onto it. This procedure will likely involve using a sheet of thin stainless steel that is slightly wider than the diameter of the finished cable. This sheet and the cable will move together along a processing line, where the outer jacket will be formed around the cable and then seam-welded to form a continuous tube. The tube will then be deformed by corrugating and compressing its diameter to match that of the otherwise-completed cable.
- Stage 9. The outer, protective layer will be applied over the stainless steel sheath. The completed cable will then be wound onto its transportation drum.

- Stage 10. The following routine factory tests will be performed:
 - Samples of the complete cable will be cut off and cooled down. The resistive properties of both the inner and outer conductors will be measured to verify that the HTS conductors achieve the correct current rating at zero resistance.
 - Samples from each cable will be measured to verify dimensional compliance and material properties. The samples of cable will be taken before and after cooling.
 - On the drum length, the capacitance of the main and outer insulation layers will be measured at room temperature.
 - On the drum length, the electrical resistance of the inner and outer copper wire quench conductors will be measured at room temperature to verify the specified value for the particular cable length.
 - On the drum length, high-voltage test terminations will be fitted. A high-voltage withstand test will be performed on both the inner and outer insulation layers. This test can be a dc voltage withstand test, but preference exists for an ac voltage withstand test, because it would permit the performance of a sensitive partial discharge test to demonstrate the absence of both major and minor insulation damage.
 - The test terminations would be cut off. Pulling eyes would be mechanically connected to each end of the cable—and in particular, to the stranded copper wire quench conductors—for use during cable installation on site. Each end of the cable would be sealed with metal end caps to render the cable completely watertight. The ends of the cable would be tied to the drum flanges. The outer layer of cable would be mechanically protected with a blanket and an outer covering of robust, sheet steel battening.
- Stage 11. At specified sampling frequencies (cumulative manufacturing lengths), longer cable lengths would be cut off for special, destructive sample tests. These tests would be similar to those performed on conventional power cables. Initially, a bending test would be performed. The cable would be cooled, and the resistive properties of both the inner and outer conductors would be measured to verify that the HTS conductors achieve the correct current rating at zero resistance. The routine high-voltage withstand test and an impulse-voltage withstand test would be performed. The cable length would be dissected for dimensional compliance.

5

VACUUM SYSTEM

5.1 Introduction

The vacuum system requirements and possibilities for a superconducting dc cable system are determined by the allowable heat leak into the cryogenic components. The intent of this section is to describe functional criteria that will enable researchers in other areas to integrate vacuum requirements and capabilities with equivalent issues for cryogenics, superconductivity, insulation, ac-to-dc converters, and power system operation. Some of the information in this section is adapted from the EPRI report *System Study of Long-Distance Low-Voltage Transmission Using High-Temperature Superconducting Cable* (see Appendix B).

5.1.1 Overview

Nearly all continuously operating cryogenic systems incorporate a vacuum as a part of their thermal insulation. A vacuum is chosen because the flow of heat in a vacuum is small compared to all other thermal insulating schemes. Vacuums have been used in all superconducting cables to date.

After the decision to use a vacuum for thermal insulation is made, several operational issues must be addressed. First, all materials outgas in a vacuum. If this process is unchecked, the vacuum will degrade with time. Second, most vacuum systems have leaks that permit air or other gases to enter the evacuated volume. In the case of a long superconducting dc cable, gas can leak into the vacuum from the cryogen-containing components, or the ambient-temperature outer container, or both. Limiting the heat flow into the cold region requires controlling both radiative and conductive heat transfer. Achieving a heat transfer of 0.5 W/m along the cable requires a vacuum level of approximately 10^{-4} Torr and the use of multilayer insulation (MLI, sometimes called *superinsulation*) that is composed of many layers of aluminum-coated Mylar film. Unfortunately, MLI has a large surface area and is a major source of outgassing in a vacuum system. Thus, the extent of both outgassing and heat leak are set by the MLI.

The design described in the EPRI report *System Study of Long-Distance Low-Voltage Transmission Using High-Temperature Superconducting Cable* (see Appendix B) proposed a buried outer steel pipe of 70-cm outside diameter (D_o) that is coaxial with a low-temperature superconducting dc cable of 16-cm diameter (D_c), as shown in Figures 5-1 and 5-2. The outside diameter was chosen to allow vacuum pumpdown and maintenance; it can be changed over a wide range without impacting heat leak or outgassing. However, the outside pipe diameter and the vacuum pumpout spacing are interrelated. The cryogenic components for the superconducting dc cable developed in this report are more complicated than those for the design in the EPRI report *System Study of Long-Distance Low-Voltage Transmission Using High-*

Temperature Superconducting Cable (see Appendix B), causing D_C , and in turn D_O , to be larger. For simplicity and consistency, and recognizing the general validity of the earlier EPRI report, the same dimensions are used for vacuum and heat leak calculations in this section.

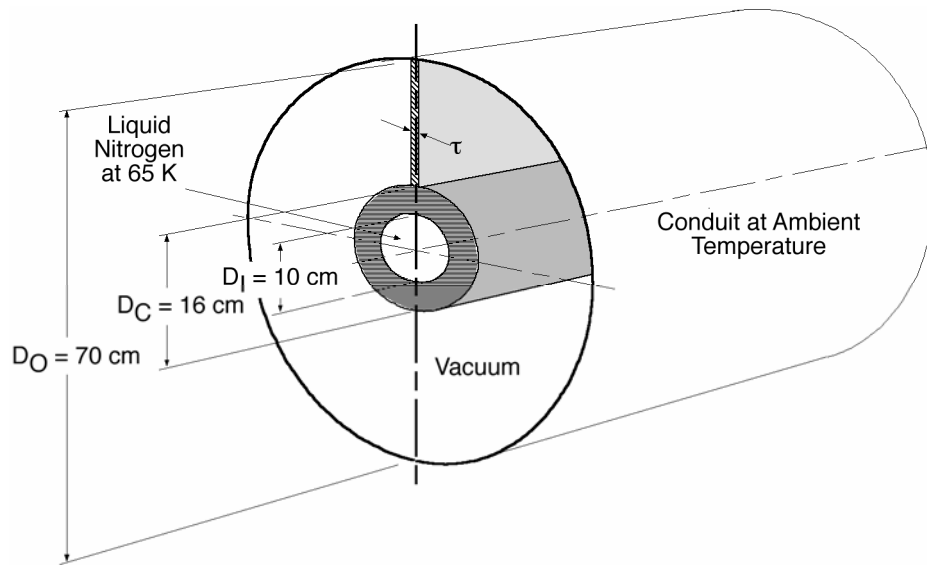


Figure 5-1
Simplified design for cryogenic and vacuum calculations

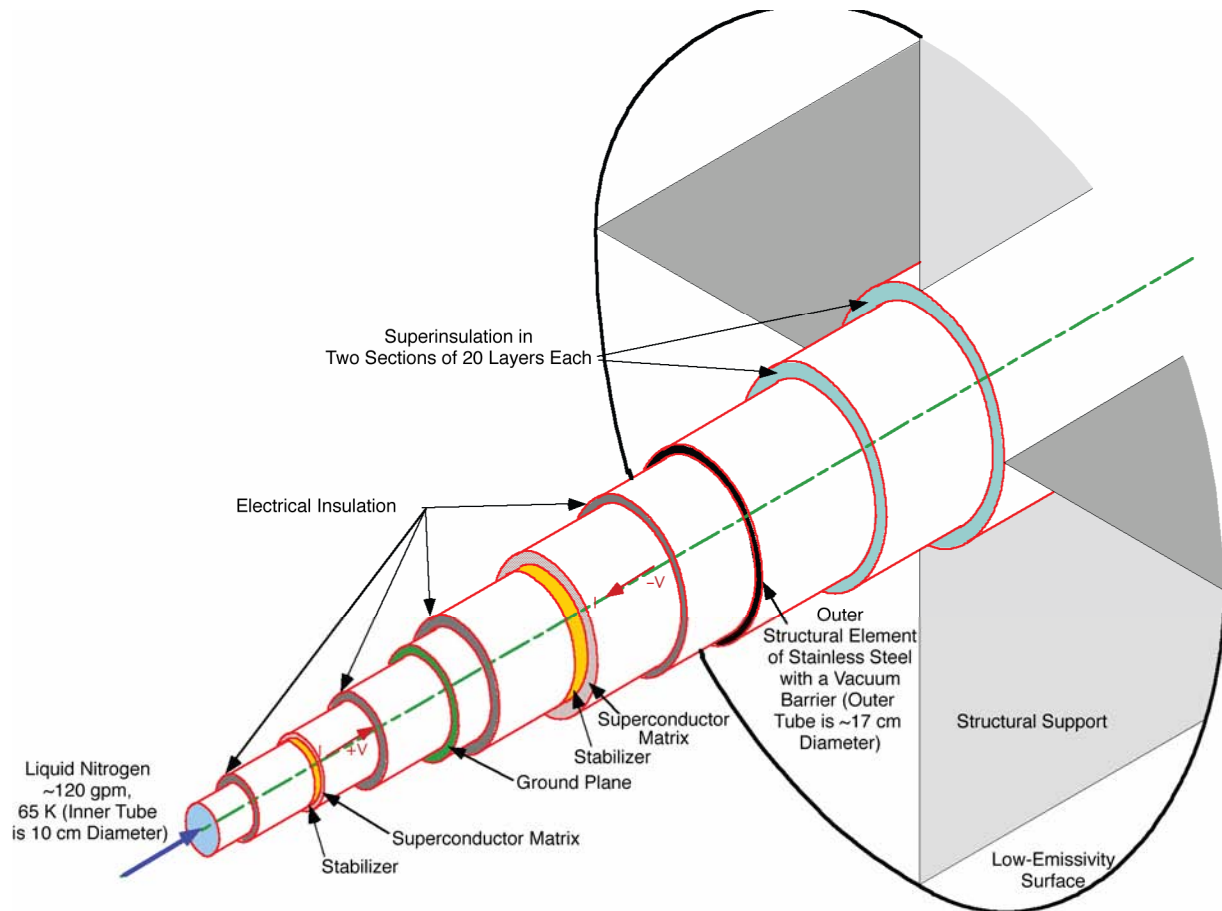


Figure 5-2
Design of the cable developed for the EPRI report *System Study of Long-Distance Low-Voltage Transmission Using High-Temperature Superconducting Cable*

© IEEE 1997; reprinted with permission [17]

Most power cables are designed to have as small an outer diameter as possible. In general, this approach keeps costs down and allows in-factory fabrication of long individual lengths. All superconducting cables fabricated to date are ac and were designed as replacements or upgrades for conventional ac cable. The expected length of such cables is from hundreds of meters to a few kilometers. The superconducting dc cable under development is expected to operate over distances of hundreds to thousands of kilometers. This increased scale demands a reevaluation of several cable system design concepts—in particular, the thermal insulating vacuum.

A critical issue in selecting the operational components of the superconducting dc cable vacuum system is the need for long-term reliability. Vacuum-insulated, flexible transfer lines are the basis for the vacuum thermal insulation in most superconducting ac cables. They are prone to failure and have a known failure rate. This is recognized by the manufacturers in their guaranteed performance. Transfer line reliability was recently investigated by researchers from Oak Ridge National Laboratory [29]. The study found that warranties for 100-m flexible transfer lines were for periods of approximately two years [29]. If this is representative of a failure rate and if it were translated into the performance of a 1000-km cable, the availability would be a fraction of a

percent. The implication is that the technology used for flexible transfer lines is probably not appropriate for long-distance superconducting cables. Addressing reliability in a system as complicated as the superconducting dc cable is beyond the scope of this report, but it must eventually be a part of a detailed design effort.

5.1.2 Heat Input

The heat flow into the superconducting dc cable is dominated by the average internal heat generation and the heat flow per unit length along the cable. This is in contrast to the typical small or short cryogenic or superconducting systems in which heat inputs from power leads and supports are dominant. The superconducting dc cable is also quite different from a superconducting ac cable in which the ac losses associated with current and field changes in the superconductor and associated stabilizer are dominant. This section addresses the calculation of heat flux through the vacuum into the cold portion of the cable; that is, the gaseous heat conduction between the outer pipe and the cold core and the thermal radiation from the ambient temperature outer vessel. The heat input associated with the radiation and convection determine the vacuum requirements for the superconducting dc cable.

5.1.2.1 Heat Conduction by Residual Gas

Residual gas conducts heat from the ambient-temperature outer shell to the cold core. The amount of heat carried depends on the residual gas pressure. Gas molecules collide with the walls of their containers and with each other. During each collision with a wall, the gas molecules approach thermal equilibrium with that wall and have a velocity that is appropriate to its temperature. As a gas molecule moves from a wall, it might hit another molecule, or it might move freely to another wall. The average distance that a gas molecule travels before hitting another gas molecule is called its *mean free path*, the value of which can be calculated from first principles. For example, the mean free path for nitrogen gas at atmospheric pressure and at 0°C is approximately 10 μm . For the geometry described in the EPRI report *System Study of Long-Distance Low-Voltage Transmission Using High-Temperature Superconducting Cable* (see Appendix B), a gas molecule will experience many collisions between the outer shell and the cold core. The mean free path increases as the pressure and temperature decrease. At a pressure of 10^{-5} Torr (0.01 μm , 1.3×10^{-3} Pa, or 1.3×10^{-3} atm), the mean free path for nitrogen gas is approximately 1 m, whereas at 10^{-4} Torr, it is 10 cm.

In terms of transferring heat from one surface to another by gases, there are two physically distinct regimes of interest. The first occurs when the mean free path is much smaller than the distance between the two surfaces. In this case, the heat transfer is almost independent of the pressure (and temperature) of the gas. For example, the heat flow in the annular portion of a superconducting dc cable with nitrogen at atmospheric pressure (300 K to 80 K; that is, greater than the liquefaction temperature of nitrogen) is approximately 200 W/m. The second regime occurs at low pressures, when the mean free path of the gas molecules is approximately the same as or larger than the separation between the two surfaces. This is often referred to as the *molecular flow regime*. Heat transport in this regime is defined by a rather complicated equation

that depends on the gas species (Z), the areas of the cold and warm surfaces, the temperatures of the cold and warm surfaces, the effective temperature of the gas as it approaches a surface, and the ratio of the specific heat of the gas at constant pressure to its specific heat at constant volume, calculated by Equation 5-1.

$$W = 2.426 \times 10^{-4} \cdot A \cdot f(Z, \gamma, T, T_1, T_2) \cdot p \cdot (T_2 - T_1) \quad \text{Eq. 5-1}$$

The real situation is somewhat more complicated than this equation might suggest, because several gas species are present in most vacuum systems. Thus, a composite or approximate equation is required in order to present a simple relationship among the important parameters. Equation 5-2 approximates the heat transfer resulting from residual gas for the superconducting dc cable geometry.

$$W (W / m) = 1.4 \times 10^{-4} \cdot p (\text{Torr}) \quad \text{Eq. 5-2}$$

In practical terms, at 0.01 μm , gaseous conduction contributes approximately 0.14 W/m along the superconducting dc cable.

5.1.2.2 Thermal Radiation

The rate at which energy is emitted per unit area of a surface depends on both its absolute temperature and its emissivity. Similarly, the rate at which energy is absorbed by a surface depends on both the effective temperature of the radiation that pervades the region around it and its absorptivity in the wavelength range associated with this effective temperature.

Thus, radiation transfers energy between and among surfaces. The net energy flow is from hotter surfaces to cooler surfaces. In the case of the superconducting dc cable, radiative heat transfer is from the ambient-temperature outer shell to the conductor core. The heat that is transferred (in J/s or W) is calculated by Equation 5-3, where ε is the emissivity of the surfaces, σ is the Stefan Boltzmann constant ($\sigma = 5.67 \times 10^{-12} \text{ W cm}^{-2} \text{ K}^{-1}$), and A is the area of the surfaces.

$$W = \sigma \cdot \varepsilon \cdot A (T_{\text{ambient}}^4 - T_{\text{cold wall}}^4) \quad \text{Eq. 5-3}$$

Equation 5-3 is only approximate, because the two surfaces of the superconducting dc cable have different areas and emissivities. However, if the emissivity is approximately 0.3 for each surface and, making a small correction for the coaxial case, the heat transfer is 75 W/m^2 , this translates to approximately 45 W/m of length along the cable, which is much too high. This heat input is essentially unchanged over the possible range of operational temperatures, from approximately 40 K to 80 K.

To reduce the heat flow to the core, it is necessary to install some type of radiation-absorbing material. Several approaches have been used for other cryogenic systems and are available for the superconducting dc cable, including the following:

- Low-thermal-conductivity solid foam in the annular space
- Low-thermal-conductivity particulates in a gas in the annular space
- Low-thermal-conductivity particulates in a vacuum in the annular space
- Low-emissivity surfaces on the ambient and cryogenic walls and a vacuum in the annular space
- MLI (multiple layers of aluminized Mylar film) in a vacuum in the annular space

Insulation materials such as foam or particulates not only affect thermal radiation but also reduce gaseous conduction. Experiments with foam indicate that the heat transfer is approximately 50 W/m^2 —a reduction from the 400 W/m^2 for air at 1 atm, but still much too high for the dc transmission line. The heat flow through particulates, even in a vacuum, is similar to that for the solid foam. Thus, the only solution is to use a vacuum, to coat the inner and outer surfaces in order to reduce emissivity, and to use MLI.

Reducing the emissivity of the inner and outer surfaces to 0.02 decreases the heat transfer to approximately 3 W/m , still higher than the acceptable level of 1 W/m for all contributions. This can be reduced further by adding MLI (layers of aluminized Mylar film).

MLI is composed of several extremely thin ($\approx 0.01 \text{ mm}$) layers of aluminum-coated Mylar film. The combination of low surface emissivity in the layers limits the total radiative heat transfer. The reduction is approximately inversely proportional to the total number of layers, n , of material. If 0.1 W/m is budgeted for radiation, at least 31 layers are required, as shown by Equation 5-4:

$$Q = \frac{Q_{\text{initial}}}{n-1} \text{ alternatively, } n = 1 + \frac{Q_{\text{initial}}}{Q} = 1 + \frac{3}{0.1} \rightarrow 31 \quad \text{Eq. 5-4}$$

Because 40 layers are often used, that number is selected here. This number of layers provides the maximum insulation in a single layup. More layers tend to reduce the insulating effect, because their weight crushes them and causes layer-to-layer contact. A bat made of 40 layers of aluminized Mylar film has a thickness of approximately 1 cm.

5.1.2.3 Combined Radiation and Gaseous Convection

Having gone through the logic and the mechanisms, it is time to refer to some practical data. Several measurements of the combined heat transfer from these combined mechanisms of radiation and gaseous conduction have been made for space and high-energy physics applications [30]. The heat flux from ambient temperature to 77 K decreases to approximately 0.5 W/m^2 (0.3 W/m along the superconducting dc cable) with 40 layers of MLI and a gas pressure of 10^{-5} Torr. These values are only slightly higher than the theoretical values, and there is little further decrease for higher vacuums. At a vacuum of 2×10^{-4} Torr, the heat flux increases

to approximately 0.75 W/m^2 . Achieving 10^{-4} Torr is considerably less expensive than achieving 10^{-5} Torr, and it takes less time. Therefore, a vacuum of 10^{-4} Torr was used for the calculations in the EPRI report *System Study of Long-Distance Low-Voltage Transmission Using High-Temperature Superconducting Cable* (see Appendix B), with the commensurate combined heat load from radiation and gaseous conduction of 0.5 W/m .

5.1.3 Some Units Used in Vacuum Systems

Different vacuum requirements exist for a variety of applications, and various units have been established for low-pressure systems. The International System of Units (SI) unit of pressure is the pascal, Pa. The pascal is the pressure that would exist if 1 kilogram of force were uniformly applied over 1 square meter ($1 \text{ Pa} = 1 \text{ kg/s}^2/\text{m}$). This unit is slowly coming into use in the area of vacuum technology. However, vacuum pressures and the capabilities of pumps and getters are often given in Torr or some other unit. The following relationships will be of use in understanding the material in this section.

- 1 atmosphere (atm) = 101325 Pa
- 1 Torr = 133.32 Pa
- 1 mm Hg = 133.32 Pa
- 1 bar = 100,000 Pa
- 1 psi = 6894.8 Pa
- 1 Pa = 0.0075 Torr
- 1 gram-mol = 22.4 liters at standard temperature and pressure (1 atm and 20°C)

5.2 Getters

This subsection describes *getters*, vacuum technology components that are in widespread use today. These components are highly effective in maintaining vacuums for many applications. However, they have limitations that affect their use as the sole element of large vacuum systems.

5.2.1 Purpose

Nonevaporable getters are typically used to maintain a high vacuum in hermetically sealed systems of various kinds. They are often used for high-temperature and cryogenic systems. In the latter case, they are typically placed in the room-temperature region of the vacuum system. They are most effective as components in applications that meet the following criteria:

- The vacuum system will be hermetically sealed for the life of the getter.
- The possibility of a leak in which air or other gas enters the system unchecked over the entire life of the system is zero.
- There is limited accessibility to the vacuum region (for example, to install or use a vacuum pump).
- Electric power is available for reactivating the getter (heating at a measurable temperature).
- The getter is not in thermal contact with heat-sensitive materials such as Mylar film.

Getters are used in a variety of applications with similarities to the superconducting dc cable. For example, many cryogenic systems including long transfer lines use getters in some way. A major advantage of getters is that they do not require electrical power during normal operation. A major disadvantage is that their ability to absorb gaseous molecules is rather limited (see Section 5.2.3, Function and Operating Characteristics).

Getters adsorb a variety of gases in a vacuum environment. Their capabilities depend on the type of material used and the species of gas in the vacuum. By far the greatest use of getters is to remove hydrogen, which outgasses from most materials (including plastics and steels) in low-pressure and vacuum environments. Getters also remove atmospheric gases and vapors from packaging materials that have desorbed from surfaces within the vacuum chamber. At a modest level, they can remove these and other gases that enter the system by diffusion through porous structures or microleaks.

5.2.2 Composition

Getters are made of structured materials that have a large surface area per unit volume and per unit mass. Several companies make getters, and most of them use combinations of the elements calcium, zirconium, iron, vanadium, palladium, cobalt, aluminum, and some of their oxides. The exact mixture and structure are usually proprietary. Exceptions are special cases in which the main impurity in the vacuum space is a specific gas or when operation is at a low temperature. For simplicity, this subsection focuses on getters that are available from SAES Getters Group, one of the main suppliers worldwide.

5.2.3 Function and Operating Characteristics

Getters adsorb gases that enter a vacuum system, typically one that is hermetically sealed. They are fabricated and transported in an inert atmosphere and are carefully positioned within the vacuum system before it is evacuated. Most vacuum systems are purged with an inert gas, typically argon or dry nitrogen, before operation. After the vacuum is established by a pump of some sort (see Section 5.3, Vacuum Pumps), the getter is thermally activated by a resistance heater.

The internal activation process depends to some degree on the getter material and its form and size. The SAES St707 getter is used as an example here because, except for nitrogen, it removes most of the gases that will be encountered in a superconducting dc cable. The St707 is a ternary alloy of nominally 70% zirconium, 25% vanadium, and 5% iron. It is available in many shapes and sizes, up to approximately 1000 mg. These getters are sold in various forms, including some with embedded heaters for activation. The St707 getters are designed to operate at temperatures of 20–200°C. However, they can operate at lower temperatures with a slightly modified performance. After they are installed, they must undergo high-temperature activation, which removes a thin, protective, passivation film. The ideal activation temperature is 450°C, which must be maintained for 10 minutes. If activation is attempted at temperatures less than 400°C, full activation cannot occur. For example, after 1 hour at 300°C, only 70% of full activation is

reached. Because getters typically operate in a fully sealed environment, they are often activated before the vacuum reaches the desired operational level—for example, when 99.9% of the air is removed—and they can assist in the final stages of pumpdown.

The St707 getter material can operate continuously at a temperature of about 200°C, at which level adsorbed gases are mobile within the material and diffuse into the bulk of the getter. When operated at a lower temperature, as they would be in an superconducting dc cable, the rate of diffusion is reduced. Depending on the amount of gas to be removed from the system, the getter might have to be reactivated, which requires heating at 450°C for 10 minutes, the same as for the initial activation.

Getter materials become saturated with residual gas molecules after some amount of exposure. As this occurs, even with reactivation, their ability to maintain the desired vacuum decreases. The total capacity of a getter depends on the species of gas to be removed. The most frequent material to be removed is hydrogen. One gram of the St707 getter material can adsorb approximately 0.01 grams of hydrogen gas. At this level, some embrittlement occurs in the bulk of the getter material. Further, as the getter is heated for reactivation, part of the hydrogen is released. Whereas reactivation is required for an St707 getter with some gas species, hydrogen and its isotopes diffuse fully into the body of the getter at ambient temperatures. Many getters are affected by extended exposure to air after they have been activated. Thus, these components must be protected or isolated in systems where repairs are expected.

5.2.4 Potential Use in Superconducting DC Cables

Several issues must be considered in the assessment of the use of getters in a superconducting dc cable. These issues include the following:

- A determination of the amounts and types of gas that will exist in the vacuum space
- Getter capacity and spacing in the vacuum area
- Getter cost
- The probability of significant leaks into the vacuum system
- Avoided vacuum pump operational cost
- The expected life of the cable
- The possible incidence of repairs; in particular, those allowing air into the vacuum space
- The need to make electric power available to activate and reactivate the getters
- Getter replacement when saturated or otherwise failed (getters are usually sized so that their longevity is greater than the expected system life)

At this time, there is no certainty that getters could be effective in the superconducting dc cable vacuum system. However, these issues must be addressed as part of an assessment of a cable design, perhaps as part of a trade study that includes some statistics gleaned from operation of

superconducting ac cables that are now being installed. Oak Ridge National Laboratory researchers concluded that, excluding leaks, ensuring a 20-year life for a 100-m section of hermetically sealed cable would require approximately 300 grams of a getter material similar to the St707 getter [29].

5.3 Vacuum Pumps

5.3.1 Purpose

Obviously, vacuum pumps are used to produce a vacuum. However, this simple statement belies the wide variety of applications in which special vacuum pumps are used. For example, vacuum pumps are used in the following applications:

- In the food industry for food desiccation and as part of the freezing processes
- In the manufacture of semiconductors
- In hazardous gas (fume) removal applications
- In autoclaves for a variety of applications
- In the impregnation of wood and other products

The use of vacuum pumps in cryogenics is a small piece of a large business. Fortunately, the range of applications for vacuum pumps and vacuum systems provides the cryogenic and superconducting industry with a choice of pumps that can be used for a range of vacuum levels and capacity.

In the areas of superconducting technology, vacuum systems are used mainly in the thermal insulation systems for superconducting magnets. A large number of vacuum pumps are used for magnetic resonance imaging systems. However, the pumps and vacuum systems used for superconducting accelerators, which may exceed 50 km in length, provides the closest parallel for the needs of the superconducting dc cable. Even though there are similarities, the accelerator magnet systems use liquid helium, the temperature of which is so low that all gases in the vacuum condense on the surface of the cryogenic enclosures, thus providing a cryogenic vacuum pump. Although they are similar at some level, superconducting accelerators and the superconducting dc cable have quite different vacuum requirements.

5.3.2 Types

There are two ways to describe the type of vacuum pumps available. One is to address the level of vacuum that the pump can maintain, and the other is to describe the dynamic, electromechanical structure of the vacuum pumps. The level of vacuum seems more appropriate for this report, although knowledge of the electromechanical structure is required for cost optimization and the detailed design process. Some vacuum pumps can operate over wide pressure ranges. However, most pumps operate more effectively and efficiently over limited pressure ranges; for example, some pumps are effective between approximately 1 atm and 1 Torr, whereas others operate best at considerably lower pressures. The common practice in cases in which vacuum levels of 10^{-2} to 10^{-5} Torr are needed is to use a roughing pump to reach the 1 Torr pressure region and then to operate another pump, a high-vacuum pump, that continues the evacuation to the desired pressure. The high-vacuum pump might be required to operate continuously to maintain the vacuum at the desired level. In some cases, a roughing pump must be used on the output of the high-vacuum pump to achieve or maintain the desired vacuum.

The most significant factor in selecting the configuration of vacuum pumps will be a life-cycle cost optimization. This will be a tradeoff between the initial capital cost, efficiency, and the long-term operation and maintenance costs, with reliability as another significant component.

5.3.3 Pumping Speeds and Pressure Drop

Most applications that require a vacuum impose the following three general requirements on the vacuum system design:

- The maximum allowable operating vacuum pressure (P_{max}) at one or more critical points or regions in the system. A variety of mechanical and structural issues affect the choice of this location and the magnitude of this parameter. In cryogenic systems, however, the allowable heat leak usually determines this pressure.
- The amount of gas (Q) to be removed. This quantity can be expressed in several forms. For example, a small crack or weld flaw might result in a leak that allows the entry of 10^{-5} grams per second of nitrogen into a vacuum system. Equation 5-5 converts this value into 0.0053 Torr-L/s.

$$10^{-5} \text{ g/s} = \frac{10^{-5}}{32} \text{ moles/s} = \frac{22.4 \cdot 10^{-5}}{32} \text{ atmosphere} \cdot \text{L/s} = \frac{760 \cdot 22.4 \cdot 10^{-5}}{32} \text{ Torr} \cdot \text{L/s} \quad \text{Eq. 5-5}$$

- The time required to achieve the operating pressure. (The value of Q for the initial pumppdown is essentially the total mass of gas in the region to be evacuated, which is the product of the density of the gas and the volume. A separate value of Q might be appropriate for continued operation of the system.)

The vacuum system designer can control the following three main parameters to meet these demands:

- The pumping speed or capacity of the vacuum pump. Pump speed, S_p , is typically specified in liters per second (L/s). The magnitude of S_p for a specific pump is a function of the inlet pressure. Under some circumstances, it also depends on the type of gas to be removed.
- The minimum allowable pressure, P_p , at the inlet to the pump—generally, $P_p \ll P_{max}$. Because not all pumps achieve the same minimum pressure, the value of P_p determines the type of pump.
- The conductance, C (specified in L/s), of the path between the pump and the location at which the vacuum is critical. The greater the effective transverse dimensions of the path, the greater the conductance; the longer the path, the lower the conductance. In practice, this quantity can be set only by some tradeoffs with other system design characteristics.

These parameters can be related by sets of equations. There are several ways to set up the definitions and the equations; the method used in this subsection allows the parameters to be expressed in general forms, independent of the fact that C and S_p change with pressure.

The relationship between the amount of gas to be removed, Q , the pump speed, S_p , and the pump inlet pressure, P_p , is given by Equation 5-6.

$$P_p \cdot S_p \geq Q, \text{ which is often written as } S_p \geq \frac{Q}{P_p} \quad \text{Eq. 5-6}$$

There is a pressure drop along the path from the region of critical pressure to the pump. The conductance along that path must allow the quantity of gas to flow without an excessive pressure drop (see Equation 5-7).

$$C \geq \frac{Q}{P_{\max} - P_p} \quad \text{Eq. 5-7}$$

To express this in a general form, the pumping speed at a location distant from the pump is defined by Equation 5-8.

$$S = \frac{Q}{P} \quad \text{Eq. 5-8}$$

This allows the calculation of the pumping speed at any location, including at the critical location; that is, where $P = P_{\max}$ (see Equation 5-9).

$$S_{\text{crit}} = \frac{Q}{P_{\max}} \quad \text{Eq. 5-9}$$

If the gas flow is too great, the local pumping speed will not be adequate to achieve the desired pressure.

Assuming that the state of equality in Equations 5-5 through 5-9 allows the determination of the pressure at the critical location, knowing only the pumping speed, S_p , the pressure at the inlet to the pump, P_p , and the conductance of the path to the pump, C (see Equation 5-10).

$$P_{\max} = P_p \left(\frac{S_p}{C} + 1 \right) \quad \text{Eq. 5-10}$$

Further, to the extent that C is not a function of the pressure, the pumping speed at the critical location, S_{crit} , is determined by S_p and C (see Equation 5-11).

$$S_{\text{crit}} = \frac{S_p C}{S_p + C} \quad \text{Eq. 5-11}$$

If there are multiple parallel paths through which the gas can be removed, the conductances of these paths are additive (see Equation 5-12).

$$C_{\text{total}} = C_1 + C_2 + C_3 + \dots \quad \text{Eq. 5-12}$$

When there are sequential paths, the net conductance is given by Equation 5-13.

$$\frac{1}{C_{\text{total}}} = \frac{1}{C_1} + \frac{1}{C_2} + \frac{1}{C_3} + \dots \quad \text{Eq. 5-13}$$

5.4 Superconducting DC Cable Vacuum Issues

There are two quite different regimes in the operation of most vacuum systems, including that for the superconducting dc line: initial evacuation and vacuum maintenance.

An initial pumpdown procedure based on the allowable time to reach operational conditions for the cryogenics was established in the EPRI report *System Study of Long-Distance Low-Voltage Transmission Using High-Temperature Superconducting Cable* (see Appendix B). To the extent that the general design of the superconducting dc cable will be similar to that of the earlier design, there will be little need to change this aspect of the design. However, the roughing pump chosen in that report was sized to pump down the system in 10 hours. Today, this appears to be much faster than needed, so a smaller pump should be adequate.

To assess the procedures and requirements for vacuum maintenance, it is necessary to establish the pressure increase that will occur along the superconducting dc cable at various distances from a vacuum pump. This was not addressed specifically in the EPRI report *System Study of Long-Distance Low-Voltage Transmission Using High-Temperature Superconducting Cable* (see Appendix B); it is described briefly in Section 5.4.2, Residual Gas, Outgassing, and Leaks. Some possible scenarios for vacuum operation are presented in Section 5.4.3, Superconducting DC Cable Vacuum Pump Capacity and Spacing.

5.4.1 Conductance and Pressure Drop in a Vacuum System

There are two different regimes for the flow of gases in a tube: a high-pressure regime and a low-pressure (or molecular-flow) regime. In the high-pressure regime, the mean free path of the gas molecules is short compared to the transverse dimensions of the tube. This is the situation at atmospheric pressure and at the beginning of the pumpdown. Collisions among gas molecules drive them from higher- to lower-pressure areas. In the low-pressure or molecular-flow regime, the mean free path is on the order of or greater than the transverse dimensions of the tube. To achieve an acceptably low heat flow into the cryogenic portion of the cable, it will be necessary to maintain pressures of approximately 10^{-4} Torr. The mean free path for gas molecules at ambient temperature at pressures of 10^{-4} Torr and 10^{-5} Torr are 10 cm and 1 m, respectively. Therefore, when the cable is cold, the gas flow in the annular space between the outer tube and the MLI on the outside of the cold portion of the cable is in the molecular-flow regime; that is, the molecules diffuse through a probabilistic process determined by collisions with the walls. The process is such that some molecules, through their random motions, arrive at the location of the vacuum pump and are removed from the system. The conductance of a tube in this regime is described by Equation 5-14, where the length, l , and the effective hydraulic diameter, d , are given in centimeters.

$$C(L/s) = 12.2 \cdot \frac{d^3}{l + 1.33 \cdot d} \approx 12.2 \cdot \frac{d^3}{l} \quad \text{Eq. 5-14}$$

Calculating the conductance for the coaxial cable geometry is straightforward, but it requires an estimate of the effective hydraulic diameter. Determining the hydraulic diameter of annular systems requires some detailed knowledge of the separators and supports for the inner tube. An effective approximation for the superconducting dc cable design is that it is composed of four quadrants, each with an effective hydraulic diameter of 20 cm. Thus, in the molecular flow regime, the conductance of a 1-km section of the superconducting dc cable is approximately 4 L/s.

For completeness, the conductance in the high-pressure regime is given by Equation 5-15.

$$C(L/s)_{Low_Vacuum_Air} \approx 190 \cdot \frac{d^4}{l} \cdot \frac{(P_{max} + P_p)}{2} \quad \text{Eq. 5-15}$$

At a pressure near atmospheric, and assuming a minimal pressure drop along the pipe, C is approximately 10^5 L/s for the cable cross section. The implication is that pumpdown time is determined by the capacity of the vacuum pump, not by the dimensions of the tube itself.

5.4.2 Residual Gas, Outgassing, and Leaks

To understand the maximum pressure in the vacuum during operation, it is necessary to estimate the outgassing and the maximum leak that can occur while maintaining normal operation. There are no hard and fast rules for this process. However, a number can be derived based on a few reasonable assumptions.

The MLI in the vacuum space has a large surface. Before the system is evacuated, this surface is exposed to the atmosphere, and it adsorbs essentially all gases—in particular, water, nitrogen, and oxygen—in the atmosphere. In addition, during its formation and handling, hydrogen not only adsorbs on the surface but also can penetrate the interior of the material. Further, the inner surface of the outer pipe will adsorb gases, and steel is known to outgas hydrogen for long periods.

5.4.2.1 Water Vapor and the Need for Purging with a Dry Inert Gas

At 27°C and 100% relative humidity, the vapor pressure of water is 24.8 mm Hg; that is, water constitutes approximately 3.4% of the total pressure. This can be translated into a mass of 1 kg of water per 100 m of length of the cable's open space before evacuation. This is a primary reason for the use of a dry, inert gas. The superconducting ac cables being developed today would have a few grams of water per 100 m if they were not desiccated. Even if the system has been kept as dry as possible, water adsorbs to the walls of the vessels and to the MLI and its interlayer spacers. The result is that 100 m of superconducting ac or superconducting dc cable can easily store a gram of water that will slowly desorb from the surface over the life of the cable. Oak Ridge National Laboratory researchers estimated that a 100-m section of superconducting ac

cable could require 3 or more grams of gas removal over a 20-year life [29]. We use this number as appropriate for the superconducting dc cable, as well. It would be reasonable to use a slightly larger number because of the larger pipe. However, there is essentially the same volume of MLI, which is the real culprit.

The 3 grams of gas per 100 meters means 30 grams per kilometer. This is essentially 1 mol of air, or approximately 22.4 liters of material, at standard temperature and pressure. Assuming it releases uniformly over 20 years (6×10^8 s) at an average gas pressure of 10^{-4} Torr, the rate of gas entering the system is approximately 0.3 L/s/km. This is a relatively small number, which will not seriously tax the capability of a small, high-vacuum pump. If this were the only input to the system and if there would be no need to open the system for repairs, getters might be adequate. However, all large and extended vacuum systems leak.

5.4.2.2 Leaks

Because of improved fabrication processes, the number and size of leaks in welded structures is decreasing, but they still exist in all large systems. Here we assume that some of the 1-km sections will have leaks of up to 0.001 cubic centimeters of air per second. This will amount to 600 L, or 1 kg, over the 20-year life of the cable. Equivalently, a leak of this magnitude introduces 300 times as much material as the outgassing. The immediate conclusion is that this type of leak is beyond the capacity of any practical getter installation because the mass of getter material must be approximately 100 times the mass of the gas to be removed.

By combining the leak and the outgassing, it is possible to calculate the required speed of the vacuum pumps. The combined gas flow, Q , is approximately 8 L/s at 10^{-4} Torr, which—conservatively—must be the pumping speed at the location of the leak. We assume that the separation between pumps is 1 km, and we further assume a worst-case situation in which this leak occurs at the end of a 1-km section and the vacuum pump in this location has failed. That is, the leak must be accommodated by the action of two pumps, each a distance of 1 km away. A hasty conclusion would be that we were quite clever (or perhaps lucky), because the sum of the two conductances is exactly 8 L/s. However, Equation 5-16 suggests that the conductance must be considerably greater than the volume of gas leaking into the system, unless the pumping speed of the pump is so great that $P_p \equiv 0$.

$$C \geq \frac{Q}{P_{\max} - P_p} \qquad \text{Eq. 5-16}$$

A possible solution is to allow the pressure to increase in those regions where there is a leak and where a pump has failed. We select a value of 2×10^{-4} Torr as the allowable vacuum in certain regions, because an increase to this pressure does not significantly increase the heat leak. The main factor is that the mass of gas is the same, and its volume, gas at pressure, has been reduced by a factor of two, to only 4 L/s, half of which must flow in each direction. This requires a pumping speed of 2 L/s in each direction at the high-pressure location. Because the pressure will decrease as it approaches the vacuum pumps, they must each have 4 L/s capacity at 10^{-4} Torr. The relationship among these variables is given by Equation 5-17.

$$P_{\max} = P_p \left(\frac{S_p}{C} + 1 \right)$$

Eq. 5-17

5.4.2.3 Impact of Cryogenic Surface on Gas Adsorption and Freezing

The surface of the cryogenic enclosure for the superconducting dc cable will operate at approximately 70 K. Most materials are solid at this temperature, and they will condense on the surface if they reach it. The vacuum space between the pipe and the outer layer of MLI will be at ambient temperature. Natural gas diffusion will allow most of the molecules to drift to the vacuum pumps, but some will be collected on the cold surface. Carbon monoxide, carbon dioxide, methane, and water will tend to freeze at the cryogenic surface. In principle, this is not an issue during operation because the condensation will be gradual and is not likely to produce a thick layer of material. When the system is warmed, the gases will probably evaporate and affect subsequent pumpdowns. A detailed assessment of this issue is an appropriate task for a more detailed design effort.

5.4.3 Superconducting DC Cable Vacuum Pump Capacity and Spacing

Several factors influence vacuum pump capacity and spacing. The most notable determinant in spacing is the length of the cable section. That value will be determined by a variety of manufacturing considerations. It is clear from Equations 5-16 and 5-17 that shorter section lengths will improve the vacuum situation. In addition, there is some effort on the development of good thermal insulation that can operate at somewhat higher pressures.

A 1-km spacing of the vacuum pumps was selected as a first estimate for calculations. It might be too long, but it is of the correct order of magnitude. The calculations in Section 5.4.2, Residual Gas, Outgassing, and Leaks, showed that a pump speed of 4 L/s would be needed at each end of a 2-km section in which there was a leak and in which a pump had failed. However, the functioning pumps must also remove gas from the other direction. Therefore, the pumping capacity at each 1-km section must be twice the pumping speed calculated, or 8 L/s. To determine the purchased pump capacity for a system, one must apply a rule of thumb based on experience. The rule is simple—always multiply the calculated pumping speed by a factor to determine the installed pump size. At 10^{-4} Torr, the acceptable multiplier is 6, which is a product of the factor of four for unknowns and a factor of one and one-half for pipe bends and other effects. Therefore, each high-vacuum pump should have a capacity of 50 L/s at 10^{-4} Torr.

Although this is not repeated while going through each calculation, every other vacuum pump could fail, and the system could still operate at the absolute worst pressure of 2×10^{-4} Torr. Further, if getters are included in each section and if there are no leaks, the vacuum pumps could be turned off to decrease power consumption and thus improve overall efficiency.

5.5 Conclusions and Observations

5.5.1 Comparison of These Results to the Previous Study

Many of the design features described in the EPRI report *System Study of Long-Distance Low-Voltage Transmission Using High-Temperature Superconducting Cable* (see Appendix B) appear to be reasonable as part of a conceptual design. However, calculations show that several components of the earlier design were over-specified. In particular, a mechanical pump with a capacity of 300 L/s was chosen for initial pumpdown of each 1-km-long section, and a 100 L/s turbo or ion pump was selected for further pumpdown to reach operational conditions and vacuum maintenance. The calculations in this section suggest that the mechanical pump can be much smaller, with the only impact being a longer evacuation period. Because cable installation is likely to require many months, the initial evacuation could occur over several days rather than in the 10 hours planned in the earlier EPRI report (see Appendix B). One might safely choose a 50 L/s mechanical pump or—because the conductance of the vacuum space is so great at high pressure—increase the separation between roughing pumps. The certainty of air leaks in such a large system implies that getters will not provide an adequate vacuum over the life of the cable.

The need for adequate conductance of the gasses in the vacuum space implies that a large outer diameter pipe will likely be required in order to ensure sufficiently low heat leak into the cryogenic and superconducting tubes. The 70-cm value chosen for the earlier EPRI report (see Appendix B) still appears to be reasonable, but a larger pipe would be better and might allow easier maintenance.

High-vacuum pumps with capacities of approximately 50 L/s at 10^{-4} Torr, spaced every 1 km, should provide reliability, in that every other pump could fail and the design vacuum of 2×10^{-4} Torr still be achieved. These pumps are approximately one-half the capacity of those chosen in the earlier EPRI report (see Appendix B). Because the conductance of the piping is limited in the high vacuum range, the separation between these pumps cannot be increased. However, it is possible that not all these high-vacuum pumps will be needed during normal operation. Assuming continuous pressure monitoring at every pump location, it might be possible to operate many of these pumps only when needed. Those pumps in areas adjacent to vacuum leaks would still have to operate continuously.

5.5.2 Issues for the Next Stage of Vacuum System Design

Both capital cost and operations and maintenance cost for various types of vacuum pumps will be required to carry out a trade study that includes life-cycle cost for the overall system. Neither the mechanical pumps nor the high-vacuum pumps are required to operate continuously. Therefore, the operating cost of the electrical power to these pumps could be avoided or reduced considerably.

The design is based on known (in fact, conservative) characteristics of heat flow through the MLI. At some point, it will be necessary to explore MLI in more detail, to compare its performance with other types of insulation, and to assess the required vacuum levels. Reducing the vacuum requirement would allow either fewer pumps or greater separation between pumps.

Although they are not specifically a vacuum issue, the supports for the cold mass and the ability to accommodate the forces associated with pulling the cable into the cryogenic tube must be explored. The struts that transfer these forces must cross the vacuum space and must not increase the heat transfer associated with the vacuum.

6

CRYOGENICS

6.1 Introduction and Summary

6.1.1 Introduction

The cryogenic issues and requirements for the superconducting dc cable fall into the following technical areas, which can be addressed more or less independently:

- Heat flow into the cold mass
- Cooling requirements of the cold mass
- Method of cryogen flow along the cable
- Separation distance between refrigeration stations
- Refrigerator technology selection

Heat flow into cryogenic systems is quite well understood, and there is a large experience base associated with the flow of liquid and gaseous cryogens. Therefore, the first four areas can be subjected to engineering analyses that apply as well today as they will some years from now when a cable is constructed. The cable and vacuum designs presented in this report have been used to calculate cryogenic requirements. The overall design of the cryogenic system is based on these calculations and known characteristics of cryogenic fluids and materials at cryogenic temperatures. The calculations and the resulting characteristics of the cryogenic portion of the cable design are described in this section.

Cryogenic refrigeration technology, however, is a moving target. In many regards, that uncertainty works to the advantage of the future of most superconducting applications, including the superconducting dc cable, because several manufacturers are actively working to improve refrigeration technology. Much of that effort is being carried out on devices whose capacities are less than the 5–20 kW that will be needed for each cryogenic station for the superconducting dc cable. However, when the cable technology is fully developed, these improved refrigeration stations will be developed by using the advanced refrigerators, either individually or in combination, to provide optimized systems. Selection of the refrigeration station technology will be based on a combination of factors and will be judged primarily on the basis of reliability and life-cycle cost.

An initial part of this assessment for the superconducting dc cable cryogenics was a review of the EPRI report *System Study of Long-Distance Low-Voltage Transmission Using High-Temperature Superconducting Cable* (see Appendix B). The superconducting dc cable concept has several significant technical differences from the earlier cable, which was designed to deliver power generated at one site to another site at a distance of 1000 miles. A brief economic evaluation resulted in the choice of a large liquifier at the power source and unidirectional flow of the cryogen—liquid nitrogen—to the power delivery end. The decision to have multiple power access points along the superconducting dc cable requires an approach for cryogen flow that is quite different. The choice of multiple power feeds and sinks suggests that a better solution is to have the cryogen flow in two paths within a single, large vacuum pipe. One flow path (referred to as the *go path*) is in the pipe called the *cryogenic enclosure*, which contains the cable body. It is possible that the cryogen will permeate the cable, as well. That design detail will be determined during later phases of the design, and the decision will likely be determined by electrical rather than cryogenic factors. The second flow path (referred to as the *return path*) is through a separate tube called the *return tube*. The cryogenic enclosure and the return tube are within the same vacuum and MLI space. However, the thermal contact between the two pipes is a design parameter that must be well controlled because it can affect the maximum temperature along the cable (see Section 6.3.4, Counterflow Heat Exchange).

A Fortran code was developed in collaboration with Oak Ridge National Laboratory staff to aid in the calculations for the cryogenics of the superconducting dc cable. This code is based on other calculations of cryogen flow in long tubes for a variety of applications at the Oak Ridge National Laboratory. The core element of this code is a commercial database, GASPAK. The code that was developed generates a DOS (disk operating system) executable file, DC_CAB200, which calculates various characteristics of the cryogenic system based on properties of cryogenic fluids, heat inputs to the system, cable layout, and cable dimensions.

This report generally uses units from the International System of Units (SI); however, some other units are used extensively in the industrial gas and cryogenic design communities. In particular, two non-SI-derived units of pressure—atmosphere and Torr—are used. The atmosphere (atm) is used in the discussion of nitrogen pressure (1 atm = 0.101 MPa), and the Torr is used to describe the quality of the vacuum (1 Torr = 133 Pa). These units are used in this report because most design tools for gas flow and cryogenic systems are based on them. In addition, the input and the output of existing programs, including DC_CAB200, are in these units.

6.1.2 Summary

Many tradeoffs are possible in the design of the superconducting dc cable. The goal of this section is to develop a design that is an engineering possibility. Four somewhat arbitrary design choices must be made in the cryogenic characteristics of the line. These are described in an order that is likely to be more easily grasped than the more logical process presented in the rest of this section. In each of these areas, the nominal design point is presented. Because the cable will be quite long and will traverse several different environments, the parameters will likely vary over a considerable range during construction.

6.1.2.1 Refrigerator Station Separation

The nominal separation of refrigerator stations is set at 20 km, which is approximately 20 times the maximum length of individual sections of cable that can be fabricated and transported. The actual separation between any two refrigerators can be greater than or less than that length. It will depend on the position of power connections, altitude changes along the cable path, and availability of ac power to run the refrigerator and the cryogenic pumps that are required to maintain pressure and flow along the cable.

6.1.2.2 Initial Temperature of the Cryogen

The ultimate selection of the temperature of the cryogen will depend on the operating characteristics of the cable and, in particular, the performance of the superconducting material used. A temperature of 66 K was used for all calculations in this section. It is just above the freezing temperature of nitrogen, which is the lowest temperature that is possible with liquid nitrogen. An advantage of this temperature is that it allows the superconductor to operate at a high critical current. The disadvantage of operating at 66 K rather than a higher temperature is that both capital and operating costs for the refrigerator will be higher. In terms of calculations of cryogenic flow and total nitrogen volume, neither would vary significantly even if the operating temperature were as high as 80 K.

6.1.2.3 Temperature Rise Along the Cable Between Refrigerator Stations

The choice of the maximum temperature rise along the cable is based on a similar set of arguments as for the initial cryogen temperature. A relatively small maximum temperature rise of 3 K was chosen in order to maintain a uniform and relatively high critical current capability in the superconductor. This value and the total heat input between cryogenic stations determine the mass flow rate of the liquid nitrogen, which is about 3 kg/s (55 gal/min.).

6.1.2.4 Maximum Pressure Drop Between Refrigerator Stations

The allowable pressure drop between refrigeration stations is perhaps the most arbitrary of the initial parameters. The choice of ~10 atm is based on recognition of the impact of altitude changes on the pressure in a fluid system. Nitrogen is only slightly less dense than water. Thus, the pressure changes by 1 atm for each 12-m change in elevation. An elevation change of 220 m (20 atm) or more will occur in many locations along a 20-km section of cable. Thus, the total pressure change along a length of cable can be 30 atm. This must be added to the minimum allowable pressure in the cable, which must be several atmospheres in order to maintain the nitrogen in a single phase during quench and fault conditions.

Nitrogen changes from a normal liquid to a supercritical fluid at about 34 atm. To avoid the complications of the varying fluid characteristics when nitrogen transitions between these two phases, it seemed appropriate to set the nominal maximum pressure—which determines the wall thicknesses of the cryogenic enclosure and the return pipe—to 31 atm. Restricting the maximum

pressure to a lower value would permit the use of thinner walls for both of these pipes. Table 6-1 lists these parameters and some of the resulting characteristics of the superconducting dc cable. Figure 6-1 illustrates the components of the cable in the pipe envelope.

Table 6-1
Design parameters of the superconducting dc cable

| Parameter | Value |
|--|---------|
| Cable core outer diameter | 115 mm |
| Distance between refrigeration stations | 20 km |
| Cable section length | 1 km |
| Liquid nitrogen mass flow | 3 kg/s |
| Cryogenic enclosure outer diameter | 18 cm |
| Cryogenic enclosure wall thickness | 3 mm |
| Return pipe diameter | 10.5 cm |
| Return pipe wall thickness | 2 mm |
| Maximum pressure | 31 atm |
| Maximum flow pressure drop | 10 atm |
| Initial fluid temperature leaving refrigerator | 66 K |
| Maximum temperature along the cable | 69 K |

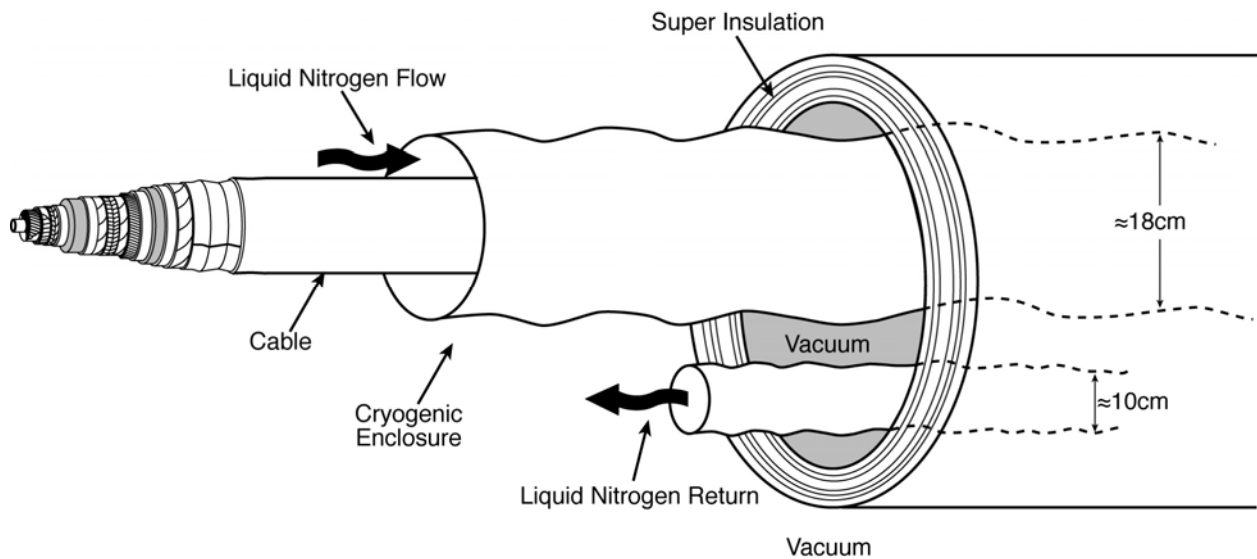


Figure 6-1
Cable in pipe envelope showing various components

6.2 Heat Flow into the Cold Mass

Heat flows into the cold mass from several sources. Because the cable is quite long, the sources of heat are considerably more extensive than for smaller superconducting devices such as rotating machines, magnetic resonance imaging magnets, and fault current limiters. This is true not only for the sources of the heat but also in the several ways in which the cable interacts with the ambient world. Here, these sources are separated into the following, physically distinct processes:

- Radiation and conduction through the vacuum
- Heat conduction along mechanical supports
- Energy losses associated with the flow of the cryogen
- Heat generated within the cable conductors
- Heat input at the vacuum and refrigeration stations
- Heat flow through the power leads

These processes are described and quantified in the following subsections.

6.2.1 Radiation and Conduction Through the Vacuum

Section 5, Vacuum Section, describes a design approach that will maintain the heat flow through the vacuum and into the cable due to radiation and convection from external sources to about 0.5 W/m or less. We use that value as a starting point for the average heat input along the length of the superconducting dc cable. Thus, radiation and convection contributes about 10 kW of heat at 66 K along the 20-km section of cable between refrigerator stations.

Calculations of the heat flow through vacuum regions are usually based on ideal conditions and do not include all the effects associated with practical construction of systems such as the superconducting dc cable. Experience has shown that heat flow is considerably greater where the MLI must be shaped to accommodate protrusions and direction changes in the cryogen flow. We assume that 2 W of heat will enter the cold mass at each joint along the external pipe—that is, every 20 m. We also assume that there will be some additional heat input every kilometer, at the location of the cable joints and vacuum pumps. Also, the instrumentation leads will enter the cold region in the area of the joints. There is little experience related to this part of the superconducting dc cable, so there is no standard method for estimating this heat load. A conservative approach is to assume a factor of ten increase in heat input per length of cable in this area. This amounts to about 25 W over the 5-m length of cable and equipment in each vacuum vault.

6.2.2 Heat Conduction Along Mechanical Supports

The superconducting dc cable has mechanical supports that span the distance between the ambient-temperature outer pipe and the cold mass that they hold in place. To maintain the position of the cold mass, the supports must resist the gravitational force associated with the weight of the cold mass, fix the axial and transverse locations and circumferential orientation of the cold mass in the vacuum, and, to an extent yet to be determined, react against the stresses associated with the contraction of the cold mass as the temperature is decreased. Various materials have been used for mechanical supports in other cryogenic and superconducting technologies. The best materials for this purpose are those with high strength (or high allowable working stress, σ_w) and low thermal conductivity (κ). One measure of the effectiveness of a material is the magnitude of a parameter, χ , which is defined by Equation 6-1.

$$\chi = \frac{\sigma_w (\text{Pa})}{\kappa (\text{W/m} \cdot \text{K})} \quad \text{Eq. 6-1}$$

One of the most popular materials for cryogenic supports is the epoxy–glass composite known as *G-11 composite*. In addition, materials based on Kevlar fiber and Nomex fiber have been used extensively. The mechanical and thermal properties of these and many other materials change significantly as a function of temperature. Thus, the choice of both the geometry and the dimensions of these supports requires detailed calculations using the temperature variation of $\chi(T)$ along the supports.

In addition to the choice of material and knowledge of its thermal and mechanical properties, the form of the supports is a crucial aspect of any cryogenic system design. The total heat flow, Q , along a material is given by Equation 6-2.

$$Q(W) = \int_{\text{Ambient}}^{T_{op}} \kappa(T) \cdot \frac{A}{l} dT \quad \text{Eq. 6-2}$$

Because G-11 composite is a heterogeneous material, the value of Q depends on the direction of the forces within the material and the surface contact characteristics. However, a standard approximation for most cryogenic calculations using G-11 structures that have constant cross section (such as rods or beams), is given by Equation 6-3.

$$Q(W) \approx 140 \cdot \frac{A}{l} \quad \text{Eq. 6-3}$$

Where:

A is the cross section of the rod (m^2).

L is the length of the rod (m).

Clearly, the heat flow along a rod is decreased by making its cross section smaller and by making its length greater. The straightforward approach to supporting a load is to use a structure that is under compression, such as the legs on a chair. However, this approach is not compatible with maintaining the heat flow level as low as possible. When heat conduction is included as a factor in the design, such as for cryogenic systems, structures under compression have such a small cross section that they tend to buckle and collapse. As a result, the best structures to support cryogenic systems are those based on elements in tension rather than those in compression.

The cold mass consists of the cryogenic enclosure, the return pipe, and the materials inside them—that is, the liquid nitrogen and the cable core. The approximate weights of these materials per meter of length along the cable are listed in Table 6-2.

Table 6-2
Weights of materials in the cold mass of the superconducting dc cable

| Material | Weight (kg/m) |
|---------------------------------|---------------|
| Cryogenic enclosure | 15 |
| Return pipe | 5 |
| Liquid nitrogen (go and return) | 20 |
| Cable core | 30 |
| Total | 70 |

We first calculate the structure required if the structure that supports this weight is under tension and gravity is the only consideration. The total cross section of a material under tension—such as Kevlar fiber or carbon fiber, the allowable working stress of which is 100 MPa (about 25% of the ultimate strength)—is about 7 mm² for a each meter along the cable.

Using Equation 6-3 and assuming that each strut is about 0.5 m long and that two are required because they are at a 45° angle, the heat load would be about 0.4 mW per meter of cable. This amount of heat is insignificant compared to other heat. However, constraining the cold mass against seismic loads and fixing it within the vacuum region requires considerably more structure. In addition, there will be some contraction of the cold mass associated with cooldown. Most of this load can be controlled at the vacuum and cryogenic vaults. However, some structure must be added to ensure that the bellows on the cryogenic vessel and the return pipe at the end of each section share this contraction. We assume that the struts will be about 25 times larger in cross section (having a heat leak of 10 mW per meter of cable) than the minimum required by the gravitational load. In addition, some solid connections will exist in the region of the joints every kilometer along the cable in the vacuum and cryogenic vaults. These joints are estimated to have heat leaks that are equal to the sum of all the struts—that is, about 10 W. Thus, heat flow along the structure contributes about 0.02 W/m.

6.2.3 Losses Associated with the Flow of the Cryogen

Much of the process of designing the superconducting dc cable is iterative. For example, the heat to be removed from the cold mass determines the total flow of cryogen along the cable, which in turn affects the total heating within the cold mass. Here, we use the mass flow (see Section 1.3.1, Practical Cable Flow and Tube Dimensions) and the resulting pressure drop to determine the amount of heat introduced into the cable by the flowing fluid. This is accomplished by calculating the temperature rise in the flowing fluid for the condition of zero heat input into the cable. This case is referred to as the *base case*.

The input parameters used for this calculation are those listed in Table 6-1. Figure 6-2 shows the temperature along the cryogenic enclosure and the return pipe for this base case, when there is no direct heat input within the cable core or from external sources of conduction or radiation. The temperature increase is 0.438 K in the return path and 0.294 K in the cryogenic enclosure. These can be thought of as friction heating of the flowing nitrogen. A similar calculation was completed for supercritical nitrogen as a check for special cases in which higher pressures might be needed—for example, in the case of significant elevation change along a section of pipe. The resulting temperature rise for the supercritical fluid was within a few percent of that for liquid.

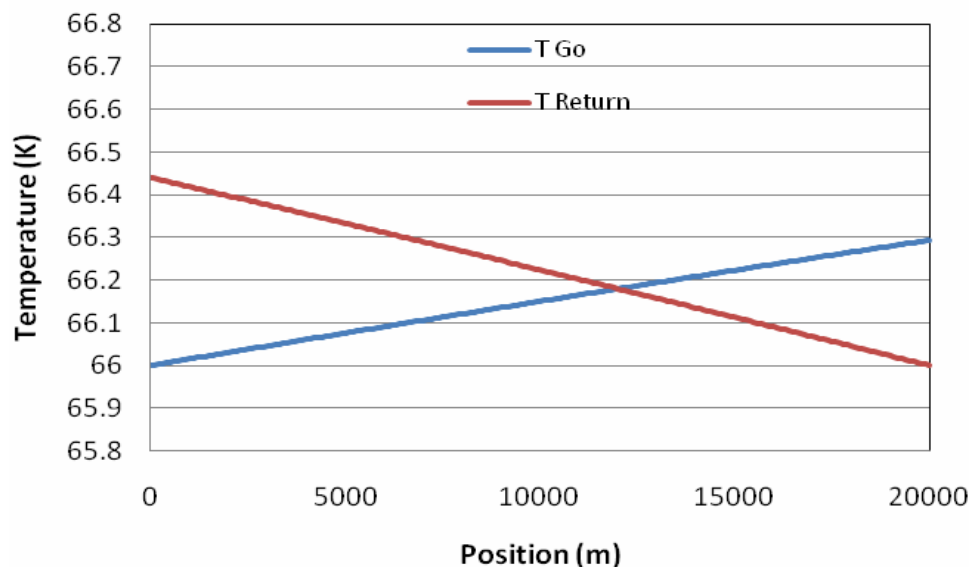


Figure 6-2
Temperature increase along the superconducting dc cable (base case)

The specific heat of nitrogen is about 2.0 kJ/kg/K, and the flow rate is 3.0 kg/s. Thus, the equivalent heating is 0.13 W/m in the return path and 0.09 W/m in the go path, which constitutes less than half the heat load from radiation and convection through the vacuum. In addition to the heat developed by the flow of the fluid, there is a pressure drop along the two paths, as shown in Figure 6-3 for liquid nitrogen and in Figure 6-4 for supercritical nitrogen.

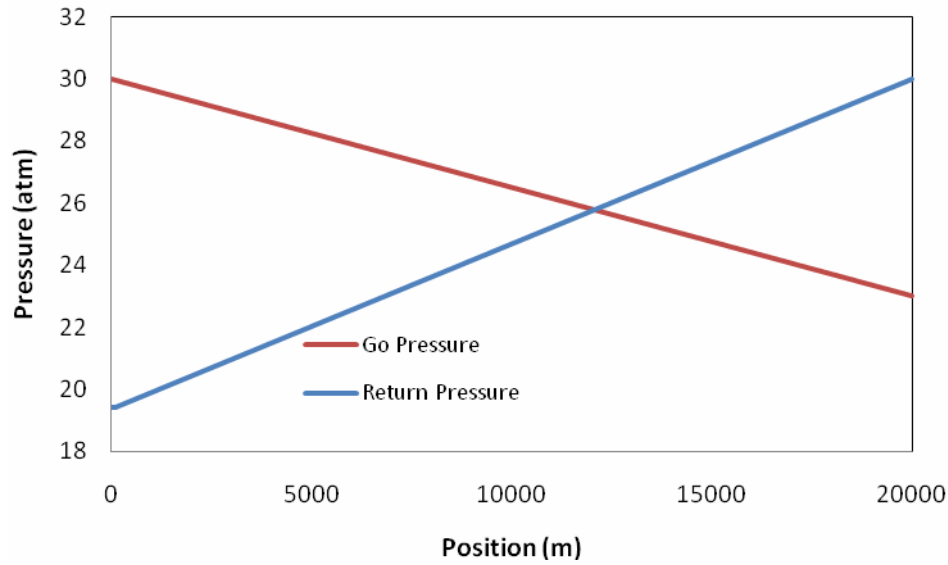


Figure 6-3
Pressure drop along the superconducting dc cable for the flow of liquid nitrogen

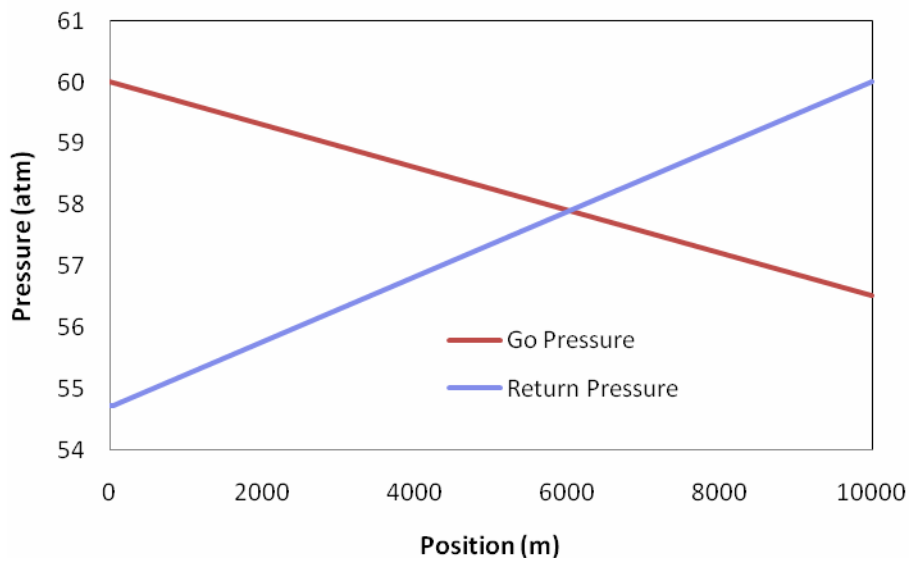


Figure 6-4
Pressure drop along the superconducting dc cable for the flow of supercritical nitrogen

Figure 6-4 is for a shorter length of pipe than that in Figure 6-3. However, the pressure drop per unit length is the same, and it is clear that liquid nitrogen and supercritical nitrogen exhibit essentially the same performance for the superconducting dc cable conditions. This pressure drop must be overcome by energy, which appears as a design requirement for compressors that are

part of the refrigerator system. The energy does not appear as a heat load at the temperature of the cable; rather, it appears as a direct power term for the electrical system that supplies power to the compressors. The power required in the pumps is given by Equation 6-4.

$$Q(W) = \dot{m}(kg/s) \cdot \frac{\delta P(Pa)}{\rho_{Nitrogen}(kg/m^3)} = \dot{m}(kg/s) \cdot \frac{\delta P(atm) \cdot 101325}{\rho_{Nitrogen}(kg/m^3)} \quad \text{Eq. 6-4}$$

The pressure drops in the go and return paths are about 7 atm and 10.9 atm, respectively. These can be combined to estimate the compressor power requirement for 20 km of cable to be about 4000 W, assuming a 53% compressor efficiency. This must be included in the room-temperature power requirements for each refrigeration system.

6.2.4 Heat Generated Within the Cable Conductors

The following three sources of heat exist within the conductors of the cable:

- Resistive losses in the electrical joints
- Hysteresis losses in the superconductor due to current variations
- Eddy current losses in the quench-stabilizing copper and the metal sheath

Splices between sections of the cable will occur each 1 km along the cable. There is no process at present for making direct superconductor-to-superconductor joints in the HTS materials that will be used in the cable. Thus, there will be some resistance between the two superconducting components at each splice in the cable. The resistance of the joint will depend on a variety of design issues. The goal is to keep the resistance as low as possible while keeping the dimensions small and maintaining structural integrity. Experience with splices in other superconducting systems suggests that the resistance of a splice that is approximately 1 m long can be maintained in the range of 2–5 nano-ohms. Here we use the higher value for the resistance of each splice in the superconducting dc cable.

The superconducting dc cable is designed to have double redundancy. That is, the two cables in parallel are thought to operate nominally at a continuous current of 100,000 A, so each cable carries 50,000 A. In fault or emergency conditions, however, each leg is designed to handle the maximum current for an extended period. The temperature rise in the cable and the flow of cryogen must be calculated for this condition. For the case in which a single-leg circuit carries the total current and the joint resistance is 5 nano-ohms, resistive heating will be about 50 W in both the go and return current legs, for a total of 100 W/km. We use this value to estimate the overall refrigeration load, recognizing that when both circuits are active, the loss in each leg is about one-fourth of this value.

Current variations that cause heating in the conductive materials are associated with the operation of the cable as a part of the grid. They are mainly caused by current ramps that occur when power is changed and by the ripple currents that are produced by the ac–dc converters. The latter heat source is localized at the converters, where power is introduced to or taken from the superconducting dc cable. These currents depend on the fraction of each converter's maximum

power capability that is being used. The largest ripple currents occur near the lower end of the usable power range of each converter, and filters will be used to reduce the amplitude of the ripple currents.

A complete description of the losses associated with the ac ripple in the superconducting dc cable is too extensive to be included in this section. The most significant part of the losses is proportional to the square of the magnitude of each harmonic current. Generally, an approach developed by Bean can be used to calculate the power dissipated in a superconductor by varying currents [31, 32]. The Bean formula can be expressed as shown in Equation 6-5.

$$P(W/m) \cong 4 \cdot 10^{-7} \sum_{all_n} \nu_n (s^{-1}) \cdot I_n^2 (A^2) \quad \text{Eq. 6-5}$$

Where:

ν_n is the frequency of the n th harmonic.

I_n is the current associated with the n th harmonic.

The power given by this equation is correct at any location along the cable. However, the losses are not continuous along the cable, because each meter of the superconducting dc cable absorbs some of the energy in the ripple currents. This attenuates the ripple currents so that they decrease as a function of distance from the converter. As a result, losses are larger close to the converter and fall to an insignificant level after about 10 km. The averaging process used for the other losses is not appropriate for this source of heat. Instead, the refrigerators near the converters must be designed to remove more heat from the section of cable that they cool than is necessary along the length of the cable. Equivalently, the refrigerators near a power node can be made to cool a shorter section of cable. The exact form of the dissipation with length will depend on the characteristics of the cable and the amplitude of the various harmonics. It will be calculated in the next phase of system design, and it will depend on the design of the converter, the operating power level, and the filters that are installed at the converter stations.

Here we assume that the converters can be controlled so that the sum of the heating from the harmonic currents at the converter will be less than 1 W/m adjacent to the source. This condition occurs if $\sum_{all_n} \nu_n (s^{-1}) \cdot I_n^2 (A^2) \leq 2.5 \cdot 10^6 (A^2 \cdot s^{-1})$, which would allow some harmonics at the

100–200 A level. Because this will occur only near the power sources, of which there are 20 or so along the cable, the contribution to the average power will be less than 0.1 W/m for the entire cable.

6.2.5 Heat Input at the Vacuum and Refrigerator Stations

Several sources of heat flow into the cryogenic system at the vacuum and refrigeration stations. Some sources—such as the extra heat that flows through the vacuum and the MLI at couplings and the supports that resist the forces associated with cooldown—are described in Section 6.2.1, Radiation and Conduction Through the Vacuum, and Section 6.2.2, Heat Conduction Along Mechanical Supports. In addition, at each vacuum station, the cryogens must be made to flow

around the splices, and yet the splices must be cooled because the heat generated in them can be as high as 100 W. The flow of nitrogen at the area of the splice can be in several tubes, which could have additional losses. The exact geometry of this interface is not certain, but an additional 2 W could flow through the vacuum and MLI in this region. In addition, there could be a vacuum break near each splice. If this occurs, the structure associated with the plate that extends from ambient to the cold mass will carry significant heat to the cryogenic fluid. Here we estimate that all these heat sources will contribute an additional 10 W at each splice, which averages to 0.01 W/m.

Cryogenic piping to and from the refrigerator also introduces some heat into the system. This issue can be approached in several ways. Because the magnitude of this heat input depends on the refrigerator design, it is typical to ascribe it to the operation of the refrigeration system. Therefore, this term is not included as a heat loss for the cable.

6.2.6 Heat Flow Through the Power Leads

The superconducting dc cable will normally operate with two different power paths, each carrying a maximum current of 50,000 A. Power will enter and leave the cable at several locations—for example, at generators, at connections to local ac power systems, and at sites where power is to be extracted. Thus, no power lead will carry the maximum current. However, the concept of reliability for the cable system requires that each path be capable of carrying 100,000 A continuously. The consequence of these design choices is that the power leads must be able to operate over a wide current range. Heat flow into the cryogenic environment caused by the current leads is due to conduction heat transfer along the lead and internal Joule (resistive) heating [33].

Considerable effort has been put into the design of power leads for superconducting systems. The starting point for most designs is a lead that is optimized to have the lowest possible heat flow into the cryogenic environment when operating at a specific design current. The heat flow at the design current in each such lead is given by Equation 6-6.

$$P(W) = [L_0(T_2^2 - T_1^2)]^{1/2} \cdot I = .046 \cdot I(A) \quad \text{Eq. 6-6}$$

Where:

P is the heat (in watts) transmitted to the colder surface at the design current, I.

T₂ is the upper temperature (~300 K).

T₁ is the lower temperature (66 K).

L₀ = 2.45 × 10⁻⁸ W Ω K⁻² is the Lorentz constant.

This formula is independent of the type of metallic conductor chosen for leads. For example, it can be achieved with copper or with stainless steel, even though the average resistivity of stainless steel is about 100 times that of hard copper.

Because the power flow in the superconducting dc cable will vary substantially to accommodate power demands, the power leads will operate at their ideal design point for only a small fraction of the time. Several approaches to the design of a power lead can accommodate this variation. This will be a major area of work during the next phase of development of the superconducting dc cable. The item of interest here is the total heat that enters the cold region. As an example, we consider three current levels: zero current, design current, and 1.4 times design current. Figure 6-5 shows the temperature distributions within a lead operating at these three current levels (zero current, $I=0$; design current, $I=I_{opt}$; and 1.4 times design current ($I/I_{opt}>1$). The temperature distribution in the lead at the design current, I_{opt} , is the bold curve. It has zero slope ($dT/dx=0$, where dT is temperature and dx is distance) at the warm end of the lead. That means there is no heat flow into or out of the lead from its ambient-temperature end. If the current is less than the design value, heat flows into the lead at that end, but because the slope at the cold end is less than for the case of the design current, less heat will flow into the cold region. When the current is greater than the design value, the lead will be heated higher than the ambient temperature at some intermediate location. Because the temperatures at the two ends are fixed, some of the heat generated within the conductor will flow to the high-temperature end, and some will flow to the low-temperature end.

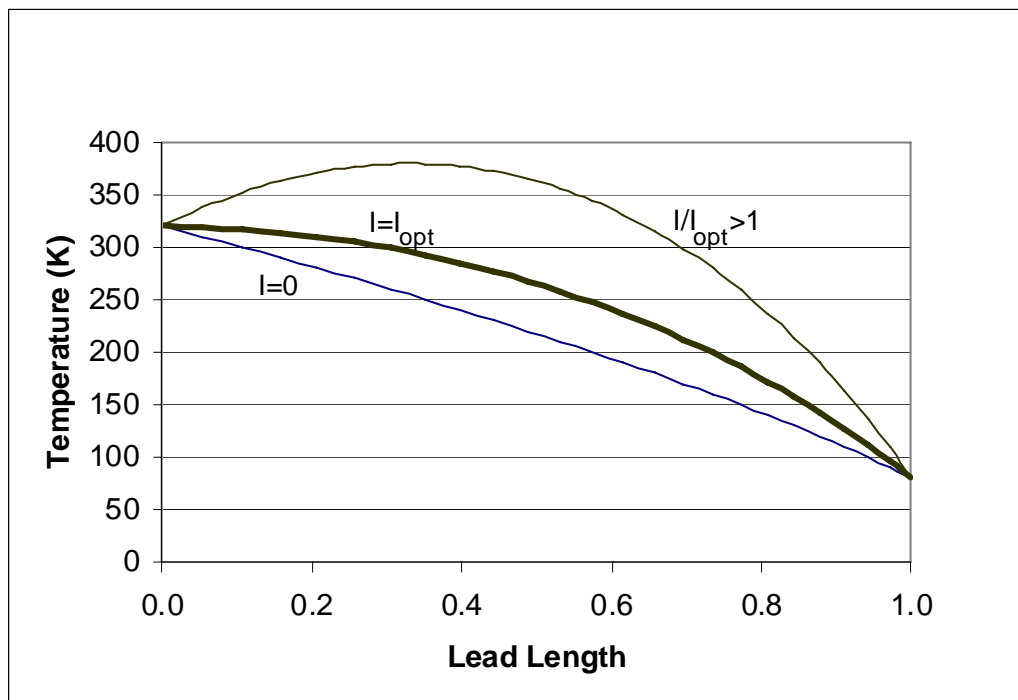


Figure 6-5
Temperature along a warm-to-cold power lead for different operating currents

6.2.7 Summary of Heat Inputs

Table 6-3 summarizes the heat inputs described in the previous subsections.

Table 6-3
Summary of heat inputs

| Heat Source | Average Heat Input | Distribution |
|---|--------------------|--------------------------------------|
| Radiation and conduction through the vacuum | 0.5 W/m | Nearly uniform |
| Heat conduction along mechanical supports | 0.05 W/m | Nearly uniform |
| Losses associated with the flow of the cryogen | 0.02 W/m | Nearly uniform |
| Heat generated within the conductor joints | 0.1 W/m | Once each kilometer |
| Heat generated in the conductors due to ripple currents | 0.1 W/m | Lumped at power conversion stations |
| Heat generated in the conductors due to power ramps | 0.05 W/m | Short duration during power changes |
| Heat input at the vacuum and refrigeration stations | 0.07 W/m | Every 1 km and 20 km along the cable |
| Heat flow through the power leads | 0.01 W/m | Lumped at power conversion stations |
| Total | ~0.9 W/m | |
| Total with 25% contingency | 1.15 W/m | |

6.3 Cryogen Flow

Heat removal requires some form of fluid flow along the length of the superconducting dc cable. Several options are available, depending on the cable's operating temperature. The performance characteristics of HTS materials suggest that they will be able to meet the demands of the superconducting dc cable at temperatures less than about 73 K. The current-carrying capability of these superconductors improves as the temperature decreases; thus, the lower the temperature, the smaller the amount of superconductor that is needed for a given current. However, the lower the temperature, the more expensive the refrigerator and the greater the operating costs. The final design will require a detailed trade study to determine the optimum temperature. Here we choose to cool the cable with liquid nitrogen at an inlet temperature of 66 K. Figure 6-6 shows the saturation pressure of liquid nitrogen, and Figure 6-7 shows the saturation density variation over the operating range of the superconducting dc cable.

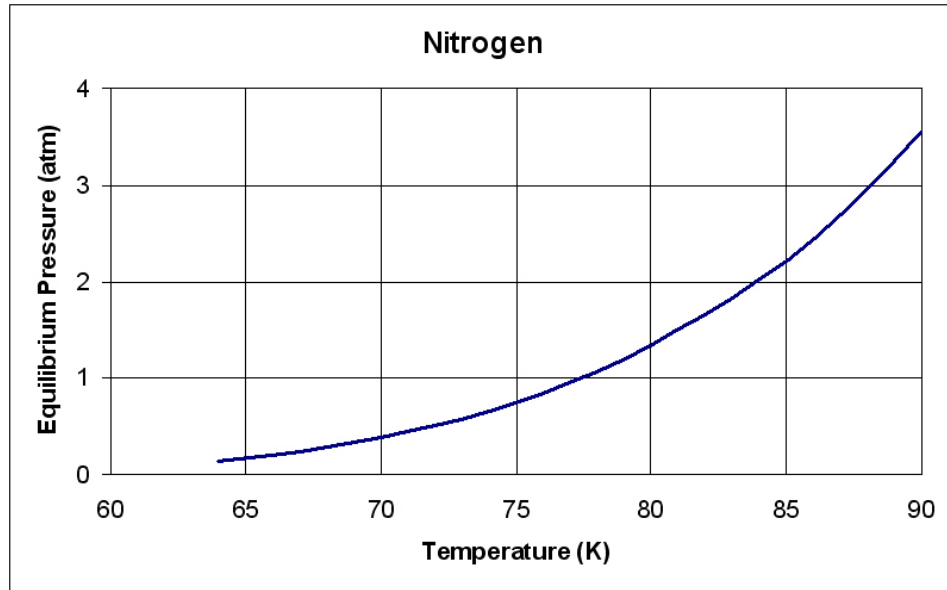


Figure 6-6
Saturation pressure of liquid nitrogen over the operating range

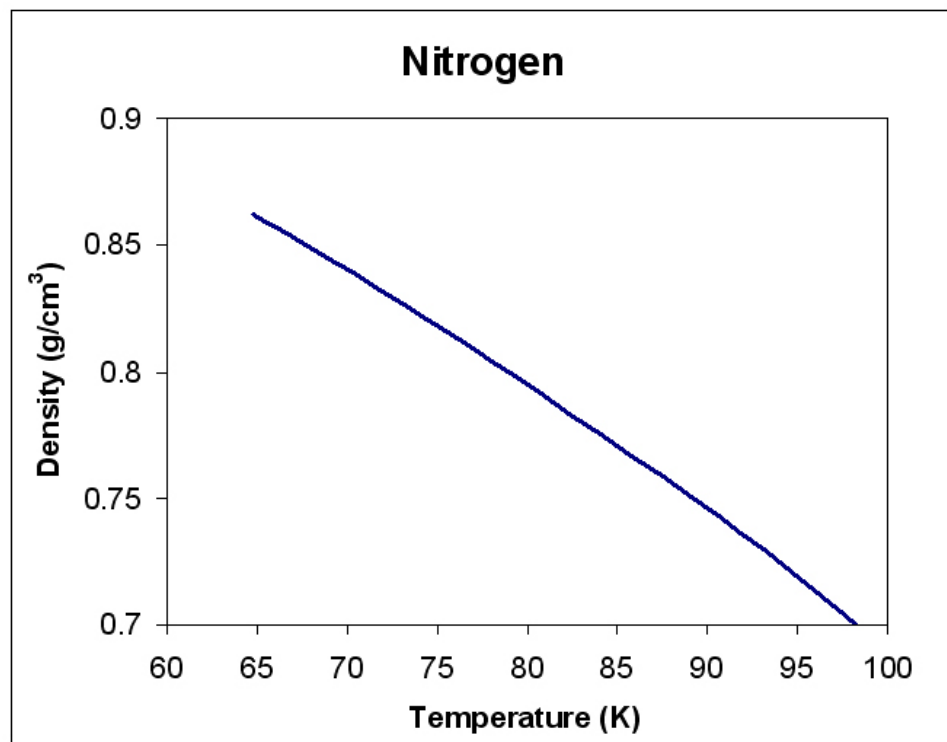


Figure 6-7
Saturation density variation of liquid nitrogen over the operating range

Data shown in Figures 6-6 and 6-7 are used in detailed flow calculations later in this section. However, these figures make it clear that, when nitrogen is in the liquid state, the chance of bubble formation is small so long as the pressure can be maintained at greater than 3 atm. The superconducting dc cable will operate at considerably higher pressures. Two fluid conditions exist that are acceptable for nitrogen in the temperature range of interest: liquid and supercritical. The pressure of the fluid determines which phase is present. The supercritical phase exists when the pressure is greater than 34 atm. We assume that the pressure will be less than this level throughout the cable and that the nitrogen will always be in the form of a single-phase liquid throughout the cable.

Figure 6-8 is the pressure-specific volume diagram for liquid nitrogen. The liquid phase exists to the left of the liquid saturation line (the red curve). Only vapor exists to the right of the vapor saturation line (the blue curve). Between the red and blue lines, the liquid and vapor phases coexist for pressures below the critical point. Lines of constant temperature and pressure coincide in the two-phase region. Typically, HTS cables operate only in liquid, so the pressure cannot be allowed to fall below the liquid saturation line for a given temperature.

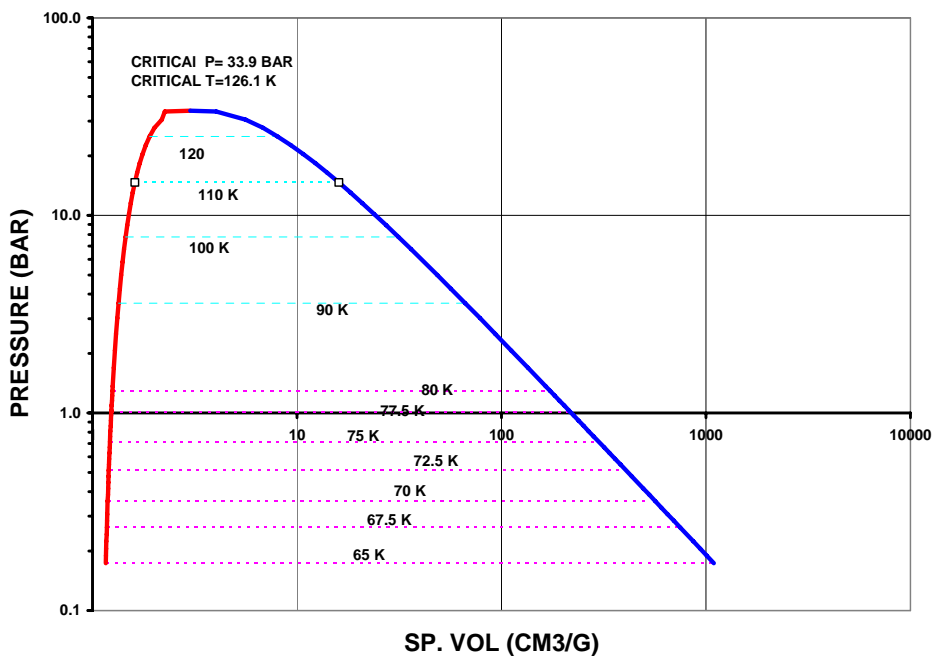


Figure 6-8
Pressure-specific volume diagram for liquid nitrogen

6.3.1 Practical Cable Flow and Tube Dimensions

The choice of parameters is an iterative process. In particular, the heat flow into the cable depends somewhat on the total flow of nitrogen. The following three general parameters fix the fluid flow characteristics and the pipe dimensions:

- Heat load per unit length of cable (~ 1.15 W/m)
- Separation between refrigeration stations (20 km)
- Maximum temperature rise during normal operation (~ 3 K)

The combination of these three parameters determines the minimum mass flow of liquid nitrogen, as shown in Equation 6-7.

$$\dot{m}(\text{kg} / \text{s}) = \frac{\dot{Q}(\text{W} / \text{m}) \cdot l(\text{m})}{C_p (\text{J} / \text{kg} / \text{K}) \cdot dT_{\text{Max}} (\text{K})} = \frac{1.15 \cdot 20000}{2200 \cdot 3} = 3.3 \text{kg} / \text{s} \quad \text{Eq. 6-7}$$

Here we choose 3.0 kg/s as the mass flow rate for this report. This is because margins have been introduced at several places, and it does not seem appropriate to have a multiplication of the margins, which has on occasion had a significant effect on overall system design. Figures 6-9 and 6-10 show the pressure drop along 20 km of cable for a 3 kg/s nitrogen flow as a function of the cryogenic enclosure diameter and the return tube diameter, respectively. To maintain pressures in the system at less than ~ 30 atm, we choose an 18-cm cryostat diameter and a 10.5-cm return tube diameter.

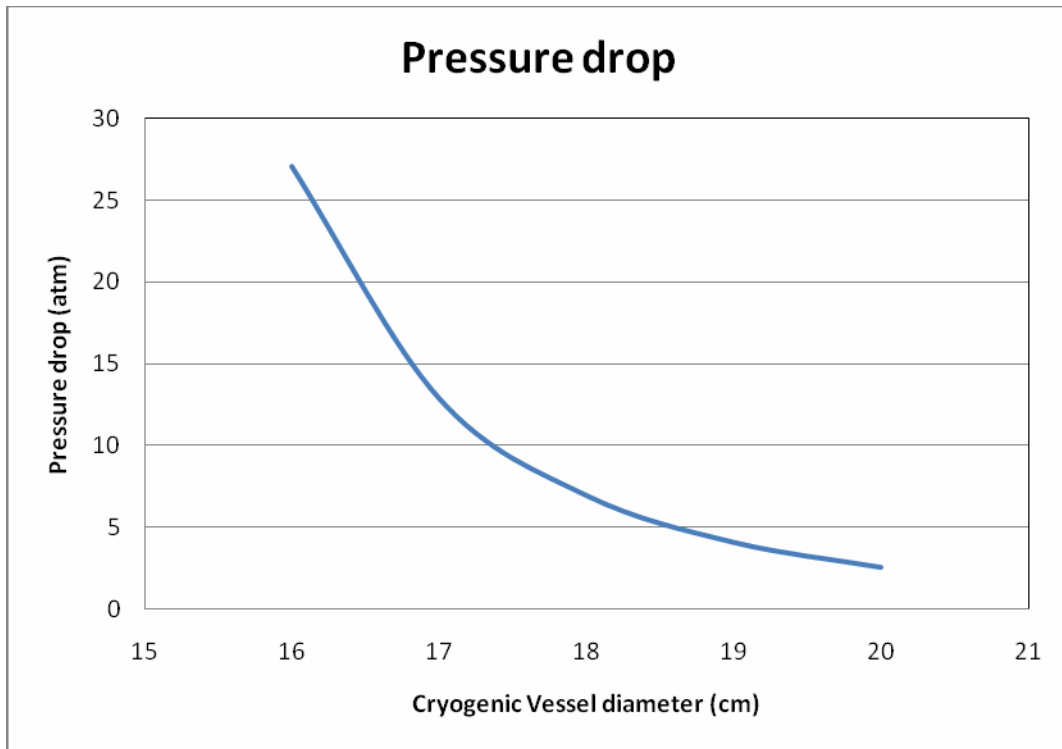


Figure 6-9
Pressure drop along the cryogenic enclosure as a function of tube diameter

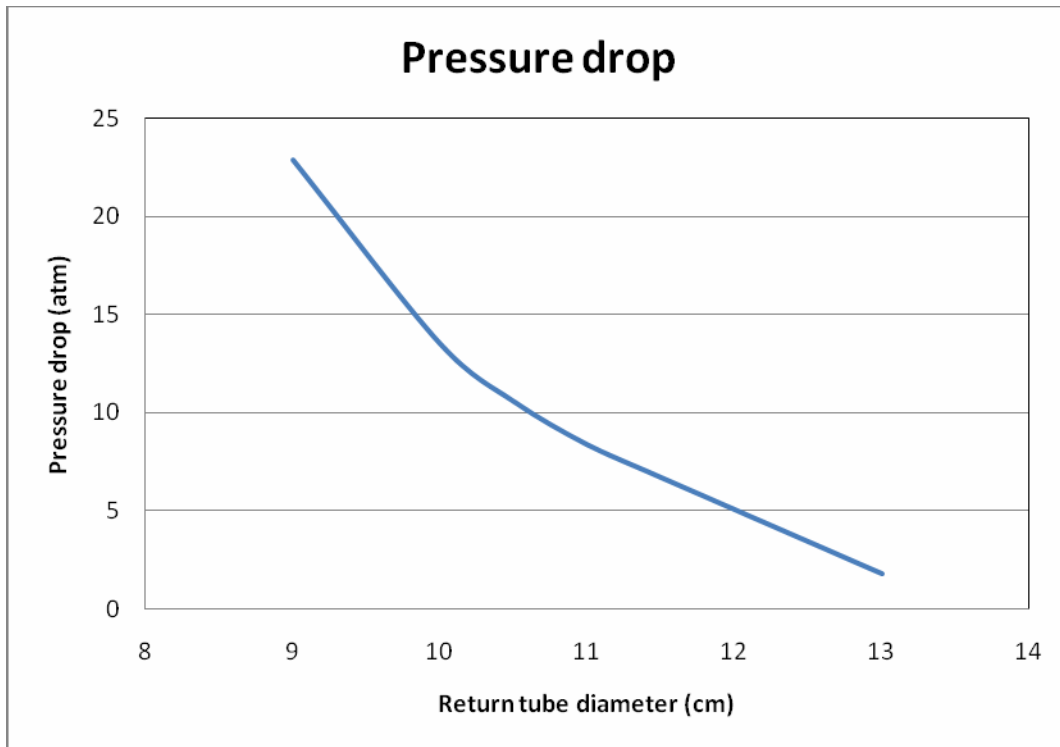


Figure 6-10
Pressure drop along the return tube as a function of tube diameter

6.3.2 Effect of Altitude Changes

The exact operating pressure of the superconducting dc cable will depend on a variety of factors, and it could vary from location to location. One important variable is the change in altitude between cryogenic stations. The density of nitrogen is about 80% of the density of water. Thus, for every 12 m of altitude change, the pressure changes by 1 atm. Figure 6-11 shows the effect of altitude on the pressure in a cable. The altitude changes shown are arbitrary, but they will likely occur at some locations along the 1000-km cable. The altitude change in Figure 6-11 is 150 m over a 10-km cable length. The starting pressure for both the go and return paths is 20 atm. In the go path (the flow is from left to right in the figure), the pressure decreases due to flow losses and the altitude change. In the return path, the pressure increases because the altitude effect is greater than the flow loss.

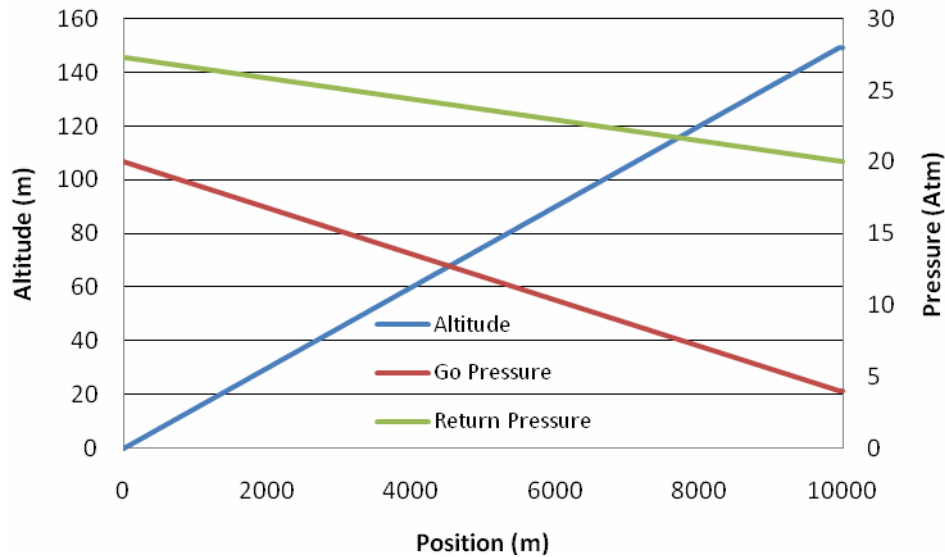


Figure 6-11
Pressure changes in a 10-km length of cable with an altitude change of 150 m

6.3.3 Temperatures During Normal Operation

During normal operation, the superconducting dc cable will operate with cryogen flowing in the cryogenic enclosure and the return tube. The temperature rise along the cable depends mainly on the various heat inputs. Here we use the average value of 1.15 W/m as the nominal heating, and we set aside for future evaluation those areas in which heating will be greater and less than this average. Part of this heat goes into each the two flow paths, and it is possible to design the system to affect the way in which the load is shared. The list of heat inputs suggests that much of the heat associated with the electrical operation of the cable goes into the cable core and thus into the cryogenic enclosure. A small shield attached to the return path can cause it to absorb most of the radiation and conduction. The calculations shown in Figure 6-12 are based on 0.65 W/m entering the cryogenic enclosure and 0.5 W/cm entering the return path. The maximum temperature rise in the cable core is about 2.5 K.

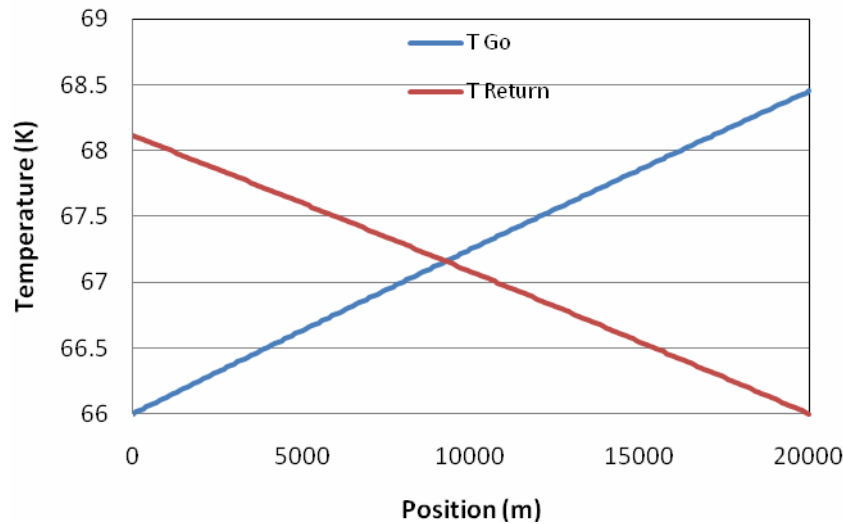


Figure 6-12
Nominal temperature rise along the superconducting dc cable

6.3.4 Counterflow Heat Exchange

Any time there are counter-flowing fluids—for example, in the go and return paths for the superconducting dc cable—there is a tendency for heat generated in one path to migrate across any connecting structures to the adjacent path. This can be visualized by considering a long, partially heated, thermally isolated, racetrack-shaped loop. This flow path might be appropriate for short cables where only one refrigerator is used and the fluid is made to flow along and back in the same cryostat. The cable proposed for the Entergy installation in New Orleans uses this cooling approach [34]. In this example, a coolant flows along the loop in one direction where there is uniform heating ($W/m = \text{constant}$) and returns in an adjacent path where there is no heating. The lower curve in Figure 6-13 shows the temperature of the coolant for the case in which there is no thermal contact between the go and return paths. The maximum temperature of the fluid is reached at the far end of the loop, the halfway point in the figure, and the temperature remains constant in the fluid as it continues along the loop that returns to the refrigerator.

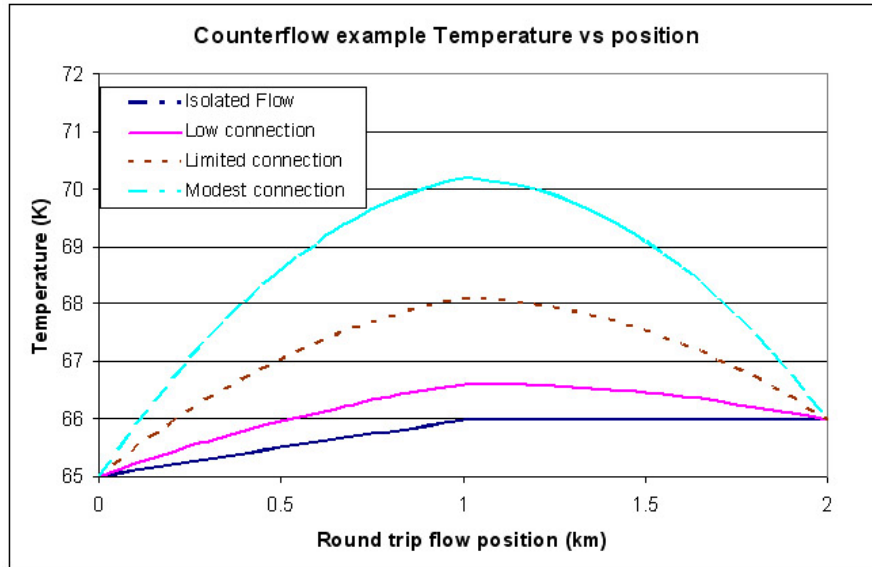


Figure 6-13
Hypothetical example of counterflow heat exchange in a constrained flow loop

Now consider what occurs if, instead of a thermally isolated loop, the second half of the path is in thermal contact with the first half, so that heat can transfer between them. To understand the counterflow effect, we consider a process in which the coolant flow is established, and then heat is applied uniformly along the first half of the path. Initially, before there is a full circuit along the path, only the outward-flowing coolant heats up. However, when the heated fluid passes the halfway mark and begins to return, it is warmer than the outgoing fluid. If heat can be transferred between the two flow paths, the return fluid will cool and the go fluid will heat up more than just from the internal heating. Because the total mass flow is constant and the total amount of heat is the same in the two cases, the outlet temperature will be the same. When the system reaches equilibrium, the temperature at the turnaround point will be the highest in the system. The three upper curves in Figure 6-13 show the increasing temperature at the turnaround position as the thermal contact between the two paths increases. The thermal contact must be maintained at a sufficiently low level for the superconductor to carry the operating current. The design of the cryogenic supports and the flow patterns within the system must accommodate this effect.

The example is instructive, but it does not apply specifically to the superconducting dc cable. Fluid flow in the superconducting dc cable does not have a simple turnaround point. Instead, the opposing flow paths have identical starting temperatures as they leave the refrigerator station in opposite directions. The base case (see Figures 6-4, 6-5, and 6-6) presents the temperature and pressure when there is neither heating nor thermal contact between the two flow paths. The temperatures shown in Figure 6-12 are those expected for typical heat inputs along the cable for the case in which there is no heat exchange between the two flow paths.

There is no way at present to specify the exact thermal contact between the two paths. Estimates of the heat transfer between the two flow paths through the vacuum and through mechanical supports indicate that the temperatures of the two paths will be close to one another and that the counterflow effect will be small. To test this estimate, we calculated the temperature under several different thermal conductivities between the two paths.

Figure 6-14 shows the temperatures along the superconducting dc cable for medium heat transfer between the go and return paths. The heat transfer capability of the cross sections for the supports between the two tubes is about twice that expected in a typical system design. Because there is no increase in temperature in this case over that of the case with no heat transfer at all, it seems that counterflow heat exchange effects will not be an issue in this design.

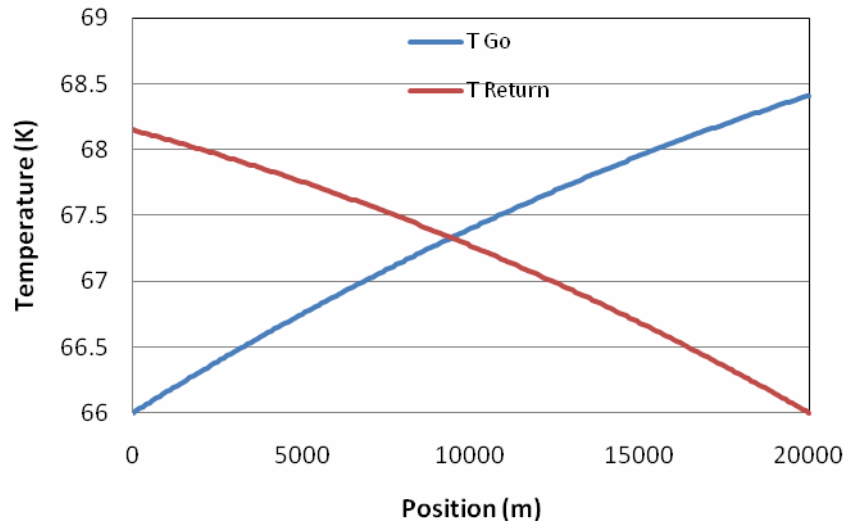


Figure 6-14
Temperatures along the superconducting dc cable for medium heat transfer

Figure 6-15 shows temperatures along the superconducting dc cable for good heat transfer between the go and return paths. The heat transfer capability of the lengths and cross sections for the supports between the two tubes is about 10 times that expected in the final design. At this level, the counterflow effect would impact the capability of the superconductors in the cable core.

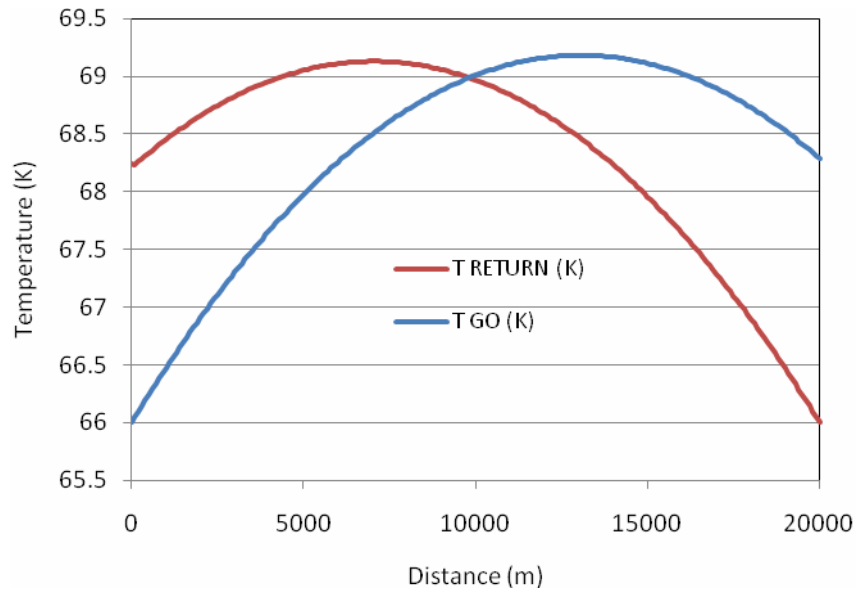


Figure 6-15
Temperatures along the superconducting dc cable for good heat transfer

6.4 Refrigerator Separation Issues

The choice of refrigerator separation distances along a superconducting dc cable will be based on an optimization process that focuses on reliability and cost. The reliability considerations will involve the operational availability of the entire superconducting dc cable. This aspect will include evaluations of mean time between failure of each refrigerator, redundancy requirements for cryogenic components, and the availability of liquid nitrogen from local industrial gas suppliers. The cost considerations will be a combination of the initial capital cost, an annualized operations and maintenance cost, and an annualized cost tied to the effective efficiency of the refrigerator and the electrical power needed for normal operation. The initial capital cost will include the cable and ancillary systems such as conventional power lines that might have to be added in some locations to provide power for refrigerator operation.

Several parameters—some that are under the designer's control and others that are associated with the local terrain—will influence the exact separation between any two refrigeration stations along the length of the cable. These parameters include the following:

- Operating pressure within the cryogenic fluid
- Allowable temperature rise between refrigerators
- Available commercial refrigerators and their capacity
- Availability of local (or hotel) power
- Results of practical tests and demonstrations of model or prototype superconducting dc cable sections

In addition, the cost, cooling capacity, and efficiency of various types of refrigerators will affect the choice of the refrigerator technology. This will in turn affect the choice of refrigerator separation distances. Because the refrigerators that will be available 20 years from now cannot be predicted, it is not possible to comment in detail on the potential effects of the different refrigerator technologies.

Perhaps the best approach to understanding the process of selecting the distance between refrigeration stations is to explore the conditions that will be encountered at three types of sites. A transcontinental cable will have sections that are represented by each of these sites. The first case is an urban or suburban environment, most likely on the outskirts of a major metropolitan area, where several converter stations of several hundred megawatt capacity will be installed within a distance of 50 km. The second case is a rural environment where no major power inputs or extractions occur for a distance of 100 km or more. The third case is a site in a remote, mountainous environment where there is a slope to the cable so that the pressure at the lower refrigerator is considerably greater than that at the upper refrigerator.

6.4.1 Case 1, Urban or Suburban Environment

For this case, the cable is likely to connect to many ac–dc end substations along a distance of about 50 km. Each substation will have some readily available form of hotel power or other local electrical power that can be used to power a refrigerator. In this environment, the choice of refrigerator separation will likely be determined by existing substations and the ability to increase their capacity and physical size to accommodate ac–dc converters of the appropriate power level. There will be instances in which the separation will be considerably less than 20 km. The general description of the cryogenics described earlier in this section can be used to determine pressure drops and the needed refrigeration power to accommodate the total heat load over these various lengths. One issue that will occur in the cable near each substation will be the ac losses in the superconductor caused by the harmonic currents that decay along the length of the cable as a function of distance from the station. Refrigerator capacity might be nearly the same in this environment as it would be for longer cable separations in remote areas.

It is not possible to determine the exact refrigeration capacity at any location. However, when there are many refrigerator stations separated by distances considerably less than 20 km, it might be possible to have the load shared from one to another and, under certain conditions, for an interim refrigerator to either have a smaller power capacity or operate at a fraction of maximum capacity. Alternatively, it might be possible to have a single refrigerator handle the heat load within the cable over a long distance and have several smaller units that accommodate the power leads at each substation. This may be an ideal separation of tasks, as the heat associated with the power lead occurs at a higher temperature than that of the body of the cable. Refrigerators that operate at higher temperatures and at variable temperatures can be designed differently and can be more efficient than those that operate only at the temperature of the cable. This is because they can be designed to use the inherently higher *Carnot efficiency* (the fraction of thermal energy that can be extracted as work in a lossless thermodynamic cycle) associated with removing heat across smaller temperature differences [35]. If the converters were made in standard sizes, it might be possible to extend the standardization to the power leads and subsequently to the refrigerators used to cool them.

One effect of smaller distances between refrigerator stations is that less fluid flow will be necessary to achieve the same limited temperature rise. As a result, the design presented earlier in this section could be adapted to have either a smaller pressure drop between refrigerators or a smaller cryogenic enclosure and a smaller return pipe. If the same size pipes are used, then it might be possible for them to have thinner wall thicknesses in these regions. Some cost savings could be associated with this change.

Bulk liquid nitrogen is usually available in most urban and suburban areas. Overall system reliability can be enhanced by having this nitrogen available on short notice or even having some liquid nitrogen storage at the substation. It might be more appropriate to have liquid nitrogen delivered to some locations rather than using refrigerators. Thus, the refrigerator separation choice might have to include this option as a factor in some locations. This approach has been used by American Electric Power and Southwire at the cable installation in Columbus, Ohio.

6.4.2 Case 2, Rural Environment

In a rural environment, there are long distances with limited local elevation changes between refrigerators, and there will be few power converter installations over distances of hundreds of kilometers. This environment is one in which a standardized refrigerator and refrigerator separation distance can be established. It will be the typical case for long-distance transmission of power. The optimization of this standard distance between refrigerator stations will be a significant part of future system design, development, and optimization. The fact that many components can be standardized will allow the development of a thorough understanding of the most important issues related to overall cable cost and reliability. Examples are the tradeoffs between refrigerator separation and the diameters and wall thicknesses of the cryogenic enclosure and the return pipe. Because the heat input per kilometer of length is roughly constant if the allowable temperature rise is unchanged, the greater the separation, the greater the required pressure drop between refrigerators. The implication is that the initial pressure (or maximum pressure, for flat terrain) must be increased as the separation increases. At some separation distance, the pressure would become so great that the nitrogen would enter the supercritical phase. Some analysis of this condition was included earlier in this section. However, the calculations were for the case in which the nitrogen was maintained in the supercritical state over the entire length of cable. Some experimentation would be needed before deciding to have one or more sections of cable operate in a regime in which the fluid transitioned from single-phase superfluid to a single-phase liquid.

6.4.3 Case 3, Mountainous Environment

The two most important considerations in selecting the separation between refrigerator stations in a mountainous environment are the effects of altitude on cryogen pressure and the limited availability of power to operate the refrigerators.

The effect of the altitude changes on the pressure of the nitrogen was introduced earlier in this section. Although altitude changes must be considered in almost all locations for the detailed design of the system and for the setting of operational limits, it is especially critical in cable sections in areas that are quite steep. The pressure rise associated with an altitude change of

200 m is greater than the pressure required to cause nitrogen to operate in the supercritical regime. It is possible in some sections to have all the fluid along the length of the cable be in this regime, but the result is a much higher absolute pressure. This higher pressure will require thicker walls for the cryogenic enclosure and for the return pipe. Fabricating sections with this capability is not a problem from an engineering sense, but choosing not to use a standard pipe dimension will introduce the need for additional spares and might lead to errors in placement of the various 20-m sections of pipe. Smaller refrigerators separated by shorter sections of cable will solve this problem, but they will require power every few kilometers.

Mountainous regions typically have few power lines, and those that exist are for long-distance, high-voltage, high-power transmission. These are the types of lines that might eventually be replaced by a superconducting dc cable. The voltages and power levels of these lines and the superconducting dc cable are not appropriate for operating the refrigerators. Thus, some form of lower-voltage power must be made available. The power can be in the form of a transmission line installed adjacent to the cable. This line will operate at a distribution voltage level and will be required only intermittently along the cable. Alternatively, a low-voltage superconducting cable can be installed in the same pipe to provide power over distances of tens of kilometers.

Regardless of the site conditions, the desire to have uniform dimensions (diameter and wall thickness) for the pipes and a standard refrigerator capacity might be the driving factor for optimizing refrigerator separation. The advantages of uniformity throughout the system are that the number of spares can be reduced and it will be easier to train system operators and technicians.

7

END STATIONS AND CONVERTERS

This section describes the converter system that will connect the superconducting dc cable to the electric power grid. Power converter technology has changed a great deal over the decades since the first significant superconducting dc power cable study at the Los Alamos Scientific Laboratory. New converter topologies will allow improved efficiency, detailed control of power flow, and overall increased flexibility of the power grid of the future. For example, the ability to design converters that can switch at frequencies much higher than the fundamental on the ac grid reduces the physical size of the converter and lowers the harmonic currents within the cable itself. The converter system outlined in this section is an initial approach to solving a complicated problem that will be encountered on a power grid that does not yet exist. The detailed design of a converter and ac system interface can be developed only in the course of considerable future research and system design.

7.1 Converter Topology

The power transmission system of the future will probably be built and operated much like today's system. That is, transmission lines will continue to be used to transfer power generated at multiple locations to loads distributed over a wide area. The lines will also be used for mutual support between areas with relatively well-balanced local generation and loads. These interconnections will accommodate a plant outage in one of these areas. This is often referred to as *sharing of spinning reserve*. New emphasis on environmental and economic factors will probably lead to increased sharing of generation resources over wide areas. Renewable power generation systems are likely to reduce the need for large, central power plants. However, if renewable generation systems such as wind or solar systems are inoperable because of lack of wind or solar radiation, support from conventional power generation plants will be needed to make up for the renewable deficiency. Also, areas with surplus power generation could support areas with generation deficiencies. Differences in seasonal or daily peak power demands could be exploited by building the transmission lines to enable sharing of distributed resources for the benefit of all. Furthermore, energy parks at remote locations might be built. There will then be a need to transmit the generated power from such parks to the load centers. This could lead to increasing the capacity of transmission lines to transfer considerable power over long distances. We anticipate a need for extremely high power (2–10 GW) and extremely long (500–2000 km) superconducting dc cables as a component of the power transmission systems of the future to serve all these purposes. Such a system must be easy to tap into in order to inject power from multiple sources and to remove power to serve loads. It is therefore envisioned that the cable will have multiple connections along its length.

The converter topology for a superconducting dc cable system that can support a large number of taps must be based on VSCs that are suitable for connection to 115–230 kV ac systems [36]. Because voltage and power are interdependent, power rating is a determining factor in the distance of the converter installation facilities from the load centers. Using converters rated at 200–300 MW would allow placement much closer to the load centers than would be possible with 1000–2000 MW converters. Such power levels typically require connection to 500–765 kV ac systems, which would require larger rights of way and one or two step-down transformers before the power could be fed into a local subtransmission or distribution network. Further, transformers and lines between the 500–765 kV systems and a 115-kV substation bus introduce losses, which is contrary to the goal of a highly efficient power grid. If these transmission losses can be avoided, the overall system will gain efficiency.

CSCs, which are used today for high-power dc systems, would be difficult to operate with a large number of terminals, whereas VSCs would allow a dc system to operate similarly to existing ac systems. CSC technologies work well for point-to-point transmission systems or for systems with only one or two taps. However, future demands for a high degree of flexibility in operating such a large-capacity transmission link would most likely require the ability to connect terminals (converters) to the cable at many locations in order to allow expansion and extension of the areas served by the cable. This possibility would be difficult to accomplish using a system based on CSC technologies, but it would be straightforward with predominantly VSCs.

A further advantage of VSCs is their ability to reverse the direction of power flow without reversing the voltage. This could reduce the need for reversing switches and simplify switching converters into and out of the system. The power load of each converter could be handled with relative ease, and the maximum overall system load would be limited only by the available generation. Therefore, dispatching generation and loads would be the same as for today's ac systems. The operational advantages and improved system efficiencies of VSC systems should compensate for the somewhat larger internal losses associated with today's VSC technologies. In the case of a large generation facility located at the end point of the dc transmission line (nuclear plants, wind farms, and large solar installations, all of which produce large amounts of power and use very little), the CSC would provide a more efficient means of injecting that power into the dc cable.

7.2 Superconducting Cable System Assumptions

All ac systems are required to be built so that the largest single element in the system can be lost without causing a major disturbance. That is, the system must ride through the loss of the largest generator, the most heavily loaded transmission line, the most critical substation bus, and so on. When this program began, it was generally thought that the loss of a cable rated at 5 GW or greater would be more than most systems could handle without collapsing. Therefore, one assumption in the analysis was that any high-power superconducting dc cable would be installed in the form of two parallel circuits, each rated to carry the total load. Thus, if the power capacity along a corridor is 10 GW, each cable would be rated for 10 GW but would be expected to carry 5 GW under normal conditions. In case of the loss of one cable, the parallel cable could carry the full load.

The rationale for a redundant system remains, but it is based solely on reliability and not on possible grid collapse if massive amounts of power are lost. An assessment of the effects of cable loss was included in the high-priority tasks for this program. An evaluation of grid response to the loss of a superconducting dc cable carrying many gigawatts has shown that the North American grid is quite robust. The study results are published in the EPRI report *Study on the Integration of High-Temperature Superconducting Cables Within the Eastern and Western North American Power Grids* (1020330) [13]. The study showed that the power grid in the eastern United States can accommodate the loss of a 10-GW superconducting dc cable and that the grid in the western United States can accommodate an 8.5-GW loss. This was not a sensitivity study, so these are not limits; it is not clear how much more power the dc cable systems could carry before some problem would occur.

Normally, each cable is connected to half of the converters. The cables could be operated with positive polarity voltage on one cable and negative on the other or with the same voltage polarity on both cables. In the latter case, both cables could be positive or negative. When one cable failed, its converters would be switched over to the healthy cable. If both cables have the same polarity, the converter that is being switched over would not require a voltage reversal. Such a switching scheme is illustrated in Figure 7-1, which assumes that the output voltages and polarities are the same for both cables and both converters.

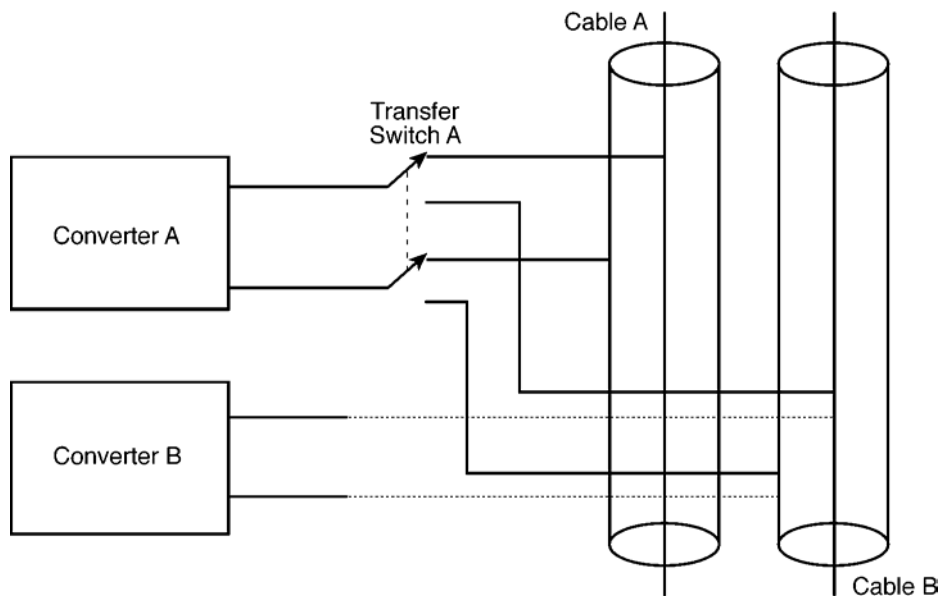


Figure 7-1
Switching arrangement to transfer converter A from a failed to a healthy cable; similar switches would be required on converter B

The switching must be performed under no load (that is, no current), and the dc capacitors (that is, those at the dc side of the converters, sometimes referred to simply as *the capacitors*) must be charged before making a solid connection to the new, healthy cable. If cable A becomes nonfunctional and can no longer carry power, converter A's current must be ramped to zero, and then the circuit with cable A must be disconnected. The voltage on the terminals of converter A must then be ramped to the same value as the voltage on converter B before the circuit between converter A and cable B is closed. If the two cables are operating in a true power-sharing mode,

these voltages will already be nearly identical, and switching will involve current transfer and the inherent issues with cable and system impedances.

The loading of the healthy cable must be rapidly increased to compensate for the transmitted power deficiency resulting from the failed cable. Also, the healthy converters that are feeding load areas suffering a loss of power should have sufficient overload capability to increase their output power and operate in the overload regime for the time it will take to switch the converters from one cable to the other. There are no commercially available switches capable of switching 5000 MW at 120 kV, because this would require a 42-kA switch. However, if it is assumed that the individual rectifiers connected to generators, as well as the individual inverters feeding the loads, will not exceed 360 MW, then 3-kA breakers can be used for the switching operations under no-load conditions. Such switching should be possible in less than 1 second. If the dc capacitor at the output of the converter has been fully discharged, *resistive switching* will be required. Resistive switching allows the capacitor to be recharged in a short time without causing a large voltage transient on the operating converter onto which the deenergized converter is connected in parallel.

A multiterminal dc system using VSCs must have a single voltage-controlling terminal. Indeed, any one of the rectifier terminals could be used for this purpose. It is assumed that the inverters will control the local dc current flow to satisfy the power schedule for the converter. It is presumed that each inverter can be scheduled to deliver a desirable amount of power and that the rectifiers can supply 100% of the scheduled power. However, it must be recognized that the semiconductors of each converter have current limits that cannot be exceeded for more than a fraction of a second. Thus, the maximum power delivered through the cable will be equal to the combined current limits of all the rectifiers. In this situation, a loss of a rectifier converter could lead to a system collapse if the remaining rectifiers do not have sufficient reserve power to pick up the lost load. Fast redistribution of the power setpoints for the converters could be used to avoid a collapse. However, it would be desirable to avoid the use of high-speed communication links for this purpose. Instead, it might be possible to use voltage droop monitoring built into the control systems of the converters to automatically adjust the power flows based on small changes in the dc voltage. System response requirements and the stability of this control strategy should be studied.

Transients arising in the dc cable from such a rescheduling of the power flows must be well damped to limit short-term cable losses. Equivalently, limiting the frequency of power changes will control the overall losses and thereby improve efficiency. A reflection-free termination would be difficult to design. However, well-designed filters on the dc side and a special high-speed converter control feature should effectively damp cable transients. Pulse-width modulation (PWM) converter systems, the type of converter that is envisioned to be needed for this application, should be able to adjust quickly in order to damp cable transients while operating with a moderate modulation frequency. However, fast voltage control of the converters might produce oscillations between the capacitor and the ac reactors internal to the converter. Detailed analysis and appropriate design will be required to avoid this condition.

7.3 Converter Station Design

A single-phase, two-level VSC is shown in Figure 7-2. For a superconducting dc cable system, the dc capacitor would be at the interface between the cable and the converters. The dc voltage is essentially constant and independent of the current, because the superconducting cable has no voltage drop. PWM techniques must be used to control the active power delivered to the ac system and, at the same time, to control the reactive power as required for proper operation of the ac system. In such a converter, the ac voltage can be synthesized with varying amplitude and phase angle at the dc side of the reactor (shown as point A in Figure 7-2). This enables control over the phase current flowing into the ac system.

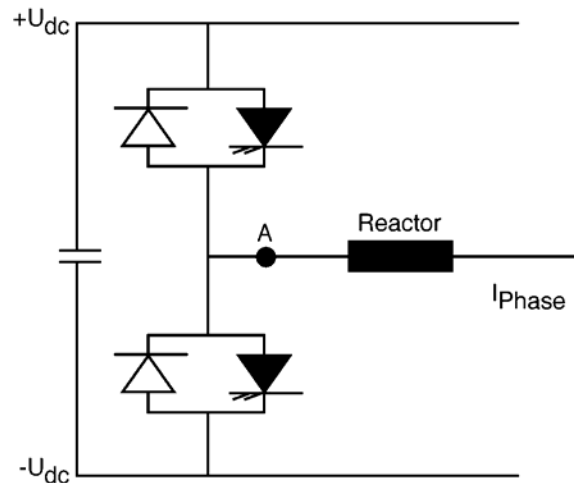


Figure 7-2
Single-phase, two-level voltage source converter

Figure 7-3 shows the output voltage from a single-phase, two-level converter operating at 9 times the fundamental ac frequency. (It is assumed that the output voltage is measured between the ac phase conductor and the negative rail of the converter.) The ratio between the modulation frequency and the fundamental ac system frequency is called the *frequency modulation ratio* (m_f), which is 9 in this case. The figure shows a converter operating with a modulation index (m_a) of 0.8, which is the ratio between the amplitude of the ac control signal (V_a) and the amplitude of the triangular control signal.

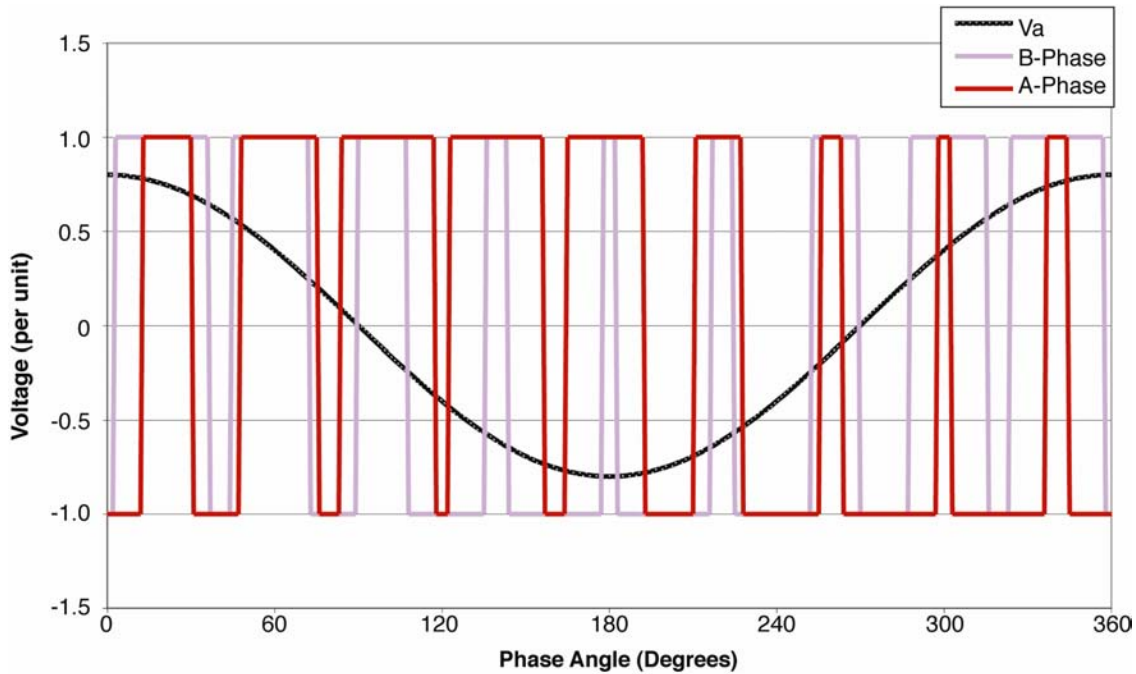


Figure 7-3
Output voltage from a single-phase, two-level pulse-width modulation converter

A modulation index of 0.8 means that there is a 20% margin between the maximum ac control voltage and the peak triangular control signal. The peak amplitude of the fundamental frequency component of the ac output voltage (V_{AO}) is expressed by Equation 7-1 for $m_a \leq 1$ [37].

$$V_{AO} = m_a \frac{V_{dc}}{2} \tag{Eq. 7-1}$$

Where:

m_a is the modulation index, which is ≤ 1 .

V_{dc} is the dc voltage.

The harmonics in the output voltage are expressed by Equation 7-2.

$$h = j(m_f) \pm k \tag{Eq. 7-2}$$

Where:

j is an integer.

m_f is the frequency modulation ratio.

k is an integer.

When assuming that m_a is ≤ 1 , for odd values of j , the harmonics exist only for even values of k . For even values of j , harmonics exist only for odd values of k [37]. If $m_a > 1$ (overmodulation), the output ac voltage from the converter contains many more harmonics. (Maximum reactive power is delivered from the converter when it operates at a modulation ratio of 1 or, if overmodulation is used, when it exceeds a modulation ratio of 1. The maximum rated reactive power generation of some high-voltage dc light schemes is approximately 50% of the converter's rated active power. In this case, the rated output power of the converter becomes 112% of the continuous active power rating.). Thus, to avoid excessive harmonic losses in the superconducting cable, overmodulation should be avoided. The waveform shown in Figure 7-3 is bipolar modulation; it is included to illustrate how a PWM converter operates. Further harmonic spectrum improvements can be accomplished by using unipolar or other modulation schemes.

The converters used to connect the dc cable and the ac system will be three-phase converters, possibly of the type shown in Figure 7-4. The phase-to-phase voltage per unit for this converter is shown in Figure 7-5.

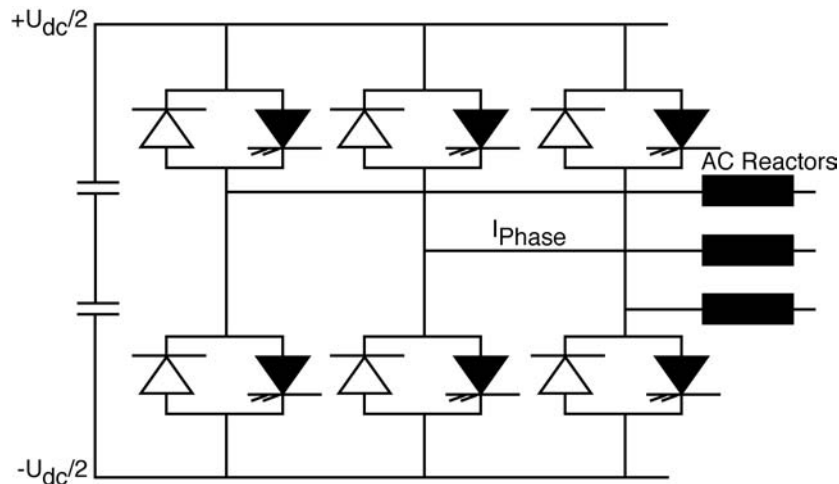


Figure 7-4
Three-phase, two-level voltage source converter

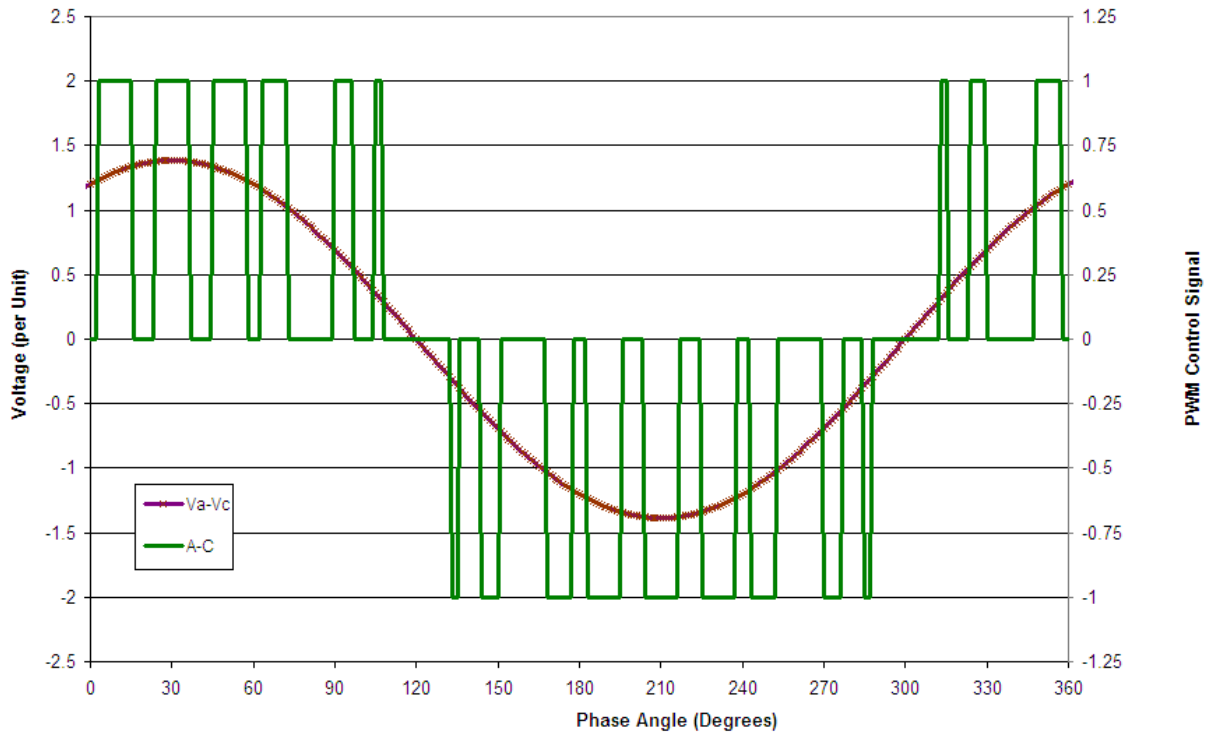


Figure 7-5
Switched phase-to-phase output voltage and fundamental ac component for the three-phase, two-level voltage source converter

The output voltage of a three-phase converter does not contain all the harmonics found in single-phase converters because some harmonics cancel. Specifically, the harmonics at m_f and multiples of m_f disappear. Selecting a switching frequency that is an odd multiple of 3 times the fundamental frequency (for example, 180 Hz, 540 Hz, or 900 Hz) avoids all even harmonics and all harmonics that are multiples of m_f . The ac harmonic currents that arise as a result of the harmonic voltages impressed on the reactor shown in Figure 7-2 do not necessarily pass through the capacitor on the dc side, because they often just circulate between two or three of the ac phases. However, under unsymmetrical ac system conditions, fundamental frequency and multiples of the fundamental frequency harmonics arise in the dc output voltage of the converter.

Under balanced conditions, the voltage harmonics on the dc side are a function of 1) the pulse modulation frequency, 2) the inductance inserted in the ac phase conductors, and 3) the size of the capacitor. The switching losses are related to the modulation frequency, which should be kept as low as possible. Although modulation frequency is one of the items to be optimized, a frequency modulation ratio equal to 9 is probably the most economical, considering losses as well as filter costs. (The modulation frequency need not be a multiple of the fundamental frequency [38].) For three-phase converters without a connection between the midpoint of the converter and the transformer's neutral, the ripple current through the capacitor at no load looks

approximately like Figure 7-6. This figure shows a 60° interval (about 2.8 ms) of the switching sequence and the capacitor current. The current has been calculated assuming a constant dc voltage. The scale depends on the size of the capacitor.

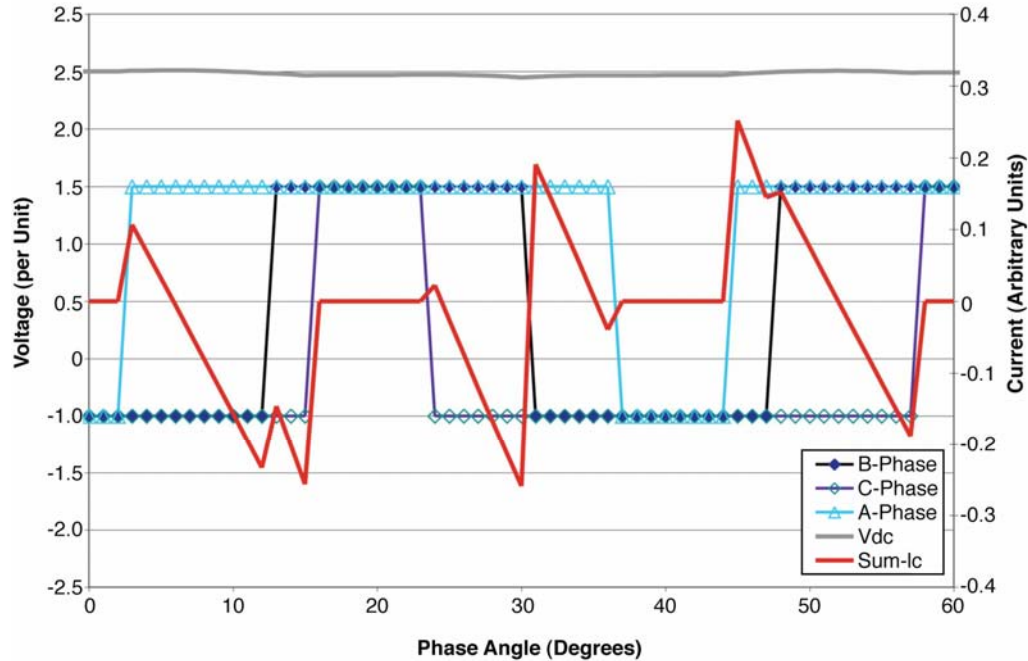


Figure 7-6
Ripple current through the capacitor at no load

Figure 7-6 shows that, during some intervals, no current flows from the dc side to the ac side of the converter. During these periods, which occur twice in any 60° interval or 12 times per cycle, the current in the cable must be stored in the capacitor. The size of the capacitor is important for control of the current fluctuations in the cable. The size of the capacitor is usually based on obtaining a reasonable charging time, as shown in Equation 7-3 [39].

$$\tau = \frac{C * V_d^2}{2 * S} \quad \text{Eq. 7-3}$$

Where:

τ is the time constant for charging the capacitor using the rated power.

C is the size of the capacitor.

V_d is the rated dc voltage.

S is the rated power of the converter.

A time constant of approximately 5 ms has been proposed for dc systems with VSCs [40]. (For time constants <2 ms, the third harmonic appears in the voltage across the dc capacitor.) For a system with a dc voltage rating of about 120 kV, a converter rating of 200 MW, and a 5-ms time constant, the capacitor should be about 140 μ F. The rated current for a 200-MW converter is 1.67 kA. If the rated current is blocked for 9° in a 60 Hz system, the voltage rise (ΔV) will be approximately 5 kV (about 4.2% of the rated dc voltage), calculated as shown in Equation 7-4.

$$\Delta V = \frac{I_c * \Delta t}{C} \quad \text{Eq. 7-4}$$

Where:

I_c is the current.

$$t = \frac{9}{360 * f}$$

This becomes a steady-state ripple current in the cable, which is an important aspect for calculation of the cable losses. Unbalanced ac system conditions such as those that arise as a result of faults, although of short duration, can be more important than the steady-state ripple currents. For example, Peter Lehn's paper indicates that a second harmonic at approximately 30% of the dc voltage would be caused by an unbalance of 10% negative sequence voltage in the ac system [41]. The system described in Lehn's paper had an equivalent time constant of approximately 2 ms [41]. Therefore, control techniques to block the negative-sequence component should be investigated to mitigate this undesirable stress imposed on the dc cable from unbalanced ac system conditions.

The choice of the capacitor is nontrivial because it can form a resonant circuit with the phase inductances. The phase leg of a VSC represents a circuit with low damping. The superconducting cable also has little damping of time-varying current flows. Thus, the capacitor must be chosen so that a resonance between the capacitor and other circuit elements is avoided. In case of ac system asymmetries, low-frequency ac components (primarily second harmonics) will appear on the dc side of the converter. This may require low-frequency damping circuits placed between the superconducting cable and the converter. Further studies are needed to explore this area fully.

7.4 Grounding of the Superconducting Cables

The superconducting dc cable system includes both superconducting and normal conducting materials. A small ac voltage drop can occur along the cable as a result of injected harmonics from the converters or transients entering the cables from the termination points. Such a voltage drop will produce a current in the resistive normal material. If the cable is grounded at more than one terminus, some of the current may circulate. Operation with continuous ground current is not allowed according to the 2002 National Electrical Safety Code; however, no specific current limit is stated [42]. Section 123D states that "on systems greater than 750V, the dc system shall

be grounded in accordance with methods specified in Section 9 of this code,” and section 092D states that “ground connection points shall be so arranged that under normal circumstances there will be no objectionable flow of current over the grounding conductors” [42].

In general, for dc systems, monopolar operation using ground return is not permitted in the United States, and for bipolar schemes, emergency operation using one pole and ground is typically limited to a relatively small number of hours per year. Compared to conventional high-voltage dc cables, the dc superconducting cable will operate at a relatively low voltage and high current. At an operating current of 50 kA, the voltage drop in a ground return would be a significant fraction of the total voltage within the system. As a result, it is impractical to allow a ground current in a superconducting dc cable. The design of the converter and overall system must accommodate this cable feature.

There is no dc voltage drop along a superconducting cable. Conventional cables have such a voltage drop, and it is a critical part of transferring current from one circuit to another. This could become an issue if the return conductors are grounded at both ends of the cable. If both ends of the cables are grounded, it would be difficult to guarantee that the two parallel, superconducting cable neutrals will always have current flows that match the current flows in the center conductor of each cable. If there is a mismatch, a net magnetic field will also arise around each of the cables, which is undesirable. Thus, it is assumed that the neutrals of the cables will be grounded at one point only. This will lead to voltage transients between earth and the neutral points of the nongrounded cable terminals, because the ac resistance of the superconducting neutral of the cable is not zero. As designed, the superconducting cable is much like an ideal coaxial cable. Thus, independent of ground connections and circuits, the neutrals will carry harmonic currents equal and opposite to those in the center conductors. Depending on cable and converter design, blocking filters might be required to limit harmonics at both the high-voltage side and the neutral side of the cable.

Transient overvoltage protection using metal oxide arresters can be installed between the neutral conductor and ground, at least at each converter station, to limit the magnitude of the voltage transients. This is a situation similar to that of existing dc links using a metallic return instead of an earth return for the neutral current. Because of the nature of the superconductors, the voltage between the neutral conductor and ground (nominally the enclosing pipes—vacuum and cryogenic) will generally be quite small. Nevertheless, the insulation between the cable’s neutral conductor and the pipe in which the cable will be installed must be sufficient to withstand the expected voltage difference. For extremely long cables, voltage rise between the neutral and ground arising as a result of geomagnetically induced currents must also be considered.

Voltages between the neutral and the cable pipes can also arise as a result of short circuits between the central and neutral conductors of the concentric coaxial cable. Figure 7-7 shows a highly simplified superconducting cable arrangement.

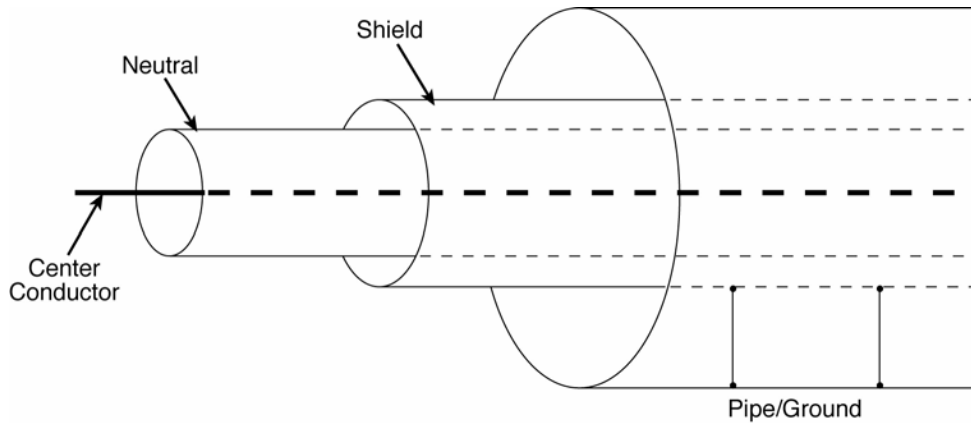


Figure 7-7
Highly simplified superconducting cable design

Assuming that the rated voltage of the cable is 120 kV, the voltage will be reduced to zero between the center and the neutral conductors at the point of the short circuit. That is, the voltage on the center conductor will go down, and the voltage on the neutral of the cable will rise. However, the neutral is coupled to the ground through neutral-to-pipe and pipe-to-ground capacitances, and possibly direct connections of a controlled resistance. The short circuit will, therefore, set up traveling waves between the center conductor of the cable and the neutral, between the neutral and the pipe, and between the pipe and ground. These waves will propagate in both directions from the point of failure. Because the propagation speeds of these waves are all different, phase displacements between the waves will arise. The propagation speed (v) is calculated by Equation 7-5.

$$v = \sqrt{\frac{1}{\mu\mu_o\epsilon\epsilon_o}} \text{ with } c = \sqrt{\frac{1}{\mu_o\epsilon_o}} \quad \text{Eq. 7-5}$$

Where:

μ is the relative permeability, a dimensionless quantity that is equal to 1.0 for a vacuum.

μ_o is the permeability of a vacuum ($4\pi \cdot 10^{-7}$ H/m).

ϵ is the relative permittivity, a dimensionless quantity that is equal to 1.0 for a vacuum.

ϵ_o is the permittivity of a vacuum (8.854 pF/m).

c is the speed of light in a vacuum.

For vacuum, the propagation speed is equal to the speed of light or 300 km/ms. Because the dielectric system between the center (inner superconducting conductor) and the neutral (outer superconducting conductor) conductors of the cable probably will include some dielectric material, possibly impregnated by some cooling medium (for example, as shown in Figure 7-8)

with a dielectric constant about 2 times that of air, the wave propagation rate can be expected to be as low as 70% of the speed of light. Also, the attenuation of the different waves will differ, because it can be assumed that the attenuation of the waves between the central and neutral conductors of the superconducting cable will be less than the attenuation between the pipe and the neutral of the cable and between the pipe and ground. This must also be considered in assessing the insulation requirement between the neutral and the surrounding pipe [43].

Comparing the simplified geometry of Figure 7-7 with the more realistic geometry shown in Figure 7-8 suggests that an analysis should be made of the grounding approach for the outer pipe and cryogenic pipe. In addition, because the vacuum enclosure will contain MLI, which has some electrically conductive components, the electric field and insulation levels between the various components should be assessed in detail for a variety of conditions.

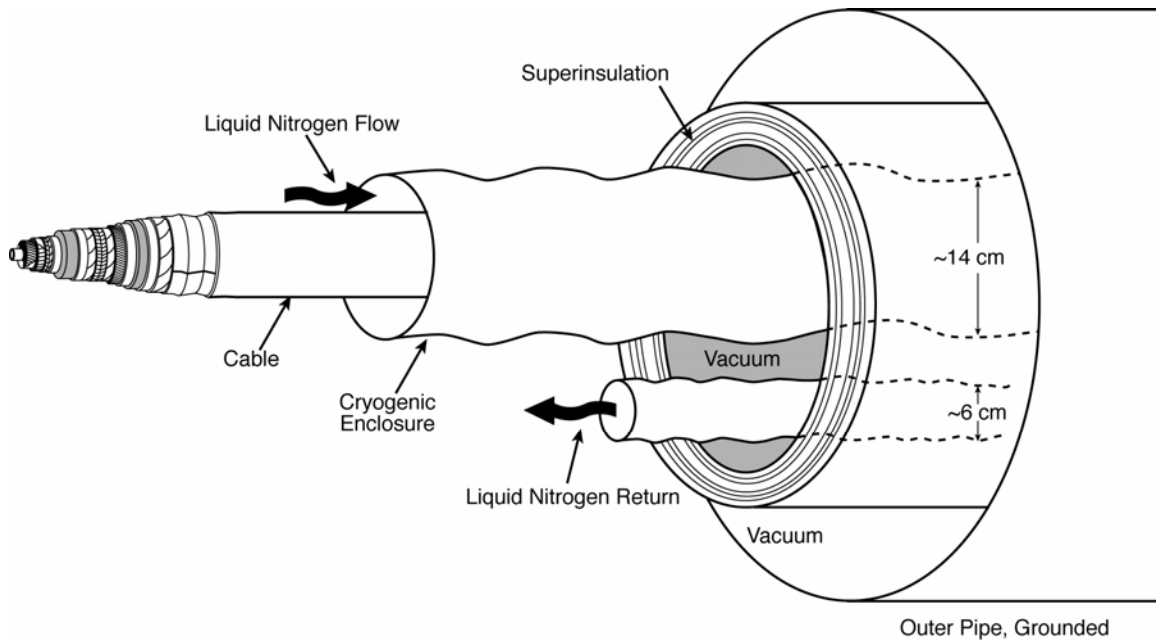


Figure 7-8
Cable in pipe envelope showing various components

7.5 Energization of the DC System

Sudden and large changes of the current in the dc cable must be avoided. However, when voltage source converters are energized from the ac system with zero voltage on the capacitor of the converter, large inrush currents would flow into the capacitor through the converters. This would cause a large inrush current into the cable to charge the capacitance. The rate of charging is limited by the cable’s surge impedance (Z_w) in ohms, which is defined by Equation 7-6.

$$Z_w = \sqrt{\frac{L}{C}} \tag{Eq. 7-6}$$

Where:

L is the inductance.

C is the capacitance.

The expected surge impedance for this cable is approximately 6–7 Ω . Thus, the cable will almost look like a short circuit to the ac system. If a step voltage of 120 kV were to be applied to the cable, the resulting current would be about 20 kA. If the cable were open ended, the reflected wave would result in 240 kV being reflected from the remote end, where the current would go to zero. This would introduce not only large, short-term losses in the superconducting cable but also a substantial overvoltage stress. In the actual case, the inrush current from the VSC will be limited by the ac-side reactors and the converter transformer. Because the ac losses in the superconducting cable are low, these waves would be lightly damped and would therefore travel back and forth between the cable ends until they eventually died out by themselves. If damping equipment is installed or losses are introduced into the system in other ways, the transients could be damped out more quickly.

The startup transients can be avoided or limited either by precharging the cable to its rated voltage or by using current-limiting devices in the ac network. Precharging could be accomplished by using a CSC at some nominal rating at the rectifier terminal. Alternatively, the converter can be energized through switching resistors to limit the inrush currents. After the cable has reached nominal voltage, other converters could be energized from the dc side before the ac breakers are closed. If the inrush currents would be unacceptably large when energizing the dc capacitor from the cable, current-limiting techniques must be used at all the connected converter terminals.

7.6 Further Research and Development Needs

Early research on superconducting cable transmission systems dealt with low-temperature superconductors using CSC technologies where dc cable applications were envisioned. This work is still relevant for the new HTS cables, which are the subject of this study. However, today's newer technologies offer possibilities for multiterminal operation using multiple VSCs, which makes it possible to consider using superconducting cables as long-distance, electric superhighways with multiple on and off ramps. Several issues demand careful study, including the following considerations for design and operation of the cables:

- Cable protection issues related to cable short circuits and rapid deenergization of the cables or parts of a cable
- Harmonic injection into the cables at steady state and during operation with voltage unbalances in the ac systems
- Energization of the cables for bumpless connection of converters to the cables

- Dispatching of power through the cable to handle load following, power flow direction changes, and so on
- Emergency transfer of power from one circuit to a parallel cable circuit in case of failure on one cable
- Crowbar or other means to ride through a temporary loss of a converter to avoid interruption of the cable current and voltage collapse of the dc cable

Although the well-known CSC technologies can be used with confidence for point-to-point transmission systems, the envisioned system using multiple VSC technologies is relatively unknown. Therefore, for design and operation of a VSC, the following should be studied:

- Converter topology for loss minimization and cost optimization, which could involve the use of soft switching converter concepts
- Harmonic filter design for blocking harmonics from entering the cables
- Control strategies to minimize injection of fundamental frequency components into the dc cable in case of an unbalanced fault in the ac system or systems
- Development of control and protection strategies for temporary loss for a converter or a set of converters in case of an ac system fault
- Development of switches and switching strategies for transfer of a converter from one cable to the parallel cable

For design and operation of the transmission system, the following should be studied:

- Performance of an ac system with multiple VSC infeeds to a major metropolitan area
- Optimization of the converter size
- Use of CSC technologies for rectifier stations with no need for power reversal as a part of the overall transmission system
- Potential interactions between converters in close proximity to each other
- Voltage control of the dc cable and strategies dealing with loss of rectifiers and inverters
- Overall reliability assessment of the transmissions system, including identification of critical failure modes and their impact on the ac system

In order to develop a viable dc superconducting cable, high priority should be given to developing and understanding the expected harmonic currents injected into the dc cable for balanced and unbalanced ac system operation. In addition, the power transients associated with starting or stopping converters must be thoroughly investigated. This information is needed for the design of the cable cooling system.

8

FABRICATION AND INSTALLATION

This section describes the various components and stages of fabrication and installation of the superconducting dc cable. (Section 4, Cable Design and Fabrication, covers the fabrication of the cable core, and Section 5, Vacuum System, establishes the vacuum requirements and describes the vacuum pipe dimensions and the distance between vacuum pumps.)

Factory-fabricated components include the following:

- Vacuum pipe
- Reflective coating
- Cryogenic enclosure and return pipe
- Cryogenic supports
- MLI
- Getters
- Factory welds
- Instrumentation
- Collar and protective end caps

Field fabrication and final assembly stages include the following:

- Site preparation
- Transportation
- Positioning in trench
- Welding of cryogenic pipes and connecting instruments
- Welding of collars to connect the vacuum pipe

Vault and manhole installation stages include the following:

- Cable pulling
- Cable splicing
- Vacuum and cryogenic component sectioning
- Vacuum pump installation and pumpdown
- Cryogenic station installation

8.1 Factory-Fabricated Components

8.1.1 Vacuum Pipe

A major goal of this program was to develop a design that would allow as much factory fabrication as possible. Just as the cable was designed to be fabricated in pieces as long as possible, the vacuum pipe and the cryogenic components are also developed for the maximum length that can be transported. Section 5, Vacuum System, describes the vacuum pipe and the radial and cross-sectional dimensions required for an adequate vacuum demanded by low heat transfer from the ambient temperature walls to the cryogenic pipes enclosing the cable and the return. Because the outer diameter of the pipe must be ≥ 70 cm, the design was developed around a pipe of this dimension. An evaluation of transportation issues suggests that pipes of this diameter could be transported with normal road requirements in lengths of at least 20 m, which is the length used for the present assessment. Figure 8-1 is an artist's concept of a completed vacuum pipe section that is ready for shipment from the factory to the installation site. The design shown in the figure was used for cryogenic and vacuum calculations.

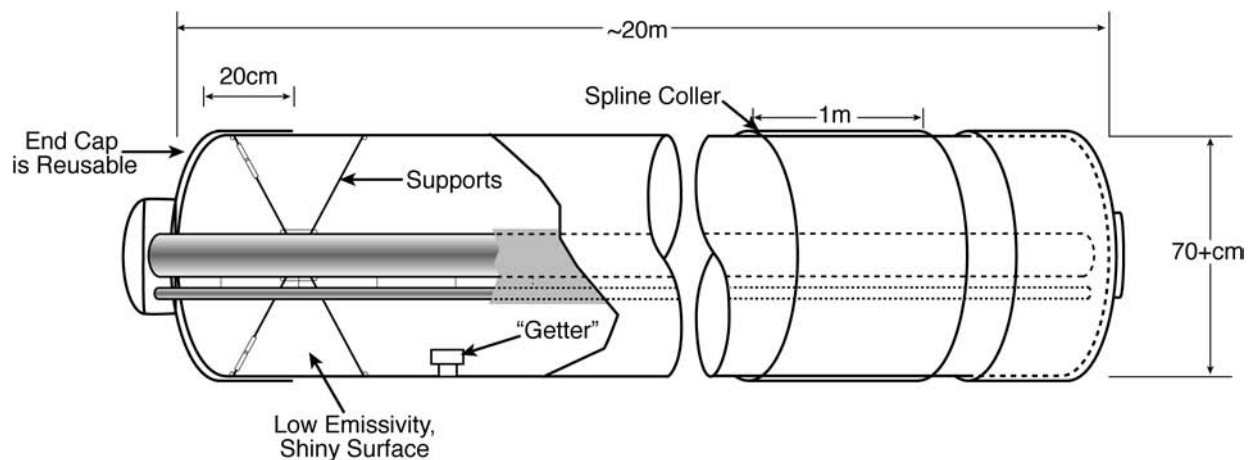


Figure 8-1
Simplified design of factory-assembled pipe for superconducting dc cable

Natural gas is transported over long distances in pressurized steel pipes. These pipes can be fabricated in several ways. Some are made from a roll of mild steel by twisting it so that welds along its length form spirals on the pipe's surface. Rather long sections of pipe can be formed in this way, with the limit being the size of the spool of steel sheet. Some large-diameter pipes are formed continuously from multiple rolls by welding the end of one roll to the beginning of the next roll. To obtain extremely long lengths, the winding and welding often occur at the installation site, shortly before placing the pipe in the ground. Another procedure uses a sheet of steel that is as wide as the circumference of the pipe, rolls it into shape, and forms a longitudinal weld (also called a *seam weld*) along the length of the section. Except for the diameter of the tube and the section length, this procedure is much the same as that used to form the outer sheath of the cable core (see Section 4, Cable Design and Fabrication). Pipe formed in this fashion has a longitudinal weld that continues along its length. Factory-fabricated natural gas pipes are either made to length or cut to length, typically 12–24 m, for transport to the installation site. Pieces of

gas pipe are prepared for installation in a trench with an external coating that prevents corrosion and provides cathodic protection. This coating stops a few centimeters from the end of each section to avoid overheating of the coating material while the pipe sections are welded together. A similar coating would be needed on the pipe for the superconducting dc cable.

Whereas the pipe used to transport natural gas operates with an internal pressure of many atmospheres, the vacuum pipe must withstand only the pressure differential between the internal vacuum and the pressure resulting from the external atmosphere and, in the case of a trench, the weight of the backfill. Although the pressure is less, the vacuum pipe must be designed on the basis of standards associated with buckling or collapse. For a given pressure, a much greater wall thickness is required to resist buckling than to accommodate a symmetrical, internal pressure. Exact wall thicknesses will be optimized during future studies and will depend on cable placement. Here we assume that existing, 70-cm diameter gas pipeline of approximately 1-cm wall thickness that can accommodate internal pressures of 30 atm will be adequate for the vacuum pipe.

An issue for the superconducting dc cable pipe that does not exist for the natural gas pipe is the potential for unplanned cooling associated with a release of liquid nitrogen, which might occur if a cryogenic pipe failed. Although the cryogenic pipes are engineered to withstand considerable overpressure, several scenarios can be conceived whereby liquid nitrogen could be released into the vacuum space. Two areas become critical in the case of a release of liquid nitrogen. The first is the pressure inside the vacuum pipe that is caused by the evaporation of the enclosed nitrogen. Each meter of cable contains about 7 kg of nitrogen. If all this liquid was evaporated and warmed to ambient temperature with no pressure relief, the vacuum pipe would have an internal pressure of about 12 atm. The stresses within the pipe at this pressure would be lower than in the equivalent natural gas pipeline. So long as the vacuum pipe remained at ambient temperature, this would not be an issue. However, if the liquid nitrogen were to appreciably cool part of the pipe, its sensitivity to stresses might be increased, because mild steel exhibits a phase transition from a ductile, austenitic material to a brittle, martensitic material when it is cooled. The temperature at which this transition occurs is determined by the chemical properties of the steel, such as the amount of carbon, chromium, and so on. The mild steel used for natural gas pipelines is generally fabricated to have a transition that is well below the lowest environmental temperature to which it will be exposed. Further analysis will be needed to assess the impact of cooling resulting from nitrogen loss on the allowable characteristics of the vacuum pipe.

After a section of pipe is cut to length, both ends must be machined to the proper surface for eventual welding to adjacent sections. The diameter and thickness of the pipes at the ends must be within a small tolerance range in order to allow rapid and automatic field welding. In addition, the ends must be beveled to accommodate a multipass weld procedure that will fill them to a smooth surface on the outside.

After the pipe is formed to the appropriate diameter and length, fixtures are welded onto the inside of the pipe at each end to support the cryogenic components. These fixtures are designed to support the weight of the loaded cryogenic pipes and to withstand the force associated with cryogenic cooldown and cable pulling.

8.1.2 Cleaning Vacuum Pipe and Installing Internal Reflective Coating

Most steels have oil, organic solvents, or other materials applied during their production. These materials are generally volatile, and they evaporate from the surface over a long period; in some cases, this process can continue for months. The gas that evaporates from the warm surface of the vacuum pipe has two effects. First, it must be removed from the vacuum space to ensure a low pressure, and thus a low heat leak, to the cryogenic components; therefore, vacuum pumps are required. Second, some of this residual material will be deposited on the surfaces of the cold MLI that is near the cryogenic components. These deposits cause the emissivity of the MLI to increase. Over time, the higher emissivity causes the heat flow into the cryogenic components to increase.

To reduce these problems, the surface of the pipe must be carefully cleaned to remove contaminants. This can be accomplished by using solvents or an abrasive procedure or both. After it is cleaned, the interior surface of the pipe is coated with a layer of low-emissivity material. The material can be applied in the form of a thin film, or it can be a low-vapor-pressure plastic sheet that is similar to, but thicker than, the aluminized Mylar film that is used for the MLI in the vacuum space. If a sheet is used, it will be attached to the surface of the steel vacuum pipe with a special, low-vapor-pressure adhesive material that further helps to seal the pipe from evaporative processes.

8.1.3 Cryogenic Enclosure and Return Pipe

The cryogenic components within the vacuum pipe assembly are separated into two tubes (see Section 6, Cryogenics). The nitrogen flows in one direction in the cryogenic enclosure with the cable core and flows in the opposite direction in the return pipe. The diameters of the two pipes are adjusted so that their hydraulic diameters are approximately 6 cm. Because parts of the surfaces are scalloped, the actual diameter of the return pipe is somewhat larger, whereas the diameter in the cryogenic enclosure is determined by the size of the cable core. These two pipes are made of an austenitic stainless steel that is chosen because it remains ductile at cryogenic temperatures (≤ 120 K).

Both the cryogenic enclosure and the return pipe have a bellows structure welded on at one end. The length of the bellow sections is selected so that after the pipes are installed in a trench, the free end of the bellows can be welded to the next section of cryogenic pipe. Welding in the factory is accomplished by an automatic welding machine. Each pipe and its associated bellows is certified to be leak-free before the MLI is applied.

The outside of each of these pipes has either a low-emissivity coating or a special surface layer that is added to reduce radiative heat transfer or both. This coating is similar to that used on the outer vacuum pipe, but the method of attachment might be different because it operates at about 70 K and will experience several thermal cycles between this temperature and ambient. Because many of the materials used to reduce emissivity are sensitive to the elevated temperatures that can occur during welding, the coatings will likely stop some distance away from the surfaces to be welded.

The extent of the movement of the cryogenic enclosure and the return pipe are determined by overall pipe length, transportation forces, thermal expansion and contraction, and the support system. The combined cryogenic pipes are surrounded by one or two bats of MLI with a total of about 40 layers.

8.1.4 Cryogenic Supports

The cryogenic enclosure is attached to the vacuum pipe by sets of supports near each end that are held in tension. Using tension elements or members is the most effective way to control heat flow into a cold region, because they can be made quite long compared to their cross section. These supports must retain their strength at all operating temperatures, and they must be strong and elastic to accommodate cable pulling forces and cooldown contraction. Stainless steel wire and Kevlar fiber rope structures have been used for this purpose in a variety of superconducting magnets.

Transverse forces will likely be greater during transportation than during operation. This is typical of many devices and will require supplemental supports. The design and extent of those supports is a task for the future. In addition, these supports will have a turnbuckle or some other adjustment or positioning mechanism that will allow the installation crew to adjust position and tension to the appropriate value when the vacuum pipes are attached to each other.

The return pipe is supported and held in position by the cryogenic enclosure; that is, a mechanical coupling holds the return pipe loosely in place and allows some axial and transverse relative movement. The return pipe might also require supplemental supports during transportation. Because both pipes contain liquid nitrogen, the thermal characteristic of the support between them has a reduced thermal requirement compared to the major support elements. However, the thermal conductivity of the support must be sufficiently low to avoid an excessive temperature inversion between refrigeration stations. The possibility of temperature excursions resulting from counterflow heat exchange is described in Section 6, Cryogenics. Detailed calculations will require future work.

8.1.5 Multilayer Insulation

The effectiveness of MLI as a thermal insulator is described in Section 5, Vacuum System. This section describes the methods used to apply the MLI and the care with which that part of the fabrication must be accomplished. MLI is made in a variety of forms from several different manufacturers. The most frequently used form is a bat of a large number of layers that is delivered to the site where it is to be installed. These bats consist of 20–50 layers of aluminized

Mylar film. Each layer is only 0.012 mm thick. Thus, MLI is extremely light, but it is also rather fragile. Additional material is often layered with the aluminized Mylar film to maintain separation between layers, to provide strength, and to hold the MLI bat in its optimal shape over long periods of use. The Mylar film, and to a lesser extent the separator, adsorbs gases. For this reason, the bats of MLI are often protected in an enclosure with a dry nitrogen or argon atmosphere until just before installation. In critical applications such as spacecraft, the installation is done in a clean room.

There are several approaches for installing the MLI on the cryogenic pipes. One straightforward procedure is described here as an example. It is quite likely, however, that more sophisticated procedures will be developed because of the large number of pipe sections. After the two cryogenic pipes are fabricated and positioned relative to each other in the factory, one or more bats of MLI will be wrapped around the combined cold structure, which is often referred to as the *cold mass*. A first bat of MLI will be installed in such a way that it is close to the cryogenic pipes. The bat will be overlapped so that there is no open space for heat to shine onto the cryogenic vessel. It will be kept in place by a tape, rope, or string. The material used to hold the MLI must be chosen carefully to avoid long-term outgassing. Tapes with a special adhesive that does not outgas or adsorb residual gas are often used for this purpose. Some space will be left at the locations where the support struts attach to the cryogenic vessel. A second bat of MLI is wrapped over the first. It will also be overlapped and positioned so that the two sections cannot be opened at the same location.

MLI will also be wrapped around each of the support struts, with particular care in the region where they connect to the cryogenic enclosure. Because there will be considerable gas flow along the cable system during the initial stages of pumpdown, the region of the struts close to the vacuum pipe will have limited MLI. In effect, this increases the hydraulic diameter of the system and reduces the load on the vacuum pumps.

8.1.6 Getters

Hydrogen gas is emitted by the steel walls of the vacuum pipe, the stainless steel in the cryogenic enclosure, the return pipe, and to some extent, the bats of MLI insulation that are wrapped around the cold mass. The pumps described in Section 5, Vacuum System, are specified to have the capacity to remove all the gas in the vacuum space down to the specified level of operation at about 10^{-4} Torr. If the vacuum system is well sealed, after some weeks or months of high vacuum, hydrogen is the most prevalent gas, and the mass flow into the system is only a fraction of the pumps' capabilities. Turning the pumps off decreases the power requirements and the operating costs of the cable. Fortunately, hydrogen is also the easiest material for a getter to remove. Depending on the getter materials and design, getters can also remove oxygen, carbon dioxide, and some other gases, but not helium. If the cable system is designed properly—that is, if there are few leaks—the getters alone should maintain a sufficient vacuum for effective operation, even if nearly all the vacuum pumps are turned off. In addition to the getters acting locally to maintain the vacuum, the cold surfaces of the cryogenic pipes will provide some additional pumping capacity for substances such as water and hydrocarbons.

Several elements—including palladium, cobalt, and zirconium—are used in the getters. The exact mix of materials and the shape and structure of the getter is based on system design. If hydrogen is the only contaminant present in the vacuum, saturation occurs after the getter material adsorbs about 0.007 grams of hydrogen per gram of getter material. Although the exact mass of getter material needed in the superconducting dc cable must be determined after some pipe sections have been built and tested, the number of getters will be sufficiently large that a special shape, and perhaps even a special material mix, can be chosen.

All commercially available getters require a high-temperature thermal activation. An electrical heater is used to drive the activation process, which varies from 450°C for 10 minutes to 300°C for 5–6 hours. These temperatures are higher than the melting temperature (or at least the softening temperature) of the Mylar film. Therefore, the getter must be placed so that heat cannot be conducted to the bats of MLI. Even thermal radiation during getter activation can raise the temperature of the Mylar film so that the thermal insulating properties of the MLI are degraded. Activation is carried out after a modest vacuum is established; otherwise, the getter material can become saturated by the initial, high-density gas in the space between the vacuum pipe and the cold mass.

A saturated getter can be reactivated by reheating it to the activation temperature. Only a fraction of the adsorbed gas is released, and most of it is redistributed within the structure of the getter, which can be reused without removing it from the vacuum space. After several reactivations, the structure of the getter weakens, and its effectiveness diminishes. The main effect is a reduction in the surface area available for adsorption.

The getter must be mounted so that it is thermally insulated from the MLI and any plastic components that are on the ambient-temperature walls. The mounting must also be located where it is convenient to establish an electrical connection. Generally, this means that the getter should be placed near one end (or perhaps at each end) of the vacuum pipes, where it can be accessed if needed. Because a series of the 20-m-long pipes will be connected in the field, an electric wire that connects to all their heaters must be installed from end to end of each 1-km section. This line operates infrequently and carries low currents, but it must be checked for continuity, electrical insulation, and resistance as the pipes are installed.

8.1.7 Factory Welds

The welds on the vacuum pipe must be much more precise than the welds in a gas pipeline, for several reasons. Installed sections of gas pipeline are typically pressure-tested with water to some safe level that exceeds the working pressure. In general, small gas leaks from the pipeline, which are usually from welds but occasionally from porosity in the base steel, cannot be detected by such a hydraulic test. However, these gas leaks are so small as to be nonhazardous, and they have little financial impact on the operation of the pipeline. The vacuum pipe for the superconducting dc cable will have a variety of internal components, including MLI, that make hydraulic testing impossible. Welds are much more critical for the superconducting dc cable's vacuum pipe, because there is no simple and effective leak-detection method, and leaks that are considered tiny for a gas pipeline can greatly impact the quality of the vacuum in the superconducting dc cable. The total leak into a 1-km section of pipe must be less than 10^{-5} g/s of nitrogen in order for the vacuum pumps and getters to function properly. Welding to this precision is considerably

different from the standard procedures for gas piping, even when much of the welding is done by a machine. Typically, vacuum and cryogenics welding personnel are trained and certified, even when most of the welding involves an inert gas and is done by special, automated welding heads. Although this issue is critical, the industrial gas community has a great deal of experience with the welding of cryogenic and vacuum systems.

8.1.8 Instrumentation

The details of the instrumentation for the superconducting dc cable are not yet decided. However, each 1-km section of cable will have several vacuum sensors and wires for activating the getters that will extend the entire length of the section. The wires for this purpose will be attached securely to the vacuum pipe and will have connectors at the ends of each individual pipe section. Just as for the MLI, these wires must be protected from excess heating that could occur during the welding process. As in other cryogenic systems, this will be accomplished by standoffs that support the conductors several centimeters away from the high-temperature regions of the welds.

8.1.9 Installation of Collar and Protective End Caps

At some point in the fabrication of the vacuum pipe, a collar will be slid over the pipe and spot-welded into position. The collar and pipe might have matching splines that can be used to ensure circumferential registry from section to section. If the registry is not adequate, the cryogenic pipes could be subjected to a twisting force that could overstress the supports. A detailed design of the system will provide information on the allowable limits for angular positioning of the cryogenic components.

After the vacuum pipe is fabricated with a collar, cryogenic components, supports, thermal insulation, getters, and any monitoring components, each end will be covered by a temporary cap to maintain cleanliness during shipping. Although they are seemingly simple items, these caps must seal the pipe from road and other environmental conditions that can easily impair the vacuum and cryogenic functions of the pipe section. These caps can be sufficiently robust to be reused many times.

8.2 Field Fabrication and Final Assembly

8.2.1 Site Preparation

Figure 8-2 shows a typical installation of a natural gas pipeline. In this example, the ground is soft enough that topsoil can be scraped or bulldozed away to prepare the bed for the pipe. Trucks with several pipe sections arrive, and a crane is used to offload the sections. To this point, the site work and preparation for the superconducting dc cable is similar to that for natural gas pipelines. The redundant nature of two full power cables considerably improves the reliability of the pathway as an element in the power grid. Therefore, the first notable difference from a natural gas pipeline installation is that two parallel superconducting dc cables will be installed.

These cables can use the same trench; the site should be wide enough to accommodate a separation of about 20 m between the two cables (see Figure 8-2). Installing the two cables at the same time will simplify logistics and use the field fabrication team more effectively.



Figure 8-2
Example of gas pipeline being delivered to site in preparation for welding

Source: Duke Energy Gas Transmission Canada

The example shown in Figure 8-2 is misleading in some ways because it is an “easy” site. Gas pipelines and the superconducting dc cable are both cross-country transmission systems; they must cross rivers, mountain ranges, deserts, and so on. In each case, special site preparation and field fabrication are required to meet the challenges associated with elevation change, temperature extremes, hydraulic conditions, and the like. These issues have been successfully addressed for natural gas pipelines, and it is expected that most of them can be addressed in a similar fashion for the superconducting dc cable.

There are two notable differences between the two systems. The first is the vacuum requirement for the superconducting dc cable, which requires active vacuum pumps approximately every kilometer. The second is the effect of elevation changes on the pipes that contain the fluids. Natural gas pipelines operate at pressures up to about 100 atm. The wall thickness of the steel pipe is chosen to withstand this pressure with some safety factor. The liquid nitrogen operates at pressures of about 5 atm, and the walls of the pipes are made to operate with similar safety factors. The density of the natural gas in a pipeline can be up to 0.2 kg/L, whereas the density of liquid nitrogen is 0.85 kg/L. An elevation change of 100 m will increase the pressure in the natural gas line by 2 atm, which is a 2% change. An elevation change of 100 m in the superconducting dc cable will increase the pressure by 9 atm, which is a 180% increase over

normal operation; if uncompensated, this increase could exceed the pressure rating of both cryogenic pipes. The approach that will be taken to compensate for the pressure change is not known at this time. However, a simple solution would be to use gaseous helium instead of liquid nitrogen in the cryogenic pipes in regions where elevation changes are important.

8.2.2 Transportation

Although Figure 8-2 provides a great deal of insight into the procedure for moving and installing the vacuum pipes at the superconducting dc cable site, it does not address the logistics issue. A 1000-km-long superconducting dc cable will have two sets of 50,000 vacuum pipes, each of which is 20 m long, that must be installed before the system can be brought into operation. The sections will be transported to the site on tractor-trailers that can accommodate nine or so pipe sections at a time (see Figure 8-3). If the construction time is on the order of three years, and a truck can make one trip per day, then, based on 250 days of operation per year, some 15 dedicated trucks will be needed. This is not a large number; even if the factory is some distance from the site and two or three days are required for transport, the number of vehicles is not exceptional.

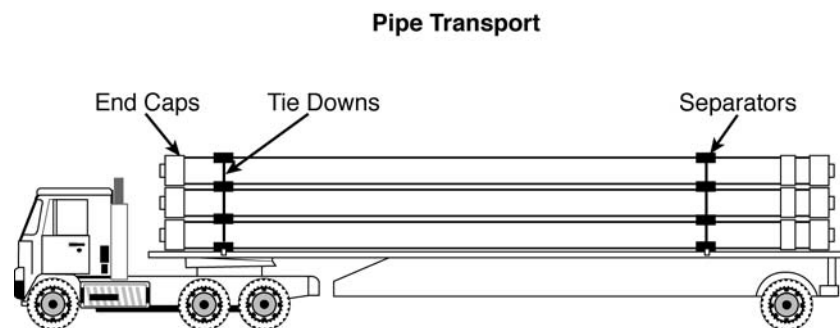


Figure 8-3
Artist's concept for truck transport of pipe sections for the superconducting dc cable

Larger issues are the preparation of the site, the availability of a space to place the 20-m sections of pipe, and a way to ensure cleanliness during the positioning and welding process. A traveling assembly building will span the trench (see Figure 8-2) to provide shelter for the pipe sections that are being processed.

8.2.3 Positioning in Trench

Setting the pipes in the trench when they are delivered to the site is, in itself, rather straightforward. However, the demands of cleanliness and the need for special welding procedures will demand some special procedures. Therefore, it is unlikely that the sections will be exposed as they are for the gas pipe shown in Figure 8-2. Some special arrangement must be made to position the pipe sections and then to use the circumferential registration to ensure proper alignment before the various components are welded together. In addition, the logistics of

installation must be coordinated with those of manufacturing and transportation to the site to ensure as short a period as possible between the time a pipe section is delivered to the site and the time that it is attached to the adjacent pipe sections. These issues affect the total number of teams that are processing the pipes and the time that it takes to complete a 1-km-long section.

Assuming that these issues are addressed as a part of the logistics for the superconducting dc cable installation, the individual steps of positioning the pipe sections begin when two sections are placed next to each other (see Figures 8-4 and 8-5). The pipe on the left is brought into a position and orientation that is determined by the previously installed section, which is to the right. To simplify the description of the installation process, the convention throughout this section is that assembly proceeds from right to left. The end cap remains on the installed section to maintain a clean environment for all the components within the pipe. When the vacuum pipe to the left is near its final position, it is anchored so that it can be moved slightly into its final position. Next, the adjacent end caps are removed and the collar is moved into position to orient the two sections circumferentially. The vacuum pipe of the left section is firmly anchored so that it cannot move with respect to the vacuum pipe in the right section.

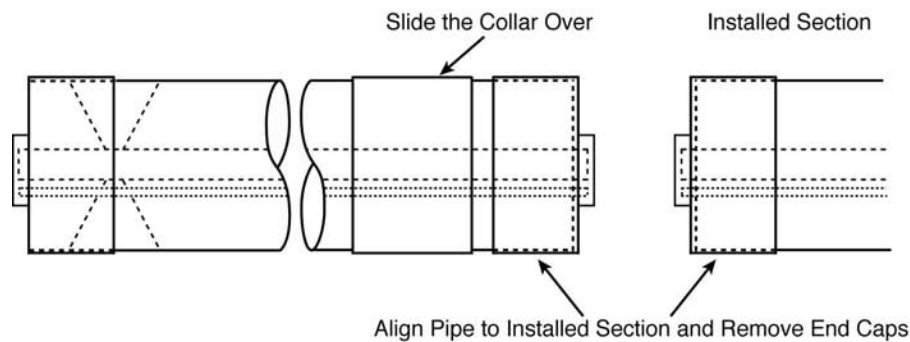


Figure 8-4
Side view of two pipe sections for the superconducting dc cable that are nearly in place

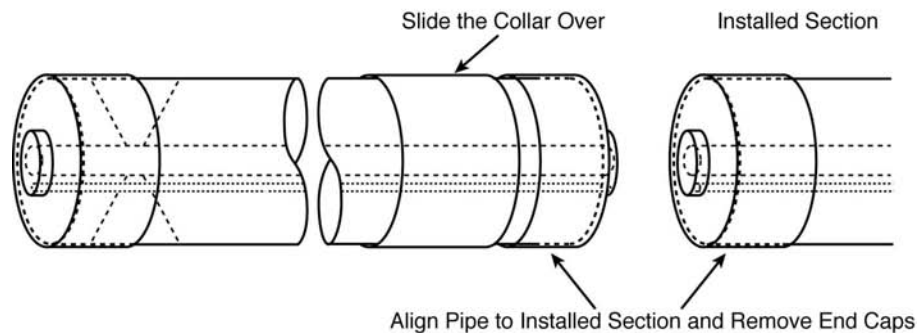
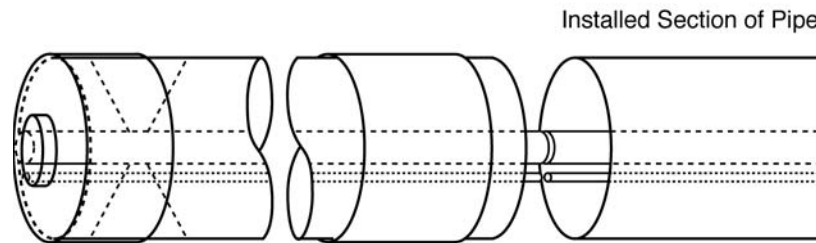


Figure 8-5
Diagonal view of two pipe sections for the superconducting dc cable that are nearly in place

8.2.4 Welding of Cryogenic Pipes and Connecting Instrumentation

After the orientations of the vacuum pipe and the cryogenic pipes are fixed, the collar is retracted to provide access to the ends of both sections (see Figure 8-6). Next, the two cryogenic pipes are welded together. This process consists of bringing the bellows on the end of the new section into contact with the pipe in the installed section. This process will occur for both the cryogenic enclosure and the liquid nitrogen return pipe. The actual welding will likely be done by robotic welding heads that are specifically designed to operate on pipes of the size and material used in the superconducting dc cable. The welding materials and the procedures used will be based on industry standards for cryogenics and vacuum. The welds will be tested to ensure that there are no leaks.



- Move the new pipe so cryogenic components are in position for welding.
- Weld the pipes together.
- Add mli over cryogenic components in and around the weld.

Figure 8-6

After the vacuum pipe of the left section is in place, the two cryogenic pipes are welded together by an automatic welder.

After both cryogenic pipes are connected, layers of MLI are installed around the newly welded sections, and the sets of supports near the opening are adjusted to hold the cryogenic components in place. These adjustments reduce the total constraint that is required to support the components during transportation. They will, however, be set to control thermal contraction during cooldown. In some cases, this requirement might increase the magnitude of the constraint. The total conduction of heat into the cryogenic environment is roughly proportional to the force used to constrain the cryogenic pipes. Thus, minimizing (optimizing) these constraints will be a goal of future design efforts.

The instrumentation leads and the wires for activating the getters are then exposed and positioned at the ends of the two sections. Continuity and resistivity are measured in both directions to ensure that all instrumentation connections are correct. The leads at the end of each section will be designed to have sufficient length for easy connection from section to section. The wires in this area will be protected from the heat produced by the welding that will occur when the two vacuum pipes are connected.

8.2.5 Welding Collars to Connect the Vacuum Pipe

Greater care is required for the vacuum pipe welds than for similar welds in a standard gas pipeline. Welds are particularly important when connecting the collars to the outside of the vacuum pipe. Preparation for this step begins with thoroughly cleaning the outer surface of the vacuum pipe and the inner surface of the collar that will be exposed to the vacuum. When these surfaces are sufficiently clean, a cylindrical sheet is introduced in the space between the two vacuum pipes. This sheet will remain at ambient temperature during cable operation, so it must have a low-emissivity material on its inner surface. The inner surface of this sheet will likely be similar to that of the vacuum pipe itself. Because most of the reflective materials are temperature sensitive, the sheet must be anchored to each pipe some distance from the location of the welds. When this sheet is in place and the cryogenic components are optically isolated from the vacuum pipe, the collar is moved into its final position. Welding proceeds circumferentially at both ends of the collar. The welds in this region can be checked by means of a temporary seal on the outside of the vacuum pipes. The completed connection between vacuum pipes is illustrated in Figure 8-7.

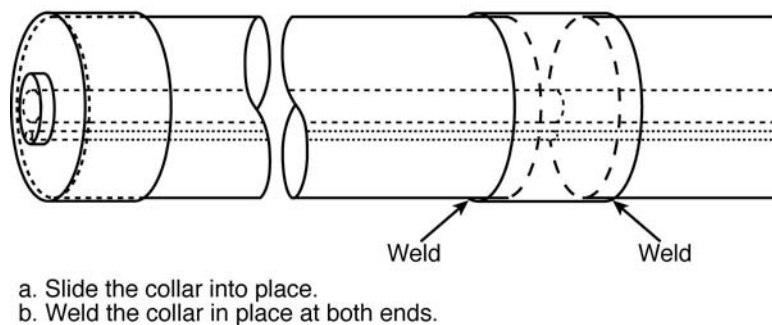


Figure 8-7

The final step in installing a section of cable is welding the collar to both pipe sections.

The trench can be backfilled with soil as the various sections are connected. The exact sequence for this procedure will depend on the specific site, including the characteristics of the terrain.

8.3 Vault and Manhole Installation

A vacuum pumping station is required approximately every kilometer along the cable, and the length of a cable core section is also about 1 km. A vault or manhole is installed as needed to house vacuum pumps and to accommodate pulling the cable core into the cryogenic pipe. The vault is similar in size and shape to those used for underground power cables. The top of the vault is at ground level. When a string of pipe sections is near completion, a vault is installed so that the last pipe section of the string extends into it (see Figure 8-8). Similarly, the first pipe of the new string also extends into the vault. A special collar arrangement, using three or four concentric collars, is installed at the ends of the pipes in the vaults. The outermost collars have several openings. One large opening is used to connect a vacuum pump, and others accommodate the instrumentation leads, power leads for getter activation, and so on.

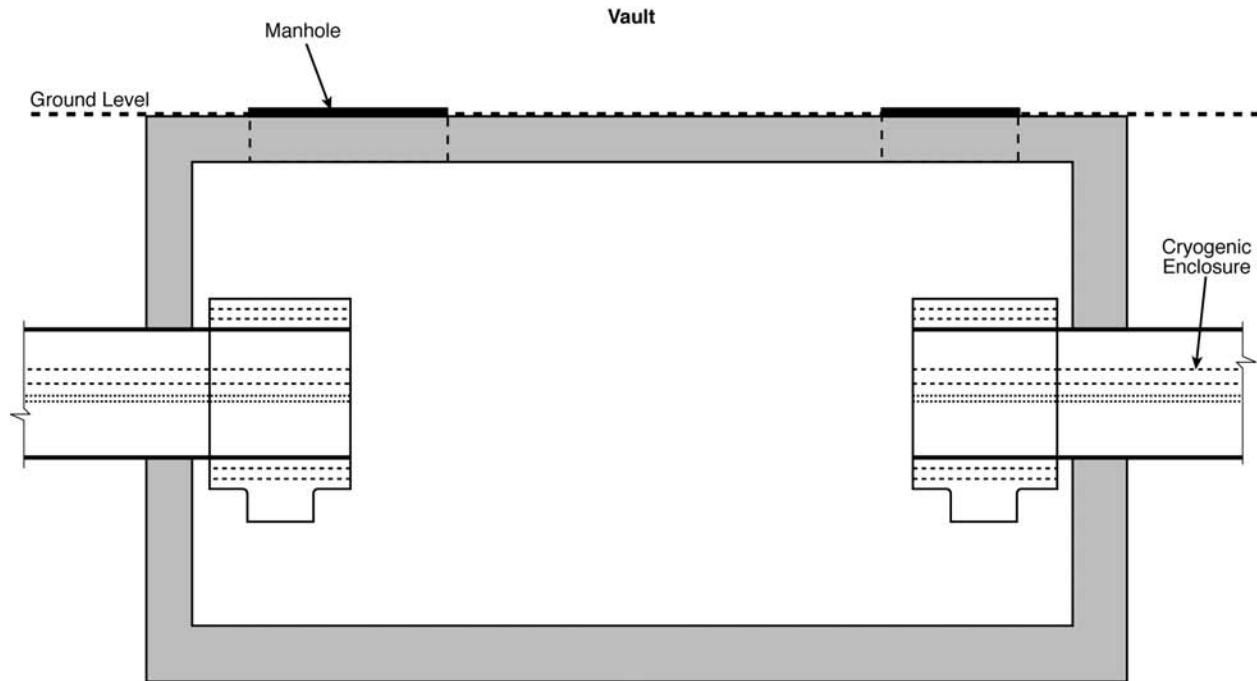


Figure 8-8
Artist's concept of the vault with the two vacuum pipes installed

The exact order of the installation of the vacuum pipes, the collars, and the vacuum pump will be determined by further studies. However, the process might proceed as follows:

1. The pipe section at the right will be sealed into place and backfill will be put in place outside the vault and around the vacuum pipe.
2. The pipe section to the left will be moved into position and carefully aligned with respect to the right section. It will then be sealed into place and the area outside the vault will be backfilled.
3. The vacuum pump (not shown in Figures 8-8 and 8-9) will be installed. An extended length of pipe and a vault with a vacuum pump installed is shown in Figure 8-9.
4. The end caps will be removed, and several special collars that will bridge the span between the installed vacuum pipes the vacuum pipe and will interface to the vacuum pump will be placed onto the ends of the installed vacuum pipes.
5. Extensions to the cryogenic enclosure and the return pipe will be welded in place.
6. Special collars that will enclose the splice will be positioned onto the cryogenic enclosure, as shown in Figure 8-10.

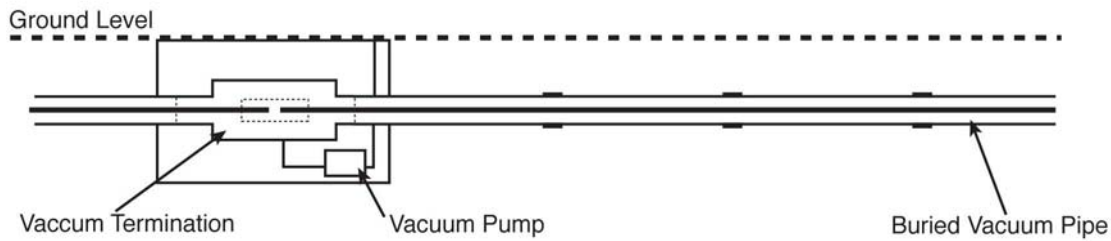


Figure 8-9
Vacuum vault with vacuum pump installed and an extended section of pipe

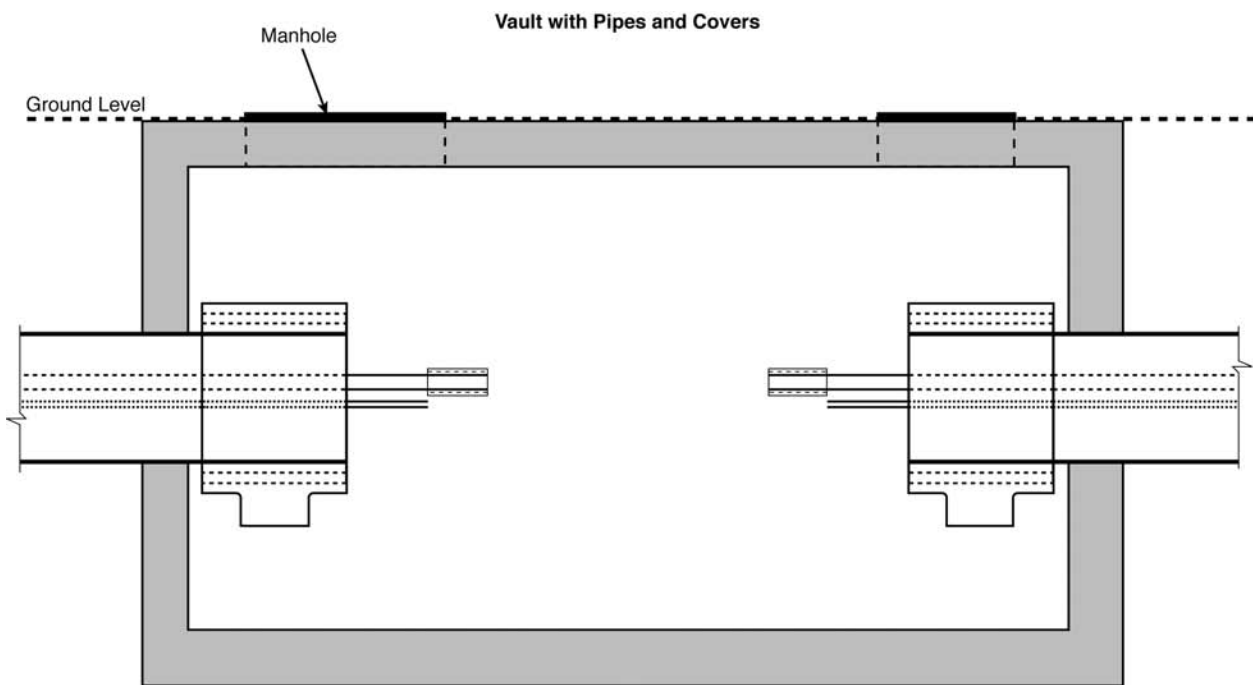


Figure 8-10
Extensions of the cryogenic enclosure to accommodate cable pulling and joint fabrication

8.3.1 Cable Pulling

After the vault installation is completed, the cable is pulled into the cryogenic enclosure to the right. This procedure is based on techniques that are standards in the power cable industry (see Figure 8-11, which shows a cable manufactured by Southwire being installed at an American Electric Power substation). One notable exception to standard cable pulling practice is the method used to control the pulling force. When pulling a conventional cable, a lubricant is applied to the outer cable surface as it is pulled into an open conduit. All the liquid lubricants in use today will become solid and possibly brittle when the liquid nitrogen operating temperature is reached. They could contaminate the nitrogen by either being dissolved and changing the characteristics of the nitrogen or by cracking into small pieces. These particles could affect the

nitrogen flow and plug certain areas (for example, at bends in small-diameter pipes and in filters). Decreased flow or an increased pressure drop along the cable would impede performance or would have to be accommodated by increasing the capacity of the refrigerator and the liquid pump, which would result in increased capital and operating costs. An approach must be developed for pulling the cable core without wet lubricants and any substance that will remain in the cryogenic vessel during operation.



Figure 8-11
Cable pull for a superconducting cable

Courtesy of Southwire

To initiate the cable pull, a rope is inserted into the cryogenic vessel at the right side of the vault; that is, at the left end of the 1-km section. Air pressure and flow are used to force the rope through the vessel so that it extends out into the next vault to the right. The rope is used to draw a robust puller into the cryogenic enclosure. After it is in place, the left end of this puller is attached to the protective cover at the end of the cable core. Figure 8-12 shows the cable core in position, ready to be pulled into the cryogenic enclosure. For simplicity, neither the rope nor the puller is shown in this view. The cable core is pulled through the 1-km cryogenic enclosure until it extends into the next vault to the right.

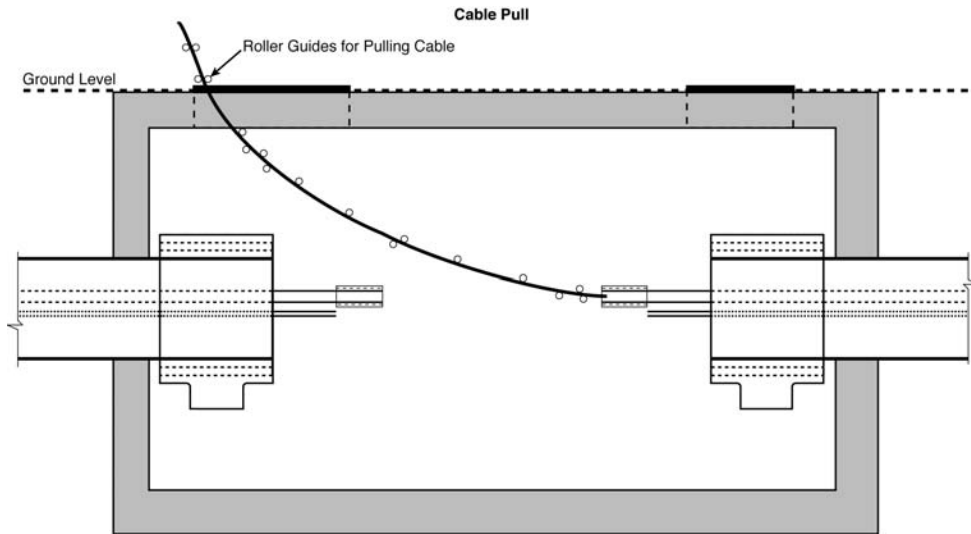


Figure 8-12
The superconducting dc cable core in place and ready to be pulled into the cryogenic enclosure

Figure 8-13 shows two cable core sections extending beyond the cryogenic enclosures and in place for splicing. The actual positions of the cable ends will be determined by a detailed cable design. Some axial overlap (not shown) will enable easier electrical connection of the various conductors. The formation of the splice and the completion of the cryogenic enclosure in the vault require extremely clean conditions; therefore, the vault is cleaned and prepared before the next step. At this point in the process, the vault appears much as shown in Figure 8-13. However, the vacuum pump might be in place, and electrical power will be available. After the cores are in position, the protective covers will be removed and cut to an appropriate length for forming a splice.

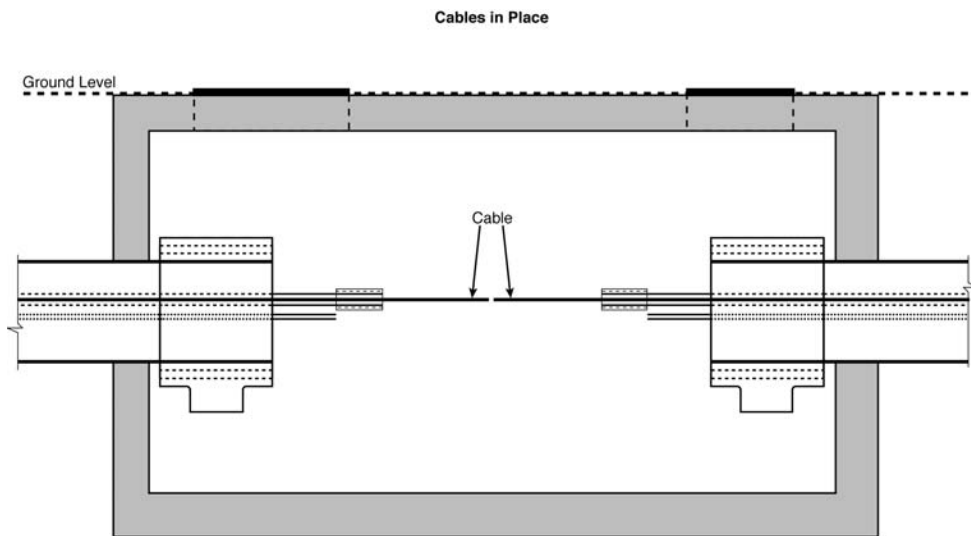


Figure 8-13
Cable cores extending into a vault in preparation for splicing

8.3.2 Cable Splicing

An artist's concept of a completed cable splice for the superconducting dc cable is shown in Figure 8-14. It is based on the cable core shown in Figure 8-15. In many regards, it is similar to the electrical splices used for conventional cables and existing superconducting ac cables; the main difference is in the number of individual wires and tapes that are required in order to form the conductors. The process is somewhat more complicated than that for conventional cables because more components must be connected and the splice must be able to accommodate some axial and circumferential stress associated with cooldown. The process begins by bringing the two cable ends into their position, unwinding all the conductors and insulators from the cables, and flaring them out in preparation for making connections. The inner tubes, or mandrels, shown in Figure 8-15 are brought together to form a rigid structure at the central bore of the cable. This tube is shown as a solid in all illustrations prepared to date, but it might be formed as a spiral structure in order to provide greater flexibility along the length of the cable. In either case, this element will be formed so that it produces an axially solid structure on which the remainder of the splice can be fabricated.

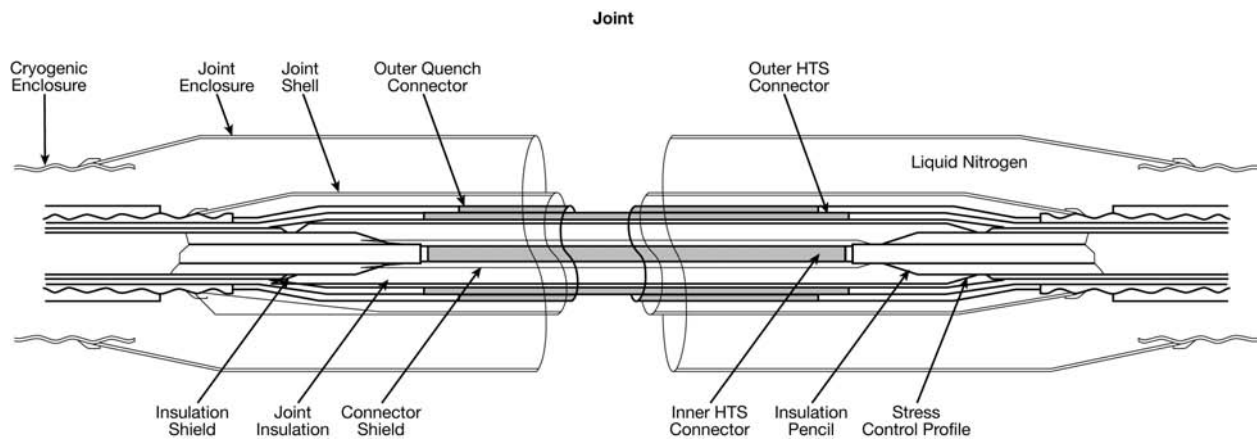


Figure 8-14
The electrical splice for the superconducting dc cable

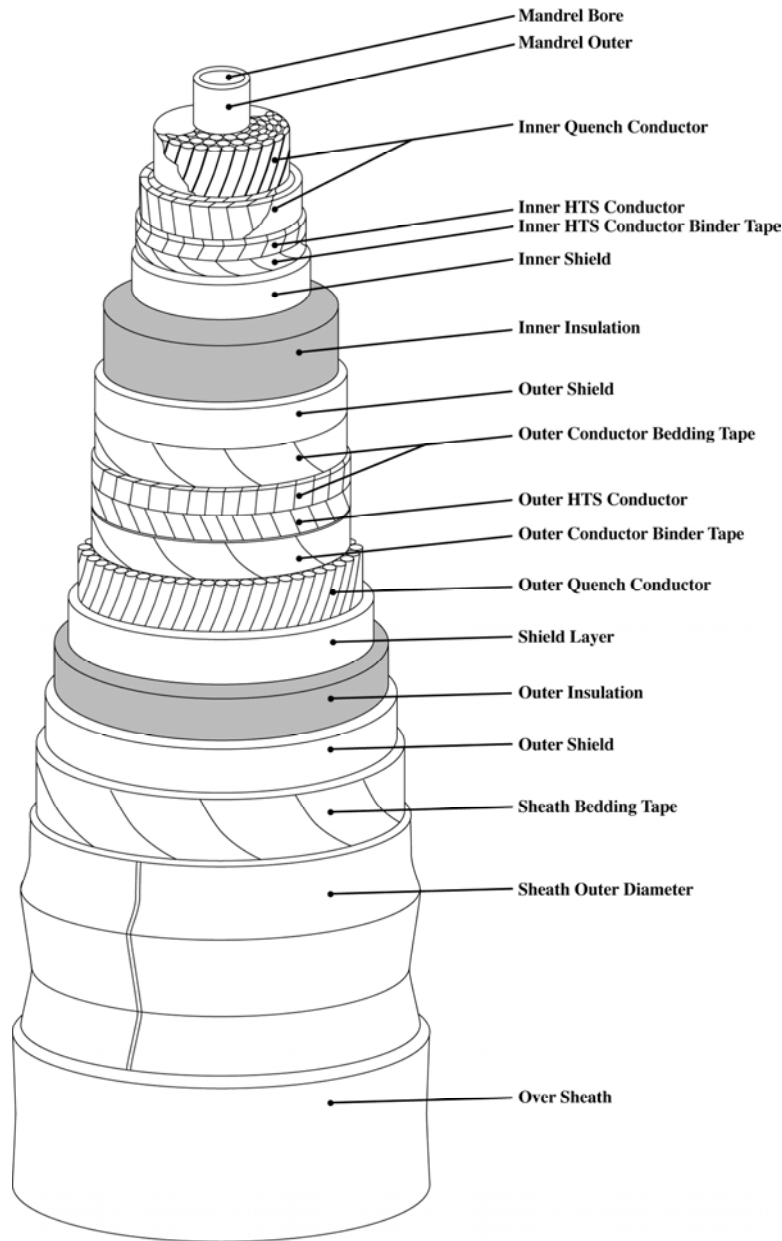


Figure 8-15
The cable core

A thin layer of protective material will be applied to the mandrel in this region to protect the conductors, which will be applied later, from any deformations associated with the mandrel's fabrication. The inner quench conductor, which is made of high-conductivity copper, is then laid into place by retwisting the individual wires from each end. The wires from the two sections are interleaved to allow a low-resistance contact. Because the quench conductor consists of many layers, the wires are interleaved layer by layer. The innermost layer is soldered, using a solder that melts at a low temperature in order to avoid damage to the protective layer. Subsequent

layers are also soldered, and the entire quench conductor can be soldered into a solid mass in the splice area. Specific details of this portion of the splice will be determined by constructing samples and testing them to determine the optimal characteristics of high strength and low resistance.

After the splice is made in the quench conductor, the HTS tapes in the inner layer are retwisted into place to form a meshed structure. It is not clear whether the HTS tapes should be soldered together layer by layer or tape by tape. The issues are the ac losses in the superconducting materials, which can be increased by soldering many conductors together, and the strength of the splice, which would be stronger if each layer formed a solid mass. In either case, the procedure is considerably more delicate than for the copper in the quench conductor, and some models and tests will be required before a specific approach can be selected.

After the HTS layer has been formed, the binder tape and insulation are applied to the splice area. Figure 8-14 shows a special conical section in the splice area that will aid in reducing the electric field in the region where materials and shapes are changing. This cone, or pencil, is effective in conventional cables and is used in existing superconducting ac cables. The insulation in the splice area is typically about twice as thick as the insulation in the body of the cable. The insulation in the body of the cable includes special, cylindrical, low-resistance shields that participate in the operation of the cable by maintaining a uniform electric field. These shields terminate at each end of the splice and are integrated with the more robust splice insulation.

The return HTS layers and the outer quench conductors in the splice region are formed much the same as the inner layers. Protective materials are included as needed to reduce mechanical strain on the superconducting layers. The positive (go) and negative (return) HTS layers are separated by the main insulation throughout the cable length as well as in the splice region. The sequence of conductors chosen in this design ensures that the magnetic field is zero in both quench conductors. Fluctuating magnetic fields introduce eddy currents in normal conductors; those currents would cause undesirable heating and losses in a superconducting dc cable.

After the splice in the outer quench conductor is completed, the outer insulation layer and any protective layers are applied to the splice. The voltage standoff of the outer insulation layer is about half that of the main insulation. Therefore, it is thinner, but the mechanical capabilities of the materials might be more important than the voltage requirement, leading to a thicker insulation than that shown in Figure 8-15.

When the conducting and insulating layers are completed, a series of system tests are performed to ensure that electrical conductivity and voltage insulation are adequate. After the joint is certified, a joint shell is installed over the entire splice. This shell connects to the outer metal surface of the cable core. The exact structure of this shell depends on several conditions that exist along the length of the cable—for example, the type of vault (vacuum or cryogenic), the existence of grid power connections (which will require power leads that will take current from cryogenic to ambient temperatures), and possibly the local terrain features (which might influence the pressure in the cryogenic enclosure and thus the flow characteristics of the liquid nitrogen).

Finally, the joint enclosure is installed on the outside of the splice. For this part of the installation, the stainless steel collars (see Figure 8-8) are moved into place and welded to form a hermetically sealed structure. Similarly, the return pipe is extended across the splice region (see Figure 8-16). The vacuum enclosure shown is either the pipe, as indicated, or a collar that has been extended and welded into place. The diameters of the cryogenic pipes are approximate; the pipes will be sized to allow nitrogen to flow along the pipe with minimum pressure drop. Figure 8-16 shows the completed splice, including the MLI blanket, which is installed to provide contiguous thermal insulation along the entire length of the cable. The MLI in this region is especially critical because it must be formed and installed by hand. Experience shows that these areas are the most critical for thermal insulation, and they are also the most likely to have gaps that allow heat to penetrate to the cryogenic environment. Supports, which might be needed to hold the cryogenic pipes in position during cooldown and normal operation, are not shown in Figure 8-16.

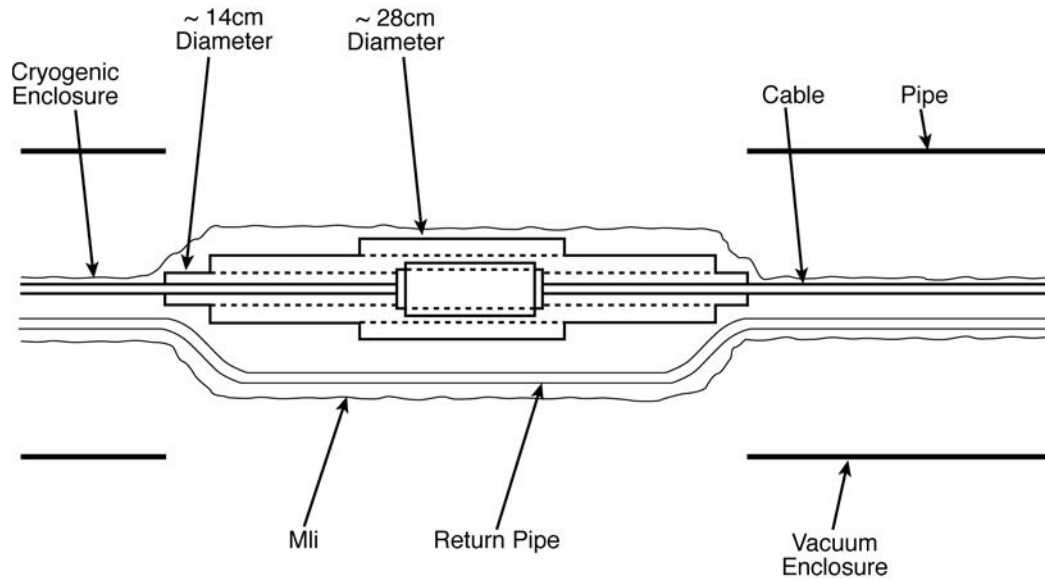


Figure 8-16
A completed splice

8.3.3 Vacuum Pump Installation and Pumpdown

After the splice is completed and tested, the vacuum enclosure is completed by moving the collars along the vacuum pipe and into place for welding. The final geometry of the vacuum enclosure in the vault is shown in Figure 8-17. After the welds on the vacuum enclosure are tested, a vacuum pump is installed in each vault. The configuration shown in Figure 8-17 is representative of how this appears after assembly. The pump is mechanically attached to the floor of the vault, and a large-diameter pipe connects the vacuum inlet on the pump to a large opening on one of the collars. The inlet diameter to the pump is large because the gas that enters it is very thin. The pump compresses the gas so that the exhaust (outlet) pipe can be much smaller. For the most part, the outlet gas contains no hazardous substances and has the same constituency as air; therefore, it can be freely exhausted into the atmosphere.

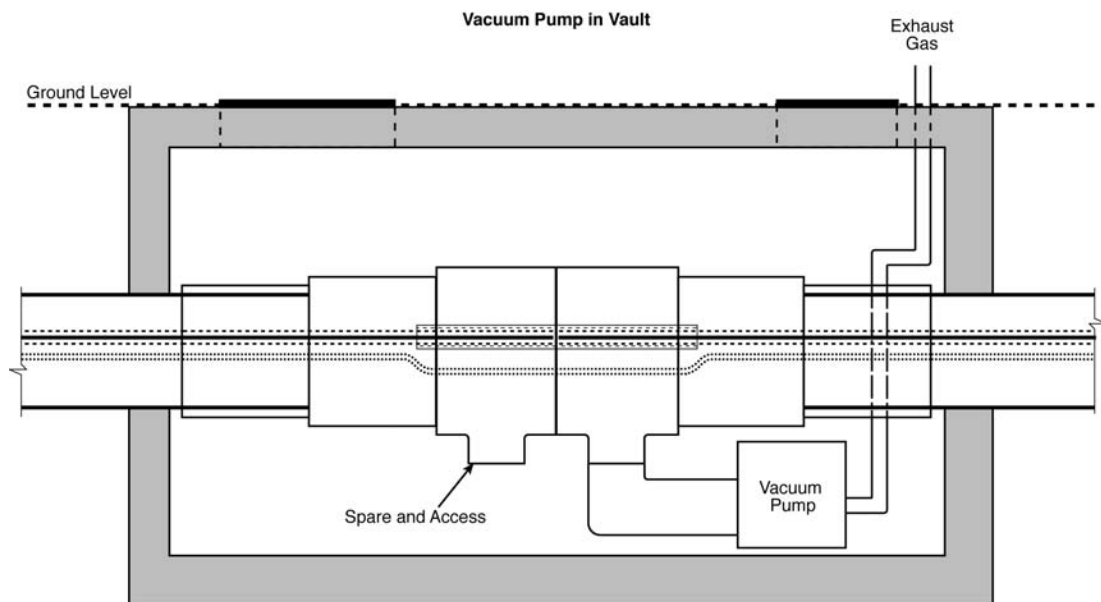


Figure 8-17
Vault for vacuum and cable splice after full installation

The electrical connections for instrumentation and getter activation circuits pass through a separate port into the vacuum pipe. This port will probably be quite small, and the second large opening will likely be held in reserve for access in case repairs are needed.

The vacuum pump and other electrical components in the vault require a low-voltage power source. Thus, some local power delivery is required along the length of the cable system. Several approaches can be effective; however, the easiest is to have an above-ground power line that is connected to the cable system at each vault. Although it is an effective and economical solution, having such a system would impact the overall reliability of the cable system. Installing underground local power at the same time as the superconducting dc cable is another potential solution. The best way to accomplish this is an issue to be resolved in the future.

8.3.4 Vacuum and Cryogenic Component Sectioning

The vacuum pumps are designed to maintain a vacuum in the sections to the right and to the left of the vault. During normal operation with no nearby leaks, the pumps can be turned off. Some failure modes—such as a breach of the vacuum pipe by some earthmoving equipment or a weld failure in a cryogenic pipe—can impact the vacuum system. In either event, if the vacuum were continuous along an entire 1000-km line, the time to restart would be prohibitive. As a result, some form of vacuum stop must be installed in every few vaults. The vacuum enclosures in those vaults will differ from that shown in Figure 8-17. Two vacuum pumps are required, and a vacuum barrier must be inserted. This barrier extends from the cryogenic pipes to the vacuum wall and must be sufficiently strong to withstand a pressure differential of 1 atm. To avoid excessive heat flow into the cryogenic components requires careful design of the shape of the vacuum break and the selection of low thermal-conductivity materials. The exact form of the vacuum break is an issue that must be resolved in the next stage of the program.

In addition, pressure relief is required in the cryogenic system to accommodate upset conditions that increase the temperature and the local pressure. This is not a serious issue, because liquid and gas flow appear to be adequate to reduce the pressure in a 1-km section in a few seconds. Therefore, it will be sufficient to install a relief valve on the two cryogenic pipes at each vault. The gas exiting the relief valve will be vented from the vault through the exhaust pipe that is used for the vacuum pump.

8.3.5 Cryogenic Station Installation

Every 10 km or so, a cryogenic refrigeration system is used to recool and repressurize the liquid nitrogen that maintains the operating temperature of the superconducting dc cable. The exact separation between refrigerators depends on many factors, especially the terrain and the pitch of the cable. In flat regions, the separation could be as large as 25 km; in mountainous areas, it could be as small as every 1 km. The parameters that determine the spacing between stations are the pressure difference along the cable and the total heat input between refrigerators. We expect that the heat input will be roughly independent of location and the pitch of the cable. However, nitrogen is nearly as dense as water, so a 100-m rise will result in a 10-atm pressure differential.

The refrigeration capacity at each station will be determined by the total heat load between it and the next refrigerator. Because heat input is roughly constant along the superconducting dc cable, the closer the refrigerators are to one another, the smaller their individual capacities must be. Thus, the refrigerators will be made in several standard sizes for use along the length of the cable. For short separations, the refrigerator might be replaced by a pump to maintain the minimum allowable liquid nitrogen pressure.

These refrigerators are installed above ground, as shown in Figures 8-18 and 8-19. They are connected into a large vault that includes vacuum pumps, and they have access to the vacuum system and the cryogenic piping in the cable sections that extend in both directions from the vault. In Figure 8-18, the pipes between the cryogenic components inside the vault and the refrigerator that is outside the vault are shown for reference.

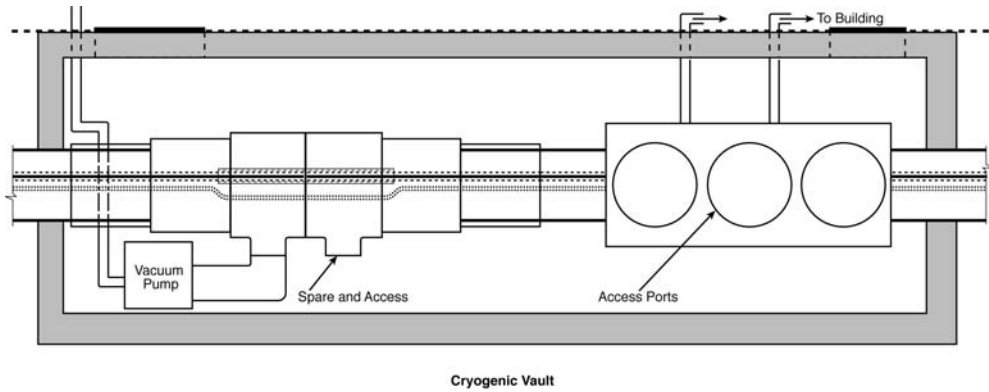


Figure 8-18
Vault for refrigeration and vacuum

As Figure 8-19 shows, the refrigerator is connected to the cryogenic pipes through the openings below the cold box. A variety of valves and separators in the vault allow both the vacuum and the cryogenic pipes in the cable section on either side to operate independently. Although the refrigeration capacities depend on their separation, it is possible to standardize the valves and connectors that are in the cold box and the vault. For reference purposes and scaling, the refrigerator is shown vertically above the vault. It will be installed so that it is out of the cable path, and the pipes shown in Figure 8-18 will connect it with the cryogenic components in the vault.

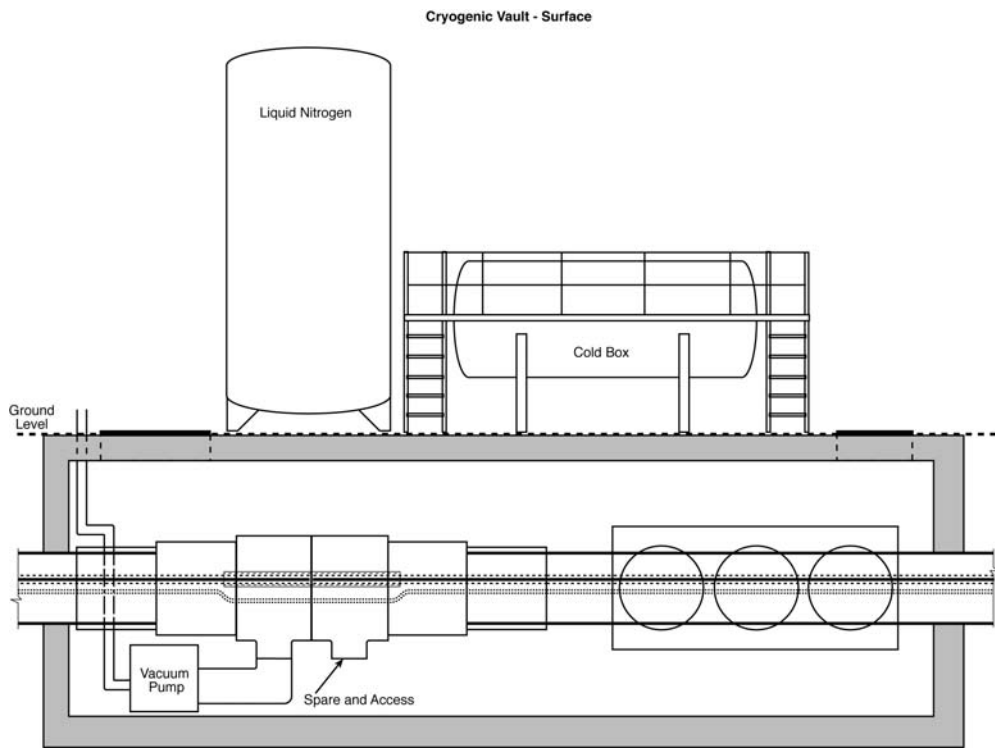


Figure 8-19
Cryogenic refrigerator and the associated vault for cryogenics and vacuum.

Figure 8-20 shows a typical pumping station for a gas pipeline. These pumping stations are used to overcome pressure losses resulting from gas flow. They are installed every 50 km or so, depending on local power availability and the flow needs of the system. The installation shown in Figure 8-20 is much the same as the refrigeration station for the superconducting dc cable. In both cases, the mechanical equipment is above ground, and the pipes are below ground. Teams that install pressurized gas pipelines will be able to adjust existing techniques to install the superconducting dc cable and its associated equipment.



Figure 8-20
Pumping station for a natural gas pipeline

Source: Duke Energy Gas Transmission Canada

9

FUTURE WORK

The assessment of the superconducting dc cable over a period of several years has resulted in an engineering design for a system that can carry large amounts of power and, the team believes, one that can operate effectively as a part of a large-scale power grid. In the process of developing an engineering solution, several questions and issues were raised for which answers are still undeveloped. In particular, in the search for a functional solution, little effort went into optimization and, from the very beginning, evaluating system costs was not a part of this program. (However, see Appendix C, in which the cost estimates from an earlier EPRI study have been updated based on understanding from the present effort). Multiple options were possible in several technical areas for some specific aspect of the design, and a functional, but perhaps arbitrary, choice was made. The use of liquid nitrogen as the coolant is an example. Other fluids can also be used, and they might be more appropriate and possibly cheaper. Some questions to answer and possible areas to study are described in the following sections.

9.1 System Test

An engineering approach has been used throughout this project. The intent from the beginning of the effort has been that the design be one that could be built today and that it would work as a technical solution to the need for massive power flow on a large-scale power grid. Nevertheless, the overall design concept has not been tested, and a model system is needed to provide a critical, early evaluation of an integrated system. The model system should include and test mechanical components (including piping, vacuum, cryogenics, and supports) as well as electrical components and characteristics (including voltage, current, power leads, and insulation). It is paramount to the justification for future activities on the superconducting dc cable that an early test of a system be carried out.

The minimum size of such a model would include several of the 20-m-long sections described in Section 8, Fabrication and Installation. It would be constructed and evaluated for vacuum integrity and cryogenics. Achieving an appropriate level of power flow in such a model is unlikely, but the initial test could easily be designed to have a high current with a low voltage across the cable, and then to operate with a low current, or perhaps no current, at the design voltage. Laboratories such as those at Oak Ridge National Laboratory have capabilities that are similar to those needed for such a test. However, it might be possible to incorporate the mechanical aspects of this design with some other superconducting cable test (for example, as an extension of or a section within an HTS ac cable).

Planning for and carrying out the research for a model test at this level is a significant effort. Although planning for this effort should begin soon, several of the other items listed in this section should be initiated rapidly so that future developments can be incorporated in the test

procedure. On the other hand, this model will be an ideal test bed for some alternative designs, particularly for the mechanical structure. The combined effort of EPRI, conductor manufacturers, and an engineering design team will be needed, and it might well take four or five years to complete.

9.2 Cryogenics and Vacuum

Two of the choices made in the design of this superconducting dc cable were to have a vacuum for thermal insulation and to use liquid nitrogen as the coolant. These choices were based on experience, and the calculations presented in Section 5, Vacuum System, and Section 6, Cryogenics, showed that they provide a functional system. However, several calculations and some tests will be necessary before making final design choices, including the following:

- Explore using cryogenics other than liquid nitrogen, especially for areas in which the cable experiences large changes in altitude.
- Explore the issues associated with pressure differences related to altitude changes along a working cable.
- Analyze the spacing of vacuum pumps along a line and the issue of operating only a few after achieving a working vacuum.
- Determine how to monitor vacuum along the line.
- Explore the concept of leak avoidance and in-place leak repairs.
- Explore the welding procedures for the three pipes, and establish the best procedures to avoid leaks into the vacuum.
- Test coatings on the inside of the external pipe to reduce heat flow into the cryogenic environment.
- Test getters for effectiveness in maintaining a vacuum over long periods.
- Use controlled vacuum leaks to test the vacuum systems and to help choose vacuum pump spacing.
- Explore different thermal insulation schemes, and include the different options in an analysis of system reliability.
- Address the impact on system reliability of the vacuum and cryogenic subsystem as part of a detailed design effort.

9.3 Insulation and Dielectrics

Of the technical areas that are critical to the eventual performance of the superconducting dc cable, perhaps dielectrics at cryogenic temperature are the least developed. The state of the art today for superconducting ac cables is represented by the use of LPP tapes similar to those used for conventional conductor ac and dc cables (specifically, oil-impregnated, laminated paper insulation cables). The LPP tape consists of a layer of polypropylene film bonded without adhesive between two layers of Kraft electrical insulation paper. Many layers of this tape are

helically lapped onto the conductor in successive and alternating directions with spacing (butt spaces) between adjacent tapes in the same layer to permit cable bending. The paper–polypropylene provides both mechanical and dielectric strength. In conventional cables, the paper tapes are impregnated with an electrical insulating oil (such as mineral oil) to secure the desired dielectric strength. In superconducting cables, the tapes are instead impregnated with liquid nitrogen, which serves a similar dielectric purpose while at the same time bringing the temperature of the conductor to a superconducting state. Short lengths (<1 km) of ac superconducting cables of this type of construction at voltages up to 138 kV have been successfully manufactured and operated in utility grids. The first dc superconducting cables will also likely use this type of dielectric insulation.

Although laminated paper-type insulations have proven successful so far, there are reasons to seek a better insulation system. In the first place, the long-term mechanical and electrical properties of today’s laminated insulation systems are not well known because no superconducting cable systems have been in operation for more than a few years. Because they were originally designed to operate reliably at room temperatures for 40 years, there is no guarantee that they would have a similar life at liquid nitrogen temperatures. However, the general mechanisms for aging of the dielectric are associated with excess temperatures, which will not occur in the cryogenic environment. The electrical and mechanical properties of most materials vary considerably with the temperature at which they are used.

More fundamentally, however, the suitability of a wet insulation, such as the laminated systems described for mass production of reliable cable, is called into question by the impracticality of performing factory testing of such cables before they are shipped. Conventional ac and dc cables are 100% factory tested for electrical performance and potential insulation defects that could produce failure in the field when the cable is first energized. The design dielectric strength of the laminated paper construction in a superconducting cable is achieved only when it is fully wetted with liquid nitrogen. Thus, to test the cable in the factory, the entire shipping reel of cable (weighing tens of tons) would have to be immersed in liquid nitrogen—a clear impracticality. Thus, with today’s superconducting cables, there is a near certainty of an occasional failure in the field as more and more systems are installed and line lengths become longer, requiring many reels of cable to be shipped. Such concerns place a high priority on the development of alternative insulation systems—for both ac and dc superconducting cables—and possibly better and more effective test methods. We recommend that research be conducted to determine the feasibility of the following options:

- One proposal for investigation is to completely separate the construction of the superconducting dc cable from that of the cryostat system in the following manner:
 - Manufacture the cable as a conventional cable without liquid nitrogen ducts or built-in cryostats
 - Separately manufacture the cryostat pipe and assemble it on site to form a robust, empty duct, as in conventional fluid-filled cable systems
 - Pull the cable length into the cryogenic pipe and joint it in a near-conventional way
 - Close and seal the cryogenic pipe, and then purge and fill it with liquid nitrogen.

In this approach, 100% factory testing of superconducting cable cores would be possible. Moreover, the cryogenic pipe dimensions, flow rate, and pressures could then be optimized to achieve the maximum hydraulic lengths, with minimal restrictions imposed by the cable.

- Another class of insulation system for conventional cables is the extruded dielectric (also known as a *solid dielectric*). This insulation is *dry* (not impregnated with a fluid) and is not laminated—much like the insulation on a common appliance cord. The materials used in this insulation include ethylene propylene rubber and XLPE. Although these two materials are not expected to work at liquid nitrogen temperatures, there is reason to believe that other synthetic resins might prove to be good extruded dielectrics for cryogenic use. An extruded, dry insulation that can provide the desired dielectric strength at room temperature, yet exhibit compatible properties at cryogenic temperatures, might be adaptable to the separate construction approach described in the previous paragraph. Factory testing could then be achieved in much the same manner as is currently performed with conventional, extruded dielectric cable. Research is needed to discover, describe, and validate potential materials suitable for dry cryogenic applications. However, notwithstanding the clear advantages of this new dielectric, keep in mind that wet designs of liquid nitrogen-impregnated insulation provide good thermal contact between the stabilizer conductor and high specific-heat-capacity liquid nitrogen. These properties would not be so good in a dry design. However, because fault currents in the dc cable are not expected to exceed the rated current by more than a factor of two and will be fairly short, the importance of good thermal contact is not nearly so important as in an ac superconducting cable.
- We recommend that a variety of dry insulation systems be selected and laboratory tested at both room and liquid nitrogen temperatures. A full suite of thermal, electrical, and mechanical tests should be carried out. The base resins used in conventional cables do not retain desirable mechanical properties at cryogenic temperatures, and other materials might not perform well electrically. On the other hand, some other resins might have the desired properties when suitably enhanced with fillers, for example. One promising area of research in this direction that is currently under way, with support from the U.S. Department of Energy, is the use of nano-scale metal oxides in an epoxy resin. A novel, *in situ* method of synthesizing the cryogenic nanodielectric has been developed by researchers at Oak Ridge National Laboratory [44]. *In situ* methods of incorporating the nano-structured materials produce improved mechanical and electrical performance over that of the base resin.
- A constant voltage is applied to the insulation in all dc cables for long periods. The result is a polarization of the insulation material, which is associated with the mobility of some of the charge carriers. When the voltage is removed, the charge polarization can remain for long periods, especially while the cable remains cold. This is an unknown area that must be explored for any solid insulation that is planned for use in a superconducting dc cable.

9.4 Cable Design and Fabrication

During the effort on the superconducting dc cable, the team developed a spreadsheet to determine cable length and weight as a function of superconductor performance, current, voltage, and the physical characteristics of the chosen materials. This approach was used to determine the cable core design presented in Section 4, Cable Design. In a sense, the spreadsheet forms a design algorithm for the superconducting dc cable. The following recommendations are made:

- This spreadsheet should be updated with new design information and new material properties for insulators and superconductors.
- In most regards, the superconducting dc cable core is not much different from existing cables. However, the use of superconductors that are tape-like and carry only a few hundred amperes will require many layers of conductor. The result is the need for multiple passes through a cabling machine for each conductive component of the cable. Existing cabling machines have limited capabilities in terms of the number of individual conductors that can be wound. Some development of cabling machines will be required before fabrication of a 100-kA cable can begin.
- If a solid insulation is used, the differences in physical properties among the insulation, the superconductor, and the underlying structure must be explored by a thorough analysis and some tests of sections of the cable, probably on a small scale initially, but eventually at full scale. Properties of interest in these tests include contraction during cooldown, yield strength, brittleness, and modulus of elasticity.
- Because of the interaction of the cable with nearby conducting materials, particularly during faults on the ac system, there is some need to explore the necessity of the extra shield that has been added to the cable core. Removing this layer of conductor and this section of insulation would reduce the diameter of the cable and simplify fabrication considerably.
- Harmonic currents that occur in the normal operation of the converters will be present in the superconducting dc cable. These variable currents will introduce heat into the body of the cable and will thus affect the refrigeration requirements. Estimates of the attenuation process have been made, but some step beyond a purely theoretical approach is needed.

9.5 Converters

Early research on superconducting cable transmission systems used CSC technologies where dc cable applications were envisioned. This work is still relevant for the new HTS cables that are the subject of this study. However, today's newer converter technologies offer the possibility for multiterminal operation using VSCs, which makes it possible to consider using superconducting cables as long-distance, electric superhighways with numerous on and off ramps. Initial investigations of the feasibility of integrating such electric superhighways into the existing ac grid, preliminary studies of the interactions between the cable and the VSC, and the design requirements for suitable control systems were the subject of research in companion projects to that which produced this report [13, 14].

Several issues demand careful study, including the following considerations for design and operation of the cables:

- Cable protection and control issues related to cable or converter dc-side short circuits and rapid deenergization of the cables or parts of a cable
- Harmonic injection into the cables at steady state and during operation with voltage unbalances in the ac systems
- Energization of the cables for bumpless connection of converters to the cables
- Dispatching of power through the cable to handle load following, power flow direction changes, and so on
- Emergency transfer of power from one circuit to a parallel cable circuit in case of failure on one cable
- Crowbar or other means to ride through a temporary loss of a converter to avoid interruption of the cable current and voltage collapse of the dc cable

Although the well-known CSC technologies can be used with confidence for point-to-point transmission systems, and they might possibly be used at one end of the envisioned system, the use of multiple VSCs in a long, radial transmission line is relatively unknown. Therefore, for design and operation of a VSC and the required control systems, the following should be studied:

- Converter topology for loss minimization and cost optimization, which could involve the use of soft-switching converter concepts
- Harmonic filter design for blocking harmonics from entering the cables
- Control strategies to minimize injection of fundamental frequency components into the dc cable in case of an unbalanced fault in the ac system or systems
- Development of control and protection strategies for temporary loss of a converter or a set of converters in case of an ac system fault
- Development of switches and switching strategies for transfer of a converter from one cable to the parallel cable
- Improved efficiency of forced-commutation converters
- The possibility of higher power-handling capabilities in forced-commutation converters

9.6 Grid Interface

An understanding of existing grid interactions has already begun. Load flow and transient stability studies have shown that integration of multi-gigawatt superconducting lines into both the eastern and western grids is feasible, but further optimization of these studies as well as other investigations are needed.

For design and operation of the transmission system, the following topics require further consideration:

- Performance of an ac system with multiple VSC infeeds to a major metropolitan area
- Optimization of converter power capacity
- Use of different types of converters at different locations
- Use of CSC technologies for rectifier stations with no need for power reversal as a part of the overall transmission system
- Potential interactions between converters in close proximity to each other
- Voltage control of the dc cable and strategies to deal with a loss of rectifiers and inverters
- Overall reliability assessment of the transmissions system, including identification of critical failure modes and their impact on the ac system
- The interface between the cable and end station components
- The need to have a voltage drop (droop) along the line of a superconducting dc cable, as is required for a conventional dc cable, to achieve control
- Reduction of the complexity of control systems for multiterminal operation
- High power capacity dc circuit breakers
- Mitigation of transients associated with faults and system events
- Improved power electronics reliability and system performance during major system upset events
- Lower costs of power electronics
- Deregulated utility structure and emphasis on distributed (renewable) generation and microgrids for increased system reliability and survivability

The control systems for a multiterminal VSC-based superconducting dc cable system must be fully assessed for all possible system conditions, events, and ac and dc faults. Although VSCs will no doubt have superior performance compared to commutated CSCs, more detailed modeling and simulations with multiple converters at the actual current and power levels proposed for the superconducting dc cable must be carried out.

9.7 Optimization and Tradeoffs

Several options will be available for detailed design issues in future superconducting dc cables. These amount to tradeoffs among a variety of parameters. A major effort in optimization should be the integration of components such as the vacuum, refrigeration, and converters into the design spreadsheet that was developed for the cable core.

Specific tradeoffs that should be evaluated include the following:

- Variations in conductor requirements as a function of operating temperature to minimize overall system cost
- Optimization of cable core length and vacuum separation versus outer pipe diameter, and spacing of vacuum pumping stations and cryogenic refrigerators
- Current and voltage for various power levels
- Other potential coolants, including helium, hydrogen, and neon
- Possibilities of non-vacuum thermal insulation

9.8 Costs

Explore costs in greater detail, which will require the following:

- Develop an algorithm for costing superconducting dc cable of the reference design and others and incorporate it into the spreadsheet described in Section 9.7, Optimization and Tradeoffs.
- Test power leads and losses. Use local refrigeration that can operate in a liquifier mode rather than just as a refrigerator.
- Develop suitable metrics to determine whether superconducting dc cable will be competitive with other system in terms of functionality and cost.

9.9 Superconductors

The superconducting dc cable has superconductor requirements that are somewhat different from other cables and many other applications. Development work on these materials is generally in the domain of the conductor manufacturers. The following are suggestions for future effort by those organizations:

- The magnetic field at the outer surface of the inner superconductor layer will be about 1 T. The current-carrying capability of superconductors is reduced in high magnetic fields. Research to improve critical currents in the presence of magnetic fields is needed.
- The present design is made to operate at a temperature range of 67–70 K. Liquid nitrogen is a good coolant well above 77 K. If the superconductors had adequate performance at this temperature, both initial and operating costs for the refrigeration would be reduced.
- The tape forms of the HTS conductors that are available today have active materials on only one side. Applying superconductor to both sides could double the current per tape and thus reduce the number of conductors and the superconductor layer by a factor of two.
- Conductor forms other than tapes should be considered. For example, a round wire conductor would be easier to form into a cable. Such a conductor must be resistant to mechanical strain.
- Superconductors fabricated so that the stabilizer and quench materials are integral parts of each tape or wire would simplify winding and fabrication. Although some HTS materials with this property exist, additional work on this form of material is suggested.

9.10 General

Several items of a general nature related to the cable should be analyzed, including the following:

- Explore the effect of increased current and losses when a single cable of a redundant pair is required to carry a double load for an extended period.
- Develop an expanded version of the spreadsheet described in Section 9.7, Optimization and Tradeoffs. The spreadsheet should include other major system components such as vacuum, cryogenics, and converter.
- Thoroughly understand the thermal impact of the power transients associated with starting or stopping converters, and appropriately design the cooling system for these transient thermal loads.

10

REFERENCES

1. I. C. Report, "Dynamic Performance Characteristics of North American HVDC Systems for Transient and Dynamic Stability Evaluations," *IEEE Transactions on Power Apparatus and Systems*, Vol. PAS-100, No. 7, pp. 3356–3364 (1981).
2. M. P. Bahrman and B. K. Johnson, "The ABCs of HVDC Transmission Technologies: An Overview of High Voltage Direct Current Systems and Applications," *IEEE Power and Energy Magazine*, Vol. 5, No. 2, pp. 32–44 (2007).
3. R. L. Garwin and J. Matisoo, "Superconducting Lines for the Transmission of Large Amounts of Electrical Power over Great Distances," *Proceedings of the IEEE*, Vol. 55, No. 4, pp. 538–548 (1967).
4. J. R. Bartlit, F. J. Edeskuty, and E. F. Hammel, "Multiple Use of Cryogenic Fluid Transmission Lines." In *Proceedings of the Fourth International Cryogenic Engineering Conference, Eindhoven, 24/26 May 1972*. IPC Science and Technology Press Ltd., London, 1972, pp. 177–180.
5. F. J. Edeskuty et al. *DC Superconducting Power Transmission Line Project at LASL: US DOE, Division of Electric Energy Systems*. Los Alamos Scientific Laboratory, Los Alamos, NM: 1980. LA-8323-PR.
6. K. Alex Müller and J. Georg Bednorz, "The Discovery of a Class of High-Temperature Superconductors" *Science*, Vol. 237, No. 4819, pp. 1133–1139 (1987). Available from <http://www.sciencemag.org/cgi/content/abstract/237/4819/1133> (accessed October 30, 2009).
7. P. Grant, "Energy for the City of the Future," *The Industrial Physicist*, Vol. 8, No. 1 (March/April 2002), pp. 22-25. Available from <http://www.tipmagazine.com/tip/INPHFA/vol-8/iss-1/p22.pdf> (accessed October 30, 2009).
8. C. Starr, "National Energy Planning for the Century," presented at the American Nuclear Society Winter Meeting, Reno, NV (November 13, 2001).
9. C. Starr, "National Energy Planning for the Century: The Continental SuperGrid," *Nuclear News*, Vol. 45, No. 2, pp. 31–35 (February 2002).
10. R. L. Cresap and W. A. Mittelstadt, "Small Signal Modulation of the Pacific HVDC Intertie," *IEEE Transactions on Power Apparatus and Systems*, Vol. 95, No. 2, pp. 536–541 (1976).

References

11. R. L. Cresap, W. A. Mittelstadt, D. N. Scott, and C. W. Taylor, "Operating Experience with Modulation of the Pacific HVDC Intertie," *IEEE Transactions on Power Apparatus and Systems*, Vol. 97, No. 4, pp.1053–1059 (1978).
12. *EPRI Underground Transmission Systems Reference Book: 2006 Edition*. EPRI, Palo Alto, CA: 2007. 1014840.
13. *Study on the Integration of High Temperature Superconducting Cables Within the Eastern and Western North American Power Grids*. EPRI, Palo Alto, CA: 2009. 1020330.
14. *Transient Response of a Superconducting DC, Long Length Cable System Using Voltage Source Converters*. EPRI, Palo, CA: 2009. 1020339.
15. P. M. Grant, "Superconductivity and Electric Power: Promises, Promises...Past, Present, and Future." *IEEE Transactions on Applied Superconductivity*, Vol. 7, No. 2, Part 1 (June 1997).
16. H. Kamerlingh-Onnes. *Communications from the Physical Laboratory at Leyden*, Vol. 120 (1911).
17. *Superconducting DC Cable Workshop: Summary Report*. EPRI, Palo Alto, CA: 2006. 1013256.
18. Navigant Consulting, Inc., "High Temperature Superconductivity Market Readiness Review," peer review presentation, July 25, 2006, for the United States Department of Energy, Office of Electricity Delivery and Energy Reliability. (Unpublished.)
19. K. J. R. Wilkinson, "Prospect of Employing Conductors at Low Temperature in Power Cables and Power Transformers." *Proc. IEE* (London) 113, 1509 (1996).
20. *EPRI Underground Transmission Systems Reference Book*. EPRI, Palo Alto, CA: 2007. 1014840.
21. *Design Concepts for a Superconducting Cable*. EPRI, Palo Alto, CA: 1994. TR-103631.
22. G. R. Blackwell, ed. *The Electronic Packaging Handbook*, CRC Press, IEEE Press, Danvers, MA, 2000.
23. A. M. Wolsky. "HTS Cable—Status, Challenge and Opportunity," for signatories of the IEA Implementing Agreement for a Cooperative Programme for Assessing the Impacts of High-Temperature Superconductivity on the Electric Power Sector (2004).
24. CIGRE Working Group 21.20. *High Temperature Superconducting (HTS) Cable Systems*. CIGRE Technical Brochure 229. June 2003.
25. CIGRE Task Force 38.01.11. *Superconducting Cables Impact on Network Structure and Control*. CIGRE Technical Brochure 199. February 2002.

26. John S. Engelhardt and Steven A. Boggs. 2001. *Room Temperature Dielectric HTSC Cable*. U.S. Patent 6,262,375 B1, filed September 24, 1992, and issued July 17, 2001.
27. *Superconducting Cable Construction and Testing*. EPRI, Palo Alto, CA: 2000. 1000160.
28. *Field Demonstration of a 24-kV Superconducting Cable at Detroit Edison: Final Report*. EPRI, Palo Alto, CA: 2004. 1011253.
29. M. J. Gouge, J. A. Demko, M. L. Roden, J. F. Maguire, and C. S. Weber, "Vacuum-Insulated, Flexible Cryostats for Long HTS Cables: Requirements, Status and Prospects," presented at the 2007 Cryogenic Engineering Conference and International Cryogenic Materials Conference (CEC-ICMC07), Chattanooga, TN, July 16–20, 2007. Available from http://www.osti.gov/bridge/product.biblio.jsp?osti_id=930989 (accessed July 7, 2008).
30. I. E. Spradley, T. C. Nast, and D. J. Frank, "Experimental Studies of MLI Systems at Low Boundary Temperatures." *Advances in Cryogenic Engineering*, Vol. 35, p. 447. 1990.
31. C. P. Bean, "Magnetization of Hard Superconductors," *Physical Review Letters*, Vol. 8, pp. 250–253 (1962). Available from <http://link.aps.org/doi/10.1103/PhysRevLett.8.250> (accessed August 31, 2009).
32. W. J. Carr. *AC Losses and Macroscopic Theory of Superconductors*. Gordon and Breach, London, 1983.
33. Martin Wilson. *Superconducting Magnets*. Oxford University Press, New York, 1983. pp. 256–270.
34. David Lindsay, Isidor Sauers, Jonathan Demko, and Chris Rey. "High Temperature Superconducting Cable," presented at the Annual Peer Review of the Superconductivity Program for Electric Systems, U.S. Department of Energy, Washington, DC, August 4–6, 2009. Available from <http://www.htspeerreview.com/pdfs/presentations/day%202/applications/6AP-High-Temperature-Superconducting-Power-Cables.pdf> (accessed August 28, 2009).
35. *Cryogenics: A Utility Primer*. EPRI, Palo Alto, CA: 2006. 1010897.
36. *Program on Technology Innovation: Superconducting DC Cable Workshop Summary Report*. EPRI, Palo Alto, CA: 2006. 1013256.
37. N. Mohan, T. M. Undeland, and W. P. Robbins. *Power Electronics: Converters, Applications, and Design*, 3rd Edition. John Wiley and Sons, Inc., Hoboken, NJ, 2002.
38. D. G. Holmes, T. A. Lipo. Chapter 3.8, "Integer Versus Non-Integer Frequency Ratios." In *Pulse Width Modulation for Power Converters: Principles and Practice*. John Wiley and Sons, IEEE Press, Hoboken, NJ, 2003.

References

39. M. M. de Oliveira. "Theoretical Analysis and Real Time Simulator Studies of an Advanced Static VAR Compensator." Licentiate thesis, Royal Institute of Technology, Stockholm, Sweden, 1996.
40. L. Lindberg. "Voltage Source Forced Commutated Converters for High Power Transmission Applications." Licentiate thesis, Royal Institute of Technology, Stockholm, Sweden, 1990.
41. P. W. Lehn, "Direct Harmonic Analysis of the Voltage Source Converter," *IEEE Transactions on Power Delivery*, Vol. 18, No. 3 (July 2003).
42. *National Electrical Safety Code 2002*. IEEE Standard C2-2002.
43. *DC Superconducting Power Transmission Line Project at LASL*. US Department of Energy, Division of Electric Energy Systems, November 1, 1972–September 30, 1979. Los Alamos Scientific Laboratory, Los Alamos, NM: 1980. LA-8323-PR.9-1.
44. I. Sauers and E. Tuncer, "Strategic Dielectric R&D for HTS and Other OE Applications," presented at the 2009 Annual Peer Review of the Superconductivity Program for Electric Systems, U.S. Department of Energy, Washington, DC, August 4–6, 2009. Available from <http://www.htspeerreview.com/pdfs/summaries/day%202/applications/3-Strategic-Dielectric-RD.pdf> (accessed October 30, 2009).
45. S. Schoenung and W. Hassenzahl. *Long- vs. Short-Term Energy Storage Technologies Analysis: A Life-Cycle Cost Study*. Sandia National Laboratories, Albuquerque, NM: 2003. SAND2003-2783.

A

ABBREVIATIONS AND ACRONYMS

This appendix provides definitions of abbreviations and acronyms used in this report.

| | |
|-----------------|--|
| BCS | Bardeen-Cooper-Schrieffer |
| Bi-2223 | Bi:Sr:Ca:Cu = 2:2:2:3 |
| BSCCO | BiSrCaCuO |
| BZO | barium zirconate |
| CSC | current source converter |
| ERCOT | Electric Reliability Council of Texas |
| FACTS | flexible ac transmission system |
| GTO | gate turnoff device |
| HTS | high-temperature superconducting, high-temperature superconductivity |
| IBAD | ion-beam-assisted deposition |
| IGBT | insulated-gate bipolar transistor |
| LN ₂ | liquid nitrogen |
| LPP | laminated paper polypropylene |
| LTS | low-temperature superconductor |
| MLI | multilayer insulation |
| PWM | pulse-width modulation |
| RABiTS | rolling-assisted biaxially textured substrates |
| SCR | silicon-controlled rectifier |

Abbreviations and Acronyms

| | |
|----------------|---|
| T _c | transition temperature |
| VAR | volt-amperes-reactive |
| VSC | voltage source converter |
| WECC | Western Electricity Coordinating Council |
| XLPE | cross-linked polyethylene |
| YBCO | YBa ₂ Cu ₃ O _{7-y} |

B

SYSTEM STUDY OF LONG-DISTANCE LOW-VOLTAGE TRANSMISSION USING HIGH-TEMPERATURE SUPERCONDUCTING CABLE

This appendix presents the previously unpublished report *System Study of Long-Distance Low-Voltage Transmission Using High-Temperature Superconducting Cable*.

System Study of Long Distance Low Voltage Transmission Using High Temperature Superconducting Cable

WO8065-12

Final Report
March, 1997

Prepared by
Longitude 122 West, Inc.
1010 Doyle Street, Suite 10
Menlo Park, CA 94025

Project Manager
Susan M. Schoenung

Authors
Susan Schoenung
William V. Hassenzahl

Prepared for
Electric Power Research Institute
3412 Hillview Avenue
Palo Alto, California 94304

EPRI Project Manager
Paul Grant

DISCLAIMER OF WARRANTIES AND LIMITATION OF LIABILITIES

THIS REPORT WAS PREPARED BY THE ORGANIZATION(S) NAMED BELOW AS AN ACCOUNT OF WORK SPONSORED OR COSPONSORED BY THE ELECTRIC POWER RESEARCH INSTITUTE, INC. (EPRI), NEITHER EPRI, ANY MEMBER OF EPRI, ANY COSPONSOR, THE ORGANIZATION(S) BELOW, NOR ANY PERSON ACTING ON BEHALF OF ANY OF THEM:

(A) MAKES ANY WARRANTY OR REPRESENTATION WHATSOEVER, EXPRESS OR IMPLIED, (I) WITH RESPECT TO THE USE OF ANY INFORMATION, APPARATUS, METHOD, PROCESS, OR SIMILAR ITEM DISCLOSED IN THIS REPORT, INCLUDING MERCHANTABILITY AND FITNESS FOR A PARTICULAR PURPOSE, OR (II) THAT SUCH USE DOES NOT INFRINGE ON OR INTERFERE WITH PRIVATELY OWNED RIGHTS, INCLUDING ANY PARTY'S INTELLECTUAL PROPERTY, OR (III) THAT THIS REPORT IS SUITABLE TO ANY PARTICULAR USER'S CIRCUMSTANCE; OR

(B) ASSUMES RESPONSIBILITY FOR ANY DAMAGES OR OTHER LIABILITY WHATSOEVER (INCLUDING ANY CONSEQUENTIAL DAMAGES, EVEN IF EPRI OR ANY EPRI REPRESENTATIVE HAS BEEN ADVISED OF THE POSSIBILITY OF SUCH DAMAGES) RESULTING FROM YOUR SELECTION OR USE OF THIS REPORT OR ANY INFORMATION, APPARATUS, METHOD, PROCESS, OR SIMILAR ITEM DISCLOSED IN THIS REPORT.

ORGANIZATION(S) THAT PREPARED THIS REPORT
Longitude 122 West, Inc.

ORDERING INFORMATION

Requests for copies of this report should be directed to the EPRI Distribution Center, 207 Coggins Drive, P.O. Box 23205, Pleasant Hill, CA 94523, (510) 934-4212. There is no charge for reports requested by EPRI member utilities.

Electric Power Research Institute and EPRI are registered service marks of Electric Power Research Institute, Inc.
Copyright © 1995 Electric Power Research Institute, Inc. All rights reserved.

ABSTRACT

High temperature superconductors (HTS) offer a potential opportunity for long distance transmission of electricity at relatively low voltage. An HTS transmission line could be less expensive than high voltage dc transmission (HVDC) because of reduced converter costs and lower line losses.

The objectives of this system study were three-fold:

- 1) To investigate possible configurations for a 1000 mile, 5000 MW HTS dc transmission line, including cooling system options
- 2) To estimate capital and operating costs of an HTS dc transmission line, and
- 3) To compare capital and life cycle costs of electricity for a long distance HTS low voltage dc (LVDC) system with an HVDC system and a gas pipeline with the same power capacity.

This preliminary analysis of an HTS low voltage dc transmission system suggests that such a system could be economically competitive with both HVDC and gas pipeline transport of bulk energy over long distances. The largest single cost item is the superconducting layer. If this can be provided at a cost around \$5/kA-m at the selected operating temperature, then the system is an attractive option. The cost of delivered electricity (¢/kWh) is strongly dependent on the cost of fuel at the source. The trade-off between systems is impacted most by capital costs and parasitic requirements.

The development of long distance HTS transmission would provide a large commercial market not only for HTS material, but also for liquid nitrogen refrigerators in the size range of several hundred kW.

CONTENTS

| | |
|--|------------|
| 1 INTRODUCTION AND BACKGROUND | 1-1 |
| 2 SYSTEM DESCRIPTION | 2-1 |
| 2.1 Superconducting Transmission Line..... | 2-1 |
| 2.1.1 HTS Material Assumptions..... | 2-2 |
| 2.1.2 Configuration..... | 2-3 |
| 2.2 Cooling System and Trade-Offs | 2-4 |
| 3 ECONOMIC ANALYSIS | 3-1 |
| 3.1 Capital Costs | 3-2 |
| 3.1.1 HTS Transmission Line | 3-2 |
| 3.1.2 High Voltage Line and Gas Pipeline Costs | 3-4 |
| 3.2 Levelized Cost Analysis..... | 3-6 |
| 3.3 Results..... | 3-8 |
| 4 CONCLUSIONS AND RECOMMENDATIONS FOR FURTHER STUDY | 4-1 |
| 5 REFERENCES | 5-1 |
| APPENDIX REFRIGERATION, VACUUM, AND ANCILLARY POWER..... | A-1 |
| Description of the System and Issues/ Choices..... | A-1 |
| Heat Input | A-3 |
| Refrigeration Options..... | A-11 |
| Vacuum | A-17 |

1

INTRODUCTION AND BACKGROUND

High temperature superconductors (HTS) offer a potential opportunity for long distance transmission of electricity at relatively low voltage. An HTS transmission line could be less expensive than high voltage dc transmission (HVDC) because of reduced converter costs and lower line losses.

The objectives of this system study were three-fold:

- 1) To investigate possible configurations for an HTS dc transmission line including cooling system options
- 2) To estimate capital and operating costs of an HTS dc transmission line, and
- 3) To compare capital and life cycle costs of electricity for a long distance HTS low voltage dc (LVDC) system with an HVDC system and a gas pipeline with the same power capacity.

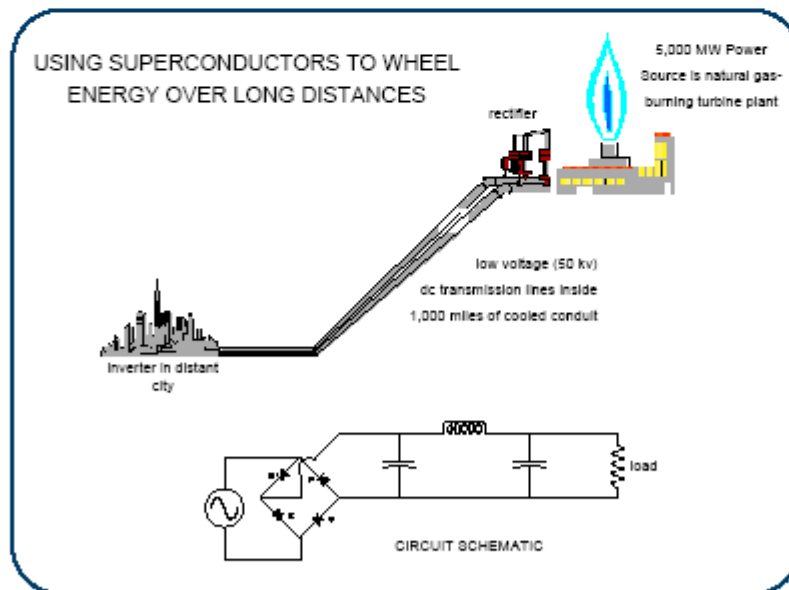


Figure 1-1 Power Plant and Transmission Line

This study was motivated, in part, by an earlier study by ABB [1], in which HVDC was compared with gas pipelines for long distance, high power transmission of bulk energy from large natural gas fields to distant urban electric loads. In that study, several routes (in Africa and South America) were examined. Another possibility is in the Middle East, from the gas fields of Qatar to the load centers in Saudi Arabia.

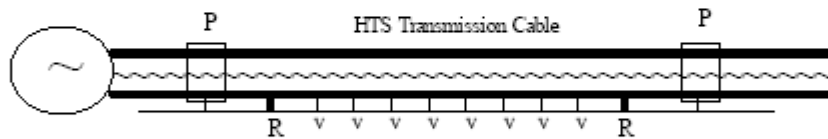
The general configuration of the system is indicated in Figure 1-1. The baseline distance was taken as 1000 miles (1610 km). A 5000 MW advanced gas turbine power plant was assumed to produce power at either the source end (for dc lines), or the load end (for gas lines). Systems analysis, including evolution of cost and cooling requirements, was carried out for the base case and then parametrized to investigate sensitivity to line length and other factors, including fuel cost and HTS operating temperature.

2 SYSTEM DESCRIPTION

2.1 Superconducting Transmission Line

The superconducting transmission system is shown schematically in Figure 2-1. The baseline system is selected to be 1000 miles (1610 km) long. A 50,000 Amp conductor carrying 5000 MW will see 100 kV across the conductors or ± 50 kV to ground. This requires a power conditioning system (PCS) with 50 kV, 5000 MW converters at each end of the line. Refrigerator stations are located every 10 km, and vacuum stations every 1 km, as described in section 2.1.2 below.

An auxiliary low-current power line at about 1.5 MW must also be provided to power the refrigerators and vacuum pumps. This line could be fed from taps on the dc line. Design of the converters for auxiliary power and for the main PCS and for the line was beyond the scope of this study.



R = Refrigerator station (100 kW_e, every 10 km)

V = Vacuum pumping station (20 kW_e, every 1 km)

P = Converter station (3 MW_e, every 100 km)

Figure 2-1 LVDC Transmission System Schematic

2.1.1 HTS Material Assumptions

Since their discovery in 1986, HTS materials have been developed from a laboratory curiosity to engineering materials serving commercial markets [2]. AC transmission cable is currently being produced by Pirelli [3], and several studies of dc distribution cables have been completed [4,5].

The key features of HTS cable are high current density (compared to metallic conductors) and low losses (due to the superconductive nature). The high current density results in a compact conductor and allows operation at a lower voltage and higher current at a conventional line. Low losses are possible with adequate cooling to maintain superconducting conditions. DC cables have inherently low loss because there is no time-varying magnetic field, only ripple. Careful cable design (including twisting) is required to minimize ac losses in ac cables.

For this study, the properties of the bismuth compound 2223 were used [6]. These include critical current density, J_c , at 77 K and zero magnetic field equal to 55 kA/cm². The relative values for decreasing temperature are shown in Figure 2-2. These are present day performance values. Improvements in the future will only help the performance of HTS products. An operating margin of $J_{op} = 0.8 J_c$ was used in this study. In addition, a 10% penalty due to resistive loss was assumed at 77K due to convention of starting J_c at measurement conditions of 1 μ V/cm. At 65 K, resistive loss is assumed to be zero.

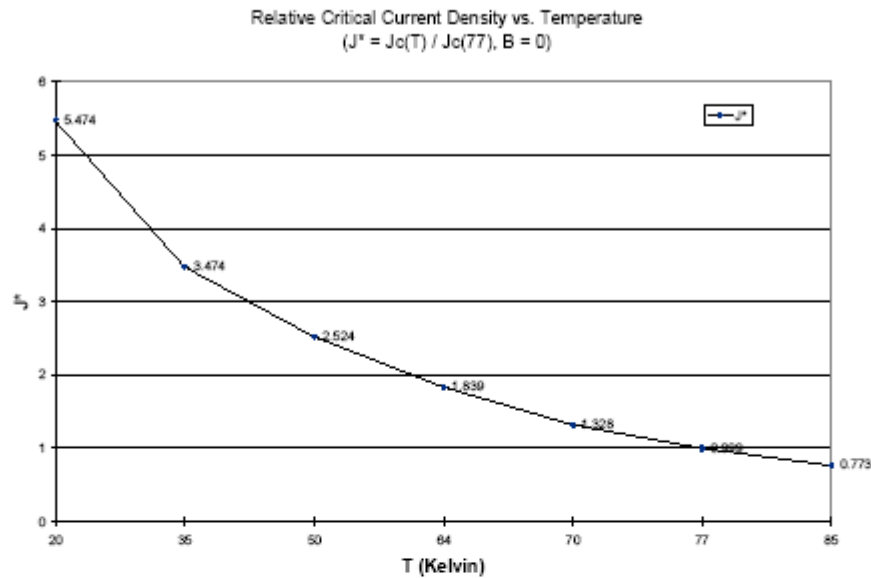


Figure 2-2 J_c for Bi-2223 [6]

2.1.2 Configuration

The study configuration for a 50 kA HTS transmission line is shown in Figure 2-3. The conductor has a parallel return path with a center ground. Electrical insulation separates the conductor paths from the support tubes and ground plane. The conductor is cooled by a flow of liquid nitrogen in the central tube. The entire conductor is supported in an evacuated conduit to reduce convection and conduction heating. Multilayer thermal insulation reduces radiation heating.

The optimized conduit diameter is approximately 0.7 m, a suitable dimension for installing in a surface trench.

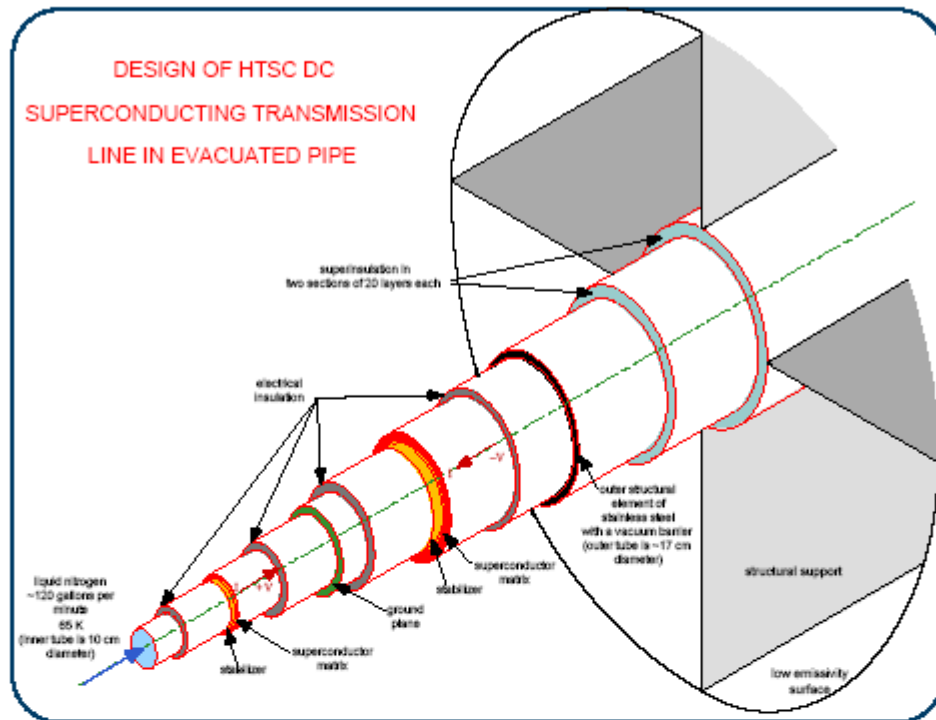


Figure 2-3 Isometric of HTS LVDC Conductor Layers

2.2 Cooling System and Trade-Offs

The baseline cooling approach for the HTS LVDC cable is liquid nitrogen at 65 K flowing in a central tube. The conductor is supported in an evacuated conduit. This approach keeps the heat flow to the conductor acceptably low, while also minimizing system cost and maintenance requirements. A heating rate of 1 Watt/m was selected as a target for design of the cooling system.

Other approaches were considered including filling the conduit with polystyrene (rather than evacuating it), cooling with gaseous helium, and cooling with the liquid nitrogen at 77 K. As described in the Appendix, these other approaches were found to be more expensive or more complicated either because of greater heat load (and hence, refrigeration requirements), more expensive cooling system components, or decreased superconductor performance. In particular, the choice of 65 K rather than 77 K as an

operating temperature results in almost a factor of 2 improvement in conductor current density, as shown previously in Figure 2-2, thus reducing the cost of superconductor. The refrigerator and conductor cost trade-offs for liquid nitrogen vs. gaseous helium cooling, including the cost of the coolant is shown in Figure 2-4.

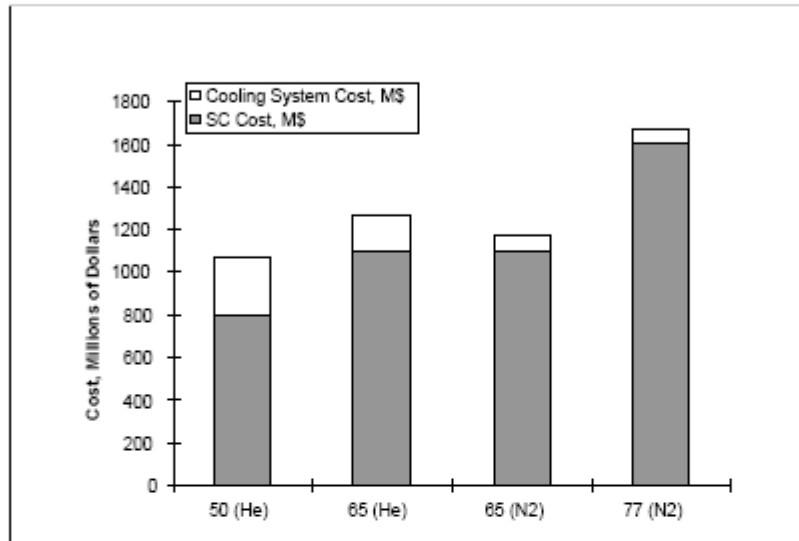


Figure 2-4 Coolant Selection Trade-Offs

The baseline system requires a total of 20 Megawatt-electric (MW_e) of refrigerator power, including a 4 MW_e nitrogen liquifier. The flow of liquid nitrogen is about 120 gallons per minute. Refrigerators with a thermal rating of 10 kilowatts-thermal (kW_t) are located at 10 km intervals along the line. The temperature rise between stations is at most 1 K, ensuring stable operation of the superconductor. Vacuum stations at each 1 km maintain a vacuum of 10^{-5} to 10^{-4} Torr in the conduit. The heat load components, in thermal Watts per meter of length (W_t/m) are listed in Table 2-1, which is also found in the Appendix.

Table 2-1
Heat Load Components

| Heat Source | Heat Input (W _t /m) |
|----------------------------------|-----------------------------------|
| Radiation and Gaseous Convection | 0.50 |
| Support Conduction | 0.05 |
| Viscous heating (pumping loss) | 0.20 |
| Miscellaneous, including leads | 0.20 |
| ac losses | 0.05 |
| Total | 1.00 |

3 ECONOMIC ANALYSIS

This section describes the economic analysis performed in this study, including capital cost estimates for the LVDC line, HVDC line and gas pipeline, as well as life-cycle costing analysis to generate electricity costs for all three systems. A flowchart of the analysis approach is shown in Figure 3-1.

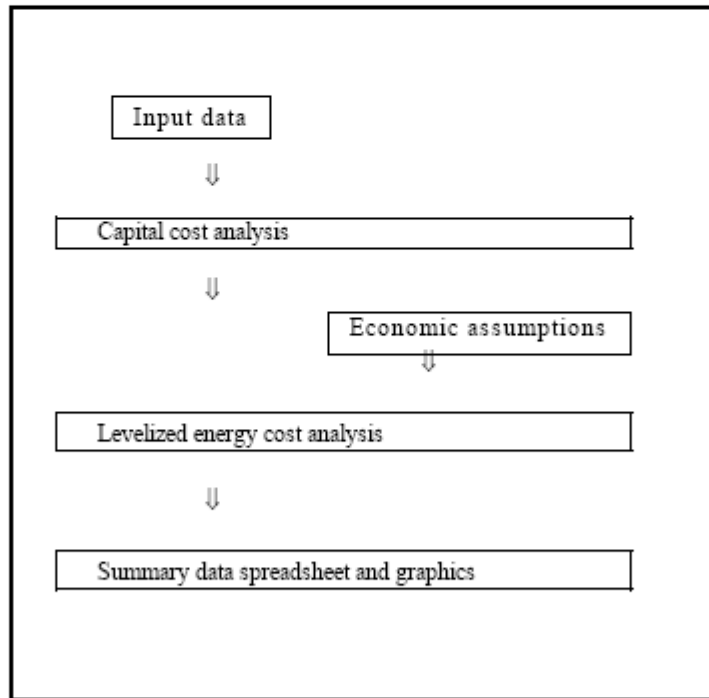


Figure 3-1 Economic Analysis Flowchart

3.1 Capital Costs

3.1.1 HTS Transmission Line

The major cost component of the HTS transmission line is the superconductor itself. The cost basis for the superconductor capital cost is \$10/kA-m for Bi-2223 operating at 77 K (i.e., $J_c=55 \text{ kA/cm}^2$) [7]. Based on the temperature curve shown previously in Figure 2-2, this translates to \$550/m for each of the two 50 kA superconductor layers operating at 65 K. No change in the material is assumed.

The remainder of the conductor/conduit package shown previously in Figure 2-3. For costing purposes, dimensions were chosen and material properties and unit costs estimated. These are given in Table 3-1. Unit cost assumptions are listed in Table 3-2, which have been adapted from References [8] and [9].

Table 3-1
Conductor Layer Dimensions and Costs

| Layer | Thickness, mm | Cost, \$/m |
|----------------------|---------------|------------|
| Inner tube | 2 | 21.8 |
| Electrical Insulator | 4 | 12.9 |
| Stabilizer | 2 | 30.1 |
| HTS | 0.5 | 550 |
| Electrical Insulator | 4 | 14.6 |
| Ground | 0.5 | 1.6 |
| Electrical Insulator | 4 | 15.7 |
| Stabilizer | 2 | 36.0 |
| HTS | 0.5 | 550 |
| Electrical Insulator | 4 | 17.3 |
| Outer Tube | 4 | 64.2 |
| MLI 1 | 20 layers | 8.3 |
| MLI 2 | 20 layers | 8.6 |
| Conduit | 4 | 131.0 |

Table 3-2
Material Cost Assumptions

| Layer | Representative Material | \$/kg |
|----------------------|-------------------------|-------------------------|
| Tubing | Stainless Steel | 4.4 |
| Conduit | Steel | 2.0 |
| Electrical Insulator | G - 10 | 6.6 |
| Stabilizer | Copper | 4.8 |
| MLI | MLI | 17 (\$/m ²) |

Combining the superconductor and conductor package costs results in a total cost of \$1450/m for the LVDC line if operated at 65 K, or \$2350/m if operated at 77 K. The relative size of the component costs are indicated in Figure 3-2 for the 65 K case.

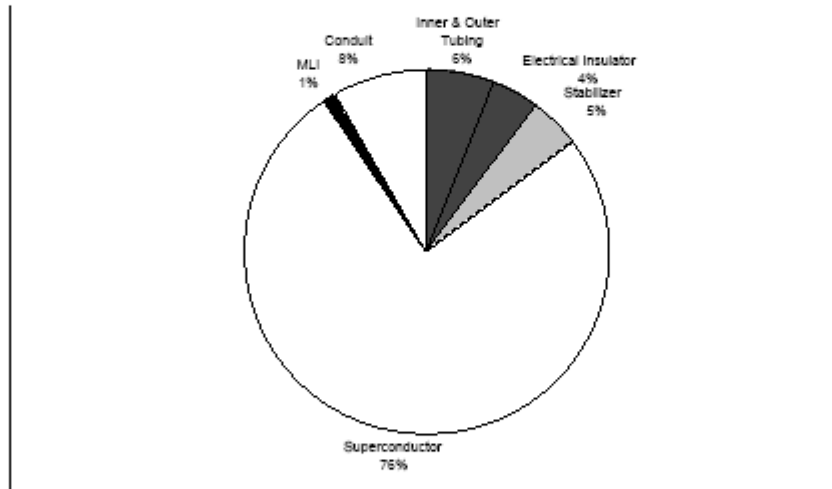


Figure 3-2 Cost Components of HTS LVDC Conductor at 65 K

The total system cost also includes converters (estimated at \$36/kW) [10] and the cooling system, which includes liquid nitrogen, nitrogen refrigerators and a nitrogen liquifier and vacuum pumping stations. This system cost is \$77 million for the 1000 mile line, as detailed in the Appendix. Capital and operating costs for the LVDC systems are summarized in Table 3-3.

Table 3-3
Costs and Operating Parameters for the 1000 miles LVDC system.

| Component | Unit Cost | Source |
|--|---|----------|
| Superconductor matrix (including silver) | \$10 / kA-m ($J_c=55 \text{ kA} / \text{cm}^2 @ 77\text{K}, 0\text{T}$) | 7 |
| Conductor components | \$350 / m (see Section 2.1) | 8, 9 |
| Refrigeration and vacuum system (LN ₂ @ 65 K) | \$45 / m + \$5 M liquifier | Appendix |
| Convertors | \$36 /kW | 10 |
| Steady state parasitic power | 32 kW/km = 4 MW (liquifier) | Appendix |
| Fixed O&M (for 1000 mi. line) | 2% of installed cost / year | |
| Variable O&M | 0.30 ¢/kWh | 8, 11 |

3.1.2 High Voltage Line and Gas Pipeline Costs

For comparison, capital cost estimates were obtained for long distance, high power HVDC lines and for large capacity gas pipelines. For HVDC, the primary sources were the ABB report mentioned previously [1] and product guide [10] and an Oak Ridge National Laboratory report [12]. For the gas pipelines, sources were published literature [13], an EPRI report [14], and ABB estimates [1].

For the HVDC system, the line and converter costs were calculated, along with the value of line losses. For the gas pipeline system (requiring 2 parallel lines, each carrying 500 million SCF/day), line costs and compressor station costs were estimated, along with the compressor power requirements. These assumptions are listed in Table 3-4. Capital cost components for all 1000 mile systems are compared in Figure 3-3.

Table 3-4
Cost Assumptions for HVDC Transmission Line and High Capacity Gas Pipelines

| Component | Unit Cost | Source |
|---------------------------|-------------------------------|--------|
| HVDC Line | \$1M / mile | 1, 10 |
| HV convertors | \$100 / kW | 1, 10 |
| Steady state losses | 8% | 1 |
| HVDC Fixed O&M | 2% of installed cost/yr | |
| HVDC Variable O&M | 0.15 ¢/kWh | 1, 12 |
| Gas Pipeline | \$1.2 M / mile each × 2 lines | 1, 13 |
| Compressor power required | 5000 HP / 100 mile per line | 14 |
| Compressor | \$131 / HP | 14 |
| Gas Pipeline Fixed O&M | 2% of installed cost/yr | |
| Gas Pipeline Variable O&M | 0.15 ¢/kWh | 14 |

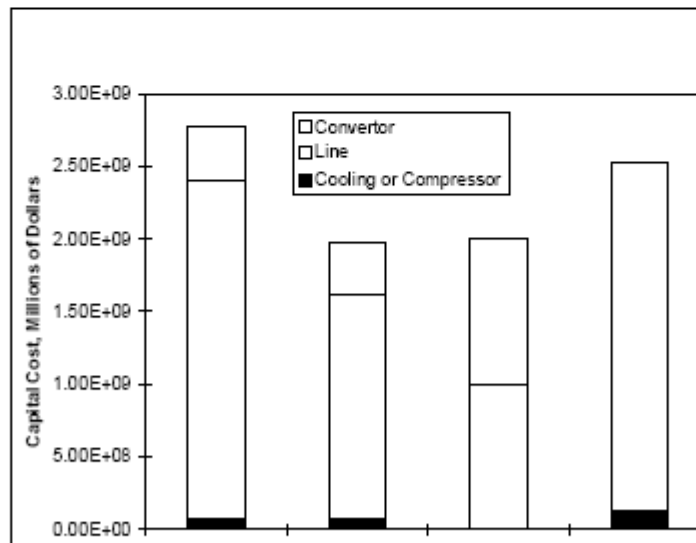


Figure 3-3 Capital Costs of 1,000 Mile Systems

3.2 Levelized Cost Analysis

Beyond capital cost comparisons, it is desirable to compare delivered electricity costs at the load for all three systems. Although the major component of the levelized or life cycle cost will be the capitalized expense, other factors also contribute, including cost of fuel and O&M costs. The fuel usage and fuel cost component varies because parasitic power requirements differ. For the LVDC system, refrigeration and vacuum system power must be accounted for, and it will scale with line length; for the conventional HVDC system, the transmission loss is typically a fraction of the power carried; for the gas pipeline, compressor power must be provided, and this also scales with line length.

The levelized cost or revenue requirement (RR) in ¢/kWh is given by Equation 1:
[15]

$$RR(\$/kW/yr) = FCR * TCC + Omf * Lom + [Omv * Lom + Ucg * HR * 10^{-6} * Lg + Uce * .01Le * (1/\eta)] * D * Ho + Uce * .01Le * R * HY/P \quad (eq. 1)$$

where:

FCR = Fixed Charge Rate or Charge Rate (1/yr)

TCC = Total Capital Cost (\$/kW)

Omf = Fixed O&M Costs (\$/kW/yr)

Omv = Variable O&M Costs (¢/kWh)

Lom = Levelization Factor for O&M Costs

Ucg = Unit Cost of Natural Gas (\$/MBTU)

HR = Heat Rate (Btu/kWh)

Lg = Levelization Factor for Gas

Uce = Unit Cost of Input Electricity (¢/kWh)

η = Storage Efficiency (kWh_{out}/kWh_{in})

Le = Levelization Factor for Electricity

R = Steady State Parasitic Power, kW

P = Output Power, kW

Ho = Operating Time per day (hr/d)

D = Operating Days per Year (d/yr)

HY = Hours per Year = 8760

In performing the electricity cost analysis, economic assumptions and operating assumptions are made. These are listed in Table 3-5.

Table 3-5
Economic and Operating Assumptions for Levelized Cost Calculations

| Variable | Value |
|-----------------------------------|-------------------|
| Inflation rate | 1% |
| Discount rate | 6% |
| Levelization period | 25 years |
| Carrying charge rate | 10% |
| System output power | 5000 MW |
| Days of operation per year | 333 |
| Fuel input (to gas turbine) | 14520 Btu/kWh-out |
| Real escalation rate, fuel | 1% |
| Real escalation rate, electricity | 1% |
| Real escalation rate, O&M | 0% |

Capital cost values are those indicated previously, plus \$500/kW for the gas turbine power plant [16].

Fuel costs vary tremendously around the world. The ABB study which motivated this work used extremely low fuel costs of 0.57 ¢/MBTU (2¢/m³). Typical delivered U.S. prices are \$3.00/MBTU. In this study, three values were considered as shown in Table 3-6. The cost of electricity as generated by the gas turbine power plant is also indicated.

Table 3-6
Fuel and Electricity Costs for Three Cases

| | Gas Cost | Generated Electricity Cost (¢/kWh) |
|------|--------------|------------------------------------|
| Low | 0.57 \$/MBTU | 2.51 |
| Mid | 1.41 \$/MBTU | 4.01 |
| High | 3.00 \$/MBTU | 6.86 |

3.3 Results

Delivered electricity costs for the three systems for line lengths ranging from 500 to 2000 miles are shown for mid-value fuel costs in Figure 3-4. The figure shows that the slope of the cost vs. distance curve varies for each technology. The figure also shows the dramatic impact of superconductor performance on cost. In this case, the difference is due to the difference in operating temperature. However, similar effects would result from reductions in the HTS material costs or improvements in HTS performance.

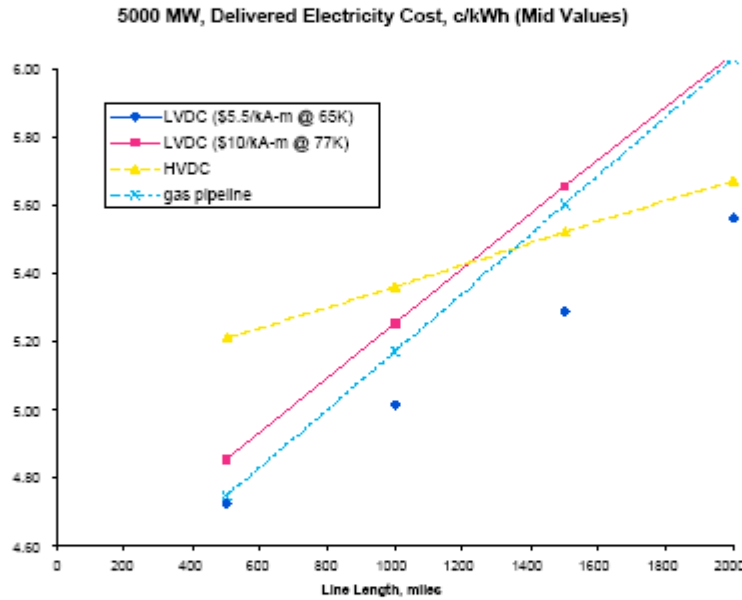


Figure 3-4 Delivered Electricity Cost for mid-value fuel

The electricity costs shown in Figure 3-4 include the levelized cost of the gas turbine generator and its fuel and O&M costs. Subtracting these out leaves the marginal or incremental cost of transporting energy by each of the three modes. These incremental costs are shown for the mid-value fuel costs in Figure 3-5. The trends are, of course, the same.

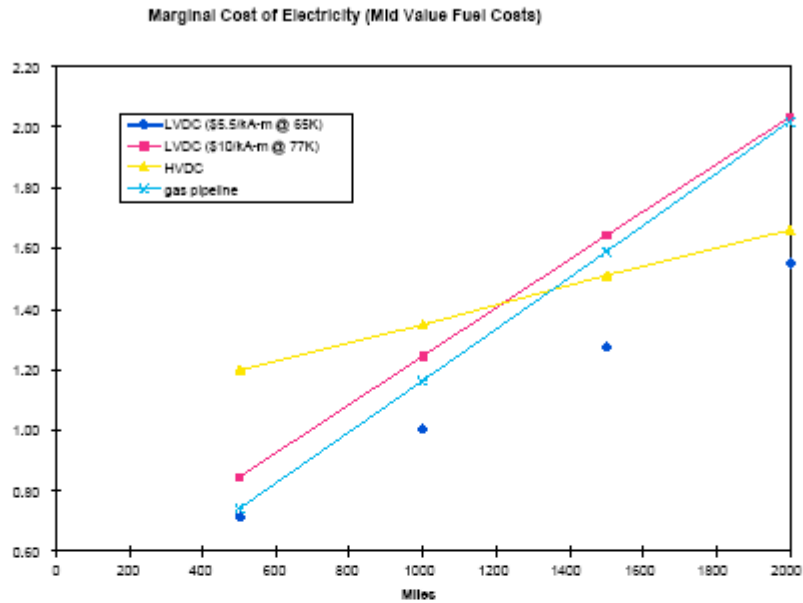


Figure 3-5 Incremental Electricity Cost for mid-Value Fuel

The extreme sensitivity of the results to the cost of fuel is shown in Figures 3-6 and 3-7, where electricity costs and incremental costs for low, medium, and high input fuel costs are shown side-by-side. The variations result from the cost of the varying parasitic power requirements for each transmission mode. A comparison of marginal electricity costs of a function of gas cost for 1000 mile lines is shown in Figure 3-8. A breakdown of the cost contributions is shown in Figure 3-9 for the mid-value incremental case at 1000 miles.

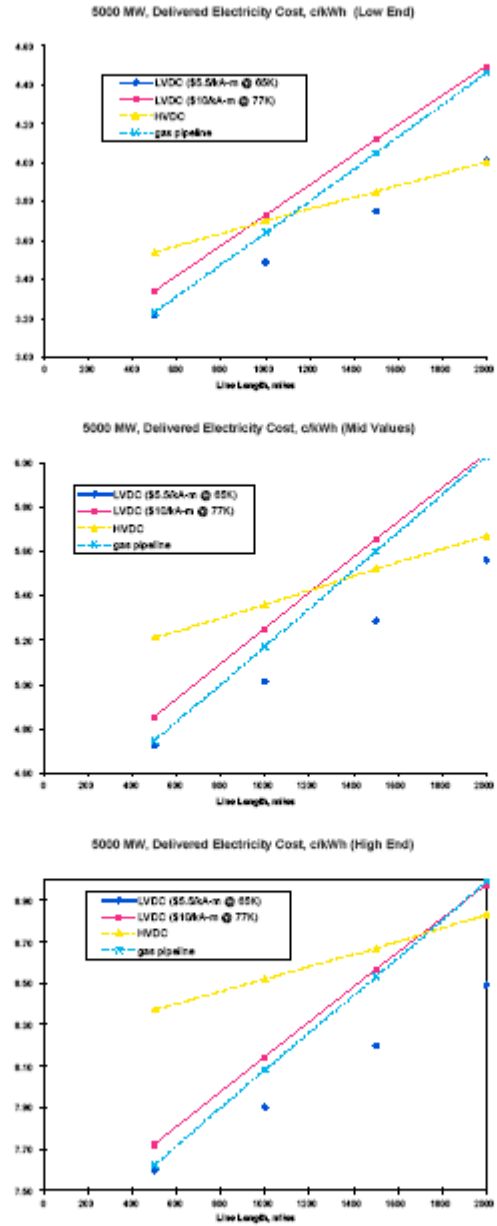


Figure 3-6 Comparative Delivered Electricity Costs

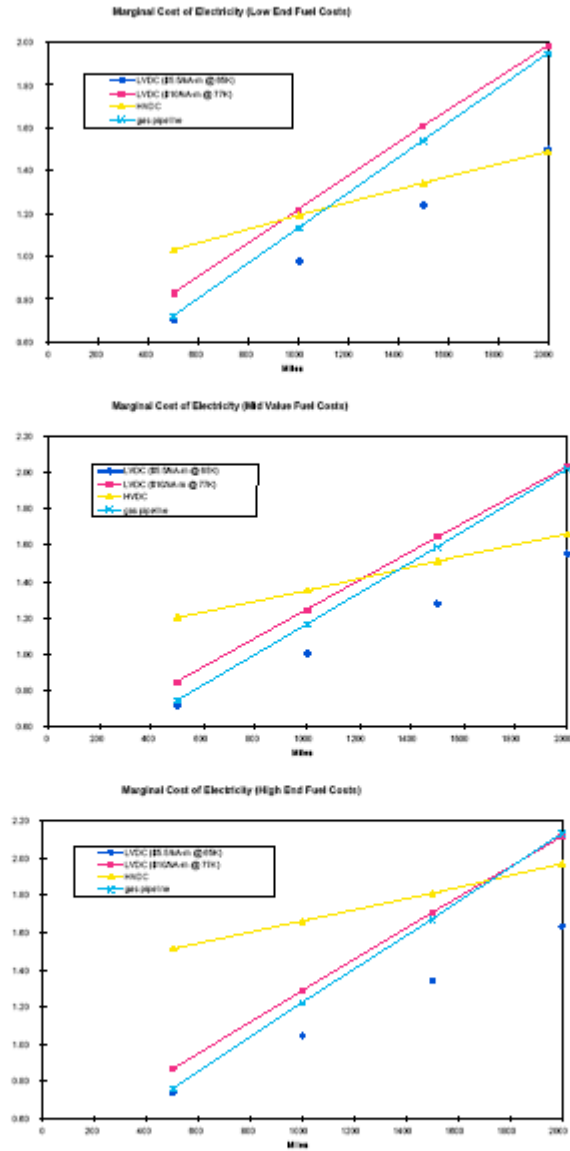


Figure 3-7 Comparative Incremental Electricity Costs

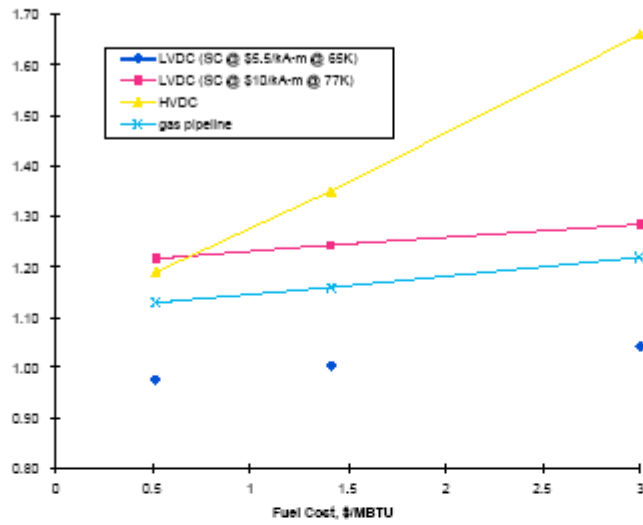


Figure 3-8 Marginal Electricity Cost as a Function of Fuel Cost for 1000 Mile System

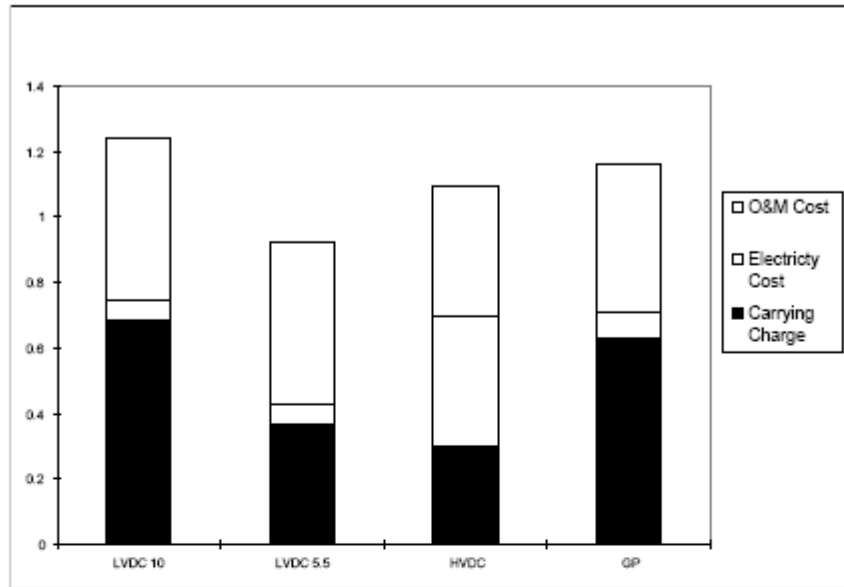


Figure 3-9 Incremental Electricity Cost Components (€/kWh)
for 1000 mile lines

4

CONCLUSIONS AND RECOMMENDATIONS FOR FURTHER STUDY

This preliminary analysis of an HTS low voltage dc transmission system suggests that such a system could be economically competitive with both HVDC and gas pipeline transport of bulk energy over long distances. The most important factor is the cost of the superconducting layer. If this can be provided at a cost around \$5/kA-m at the selected operating temperature, then the system is an attractive option. The cost of delivered electricity (¢/kWh) is strongly dependent on the cost of fuel at the source, since this component contributes nearly to all the power transmission options. The trade-off between systems is impacted most by capital costs and parasitic requirements.

The development of long distance HTS transmission would provide a large commercial market not only for HTS material, but also for liquid nitrogen refrigerators in the size range of several hundred kW. The nitrogen reaching the end of the transmission line might also have economic value, which has not been evaluated in this study.

Several issues which are recommended for further study before proceeding to system design include:

- The sensitivity analysis has been performed with line length as a variable. It would also be interesting to consider the sensitivity to power level.
- Details of the conductor packaging (e.g., specific selection of stabilizer and insulation) need additional consideration.
- Details of providing auxiliary ac power, such as low power take-offs along the line have not been established.
- Design of a subcooled refrigerator for operation at 65 K is needed.
- Vacuum requirements need more detailed evaluation, vacuum pressure needs to be optimized, and pumps including distributed pumping must be specified.
- Line cooldown must be addressed, including thermal contraction issues.
- A trade off between flow rate and refrigerator spacing is needed.

These items would provide a refinement to the system analysis and a basis for development efforts leading up to implementation of an HTS LVDC transmission system.

5 REFERENCES

- [1] A. Clerici, A. Longhi, B. Tellini, "Long Distance Transmission: the DC Challenge," presented at the Sixth International Conference on AC and DC Transmission IEEE Conference, London, UK. (May 1996)
- [2] P. Grant, "Superconductivity and Electric Power: Promises , Promises...Past, Present, and Future," Paper #PG-4, presented at the Applied Superconductivity Conf., Pittsburgh, Aug. 1996.
- [3] D.M. Buczek, et al, "Manufacturing of HTS Composite Wire for a Superconducting Power Transmission Cable Demonstration," Paper #MW-1, presented at the Applied Superconductivity Conf., Pittsburgh, Aug. 1996.
- [4] Superconducting Low Voltage Direct Current (LVDC) Networks. Electric Power Research Institute, Palo Alto, CA: April 1994. Report TR-103636.
- [5] J. Oestergaard, "Superconducting Power Cables in Denmark - a Case Study," paper #LMB-1, presented at the Applied Superconductivity Conf., Pittsburgh, Aug. 1996.
- [6] Personal communication - American Superconductor Corp., Aug. 1996.
- [7] Department of Energy near term cost target
- [8] Conceptual Design and Cost of a Superconducting Magnetic Energy Storage Plant. Electric Power Research Institute, Palo Alto, CA: April 1984. Report EM-3457.
- [9] "Independent Cost Estimate for the SMES-ETM," prepared by the Power Associates, Inc. and Cosine, Inc., for the Defense Nuclear Agency.
- [10] L. Philipson, editor, "Introduction to Integrated Resource T&D planning," ABB Power T&D Co., Cary, NC, 1995.
- [11] S. M. Schoenung, et al, "Capital and Operating Cost Estimate for High Temperature Superconducting Magnetic Energy Storage," Proc. 54th American Power Conference, Chicago, IL, 1992.
- [12] Comparison of Costs and Benefits for DC and AC Transmission. United States Department of Energy, Oak Ridge TN: February 1987. Report ORNL-6204.
- [13] Warren R. True, "Pipeline Economics," Oil & Gas Journal, November 27, 1995, pp. 39-58.
- [14] Pipelines to Power Lines: Gas Transportation for Electricity Generation. Gas Research Institute and Electric Power Research Institute Palo Alto CA: January 1995. Report TR-104787.
- [15] R. B. Schainker, "A Comparison of Electric Utility Energy Storage Technologies," presented at ASCE Energy '87 Conference, American Society of Civil Engineers, 1987.

- [16] Technical Assessment Guide - Electricity Supply - 1989. Electric Power Research Institute, Palo Alto, CA: Sept. 1989. Report P-6587-L.

APPENDIX REFRIGERATION, VACUUM, AND ANCILLARY POWER

Description of the System and Summary of Issues / Choices

The conductor / conduit system was shown previously in Section 2. The sketch in Figure A-1 shows the system as it was analyzed for thermal and structural parameters.

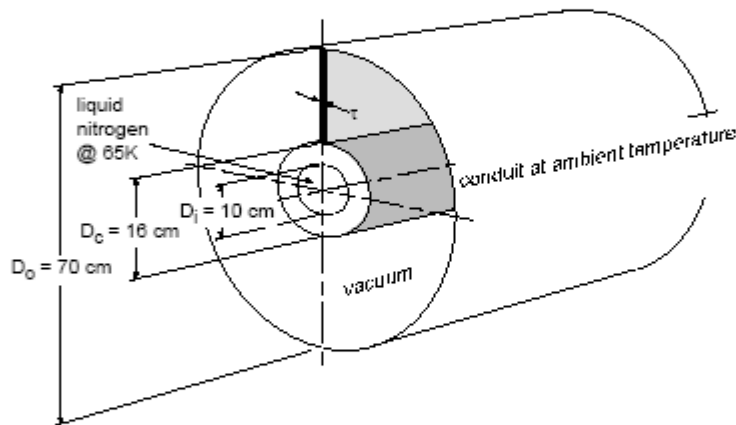


Figure A-1 Conductor/Conduit Analysis Sketch

Several options for coolant, the refrigeration process, and vacuum level were investigated. The system selected is driven by a requirement to achieve a total heat input into the cold portion of the superconducting DC transmission line of less than about one watt per meter ($1 \text{ W}_t/\text{m}$) of length. This total heat input is budgeted among the various heat sources, namely: radiation, gaseous convection, support conduction, miscellaneous, and pumping or friction losses. An additional heat input is the ac losses in the superconductor due to currents induced by voltage ripple.

A-1

The following temperature choices were made. First, based on the characteristics of the superconductor, the operating temperature should be below about 75 K. Second, a maximum temperature rise of 1 K between refrigeration stations was selected to achieve uniform superconductor performance. This choice also provides some operational redundancy because the superconducting dc line can perform at or near capacity with a 2 K temperature rise, which would occur if one refrigerator were out of service. Third, the use of single-phase, liquid nitrogen was selected instead of gaseous helium to reduce system complexity and friction associated with viscous flow. This choice means the operating temperature must be between the freezing point of nitrogen, about 63 K, and its boiling point, about 78 K. An operating temperature of 65 K was selected because the current carrying capacity of the superconductor – a major cost item – is considerably improved at this lower temperature. The refrigeration costs increases by about 25 % when the temperature is decreased from 77 K to 65 K, according to system vendors. [A1]

The system requires relatively a large liquifier at the power generation end. It produces 21,600 liters of liquid nitrogen per hour at 65 K. This is a moderately large refrigeration system. Several refrigerators this size or larger are installed in industrial locations in the United States every year [A1]. This liquid nitrogen is pumped along the entire length of the line, being re-cooled by refrigerators when the temperature increase exceeds the 1 K limit. For the cooling requirement of 1 W_t/m, the separation between refrigeration stations was chosen to be 10 km.

The goal of a total heat input of 1 W_t/m is a more serious requirement on the vacuum system than on the refrigeration system. Radiation and gaseous convection are controlled by using multilayer insulation and by evacuating the space between the ambient temperature outer pipe and the core. Approximately 40 layers of superinsulation is adequate, but a vacuum of at least 10⁻⁴ Torr is required. This requires frequent pumping stations, approximately every kilometer, each with a combination of vacuum pumps.

A-2

The total electrical power load for each refrigerator is about 100 kW_e, including a 25 % margin. The 10 vacuum stations over the 10 km require about 200 kW_e. Power for this equipment is supplied by an ac transmission line which is powered from the dc line via taps every 100 km. If power flows in both directions from the dc tap, the maximum power in the ac line will be about 1.5 MW.

Several issues remain before proceeding to a cryogenic system design.

- Design of a subcooled refrigerator for operation at 65 K is needed.
- Vacuum requirements need more detailed evaluation, vacuum pressure needs to be optimized, and pumps including distributed pumping must be specified.
- Line cooldown must be addressed, including thermal contraction issues.
- A trade off between flow rate and refrigerator spacing is needed.

Heat Input

The total heat flow into a dc superconducting transmission line will be dominated by the average heat input per unit length. This is in contrast to the typical small and/or short cryogenic systems where heat input from power leads and supports are typically the dominant effect. It is also very different from an ac transmission line where the ac losses associated with current and field changes in the superconductor and associated stabilizer are dominant. The six major sources of heat input in a dc superconducting transmission line are:

- 1) thermal radiation from the ambient temperature outer vessel,
- 2) gaseous convection between the outer vessel and the conductor package,
- 3) conduction in the mechanical supports for the core conductor package,

- 4) miscellaneous heat flow at the location of joints, connections, power leads, etc.,
- 5) viscous heating associated with flowing the cryogen through the conductor, and
- 6) ac losses due to current ripple in the superconductor and stabilizer.

Here the different sources of heat input to the HTS dc superconducting transmission line are described and their magnitudes are estimated. These values determine the refrigerator vacuum and superinsulation requirements.

Radiation

The rate of energy emitted per unit area of a surface depends on the temperature and the emissivity of the surface. Similarly, the rate of energy absorbed by a surface depends on the effective temperature of the radiation that pervades the region near the surface and the absorptivity of the surface in the wavelength range associated with this temperature. Thus, radiation transfers energy from surfaces at one temperature to other surfaces at lower temperatures. In the case of the dc transmission line, heat flows from the ambient temperature outer shell to the 65 K conductor core. The heat that is transferred (in Joules/sec or Watts) is

$$W = \sigma \epsilon A (T_{\text{ambient}}^4 - T_{\text{cond}}^4)$$

where ϵ is the emissivity of the surfaces, σ is Boltzman's constant ($= 5.67 \times 10^{-12} \text{ W cm}^{-2} \text{ K}^{-4}$), and A is the area of the surfaces. This equation is only approximate because the two surfaces of the transmission line have different areas and emissivities. However, if the emissivity were about 0.3 for both surfaces, and making a small correction for the annular case, the heat input would be $75 \text{ W}_t/\text{m}^2$. This translates to about $45 \text{ W}_t/\text{m}$ of length along the transmission line, which is much too high.

A-4

To reduce the heat flow to the 65 K core it is necessary to install some type of radiation absorbing material. Several approaches are available including:

- solid foam insulation in the annular space,
- particulates in gas in the annular space,
- particulates in vacuum in the annular space,
- low emissivity surfaces on the ambient and cryogenic walls, and
- superinsulation (multiple layers of aluminized mylar) in a vacuum in the annular space.

An insulation material such as foam not only affects thermal radiation, but it also reduces components of the gaseous conduction. Experiments with foam [A2] indicate that the heat transfer is about 50 W/m^2 , a reduction from the 400 W/m^2 for air at one atmosphere, but still much too high for the dc transmission line. The heat flow through particulates, even in a vacuum, are similar to that for the solid foam. Thus the only solution is to use a vacuum, to have the inner and outer surfaces coated to reduce emissivity, and to use superinsulation.

Reducing the emissivity of the inner and outer surfaces to 0.02 decreases the heat input to about 3 W/m , still higher than the acceptable level of 1 W/m for all contributions. This can be reduced further by adding layers of superinsulation or multilayer insulation (MLI).

Superinsulation is a term used for multiple very thin ($\approx 0.01 \text{ mm}$) layers of aluminum-coated mylar. This material is in the vacuum space and has a thickness of approximately 1 cm for 40 layers. The combination of low surface emissivity in the layers limits the total radiative heat transfer.

The reduction is approximately inversely proportional to the total number of layers, n , of material [A3]. If 0.1 W/m is budgeted for radiation, then at least 31 layers is required:

$$Q = \frac{Q_{\text{initial}}}{n-1} \quad \text{or} \quad n = 1 + \frac{Q_{\text{initial}}}{Q} = 1 + \frac{3}{0.1} \rightarrow 31 \text{ layers.}$$

Since 40 layers is often used [A4], it is selected here. This number of layers provides the maximum insulation in a single layup. More layers tend to reduce the insulating effect because their weight crushes them and causes layer to layer contact.

Gaseous Convection

Residual gas transmits heat from the ambient temperature outer shell to the 65 K core conductor. The amount of heat transmitted depends on the residual gas pressure. There are two regimes for this heat transfer. If the gas density is high, i.e., the molecules collide many times between the inner and outer surfaces, the heat transfer is nearly independent of pressure. If the density is low, i.e., the molecules are likely to travel from the outer surface directly to the inner surface without a collision, then the heat transfer is roughly proportional to the pressure. This is called the molecular flow regime. At a pressure of 10^{-5} Torr (0.01 microns, or 10^{-3} Pa), the mean free path for nitrogen gas is about 1 m. For the transmission line geometry the heat input in Watts/meter is given by [A2]:

$$W = 1.4 \times 10^{-4} p(\text{Torr})$$

At 0.01 microns, gaseous conduction should contribute about 0.14 W/m.

Several measurements of the combined heat transfer from these two mechanisms radiation and convection have been made for space and high-energy-physics applications. The heat flux from ambient to 77 K decreases to about 0.5 W/m² (0.3 W/m for the transmission line) at 40 layers of superinsulation and a gas pressure of 10^{-5}

Torr. These values are only slightly higher than the theoretical values and there is little further decrease for higher vacuums. At a vacuum of 10^{-4} Torr the heat flux increases to about 0.75 W/m^2 . Achieving 10^{-4} Torr is considerably less expensive than 10^{-5} Torr, and it takes less time. Thus, a vacuum of 10^{-4} Torr is used for further estimates and a heat budget of 0.5 W/m is used for the combined heat loads from radiation and gaseous convection.

Structural Supports

The central conductor core must be supported vertically against gravity and transversely against any off-centering forces. This might be accomplished with solid disks or bobbins, however, such a structure would limit gas flow in the annulus. The result would be either a higher pressure vacuum, or an increase in the vacuum pumping requirements. Rather, the supports will be thin spider structures, with most of the forces contained by tension elements. The minimum structure occurs when the weight of the conductor bundle is supported from the top of the outer pipe by a tension member.

The support thickness and resulting conduction input were calculated as follows: The minimum thickness of support structure is that for a tension member (in this case G-10) carrying the weight of the conductor and tubing, filled with liquid nitrogen. Referring back to Figure A-1, the force per unit length is:

$$F_L = \rho V/L = \rho A = \sum (\rho_i A_i)$$

where ρ is density and A is cross sectional area of each layer, i.e. the central flow channel, the layers of tubing, and the layers of conductor.

Assuming the solid cross section has a density midway between that of steel (440 lb/ft^3) and copper (558 lb/ft^3), or $\rho_{\text{conductor}} = 500 \text{ lb/ft}^3$

then, with $\rho_{\text{liquid nitrogen}} = 50.4 \text{ lb/ft}^3$, and referring to the dimensions in Figure A-1,

$$F_L = 2.3 \text{ lb/cm}$$

A-7

The thickness required to support this weight is given by:

$$\tau = U/F_L$$

where U is the tensile strength of the support material. Assuming G-10,

$U = 400$ MPa. This gives the minimum $\tau = 2.6$ microns, which is a small structural requirement!

Allowing for margins of safety and ease of fabrication, consider a practical value to be $\tau = 10$ microns. (This is an equivalent thickness, since the actual configuration would likely be intermittent supports along the length of the conduit.)

Calculating the conduction heat input per unit length resulting from this support structure:

$$q_L = \tau \int k(T) dT / l$$

where $\int k(T) dT$ is the integrated thermal conductivity over the temperature range 65 to 300 K, approximately = 150 W/m for G-10,

and l is the radial distance from the cold core to the warm conduit, approximately 0.25 m. This gives $q_L = 0.006$ W_t/m.

There may occasionally be excessive forces (seismic, etc.) requiring some additional structure (bumpers, e.g.) for motion limitation. Thus, a budget of 0.05 W_t/m is allowed for heat flux due to the mechanical supports.

Miscellaneous Heat Load

Using an engineering rule of thumb, it is assumed that the heat load from penetrations through the superinsulation will increase the total heat flux from radiation and gaseous convection by about 20%, or 0.1 W_t/m. Extensive piping will be required at the refrigerator connection to the transmission line, and may be required for areas of stress

A-8

relief that accommodate the thermal contraction of the line during cooldown. This may amount to several hundred watts for each refrigerator. Power leads contribute about 1 W_t per kA based on catalog information from America Magnetics, Inc. This contributes approximately 100 W_t at each end of the line and a few watts along the line for the smaller power leads that extract energy for refrigeration and vacuum pump power. This loss is negligible. A budget of 0.20 W_t/m is allowed for miscellaneous heat input.

Friction or pumping loss

The friction or viscous heating, loss is based on the total amount of cryogen flowing along the transmission line, \dot{m} , the pressure drop between refrigerators, Δp , and the density of the liquid, ρ .

$$W_t = \dot{m} \Delta p / \rho$$

The pressure drop in the line (for a 4" diameter pipe) is found from the following expression [A2], in English units:

$$\Delta p(\text{psi} / \text{ft}) = 0.15 \times 10^{-6} q^2 (\text{gal} / \text{min})$$

Using 0.85 kg/liter as the density of liquid nitrogen at 65 K, the flow rate is 5.8 liter/second or about 100 gal/min. The flow velocity is 1.35 m/s. The pressure drop over 10 kilometers is 50 psi, or 0.34 MPa. Plugging this into the equation, the viscous loss or heat input is 2 kW_t or 0.2 W_t/m .

Heat Input from ac Losses in the Conductor

The power conditioning system (PCS) converts ac to dc. However, the voltage on the dc line contains some ac at frequencies associated with the characteristics of the switching method in the PCS (usually at 6 or 12 times the main frequency [A5]). These ac components produce currents in the superconductor and stabilizer. For conventional dc transmission lines the voltage distortion (ripple) is limited by ANSI/IEEE standards [A6] to a maximum of 1% for an individual frequency and 2-5% total. Losses at 1%

ripple would be unacceptably large for the baseline HTS material and configuration. (A 1000A ac component would mean 0.5 W_t/m heat load for today's HTS material [A7].) The allowable current ripple in the HTS line is determined by the total refrigeration load. In order to maintain 1 W_t/m total heat input, the ac current contribution must be limited to about 0.05 W_t/m. This can be achieved by:

- Filtering the power output from the ac-to-dc convertor (a variety of methods are available [A8]).
- Selecting an HTS conductor material and configuration with inherently low ac losses.

Total Heat Input

The total heat input to the transmission line is the sum of the above individual values, as summarized in Table A-1 below. The total 1.0 W_t/m is a conservatively high value.

Table A-1 Heat sources and heat input values for dc superconducting transmission line.

| Heat Source | Heat Input (W_t/m) |
|----------------------------------|---------------------------|
| Radiation and Gaseous Convection | 0.50 |
| Support Conduction | 0.05 |
| Viscous heating (pumping loss) | 0.20 |
| Miscellaneous, including leads | 0.20 |
| ac losses | 0.05 |
| Total | 1.00 |

Refrigeration Options

Operation over long distances at temperatures below 80 K requires the use of a cryogen that:

- 1) has sufficient heat capacity to remove the approximately $1 W_t/m$ that enters the system,
- 2) can be pumped without excessive heat input due to frictional losses, and
- 3) remains fluid at the operating temperature and pressure.

Liquid nitrogen and gaseous helium and were considered for use in the dc transmission line. A liquid nitrogen system was chosen because it has smaller capital and operating cost and a simpler transmission line cross section. The gaseous helium alternative is discussed at the end of this section.

The characteristics of liquid nitrogen of interest here are

| | |
|-----------------|---|
| Melting point | $T_{\text{melt}}=63.14 \text{ K}$ |
| Boiling point | $T_{\text{boil}}=77.40 \text{ K @ } 1 \text{ Atm}$ |
| Specific heat | $C_p=2 \text{ kJ/kg/K}=13.5 \text{ Cal/mole/K}$ |
| Enthalpy Change | $H_{\text{ambient}} - H_{65\text{K}} = 1800 \text{ Cal/mole} = 270 \text{ kJ/kg}$ |
| Density | $\rho = 850 \text{ kg/m}^3$ |

The melting point of 63 K establishes an operating temperature between approximately 64 K and the boiling point, 77 K. Subcooled, single-phase liquid nitrogen at 65 K was chosen as the cryogen for three reasons. First, performance of the superconductor improves as the temperature is lowered. Second, pressure drop (friction) is less for subcooled-liquid flow than for two-phase flow. Third, 65 K was chosen because the increased cost of refrigeration between 77 K and 65 K is more than offset by the reduced cost of superconductor.

The cryogenic system consists of a large liquifier at the power input end, which produces 65 K liquid nitrogen that is pumped the 1000 mile (1610 km) length of the dc transmission line. The $1.0 \text{ W}_t/\text{m}$ heat input causes the temperature of the liquid to rise as it flows along the line. Smaller refrigerators are placed along the transmission line to ensure that under normal operation the temperature does not exceed 66 K. The 65 K liquid nitrogen leaves the refrigerators at a pressure of 10 Atm. By the time it reaches the next refrigerator along the line it has warmed up by approximately 1 K and the pressure has decreased to about 7 Atm. Each refrigerator provides cooling from 66 K to 65 K and boosts the pressure of the liquid nitrogen back up to 10 Atm.

A-12

One advantage of this system, and the margins of 25 % or so in the refrigerators, is that the line should be able to operate at the specified power level even if one refrigerator is out of service. In this case, the adjacent refrigerators can boost their cooling so that the temperature rises at most to 66.5 K and the pressure always remains greater than 3 Atm, which assures single phase flow. The 25 % margin also assists in system cooldown.

There is a trade off between liquid nitrogen flow rate and refrigerator spacing. Since the maximum temperature rise for normal operation is constrained by superconductor performance to 1 K, if the separation between refrigerators were increased, the flow rate and thus the size of each refrigerator would also increase. Total refrigeration along the line goes up slightly because frictional losses also increase. But, since the per kW cost of refrigeration decreases with unit capacity, the total cost of refrigeration along the line is not affected by increasing or decreasing refrigerator separation by a factor of two or so. Similarly, the total power required to operate the refrigerators is also relatively insensitive to separation or total flow rate. However, both the cost of the initial liquifier and the power required for its operation are roughly proportional to the total liquid nitrogen flow rate. For any given site, the refrigerator spacing and flow rate may be optimized to meet the market for liquid nitrogen at the power delivery end of the transmission line.

For this study of a 1000 mile long dc transmission line, a refrigerator separation of 10 km was selected. Thus, 160 identical units each delivering 10 kW_t of refrigeration at 65 K are required. Though refrigerators in this size range exist today, the market is small. Larger markets exist for both much larger, 1 MW_t equivalent, and smaller, 200 W_t units. However, the need for 160 identical refrigerators is sufficient to warrant a special design and take advantage of large-scale production techniques, both of which will reduce cost and improve efficiency.

Since these 10 kW_t refrigerators will be designed to operate continuously in one mode (We neglect the issue of cooldown), the efficiency, at 65 K, should be better than 50 % of

Carnot. This means that the electrical power per refrigerator will be about 80 kW_e. We add 25 % to cover the operation of ancillary equipment and as a safety factor to arrive at 100 kW_e per unit, or 16 MW_e for the entire transmission line.

The cost of individual refrigerators in this input power range vary from about 350 to 500k\$ each. Refrigerators for lower temperatures cost somewhat more. Discussion with some manufacturers, present and past, suggests that savings of a factor of two or more will be possible for quantities of 100 or more. The cost reduction would be even greater if existing refrigerators did not use mass produced parts wherever possible, for example, the compressors. The estimated cost of the refrigerators in quantity is 200 k\$ each for a total budget of 32 M\$ for the entire transmission line.

The single refrigerator at the power generation end of the transmission line must have the capacity to produce 5 kg/s of liquid nitrogen from ambient air. This liquifier provides 1.35 MW of cooling at temperatures from ambient to 65 K. The total electrical power needed for this unit is about 4 MW, and it will cost about 5 M\$. Refrigerator and liquifier parameters are given in Table A-2.

Table A-2 Refrigerator capacity and cost for liquid nitrogen as a function of temperature. Total cost includes liquifier.

| Temperature | Liquifier | Liquifier | Refrigerator | Efficiency | Refrigerator | System |
|-------------|--------------------|-----------|---------------------|------------|--------------------|--------|
| | Power | Cost | Power | | Power | Cost |
| (K) | (MW _e) | (\$M) | (W _t /m) | | Total | Total |
| | | | | | (MW _e) | (\$M) |
| 65 | 4 | 5 | 1 | 0.12 | 20.0 | 37.0 |
| 70 | 4 | 5 | 1 | 0.14 | 18.0 | 32.0 |
| 75 | 4 | 5 | 1 | 0.16 | 16.0 | 28.0 |
| 77 | 4 | 5 | 1 | 0.17 | 15.0 | 26.0 |

Gaseous helium

Gaseous helium was also considered for the coolant. Characteristics necessary for a comparison with a liquid nitrogen system are:

Specific heat $C_p = 17 \text{ kJ/kg/K} = 4 \text{ Cal/g/K} = 1 \text{ Cal/mole/K}$

Density $r = 0.80 \text{ kg/m}^3 @ 1 \text{ Atm} @ 65 \text{ K}$

Viscosity $\eta = 70 \text{ micropoise} @ 80 \text{ K} = 7.0 \times 10^{-7} \text{ kg/ms}$

Whereas data was available for the pressure drop in flowing liquid nitrogen, it must be calculated for gaseous helium. In addition, the viscous flow losses depend on the flow regime. Thus the approach used here to obtain a comparison between a liquid nitrogen and a gaseous helium system is to assume initially that the flow characteristics are the same, and then to iterate to obtain a solution for the gaseous helium that can be compared to the liquid nitrogen system.

If the viscous heating in the flowing helium were the same as for the liquid nitrogen, about 2 kW over 10 km, then the total heat input would still be 10 kW. The helium mass flow necessary to remove 10 kW with a temperature rise of 1 K is about 0.56 kg/s, which requires a flow velocity of 4.35 m/s in the inner tube. The pressure drop in a fluid is given by

$$\Delta P = 2f\rho_w v^2 L / D,$$

where f is the friction factor, v is the fluid velocity, L is the length of the pipe, and D is the hydraulic diameter. The friction factor depends on the flow regime, which can be determined by calculating the Reynolds number:

$$\text{Re}_D = \frac{\rho v D}{\eta} = 10.8 \times 10^6,$$

which implies turbulent flow. The friction factor for smooth surfaces is found from [15] to be 0.003. Thus the pressure drop is:

$$\Delta P = 2f\rho_{\text{He}} v^2 L / D = 2 \times 10^5 \text{ Pa} = 2 \text{ Atm} .$$

The total viscous flow loss is given by the same relation used for liquid nitrogen:

$$W = \frac{m\Delta p}{\rho} = \frac{2 \times 10^5 \times 0.56}{20 \times 0.87} = 6.44 \text{ kW}$$

or 0.64 W/m instead of the 0.2 W/m viscous loss for liquid nitrogen. The temperature rise for this case would be 1.4 K over 10 km. Since other assumptions in the design assume the allowable temperature rise is only 1 K, some aspect of the design must be changed. The straightforward approach used here is to maintain the 10 kW for each refrigerator for line cooling. This is accomplished by reduce the spacing between refrigerators. (It also increases the total number of refrigerators.) This occurs at a refrigerator spacing of 7.0 km.

However, there are two additional heat inputs to the system. Whereas the nitrogen all flowed in one direction, the helium must be returned. There is viscous heating associated with the return helium in a separate tube, which is thermally insulated from but near the conductor tube. This is also 0.64 W/m, which requires an additional 4.5 kW for each refrigerator. The second is the additional heat input due to the increased area and cold mass that receives heat from all the same sources mentioned above. This is estimated to be an additional 3 kW. Thus the total heat load for each of the refrigerators spaced every 7 km is 17.5 kW.

The cost of the helium, based on a unit cost of \$3/liquid liter \$18/kg, is \$12 M. This amount is appropriate for a volume 20% greater than the two 10 cm diameter tubes. The cost of the additional pipe, superinsulation, and associated structure for the gaseous helium return is \$30 M.

A-16

The costs and power requirements for the gaseous helium refrigeration system are described in Table A-3.

Table A-3 Refrigerator capacity and cost for gaseous helium as a function of temperature. Total cost includes helium cost and return line.

| Temperature | Helium | Line | Refrigeration | Efficiency | Power | Refrigerator |
|-------------|--------|-------|---------------------|------------|--------------------|--------------|
| | Cost | Cost | Power | | Required | System Cost |
| (K) | (\$M) | (\$M) | (W _t /m) | | (MW _e) | (\$M) |
| 50 | 30 | 12 | 2.5 | 0.06 | 81.0 | 232.5 |
| 55 | 30 | 12 | 2.5 | 0.08 | 61.8 | 184.5 |
| 60 | 30 | 12 | 2.5 | 0.10 | 48.5 | 151.4 |
| 65 | 30 | 12 | 2.5 | 0.12 | 40.8 | 132.0 |
| 70 | 30 | 12 | 2.5 | 0.14 | 35.4 | 118.5 |
| 75 | 30 | 12 | 2.5 | 0.16 | 30.9 | 107.3 |
| 77 | 30 | 12 | 2.5 | 0.17 | 28.1 | 100.1 |

The costs of the liquid nitrogen and gaseous helium refrigeration systems are compared in the Figure A-2.

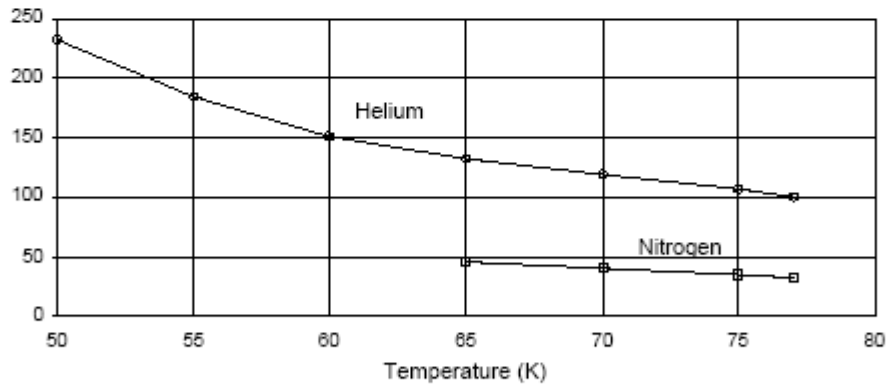


Figure A-2 Refrigerator Cost (\$M) for Liquid Nitrogen and Gaseous Helium Cooling Systems

Vacuum

The goal of the vacuum system is to maintain a pressure of about 10^{-5} Torr. This implies both a high vacuum pump and a roughing pump. The capacity of these are determined by the more stringent of two conditions. The first is initial pump down time and the second is the stable vacuum that can be achieved with the outgassing load (mostly water) associated with the multilayer thermal insulation.

The roughing pump is sized for pumpdown over a length, L , of 1 km in a period, t , of about 10 hours. The capacity is given by [A9]

$$S \text{ (liters/s)} = [V/t] \ln(p_i / p_f) \cong 0.3 L \text{ (m)} = 300 \text{ liters/s,}$$

where v = volume = area \times length, L

Roughing pumps consisting of a mechanical booster and single stage pump of this capacity are commercially available. The cost for these pumps is about 5 k\$ each and the power requirement is about 7 kW_e.

Several high vacuum pumps, e.g., turbo pumps and ion pumps, are available for the pressure range of 10^{-2} to 10^{-5} Torr. To achieve the same pumpdown time as for the backing system will require a pump with a capacity of about 100 liters/second.

Equilibrium pressure is a more difficult issue as it is difficult to estimate the outgassing rate for the superinsulation. Outgassing decreases with time, and, once it is cold, the transmission line will act as a cryopump for part of the water from the superinsulation.

The outgassing is proportional to the total area of material, i.e., to the product of the outer diameter of the conductor package times the number of layers of superinsulation. Outgassing decreases with time, so the equilibrium rate will be the value after several days. In this case, it is estimated that the total outgassing after 10 days will be about 10^{-1} Torr/s. Achieving 10^{-4} Torr will require a pump having a capacity of 1000 liters/s. This requirement is much more stringent than the pumpdown time. Pumps of this capacity cost approximately 20 k\$ each in large quantities and require about 15 kW to

A-18

operate. This gives a electrical power requirement of about 22 kW/km or a total of 35 MW_e for the entire line. The vacuum system is summarized in Table A-4.

Table A-4 Vacuum system components, power, and costs for HTS dc superconducting transmission line.

| Component | Quantity | Unit Power | Unit Cost | Total Power | Total Cost |
|------------------|----------|--------------------|-----------|--------------------|------------|
| | | (kW _e) | (\$k) | (MW _e) | (\$M) |
| Roughing Pump | 1600 | 7 | 5 | 11 | 8 |
| High Vacuum Pump | 1600 | 15 | 20 | 24 | 32 |

Appendix References

- [A1] Private Communication, Robert Powell, PSI, 1996
- [A2] Russell B. Scott. Cryogenic Engineering. Met-Chem Research Inc., Boulder, CO 1963 Edition, reprinted 1988.
- [A3] I. E. Spradley, T. C. Nast, and D. J. Frank, "Experimental Studies of MLI Systems at Low Boundary Temperatures," Adv. in Cryogenic Engineering. Vol. 35, p. 447 (1990).
- [A4] Ted C. Nast. A Review of Multilayer Insulation, Theory, Calorimeter Measurements, and Applications. Lockheed Palo Alto Research Laboratory Report, Palo Alto, CA.
- [A5] J. Arrillaga, High Voltage Direct Current Transmission. The Institution of Electrical Engineers, Power Engineering Series 6, London, 1983.
- [A6] ANSI/IEEE Standard 1030-1987. IEEE Guide for Specification of High-Voltage Direct-Current Systems. Part I - Steady-State Performance. IEEE, New York, NY, 1987.
- [A7] Los Alamos National Laboratory data, unpublished, 1996.
- [A8] Superconducting Low Voltage Direct Current (LVDC) Networks. Electric Power Research Institute, Palo Alto, CA: April 1994. Report TR-103636.
- [A9] A. Roth. Vacuum Technology. Elsevier Science Publishing, New York, NY 1990, 3rd Edition.

C

ECONOMIC CONSIDERATIONS

This appendix provides updated cost estimates for the previously unpublished report *System Study of Long-Distance Low-Voltage Transmission Using High-Temperature Superconducting Cable*, which is presented in Appendix B. Most of the original estimates have been updated to reflect present-day costs of various materials, and some additional items have been included. The cost estimates in this appendix represent the cost per meter and per kilometer of an installed cable. They do not include the costs associated with testing and cooldown of the cable before it is put into operation. The quantitative changes are shown in the tables.

The following items describe the updates to the original estimates and the assumptions used in producing the updated estimates:

- Unit costs of materials such as steel and multilayer insulation were updated.
- Costs of equipment, such as vacuum pumps and ac–dc converters, were updated.
- Trenching costs were added.
- Contingencies were added. The contingency figures vary from 25% for conventional equipment to 50% for new equipment. A larger contingency might have been used were it not for the experience of the industrial gas community in building cryogenic systems and lines.
- A variable cost, ranging from US\$5/kA-m to \$US100/kA-m for operation at 77K with a self-magnetic field, was used for conductors. Because this cost is a variable, it does not have a contingency.
- Only capital costs per kilometer and per mile are calculated.
- No comparisons with other technologies are provided.
- Operating and maintenance costs are not estimated.
- Efficiencies of components and overall efficiency of transmission are not included.
- The annualized cost of delivered energy is not calculated.

Table C-1 presents cost estimates for the cable core material, including both 1996 costs and costs as of October 28, 2009. Costs of metals have retrenched considerably since January 2008. Higher costs could have been used in this appendix, but the cost of the superconductor at today's prices completely overwhelms all other costs, as shown in Table C-1.

Table C-1
Cable core material cost assumptions

| Layer | Material | US\$/kg (1996) | US\$/kg (2009) |
|-----------------------|-----------------------------|-------------------------|-------------------------|
| Tubing | Stainless steel | 4.4 | 5.5 |
| Conduit | Steel | 2.0 | 2.5 |
| Electrical insulator | G-10 | 6.6 | |
| Electrical insulator | Solid core or wrapped paper | | 10.0 |
| Stabilizer | Copper | 4.8 | 5.5 |
| Multilayer insulation | Multilayer insulation | 17 (\$/m ²) | 25 (\$/m ²) |

Note: All costs are in present-day dollars. Unit cost differences are based on market quotations for materials on October 28, 2009.

Table C-2 presents the cable costs of non-superconducting components and fabrication. The table includes material dimensions, which were used to obtain total weights and areas.

Table C-2
Cable costs of non-superconducting components and fabrication

| Layer | Thickness (mm) | US\$/m (1996) | US\$/m (2009) |
|-----------------------------------|----------------|---------------|---------------|
| Inner tube | 2 | 21.8 | 27.3 |
| Electrical insulator | 4 | 12.9 | 19.5 |
| Stabilizer | 2 | 30.1 | 34.6 |
| Electrical insulator | 4 | 14.6 | 22.1 |
| Ground | 0.5 | 1.6 | 2.0 |
| Electrical Insulator | 4 | 15.7 | 19.6 |
| Stabilizer | 2 | 36.0 | 45.0 |
| Electrical Insulator | 4 | 17.3 | 26.2 |
| Outer tube | 4 | 64.2 | 80.3 |
| Multilayer insulation 1 | 20 layers | 8.3 | 12.2 |
| Multilayer insulation 2 | 20 layers | 8.6 | 10.8 |
| Conduit | 4 | 131.0 | 163.8 |
| Total (no superconductors) | | 362.1 | 463.3 |

Note: All costs are in present-day dollars. Unit cost differences are based on market quotations for materials on October 28, 2009.

Table C-3 presents the cost per meter for a 1600-km, 5-GW, low-voltage dc system.

Table C-3
Cost per meter for a low-voltage dc system

| Component | Unit Cost (US\$) |
|--|----------------------------------|
| Superconductor (77 K, self field) | Variable, \$5/kA-m to \$100/kA-m |
| Superconductor | Variable \$600/m to \$12,0000/m |
| Conductor components | \$463/m |
| Conductor contingency (50%) | \$231/m |
| Fabrication (25% of conductor cost) | \$174/m |
| Trenching | \$300/m |
| Field installation (3 person-hours per meter) | \$300/m |
| Refrigeration and vacuum system (with liquid nitrogen at 65 K), including initial liquefier (see note) | \$70/m |
| Contingency on conventional elements (40%) | \$338/m |
| Total for non-superconducting components | \$2476/m |
| Converters (US\$150/kW), 5 GW at each end [45] | \$932/m (for 1600-km line) |
| Converters (US\$300/kW), 5 GW at each end [45] | \$1864/m (for 1600-km line) |

Note: Costs of vacuum and cryogenic systems have approximately doubled since 1996. This might be surprising, but system reliability, such as mean time between failures, has also doubled. As a result, operations and maintenance costs, which are not included, will be considerably reduced. To compensate for this difference in quality, an inflation factor of 1.5 is used for both vacuum systems and refrigerators.

Table C-4 presents the cost per meter for a 1600-km, 5-GW, low-voltage dc system, with superconductor costs ranging from US\$5/kA-m to US\$100/kA-m.

Table C-4
Cost per meter for the low-voltage dc system with different superconductor costs

| Component | Cost (US\$/m) | Cost (US\$/m) | Cost (US\$/m) | Cost (US\$/m) |
|--|---------------|---------------|---------------|---------------|
| Unit Superconductor Cost (US\$/kA-m) | 5 | 18 | 50 | 100 |
| Superconductor | 600 | 2000 | 6000 | 12000 |
| Conductor components | 463 | 463 | 463 | 463 |
| Conductor contingency | 231 | 231 | 231 | 231 |
| Fabrication | 174 | 174 | 174 | 174 |
| Trenching | 300 | 300 | 300 | 300 |
| Field installation | 300 | 300 | 300 | 300 |
| Refrigeration and vacuum system | 70 | 70 | 70 | 70 |
| Contingency on conventional elements | 337 | 337 | 337 | 337 |
| Total cable cost without converter | 3076 | 4476 | 9076 | 12,476 |
| Total cable cost with converter (US\$150/kW) | 4008 | 5408 | 10,008 | 13,408 |
| Total cable cost with converter (US\$300/kW) | 4940 | 6340 | 10,940 | 14,340 |

The relative costs of the various components with superconductor costs of US\$5/kA-m, US\$18/kA-m, and US\$50/kA-m are shown Figures C-1 through C-3. (A similar pie chart with a superconductor cost of US\$100/kA-m is not included because it was not informative; the cost of the superconductor is approximately 88% of the total cost.)

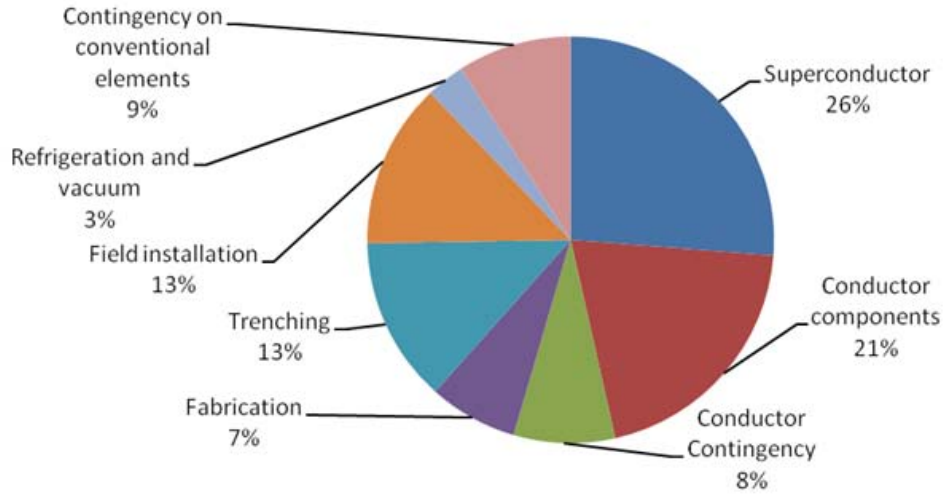


Figure C-1
Relative costs of materials for superconducting dc cable (excluding converters) with superconductor at US\$5/kA-m

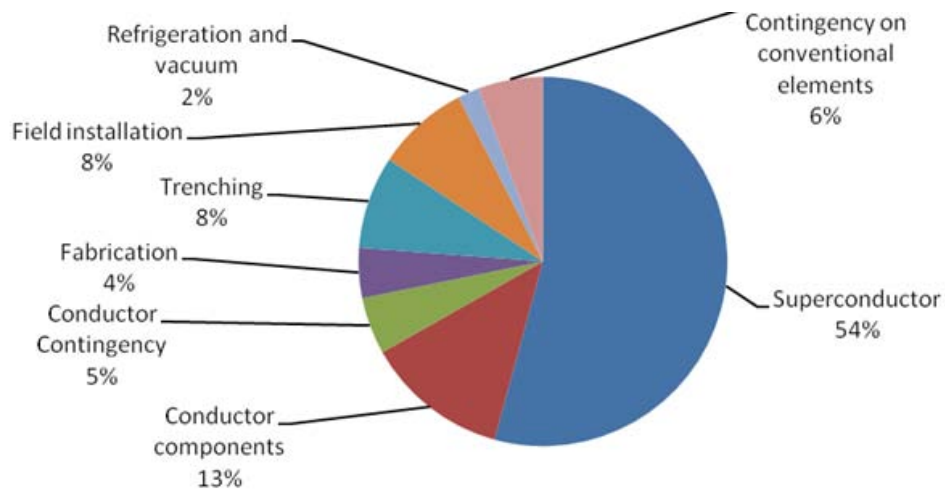


Figure C-2
Relative costs of materials for superconducting dc cable (excluding converters) with superconductor at US\$17/kA-m

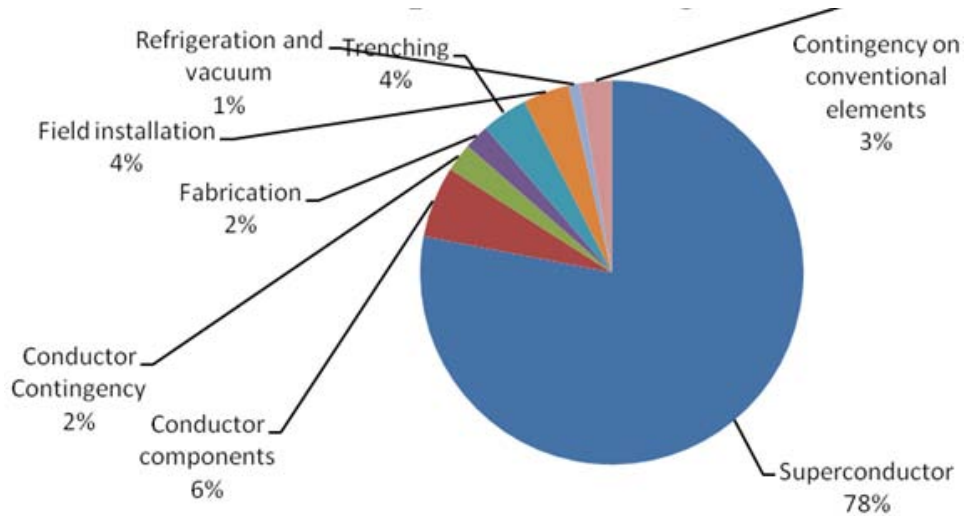


Figure C-3
Relative costs of materials for superconducting dc cable (excluding converters) with superconductor at US\$50/kA-m

These costs can also be expressed as cost per kilometer or cost per mile. Cost per mile is the typical price quoted in the media for comparisons of various power transport systems. Table C-5 presents cable costs per kilometer and per mile for a 1600-km (1000-mile), 5-GW, low-voltage dc system with superconductor costs ranging from US\$5/kA-m to US\$100/kA-m.

Table C-5
Cost per kilometer and per mile with different superconductor costs

| Component | Cost | Cost | Cost | Cost |
|---|----------|-----------|-----------|------------|
| Unit Superconductor Cost (US\$/kA-m) | 5 | 18 | 50 | 100 |
| Cable cost per kilometer (US\$ millions) | 3.0 | 4.4 | 9.1 | 12.5 |
| Cable cost per mile (US\$ millions) | 4.9 | 7.2 | 14.5 | 20.0 |
| Cable cost per kilometer with converter at US\$150/kW (US\$ millions) | 4.0 | 5.4 | 10.0 | 13.4 |
| Cable cost per mile with converter at US\$150/kW (US\$ millions) | 6.4 | 8.7 | 16.0 | 21.5 |
| Cable cost per kilometer with converter at US\$300/kW (US\$ millions) | 4.9 | 6.3 | 10.9 | 14.3 |
| Cable cost per mile with converter at US\$300/kW (US\$ millions) | 7.9 | 10.2 | 17.5 | 23.0 |

In addition to the changes in material costs, the capabilities and costs of converters have changed. We assume that the 1600-km (1000-mile), low-voltage dc line will have a 5-GW CSC at the power input and a 5-GW VSC at the receiving end. Converter costs depend on the type and power capacity of the converter. VSCs are more expensive than CSCs. Costs of US\$150 to US\$300 have been used in several studies evaluating electricity storage systems, including a study performed for Sandia Laboratories [45]. Here we compare overall system costs using both US\$150/kW and US\$300/kW. The total cost of the converters for these two cases are US\$0.75 billion and US\$1.5 billion, respectively, for each end of the line. The total cost per mile

for converters is US\$1.5 million and US\$3 million (US\$0.95 million and US\$1.9 million per kilometer), respectively. Figures C-4 through C-7 show the relative costs of materials with superconductor costs at US\$50/kA-m and US\$5/kA-m and converter costs at US\$300/kW and US\$150/kW.

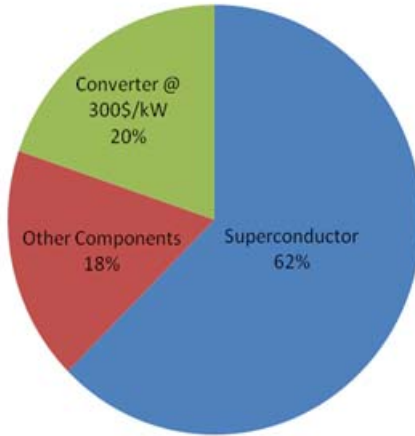


Figure C-4
Relative costs of materials for superconducting dc cable with superconductor at US\$50/kA-m and converters at US\$300/kW

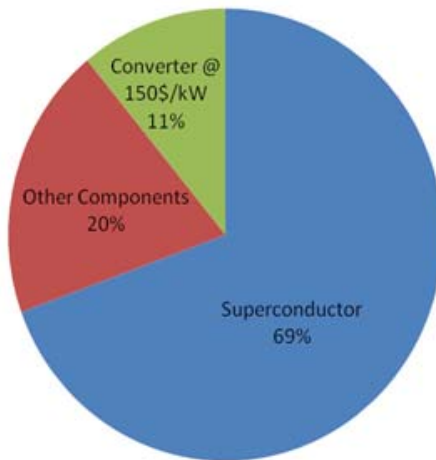


Figure C-5
Relative costs of materials for superconducting dc cable with superconductor at US\$50/kA-m and converters at US\$150/kW

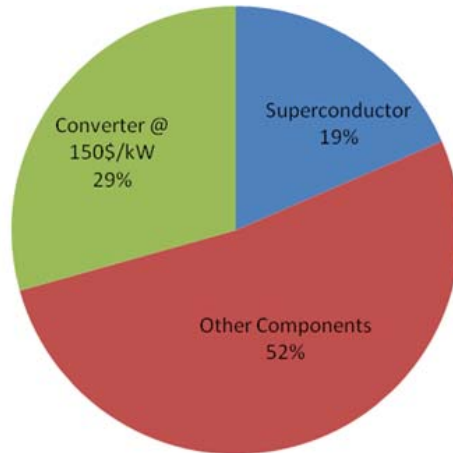


Figure C-6
Relative costs of materials for superconducting dc cable with superconductor at US\$5/kA-m and converters at US\$150/kW

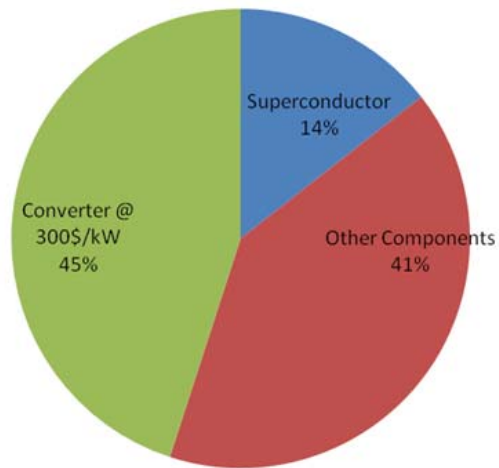


Figure C-7
Relative costs of materials for superconducting dc cable with superconductor at US\$5/kA-m and converters at US\$300/kW

The Electric Power Research Institute Inc., (EPRI, www.epri.com) conducts research and development relating to the generation, delivery and use of electricity for the benefit of the public. An independent, nonprofit organization, EPRI brings together its scientists and engineers as well as experts from academia and industry to help address challenges in electricity, including reliability, efficiency, health, safety and the environment. EPRI also provides technology, policy and economic analyses to drive long-range research and development planning, and supports research in emerging technologies. EPRI's members represent more than 90 percent of the electricity generated and delivered in the United States, and international participation extends to 40 countries. EPRI's principal offices and laboratories are located in Palo Alto, Calif.; Charlotte, N.C.; Knoxville, Tenn.; and Lenox, Mass.

Together...Shaping the Future of Electricity

Programs:

Technology Innovation

Increased Transmission Capacity

© 2009 Electric Power Research Institute (EPRI), Inc. All rights reserved. Electric Power Research Institute, EPRI, and TOGETHER...SHAPING THE FUTURE OF ELECTRICITY are registered service marks of the Electric Power Research Institute, Inc.

1020458

Electric Power Research Institute

3420 Hillview Avenue, Palo Alto, California 94304-1338 • PO Box 10412, Palo Alto, California 94303-0813 USA
800.313.3774 • 650.855.2121 • askepri@epri.com • www.epri.com